SPS

Rapport des étudiants 34

REMOTE SENSING AND SOIL SCIENCE OF THE KAYA AREA (BURKINA FASO)

E. Elkenbracht
A. ten Holte
L. Otter
T. Slaa
February 1995

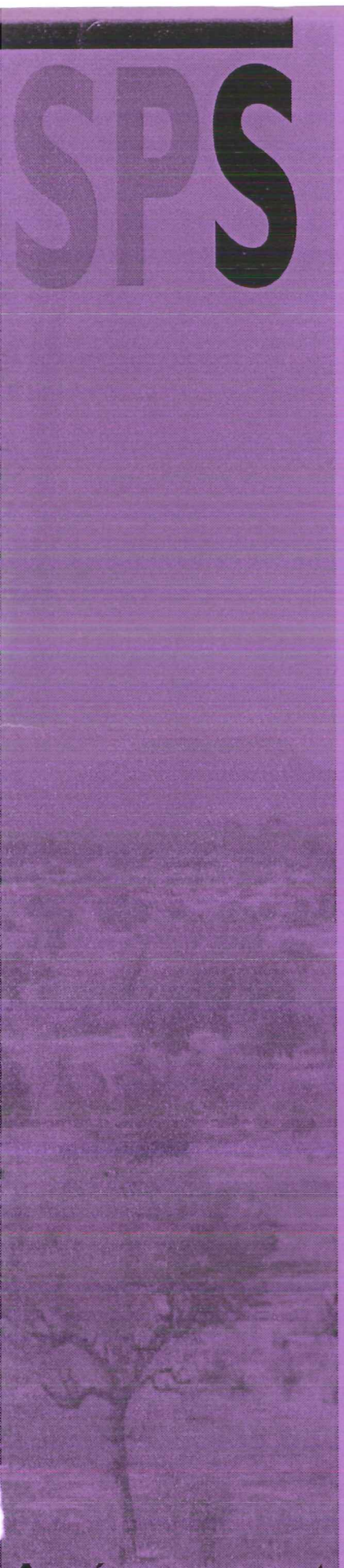

Aménagement et Gestion
de l'Espace Sylvo-Pastoral au Sahel

Antenne Sahélienne de l'Université Agronomique Wageningen Pays-Bas
et de l'Université de Ouagadougou Burkina Faso

PUBLICATIONS DEJA PARUES:

Documents du projet (rouge)

1	B. van Koppen & N. Groesz	Research Proposal: "gender in the optimalization of tenure arrangements with regard to landesque capital"
2	J. Oostveen (red.)	Werkplannen juni 1991
3	B. Lekanne dit Deprez	Silvopastorale gebieden als sociale ruimte bij de Mossi van Burkina Faso
4	E. Frederiks	Algemene informatie ten behoeve van bezoek aan de Universiteit van Ouagagdougou
5	E. Frederiks	Programme Sahélien UAW: Activités 1985 - 1992 et l'avenir
6	M. Bloemberg (red.)	Rapport du 1er atelier du programme de recherche SPS à Ouagadougou (du 14 au 18 décembre 1992
7	A. de Wit	Manuel pour mésurer la sève des arbres avec le "Dynamax sap flow system flow32"
8	L. Stroosnijder & W. Hoogmoed	Zelfevaluatie VF-Sahel (VF 91.61), februari 1993
9	A. Ran	Hoe, wat, waar in Burkina Faso: studentenhandleiding Steunpunt Sahel
10	M. Rietkerk & F. Hien	Mesures de régénération au Sahel
11	A. Mando	Role des termites dans la régénération des sols dégradés au Sahel
12	L. Stroosnijder & W. Hoogmoed	"Management of natural resources in the sahel", subprogramme of the VF-programme "Sustainable land use in the tropics"
13	M.A. Mulders	Rapport sur les activités de télédetection du programme SPS, juillet 1992 - mai 1993
14	M.A. Mulders, J. van Rooijen et A. Casterad	Data processing as preparation for soil and land degradation studies in Burkina Faso
15	A. Bleumink	Manuel pour l'utilisation de l'enregistreur de données DELTA-T logger
16	E. Frederiks (red.)	Rapport Annuel 1992, Antenne Sahélienne UO/UAW (version française et néerlandaise)
17	H.J.F. Savenije	Sylvicultural management practices in the Sudan and Sahel zone with an emphasis on the silvopastoral vegetations: a compilation of literature
18	J.W. Nibbering	Manuel de quelques techniques de mesures agro-économiques et le traitement des résultats
19		Rapport Annuel 1993, Antenne Sahéliene UO/UAW, mars 1994
20	J.W. Nibbering	Méthode et résultats de quelques transects effectués le long des routes de circulation pour inventorier l'état et l'utilisation des terroirs au niveau régional
21	J.W. Nibbering	Glossaires français-néerlandais et néerlandais-français de termes utilesés dans l'étude des aspects sociaux et économiques de l'agriculture

Publications de l'Antenne (vert)

1	S. de Bie & C. Geerling	IUCN-Paper: "Ecological Limits to the conservation and sustainable exploitation of natural resources"
2	W. van Driel & A. Ran	Risques et contraintes pour l'intensification de la riziculture dans deux bas-fonds aménages de la province de la Comoë, Burkina Faso
3	J.J. Kessler & K.F. Wiersum	The multi-dimensional nature of silvo-pastoral areas in the Sahel region
4	L. Stroosnijder	Afrika studiedag 16 december 1992: "Ecologisch kwetsbare gebieden in Afrika"
5	L. Stroosnijder, W. B. Hoogmoed and J.J.A. Berkhout	Séminaire International sur la gestion agroclimatique des precipitations, décembre 1991: "Modelling effects of water conservation tillage in the semi-arid tropics"
6	W.B. Hoogmoed J.J.A. Berkhout L. Stroosnijder	Séminaire Internationale sur le travail du sol en zones arides et semi-arides, organisé par l'ANAFID, 22-23 april 1992: "Soil tillage options for water management under erratic rainfall conditions"
7	M. Rietkerk, F. Hien L. Stroosnijder	"Dominance des caractères des croûtes sur les types de sols dans les terrains sylvo-pastoraux dégradés au Sahel"
8	J.J. Kessler	Agroforestry and Sustainable Land-use in Semi-arid Africa. In: Zeitschrift für Wirtschaftsgeographie, Jg. 37 (1993), Heft 2, S. 68-77, Frankfurt a.M.
9	J.J. Kessler & K.F. Wiersum	Ecological Sustainability of Agroforestry in the Tropics. In: Entwicklung und Ländlicher Raum 5/93, vol 27 (5): 8 - 11, 1993
10	K.F. Wiersum	Systèmes indigènes d'exploitation et de gestion de la végétation boisée au Sénégal: cadre d'analyse. In: La Foresterie Rurale au Sénégal: participation villageoise et gestion locale, Leiden Development Studies, No. 12: 135 - 159, 1993
11	L. Stroosnijder	Population Density, Carrying Capacity and Agricultural Production Technology in the Sahel. Paper presented at the 1994 Danish Sahel Workshop, 6-8 January 1994, Sandberg Manor, Sonderborg, Denmark
12	A. Mando, W.F. van Driel & N. Prosper Zombré	Le rôle des termites dans la restauration des sols ferrugineux tropicaux encroûtés au Sahel. Contribution au 1er Colloque International de l'AOCASS: Gestion Durable des Sols et de l'Environnement en Afrique Tropicale, Ouagadougou, 6 - 10 décembre 1994
13	A.H.M. Schutjes & W.F. van Driel	La classification locale des terres par les Mossi: paysans et pédologues parlent-ils le même langage ? Contribution au 1er Colloque International de l'AOCASS: Gestion Durable des Sols et de l'Environnement en Afrique Tropicale, Ouagadougou, 6 - 10 décembre 1994
14	H.B. Tammes, R.B. Kaboré & W.F. van Driel	L'effet de la matière organique sur la formation des croûtes et l'érosion des sols sableux au Burkina Faso. Contribution au 1er Colloque International de l'AOCASS: Gestion Durable des Sols et de l'Environnement en Afrique Tropicale, Ouagadougou, 6-10 décembre 1994

REMOTE SENSING AND SOIL SCIENCE OF THE KAYA AREA (BURKINA FASO)

Ernestine Elkenbracht
Adrienne ten Holte
Loes Otter
Trinette Slaa

1994

Burkina Faso, Antenne Sahelliene student report nummer 32
Wageningen Agricultural University, department of soil science and geology.

ACKNOWLEDGEMENTS

This research described in this rapport was only possible with help of many people. We would like to thank all of them.

In first place we like to thank the staff of Antenne Sahelienne. They provided all the basic supplies for our stay and research in Burkina Faso. Without our chauffeur Babba we would not have reached every nook and corner of our fieldwork area.

During the research in Wageningen Maarten Tromp was very helpful in computer and remote sensing work. Toine Jongmans was a good teacher in micromorphological analysis. The soil map was digitized with ARC-INFO and this would not be possible without the assistance of John Stuiver and the finishing touch by Heleen Wessels. Jan van Doesburg en Bram Kuiper assisted in analysing the soil and rock samples.

Gerrit Epema and Dick Legger were our supervisors during a part of the fieldwork in Burkina and the research in Wageningen. Their enthusiasm, ideas and support were very stimulating, but without the cups of tea and coffee of Dick we would not have survived.

Ernestine Elkenbracht
Adrienne ten Holte
Loes Otter
Trinette Slaa

PREFACE

The present student research is a part of the interdisciplinary research programme "Aménagement et Gestion de l'Espace Sylvo-Pastoral au Sahel (SPS)", which is carried out by the Agricultural University Wageningen in cooperation with the University of Ouagadougou (Burkina Faso). Preparations have been made in Wageningen in October 1993. The actual fieldwork has been performed in November-December 1993 in the area near Kaya (Burkina Faso) by the 4 students. Analysis of the data and report writing was performed mainly in the first half of 1994. In the last phase parts of the report were somewhat reorganised and edited by the supervisors, but the students remain responsible for their specific parts. The chapters have been written by: Ernestine Elkenbracht, chapters 1, 2, 3.1, 4, 5.3.3, 5.3.4, 6; Adrienne ten Holte, chapters 1, 2, 3.1, 4, 6; Loes Otter, chapters 1, 2, 3.2, 5.1.3, 5.1.4, 5.2, 5.3.2, 6; Trinette Slaa, chapters 1, 2, 3.2, 5.1.1, 5.1.2, 5.2,5.3.1, 6. For all students the credits are given to an "Afstudeervak bodeminventarisatie en landevaluatie" of 21 study points. We think that this report is an important step in our knowledge on soil science of the Kaya area and the possibilities of remote sensing. We are very much confident that this report is a good base for further work in the field of remote sensing and soil science for the Province of Sanmatenga at both detailed and reconnaissance scale.

Dr. Gerrit F. Epema
Ir. Dick Legger
(supervisors)

TABLE OF CONTENTS

1. INTRODUCTION 1

2. MATERIALS 3

3. METHODS 7
3.1 METHODS FOR SOIL MAPPING 7
3.2 METHODS FOR REMOTE SENSING 8

4. STUDY AREA 15
4.1 GENERAL 15
4.2 GENESIS 17
4.3 SOIL MAPPING UNITS 29

5. REMOTE SENSING 39
5.1 FIELD AND LABORATORY REFLECTANCE 39
5.1.1 Spectral differences between major soil and vegetation types . . . 39
5.1.2 Spectral characteristics of various shrubs and grasses 42
5.1.3 Spectral characteristics of bare surfaces in the field. 44
5.1.4 Analysis of laboratory reflectance spectra for soil surface characteristics. 51
5.2 COMPARISON BETWEEN FIELD AND SATELLITE REFLECTANCE 57
5.3 ANALYSIS OF LANDSAT TM IMAGERY 63
5.3.1 UNSUPERVISED CLASSIFICATION FOR LANDSCAPE MAPPING 63
5.3.2 MIXTURE MODELLING OF LANDSAT TM DATA 83
5.3.3 SPECTRAL VARIATION WITHIN SOIL MAPPING UNITS . . 87
5.3.4 AERIAL PHOTOGRAPHS AND LANDSAT TM FOR SOIL MAPPING 107

6. CONCLUSIONS AND DISCUSSION 109

REFERENCES 113

APPENDIX 2.1 CHARACTERISTICS OF LANDSAT THEMATIC MAPPER IMAGES 117

APPENDIX 2.2 CHARACTERISTICS OF THE REFERENCE PANEL 119

APPENDIX 3.1 FILE AND MAP COORDINATES OF TM IMAGES 121

APPENDIX 3.2 MINI-IRIS REFLECTANCE MEASUREMENTS 122

APPENDIX 4. SOIL PROFILE DESCIPTIONS 127

APPENDIX 5.1 SHORT DESCRIPTION OF LABORATORY SAMPLES 153

APPENDIX 5.2 CHEMICAL COMPOSITION (X-RAY FLUORESCENCE) 155

APPENDIX 5.3 MINERALOGICAL COMPOSITION (X-RAY DIFFRACTION) . . 158

APPENDIX 5.4 ORGANIC CARBON AND FREE IRON CONTENT 160

APPENDIX 5.5 ABSORPTION FEATURES OF LABORATORY SAMPLES 161

APPENDIX 5.6 A SELECTION OF UNMIXED IMAGES 166

APPENDIX 5.7 STATISTICAL RESULTS OF UNMIXING 170

1. INTRODUCTION

The Sahel region is confronted with a degradation of the natural environment. The reduction of soil fertility is followed by a reduction of agricultural yield. Erosion of sensitive surfaces becomes more severe by reduction of vegetation cover. Physical degradation is accompanied by a marginalisation of some societal groups.

To understand the causes of physical degradation of an area it is necessary to have knowledge of biotic and abiotic aspects of the area. Knowledge about soil properties and

The interdisciplinary research program "Aménagement et Gestion de l'Espace Sylvo-Pastoral au Sahel (SPS)" is carried out by the Agricultural University Wageningen in cooperation with the University of Ouagadougou (Burkina Faso). Its objective is to find an interdisciplinary solution to determine the production level, the management type and the roll of village communities in durable management of natural resources in the Sahel.

This report is written in the framework of this program and presents a study of soil and remote sensing aspects of the Kaya area, Burkina Faso and is performed in November and December 1993. Its objectives are:

1. to construct an easily understandable and reliable soil map.
   This has been performed by:
   a. studying the genesis of the area;
   b. mapping the soils using of satellite images, aerial photographs and fieldwork.

2. to understand the Landsat Thematic mapper satellite images of the area for mapping:
   More specifically the following has been studied:
   a. the relation between soil and vegetation reflectance and their properties;
   b. the relation between field reflectance and at-satellite planetary reflectance and between field reflectance and laboratory reflectance;
   c. possibilities of landscape classification based on satellite images and fieldwork;
   d. the abundance of typical surfaces within a pixel using mixture modelling;
   e. the variation in spectral values within one soil mapping unit using geostatistics.

It is believed that the results of this study are a good base for further work in the field of remote sensing and soil science for the Province of Sanmatenga at both detailed and less detailed scale.
The study was carried out by researchers of the Soil and Geology Department and by students in Physical Geography and in Forestry.

2. MATERIALS

The materials used for remote sensing are: imagery from air and space, instruments to determine reflectance in the field and in the laboratory and the main programmes to analyze the remote sensing data.

AERIAL PHOTOGRAPHS

Two sets of stereoscopic aerial photographs were available: 1) photos of scale 1:50 000, from October 1981, and 2) photos of 1:30 000 from January 1982, which were enlarged to a scale of 1: 15 000. The aerial photographs were supplied by the 'Institute Geographique de Burkina' (IGB).

LANDSAT THEMATIC MAPPER.

The Landsat Thematic Mapper (TM) satellite records reflected radiation of the earth surface. It has a swath width of 185km. TM-images have 7 bands, 3 in the visible light (VIS), 1 in the near-infrared (NIR) part of the spectrum, 2 in the middle-infrared part (MIR) and 1 in the thermal-infrared part (table 2.1).

Imagery of Landsat Thematic Mapper (TM) of two dates were used in this research: January 8, 1991 and May 7, 1988. Landsat TM records reflected radiation of the earth surface. The TM-sensor has a ground resolution of 30 * 30m. Based on data of the satellite, EOSAT, the supplier of the data, applied a geometrical correction of the data of both dates and resampled the imagery to a spatial resolution of 25 * 25m. The type of geometric projection used was UTM (Universal Transverse Mercator). The "standard systematic correction" has a maximum error of 250m. For a more extensive description of characteristics of the imagery one is referred to appendix 2.1. A subset of the research area was taken from the January and May images. Print outs of the subsets were used for field preparation and orientation. As the research was focused on reflected radiation between 400 - 2500nm the thermal-infrared band (6) was not used.

Table 2.1 Landsat TM bands and wavelength (Markham and Barker, 1985 and Buiten and Clevers, 1990).

1	451.8 - 518.0nm	VIS
2	528.8 - 609.4nm	VIS
3	624.4 - 693.0nm	VIS
4	776.0 - 905.1nm	NIR
5	1 567.6 - 1 784.5nm	MIR
6	10 400 - 12 500nm	TIR
7	2 097.2 - 2 347.4nm	MIR

CROPSCAN

A Cropscan radiometer is one of the two instruments used to determine field reflectance. It is a radiometer with eight sensors for the incoming radiation and eight sensors for the reflected radiance, an A/D converter and a Tandy 102 field computer (Anonymous, 1990). The data can be transferred to a PC for further analysis. This multispectral radiometer measures in eight wavelength bands at respectively: 490, 550, 670, 700, 740, 780, 870 and 1050 nm. In order to determine reflectance for all bands, reflected radiation from the surface has to be divided by incoming radiation and multiplied with an instrument and band specific calibration factor. Since reflected radiation and incoming radiation are measured at the same time, the instrument can be used under many atmospheric conditions. Another important feature of the instrument is the speed: one measurement takes less than 2 seconds.

MINI-IRIS

The Mini-IRIS is a spectroradiometer, which is designed to determine field reflectance with a high spectral resolution between 0.4 and 2.5μm in real time. The resolution is 10nm between 0.4 and 1.0μm and is selectable for either 24nm from 1.0 - 2.5μm (first grating) or 8 nm from 2.0 - 2.5μm (second grating). The spectrometer uses two sensors: one silicon detector for the range of 0.4 - 1 μm, and a PbS detector for the range between 1 and 2.5μm (Anonymous, 1993). Reflectance is determined by measuring the target and subsequently measuring a reference panel, multiplied with a correction factor. With the used tripod, the distance between Mini-IRIS lens and ground surface was 105cm. In this case, the spatial resolution is 24 * 24cm. Height of the instrument influences the spatial resolution. When the mini-IRIS is used on slopes, the target-lens distance may be less than 105cm. In this case the spatial resolution can be calculated as follows:

$$b = [(2.5 / 11) * a]^2$$

b = spatial resolution (cm^2)
a = height of mini-IRIS (lens - ground distance in cm)

Incoming radiance is determined by measuring a barium sulphate reference panel. This panel is attached to the tripod and is measured prior to any target measurement. The barium sulphate reference panel has almost a Lambertian surface, but reflectance does not reach 100%. In appendix 2.2 reflectance percentage of the used panel as function of wavelength is given. In Chapter 3.2 these reflectance percentages are used to calculate the total amount of incoming radiance. All signals of the Mini-IRIS have to be corrected for the dark current. Dark current is the signal given by the sensor when all light is blocked from the detectors.

INFRA ANALYZER

The Infra Analyzer is a laboratory spectroradiometer with an active light source. It is able to measure reflectance from 700 to 2500nm on small samples. Spectral resolution is 3nm. This instrument located at the "Laboratorium voor grond- en gewas onderzoek" in Oosterbeek, the Netherlands, is used for measuring reflectance of reference samples taken from the field.

COMPUTER PROGRAMS

The most important programs, used during this research, are:

- IDRISI A simple GIS system with modules for analysing remotely sensed data (Eastman, 1992). It can use vector and raster images and contains modules of image processing, statistical analysing, database management, cartographic display and analysis system, and a map digitizing system. Being the only image processing program available in Burkina Faso, January and May images were converted from ERDAS to IDRISI format (Chapter 3.2) for use during the fieldwork period of the research.

- ERDAS A program incorporating functions of image processing and raster Geographic Information Systems (GIS). These functions include collection, viewing, alteration and analysis of remotely sensed data and other raster data sets (Anonymous, 1990). Both ERDAS installed on PC and on the workstation (running under UNIX) have been used. ERDAS is used for most processing of Landsat TM-images (chapter 3 and 5).

- SIPS Spectral Image Processing System (SIPS) is an advanced program which originally was developed to analyze imaging spectrometer and other remote sensing data (Kruse et al, 1993). This program is developed as an application in IDL and runs under UNIX. In this study a module to unmix pixels has been used. The unmixing procedure of the Landsat TM data is described in Chapter 5.3.2.

- DISPEC A program developed to display and process the mineral spectra (Anonymous, 1991). It includes an absorption feature finding algorithm, and can be applied to quantify the characteristics of the absorption features in the mineral spectra such as depth, area and asymmetry. In this study (Chapter 5.1), DISPEC is used to analyze reflectance spectra measured by the Infra Analyzer.

- ARC-INFO

  The ARC-INFO database system consists of two components: ARC handles where the features are and INFO the feature descriptions and their relation. The soil boundaries on the aerial-photographs were digitized and transferred to an overlay of a satellite imagery (Chapter 3.1), using ARC-INFO (version 6.0). The data were edited in with ARCEDIT and the legend created with ARCPLOT (Anonymous, 1992a and b).

3. METHODS

3.1 METHODS FOR SOIL MAPPING

FIELDWORK

In the field an aerial photo-interpretation of nine photographs was validated and were necessary corrected. Next to numerous surface, road cut and gully bank observations, the different soil units were studied through a limited number of auger hole observations and soil profile describtions, using the FAO guidelines (FAO-ISRIC, 1990). Of each horizon of the soil profiles and of some rocks samples were collected for analyses. Of about 50 samples the pH and EC (1:2.5) was determined in the field, using Hanna's pH and dissolved solid testers.

SOIL MAP

Combining band 7 of the acquisition of May, 1988 with bands 4 and 1 of the January, 1991 tapes with ERDAS gave, after stretching, the clearest image, including that on the geology. The soil map, originally represented by interpretation lines on the nine aerial photographs, was digitized with ARC-INFO. In order to match the aerial photographs with the image and with each other, on each photograph five clear reference points were selected. For proper matching the location of these reference points had to be as far as possible of each other and partly in the overlay with adjacent aerial photographs. The coordinates of these reference points were determined by recording the coordinates of exactly the same points on the image with the option "curses" in ERDAS. As a result the digitized soil map has the same grid as the image and can be used as cover over the image.
When, by deformation at the edges of the aerial photographs, the polygons did not match in the transition zone of two photos, the polygons were rotated or moved with ARCEDIT, untill the interpretation lines corresponded with clear boundaries or other topgraphic features still visible on the image. After correcting all errors, the polygons were labelled. Next these labels were replaced with their corresponding colour, hadge and soil code in such a way that the image was still visible, giving an impression of the variability in each of the designated soil units.
The legend is produced in ARCPLOT and build up hierarchical: e.g. the geology is presented by a colourgroup, the geomorfology by the hue in a colourgroup and the surface material by the hadge. If necessary, an additional code represents the height of the geomorfological unit.

LABORATORY WORK

With X-ray diffraction the different crystalline minerals in samples were analyzed. With röntgen fluorescence the total elementary composition was determined. Thin sections of undisturbed soil samples were made to study soil processes that have or are taking place and to show the arrangement of individual soil particles. Of a selected number of samples the CEC (pH 7.0, M NH_4OAc), exchangeable Na, K, Ca and Mg, pH-H_2O and -KCl and the EC (all three at 1:2.5), the $CaCO_3$ equivalent and texture were determined, using standard FAO procedures (van Reeuwijk, 1987).

3.2 METHODS FOR REMOTE SENSING

PREPARATION PHASE

In the preparation phase the following was performed:
1) retrieving satellite data from tape to disk of the study area
2) matching of different bands and dates of satellite imagery
3) georeferencing of satellite imagery
4) displaying, printing and analysis of images

Two Landsat Thematic Mapper scenes of January 8, 1991 and May 7, 1988 were available for this study. After previewing and using information of EOSAT, data of the study area were retrieved from tape and copied to disk. Two subsets were made covering all bands of both dates of the study area.

When displaying some band combinations of the January subset, it appeared that the images were fuzzy. Band 3 and 7 were displaced. Before the subset could be used, band 3 and 7 had to be shifted upwards by some pixels. Trial and error showed that these bands should be shifted 6 pixels.

For making multitemporal images of the study area, it was necessary to match the two subsets. The May subset was matched to the subset of January. This was done by trial and error and visual judgement. The result was an image of 12 bands, six bands of the January subset and six of the May subset. Matching of both images was not done using the sattelite derived map coordinates, because this result was worse than the result of the trial and error method.

The outer boundaries of the January and May subsets do not show an exact match. Therefore the multitemporal image is slightly smaller than the original subsets. Map and file coordinates of January, May and multitemporal subsets are given in appendix 3.1 if these subsets will be used for further study.
The multitemporal image map coordinates are similar to the map coordinates of the January subset. To achieve the original map coordinates of May, given by the sattelite, the following calculation has to be performed:

X map coordinate of January subset + 125 m = map X coordinate of May subset
Y map coordinate of January subset + 100 m = map Y coordinate of May subset

This difference in geometry between the two dates falls within the expected range. The accuracy of the sattelite derived geometric correction is $\pm$250 m in the worst case. For all images, maps and locations UTM coordinates of January are used.
In the preparation phase most image processing was performed using ERDAS. For the use of the satellite data in Burkina Faso, the ERDAS-files were also converted to IDRISI-format.
For a preliminary selection of locations of interest different images were inspected. A very useful image, showing a range of zones and variation within these zones is presented in figure 3.1. Based on the images and an analysis of the digital numbers of a range of pixels, hypotheses were made and locations for visit were determined.

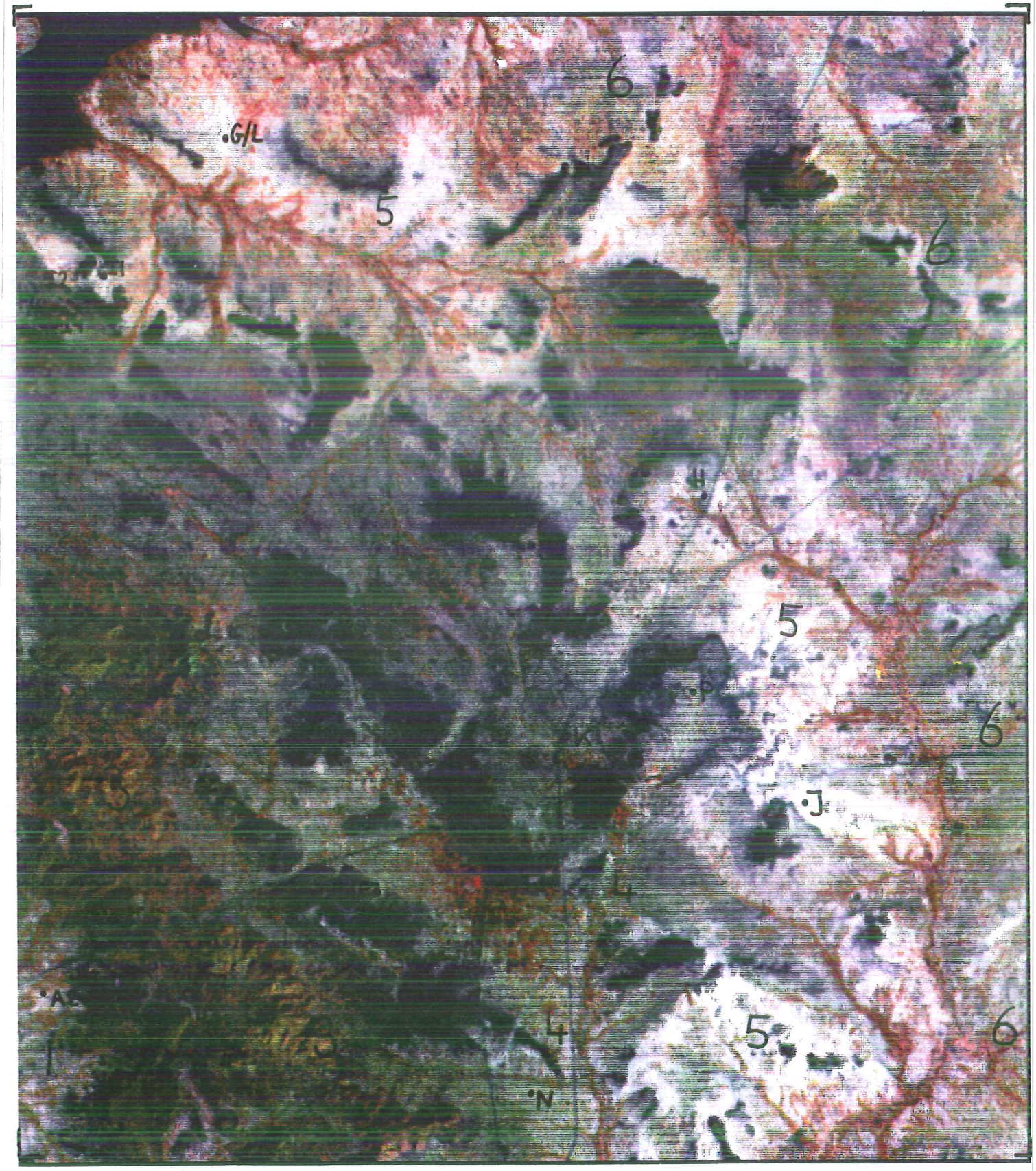

Figure 3.1 A Landsat TM colour composite of January, 1991 of bands 4, 5 and 3, coloured respectively red, green and blue.
(on transparant: 1-6 zones; A1, A2, B, ... day characters; see table 3.1 for explanation)

FIELDWORK

Before starting the field reflectance measurements with the Mini-IRIS spectrometer, it was necessary to gain a good impression of the area. So as to make a sound interpretation of the satellite images. With knowledge of landscape, reflectance characteristics and geological formations, locations of interest are selected. In every zone, one or more locations, which are representative for the zone, are selected. Differences in landscapes and geological formations are considered when selecting the locations.

At each location, reflectance measurements of different surface types are taken. Before taking measurements, surfaces and vegetation typical of the location were marked with a sign. The signs are used for numbering the places and for easy recognition. When selecting the typical surfaces, special attention was given to differences in soil types, surface sealing, structure, colour, vegetation and stone type. In addition, at every location a description was made of vegetation, relief, soil, slope, geomorphology and landcover. Also at every reflectance measurement a short description of each surface type and vegetation cover was made.
At every site the following measurements were carried out:

- First grating (400 nm - 2500 nm): reflected radiation of reference panel, reflected radiation of target, darkcurrent
- Second grating (400 nm - 1000 nm, 2000 nm - 2500 nm): reflected radiation of reference panel, reflected radiation of target, darkcurrent.

The reference panel and the darkcurrent signal are described in chapter 2. Darkcurrent signal and reflected radiance of the reference panel are used for calculating reflectance of the target.

At some locations two other types of measurements are taken. For determining the type of atmosphere the diffuse incoming radiation is measured. This is carried out in the same way as a normal target measurement, be it that in stead of the target, the shaded reference is measured. The shading was done by holding a panel at approximately 4 m (Epema, 1992). The second type of measurement is carried out in order to determine the influence of water on soil reflectance. This is carried out by wetting the soil after the reflected radiation of the dry soil was measured. Subsequently, radiation reflected by the wet soil is measured again.

In table 3.1, a short description of all locations is given. Day characters in table 3.1 correspond with characters in figure 3.1. Figure 3.1 shows the geographical position of all locations. In zone 6 no measurements are taken because of a defect of the Mini-IRIS. An overview of all surface reflectance measurements plus descriptions is given in appendix 3.2.

Tabel 3.1 Locations of Mini-IRIS measurements

day/location	zone	geological formation	description	cover
A1	2	red schists	plateau	bare soil 64% (gravel 24%, crusts 40%), shrubs 1%, grass 35%
A2	1	red schists	erosion plane with some small sanddunes	bare soil (crusts/sandy/gravel) 94%, shrubs 1%, grass 5%
B1	2	red schists	plateau	bare soil (laterite/gravel/crusts) 65%, shrubs 10%, grass 25%
B2	1	red schists	kaolinitic erosion plane	bare soil (sandy/crusts) 100%
C1	3	green schists	hill	bare soil (gravel/rock outcrops) 10%, trees and shrubs 5%, grass 85%
C2	3	green schists	cultivated hill with some quartz rock outcrops	bare soil (crusts/sandy/rock outcrops) 40%, fields 55%, trees 5%
D1	3	red schists	fields in valley	bare soil (gravel/crusts) 75%, shrubs and trees 15%,grass 10%
D2	3	red schists	longitudinal hill	bare soil (rock outcrops) 10%, shrubs 20%, grass 70%
D3	2	red schists	plateau	bare soil (crusts/laterite/ gravel) 10%, shrubs and trees 15%, grass 75%
E1	4	red schists	fields in valley	bare soil (crusts/sandy) 85%, trees 10%, grass 5%
E2	4	red schists	plateau	bare soil 80% (gravel 50%, crusts/sandy 30%), grass 20%
E3	4	red schists	plateau	bare soil (gravel) 29%, trees 1%, grass 70%
F	4	green schists	top of hill	bare soil (gravel/rock outcrops) 90%, grass 10%
H	5	granite	erosion plane	bare soil (crusts/sandy) 90%, shrubs 1%, grass 9%
I1	4	granite	kaolin erosion plane	bare soil 75% (gullies 5%, crusts/gravel/sandy 70%), trees 1%, shrubs 4%, grass 20%
I2	4	manganese	longitudinal hill	bare soil (rock outcrops) 80%, shrubs 20%
I3 (idem F)	4	green schists	top of hill	bare soil (gravel/rock outcrops) 90%, grass 10%
I4	4	green schists	non-cultivated valley	bare soil 80% (quartz rock outcrops 55%, black rock outcrops 20%, sandy 5%), grass 20%
J	5	granite	kaolin erosion plane with granite outcrops and small sanddunes	bare soil 90% (granite rock outcrops 6%, sandy 20%, crusts 55%, gullies 10%, laterite 3%), trees 1%, grass 5%
K	4	green schists	fields	bare soil (crusts/sandy) 20%, trees and shrubs 10%, grass 70%
L1	5	granite	erosion plane with small sanddunes	bare soil 60% (crusts 45%, gravel 5%, sandy 10%), shrubs 10%, grass 30%
L2	5	granite	fields	bare soil (crusts/sandy) 70%, trees and shrubs 15%, grass 15%
N	4	green and red schists	fields	bare soil (crusts/sandy) 87%, trees 10%, grass 3%
O	5	granite	plateau	bare soil 69% (gravel 40%, crusts 29%), trees 1%, shrubs 20%, grass 10%
P	4	red schists	plateau (laterite edge and fields in centre)	bare soil (laterite/gravel/crusts/sandy) 70%, trees 10%, grass 20%
Q	4	red schists	plateau (airfield)	bare soil 70% (gravel 50%, crusts 20%), shrubs 5%, grass 25%

FIELD REFLECTANCE

The Mini-IRIS measures the amount of reflected radiance of a target per band. In order to calculate the reflectance of a target, the reflected radiance must be divided by the total amount of incoming radiance. Incoming radiance is determined by measuring the reference panel. Target signal and reference signal must be corrected for the darkcurrent of the Mini-IRIS. Because the reference panel does not reflect 100% (appendix 2.2), a second correction is needed.

In this way reflectance can be calculated:

$$[(T - D)/(R - D)] * C = RTS$$

T = reflected radiance of a target in digital numbers (DN)
D = darkcurrent of the Mini-IRIS in DN
R = amount of reflected radiance of reference panel in DN
C = correction factor for reference panel
RTS = reflectance target signal

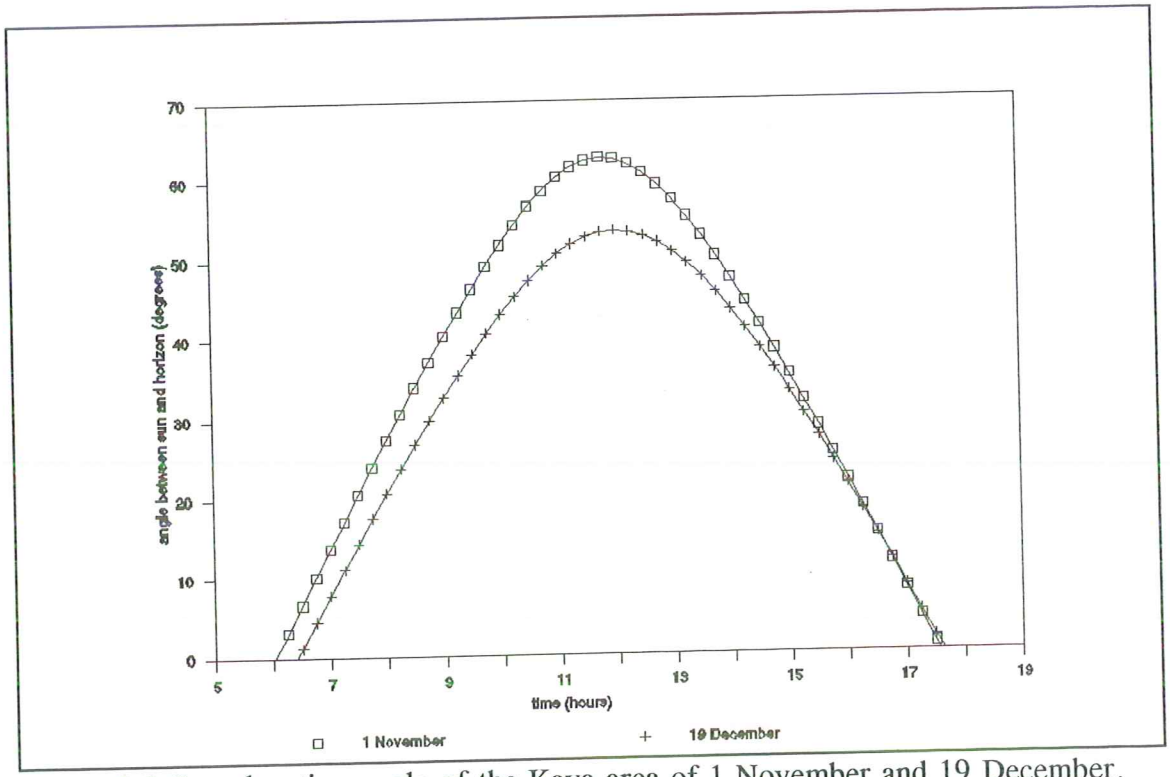

Figure 3.2 Sun elevation angle of the Kaya area of 1 November and 19 December.

Field reflectance is influenced by a number of factors other than soil and vegetation. One of these factors is difference in sun elevations during measurements. During low sun elevations, the reflectance varies significantly from hour to hour. When the angle between horizon and sun exceeds 25°, variation in reflectance is only 10% at a flat surface (Epema, 1992). Sun elevation for Burkina Faso is calculated for November 1 and

December 19 (figure 3.2). This calculation is done after M. Iqbal (1983). Figure 3.2 shows that the sun elevation angle exceeds 25° at eight o'clock in the morning. So, after eight am the sun angle does not have a large influence. To prevent substantive reflectance changes, field reflectance measurements were never carried out before this hour. After about noon measurements were stopped. At this hour the Mini-IRIS caused shading at the reference panel. In the afternoon, no measurements were carried out.
It has to be noted that some problems occurred with the newly developed Mini-IRIS instrument. Main problems refer to low S/N ratio above 1000nm, and probably saturation of the signal. In chapter 5.1.3 this problem is treated more extensively.

4 STUDY AREA

4.1. GENERAL

4.1.1 Location of the area

The study area is located around the township of Kaya in Burkina Faso, between 1 460 000 -1 444 000 and 700 000- 715 000 UTM about 100 km NNE of the capital, Ouagadougou.

4.1.2. Climate

Kaya is situated between the 500 and the 620 mm isobytes. The rainy season runs from May untill October with a maximum of around 200mm in August. Table 4.1. gives the precipitation data of the Kaya station.

Table 4.1. Precipitation in Kaya during the rainy season (averages over 1970-1989).

May		June		July		August		Sept.		October		Total	
mm	days	mm	days	mm	days	mm	days	mm	days	mm	days	mm	days
34	4	93	7	148	9	216	12	111	8	18	2	620	42

Source: Direction de la Météorologie, données journalières 1970-1989 pour les 11 stations pluviométrie du Centre-Nord, Ouagadougou (available on fiches).

The temperature varies little over the year. Table 4.2. gives an example of the maximum and minimum monthly temperatures. Between February and April, the anticlone of the Sahara causes the very hard, dry and hot Harmattan wind (Casenave and Valentin, 1989).

Table 4.2. Average monthly maximum and minimum temperatures (°C) in Kaya.

	J	F	M	A	M	J	J	A	S	O	N	D
Maximum	32	35	38	39	38	35	32	31	32	36	36	34
Minimum	17	20	23	25	25	23	22	21	21	22	19	16

Source: ICRISAT, 1988

The climate corresponds with the Sahelo-Sudanese climate of Aubreville. The climatic characteristics of Ouagadougou, which is slightly more humid, are (FAO, 1977):

Winter type: 'Tp', too warm for cryophilous plants such as wheat
Summer type: 'G', warm enough for cotton, summer days are very hot
Temperature regime: 'TR', Hot tropical
Humidity: 'mo', semiarid monsoon
Annual precipitation: 620 mm (Kaya)
Annual evaporation: 2550 mm
Leaching rainfall in humid season: 300mm
Drought stress in dry season: 1920mm
Humid season: months 7-9
Dry season: months 11-5

4.1.3. Soil temperature and moisture regimes

Deep, well drained soils in Kaya, in which all rain infiltrates whenever the soil moisture content is below field capacity with no run-on, having an iso hyperthermic temperature regime and an aridic tropustic (= iso-temperature) moisture regime (tentative subdivision). Iso-hyperthermic means a mean annual soil temperature of 22°C or higher and the difference between mean summer and winter temperature is less than 5°C at a depth of 50cm. Aridic tropustic is defined as limited in moisture but moisture is available when conditions are favourable for plant growth and the soil is less than 180 consecutive days completely or partly moist (Soil Survey Staff, 1975; van Wambeke, 1982). Sealing has the effect that the moisture regime of these soils comes close to aridic.

4.1.4 Vegetation

The study area covers the following vegetation units (FAO, 1977):
-Unit 4e 'dry savanna'. In this wooded savanna Acacia predominates but also many broad leaved trees e.g. *Combretum and Terminalia* occur in association with *Adansonia digitata, Sclerocarya, Celtis, Ziziphus and Gymosporia.* The grasses comprise mainly *Andropogon gayanus, variuos Hyparrhenia and Pennisetum* and some *Cymbopogon, Loudetia and Ctenium.*
-Unit 4g 'thornbush savanna' (north of unit 4e). This is an intermediate zone between the wetter wooded savanna and the subdesert types. Grasses are generally less than one metre high and include *Chrysopogon aucheri, Aristida stipoides, Cenchrus ciliaris and Sporobolus variegatus*. Trees and shrubs are generally Acacia and Commiphora. In the valleys there are taller grasses such as *Hyparrhenia and Beckeropsis*.

4.2 Genesis

4.2.1. Geogenesis

Similar to 75-80% of Burkina Faso, the area around Kaya consists of Precambrium D (Antebirrimian) and C (Birrimian) crystalline formations with strongly weathered plateaus, often covered with hardened plinthite (iron) crusts.

The Antebirrimians, the oldest identified formations in Burkina, are of archean age. It is likely that between 3000-2700 MA these, in origin marine, series have been deposited on a katarchean sial crust of more than 3000 MA old. During the Liberian mountain formation, at 2660 $\pm$ 135 MA (determined with potassium-argon on amphibole), these residual volcanic or pyroclastic-sediment formations (ortho amphiboles-pyroxene, ortho leptynites) or other sediments (skarns, quartzites, gneisses, leptynites, biotite migmatites) in a predominant granitic-migmatic mass have been folded and metamorphized. Weathering and erosion transformed these formations to the present peneplain with altitudes of 250 to 300m.
Between 2400-2300 MA the area subsided and was inundated by the sea. During the same period, folds of the Liberian formations, that run N.NE to NE or N60°W to N80°W, created narrow chains of single or parallel 20-50km long and 400-500m high volcanos and, less frequently, Inselbergs. The latter mostly consist of homogene granitic facies and associated rocks (granites, granodiorites, syenites and alkaline granophyres).
During the Birrimian, pyroclastic sediments were deposited in the folds that now consist of metamorphized basic volcanites, pyroclastics and clay to sand sediments.
Around 2170 MA an early tectomagmatic phase, characterized by granodiorite intrusions, concluded the era of subsidence and the accompanying deposits of volcanic sediments.
Between 2170-2100 MA substantial amounts of mainly clayey quartz and sands were deposited. The most important part of this so called Eburne mountain formation (folding and metamorphosis) took place between 2100 and 1950 MA, with a peak at 2000 MA. It was characterized by major intrusions of syn to tarditectonic granite that locally rejuvenated both the Birrimian folds and the Liberian chains. The Eburnee activity ended between 1800 and 1500 MA with complex post tectonic magmatic intrusions of alkaline character.
Between 1300 and 1000 MA the Crystalline Basement peneplain, with its eroded craters, is covered again during a marine transgression.
Burkina Faso was not affected by the Precambrium B and no traces of the Precambrium A have been found in the Kaya area. Also there are no signs of geological evolution during the Primar and Secondar until the end of the Tertiar.
At the end of the Eocene (37 MA) the landscape consists of a slightly undulating peneplain, submitted to strong weathering and leaching. During the Neogene (25-2 MA), especially its last 3 million years -the Pliocene- with its various rainy periods, pedogenetical processes created slopes with plinthite that, during drier periods, hardened into extremely hard iron crust.

Combination of geological maps (Hottin and Ouedraogo, 1975; Ducellier, 1961, 1963) with own findings indicates that the Kaya area consists of the following series:

Precambrian D (Antebirrimian): Migmatites and undifferentiated granites

Precambrian C (Birrimian)

-Metamorphised non igneous (parametamorphic) rocks (= Riziam = red schists)
-Metamorphised igneous (orthometamorphic) rocks -Basic and intermediate rocks (= Dacola = green schists) -Ultrabasic rocks

Post Birrimian basic rocks

-Syntectonic acid rocks such as calco-alkaline rocks

The Dacola and Riziam group are associated and partially even interstratified. Both have a schist structure and only their original parent material differs (Ducellier, 1961). The Riziam group has a large extension in the surroundings of Kaya. It has been affected by an insignificant and superficial metamorphosis. It consists of outcrops of predominantly clayey schists alternating with quartzites with colours that vary between ocer, yellow, chestnut brown, red, purple and white. The red colour is caused by hydrated sesquioxides (goethite, limonite). Some exceptional or rare rock types, such as manganese schists, have been found in it. Analysis of such a "manganese band" in the Kaya area showed 17% MnO, (Table 4.3, sample 3) what is comparable with the amount of 19% found in another part of the country (literature!!!).

The Dacola group, consisting of calcium rich metamorphised gabbros and andesites (or dolerites) -respectively coarse grained basic and fine grained intermediate igneous rocks-, originally have been formed under high temperature. It is partially metamorphized tectonically, a process, called retromorphosis, leading to small zones of varying age and degree of metamorphosis. In rocks with a low metamorphosis the original structure is still visible. Those with some more metamorphosis are the greenschist facies, characterized by the presence of chlorite, with its typical green colour, and calcic silicates such as epidotes. The presence of amphibole indicates places with a higher degree of metamorphosis, the amphibolite facies.

In general the Calco-alcaline rocks are microcline and contain quartz, plagioclase (oligoclase and sometimes andesine, but no albite), also indicating a transformation from greenschist to amphibolite facies by a higher methamorphosis. Other minerals, mostly less than 10%, are of secondary importance. In the calco-alcaline group the granite outcrops occupy a large surface of the Kaya area, appearing in different large formations. Often they are heterogeneous or migmatic (alternating light -quartz, feldspars- and dark -schists, gneisses, amphiboles- layers). In regions with abundant outcrops, their contours are frequently parallel to the direction of the inbedded schisteuses rocks.

Table 4.3 Mineralogical composition of some rock samples found in the Kaya area

	SiO_2	TiO_2	Al_2O_3	Fe_2O_3	MnO	MgO	CaO	Na_2O	K_2O	P_2O_5	BaO	No	Ni	Pb	Rb	Sr	V	Zn	Zr
no	%											ppm							
4	46.7	1.9	16.2	16.2	0.3	4.1	7.4	0.8	0.1	0.1	tr	4	116	13	10-	123	480	55	123
26	57.4	1.7	12.7	13.0	0.2	3.1	8.3	0.5	tr	0.1	tr	26	40	14	10-	53	347	46	112
19	50.9	0.9	11.8	10.3	0.2	11.6	8.8	2.7	1.0	0.3	0.1	19	184	10	31	773	167	66	60
27	54.2	0.9	23.4	12.1	tr	0.1	0.1	1.0	1.5	0.1	tr	27	131	22	57	130	176	38	184
25	61.0	0.7	15.0	6.3	0.1	3.5	4.8	4.2	2.7	0.3	0.1	25	27	18	112	795	107	61	179
3	60.9	0.4	10.3	5.6	16.8*	0.2	1.2	tr	0.1	0.1	tr	3	348	41	10-	137	103	184	103
40	71.1	0.6	14.3	4.1	0.1	1.4	3.5	3.8	1.4	0.1	tr	40	10-	11	62	109	102	32	234

No.						
4	Am++++	Ep+	Pl+			greenschist
26	Am+++	Ep+	Pl+	Sm+	Ch+	greenschist
19	Am++++	Ch+	Pl++	Mi+		actinolyte
27	Mi					redschist
25	Am++	Or+	Pl+++	Mi+		granite
3	Sp+++					manganese band
40	Pl+++	Mi++				

Am = amfibole, a Ca/Mg rich Al poor (tremolite/ actinolite) type;
Ch = chlorite; Ep = epidote; Mi= mica;
Or = K-feldspar; Pl = plagioklase
Sm = smectite; Sp = spessartite

tr (trace) < 0. 05
- below detection limit
* more than highest standard sample

4.2.2 Pedogenesis

Large amounts of water, under humid tropical conditions percolating through well drained soils, caused deep and strong weathering, strong leaching of silica and cations, and a subsequent drop in pH. By a change in climate (rise of the sealevel) the depth of the groundwater decreased,

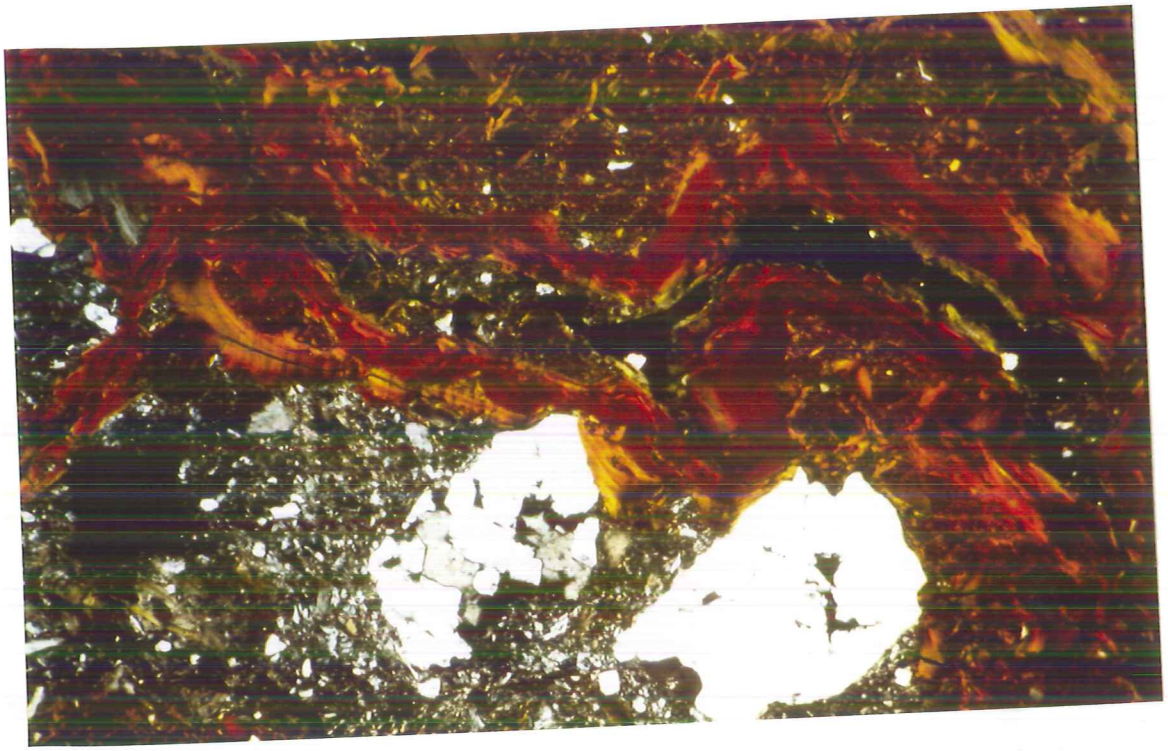

Figure 4.1 Clay coatings in the subsoil of profile 93-4

leading to greying and plinthisation. As a result the iron, released by the weathering,

concentrated in abundant iron mottles which, during following, drier periods or seasons, hardened irreversible to iron concretions. Weathering of primary minerals, still present or precipitated in rich -possibly even salty- dust, in combination with the reverse from an excess of rainfall (= percolation) to an excess of evaporation (= capillary rise), caused a strong increase of the base saturation. This resulted in a higher pH, and probably also of the sodium saturation (ESP). Note that strongly weathered soils contain low activity clays (low CEC values) that do not require high amounts of cations to increase their base saturation substantial. Both the higher pH and ESP caused clay particles to disperse after which, during torrential rainstorms, they could be transported with percolating rainwater. In the subsoil this clay precipitated as clay coatings (Figure 4.1) in pores and on iron concretions.

A combination of clay coatings, which reduce the hydraulic conductivity, and an increased rainfall, raised the groundwater table once again. Under alternating reduced and oxidized conditions, both ferrolysis (Brinkman, 1979) and iron accumulation occurred, especially along preferent waterflows such as cracks and root channels (Figure 4.2). As a consequence the soils experienced losses of cations and aluminium and the relative silica content increased.

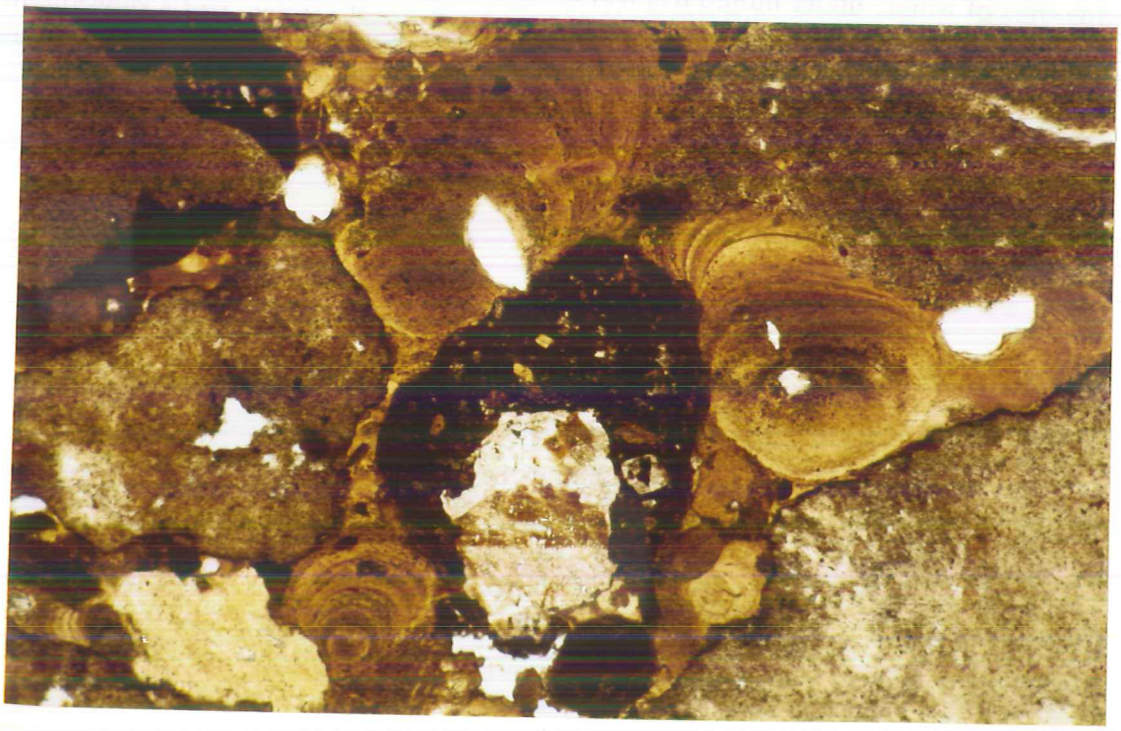

Figure 4.2 Ferrolysis of clay cutans accumulated along preferent water channels in profile 93-2

Especially in the highest part of the iron crust, the expected relative increase of iron and decrease of aluminium and cations is reflected in the 'semi quantative estimation of the mineralogy' of samples of profiles 93-2, 3 and 4 (Appendix ??). The sharp decrease in the amount of silica (from 80 to 15%) indicates that ferralitisation (strong leaching -also of silica- under well drained

conditions) has been more pronounced than ferrolysis (relative increase of silica content by preferent removal of aluminium under poorly drained conditions). The absolute reduction in in aluminium becomes clear if its content is compared with that of TiO_2, Co and V, stable components with a constant absolute amount. Their content increases from respectively 0.5 to 3.3%, 0 to 750ppm and 100 to 700ppm, and Fe_2O_3% increases from 5 to 65%, while that of aluminium stays more or less between 10 and 25% (Figures 4.3A and B). Contents of less than 17% aluminium were only found in samples from red schists. Not any Ca and Mg, or Na or K was found at a Fe_2O_3% of resp. >20, >25 and >40.

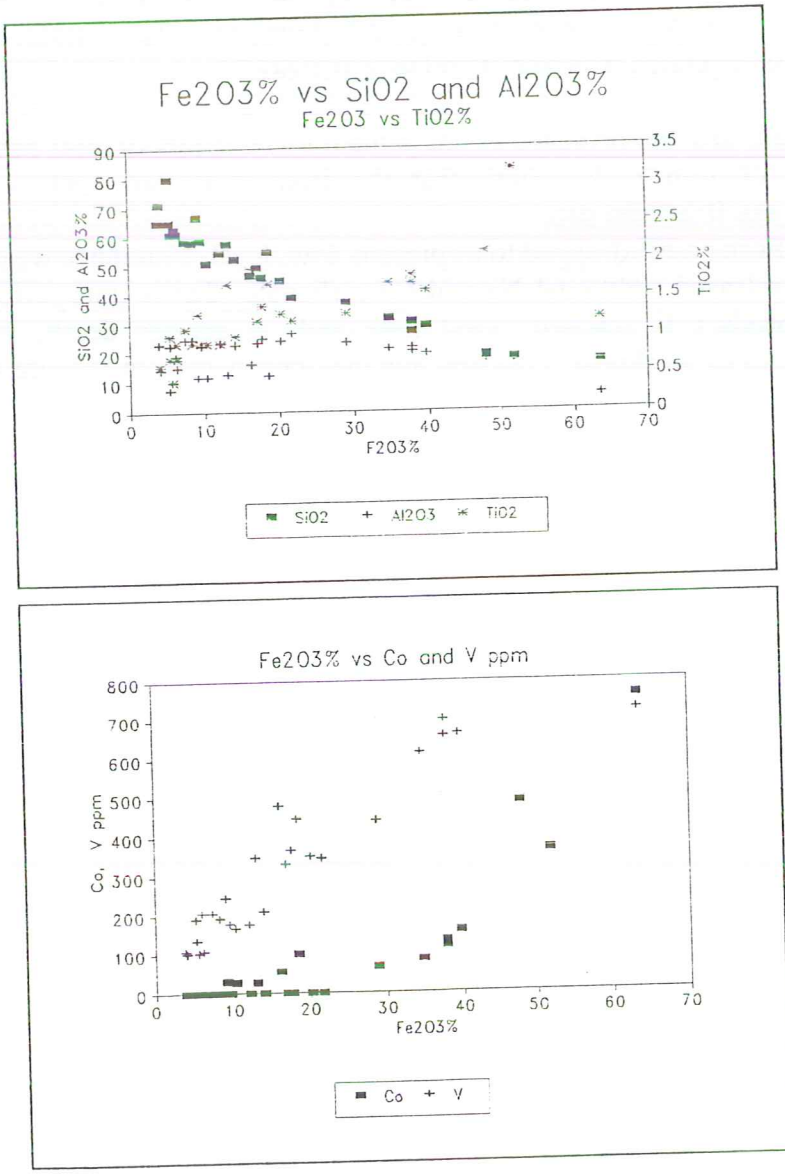

Figures 4.3a and b. Relation between the Fe_2O_3% versus the SiO_2%, Al_2O_3% and TiO_2% (4.3A), and versus the Co and V contents -in ppm- (4.3B) of soils in the Kaya region.

The above mentioned processes, related to risings and lowerings of the groundwater table, repeated themselves several times, resulting in alternating iron and clay cutans, the former being responsible for the changing colours in or on the clay skins. Red clay coatings, for example, could have been covered by iron during the weathering proces after which a new layer of clay was precipitated. The latter was than affected by ferrolysis giving many clay coatings the often observed grainy appearence. That clay precipitation occured in different faces is also shown by the presence of clay coatings on fragmented -result of having been subjected to ferrolysis- clay coatings. The main effect of the repeated rising and lowering of the groundwater table and the leaching processes was the removal of silica and aluminium, the continued plinthisation and hardening of the precipitated iron and its relative increase.

Both analytical data and the presence of the numerous remnants of iron melters, used for the local production of iron tools, show that the iron stone can contain sufficiently high concentrations to use it as iron ore.
Finally the groundwater table dropped to its present, low, level. Continued weathering, especially of granodiorites, released additional Na and Ca carbonates that is transported to places where their solubility product is reached. First lime and, at greater depth, sodium carbonates precipitated in zones of weakness, covering any clay cutans present (Figure 4.4).

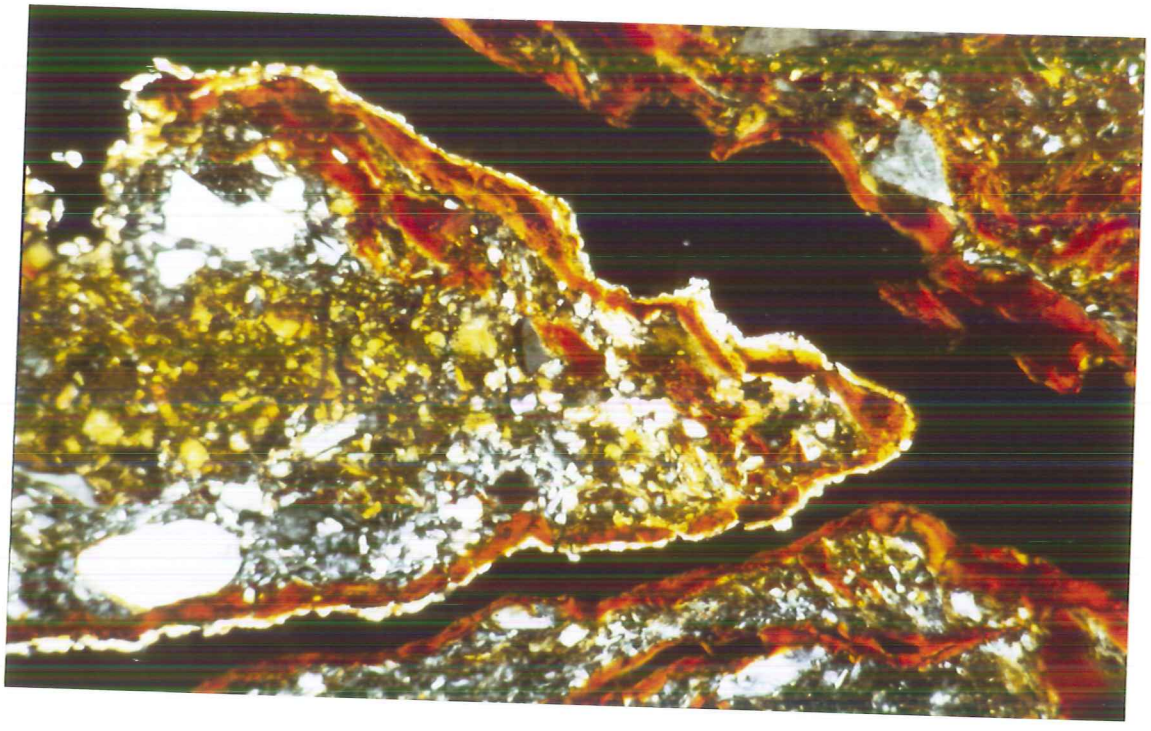

Figure 4.4 Carbonate precipitation on clay coatings of profile 93-4

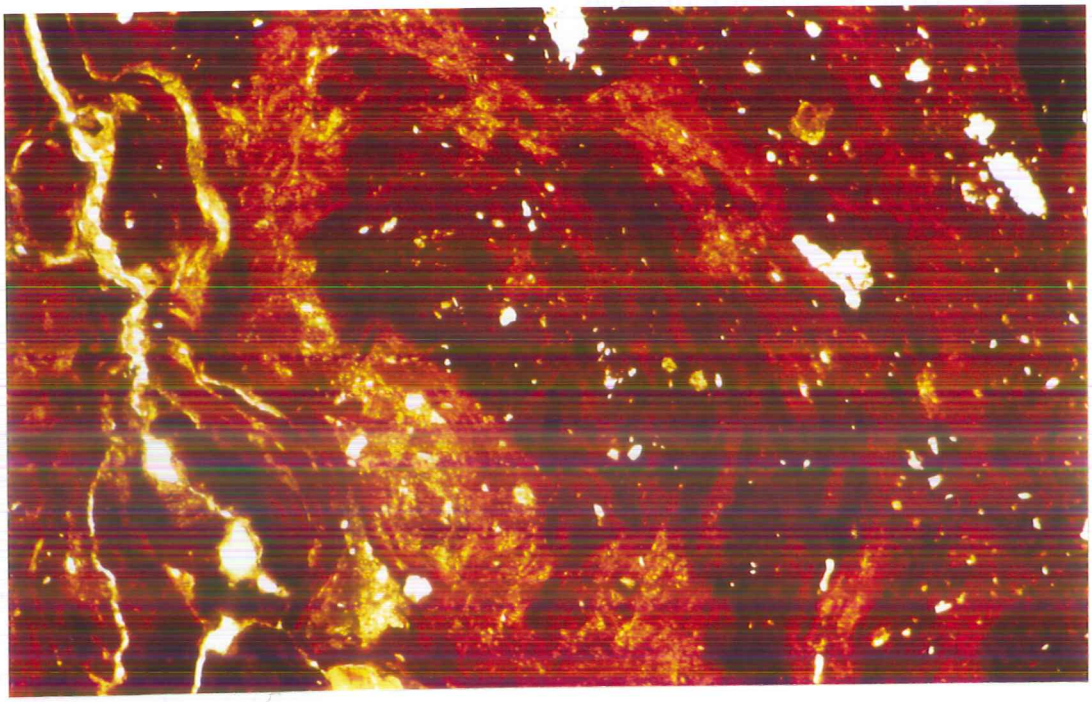

Figure 4.5 Plinthite, pores with small in-fillings of clay and small quartz crystals.

Where, by erosion, plinthite emerged to the surface it dehydrated and hardened irriversible. At the moment the hardened plinthite, iron stone or 'cuirass', as the French call it, or -confusingly- also called 'laterite', does not permit any infiltration of water. However, thin sections of these crusts reveal the processes such as clay and iron precipitation and ferrolysis, that took place during the long period of their genesis (Figure 4.5).

Mainly by retrograding erosion the iron crusts are desintegrating. As a result horizons having been protected for millions of years now start to erode, causing lime concretions to surface. The rate of erosion is excellerated at places where layers with high sodium carbonates contents, accompanied by high pH values, are reached. These layers are located just below those with lime (= gray grains) accumulation, as visible in Figure 4.6.

On granodiorite and red schist but not on green schists iron crusts were found. The fact that the green schist have an iron and silica content that is very close to that of the parent material of the red schists (Table 4.4) indicates that both are of the same origin, the latter being less metamorphized or more weathered than the former.

As a consequence of leaching Fe^{++} and Fe^{+++} contents increased relatively. At places the same applies to Al making the formation of new minerals, such as respectively iron (hydro)oxides (Figure 4.7) and kaolinite (Figure 4.8) possible.

Table 4.4 Comparison of the Si% and Fe% in the parent material and the (weathered and leached) topsoil of various geological formations.

Geological fromation	Parent rock SiO_2	Parent rock Fe_2O_3	Topsoil SiO_2	Topsoil Fe_2O_3	Presence of hardened plinthite
red schist	52	14	18	52	yes
green schist	57	13	80	5	no
granodiorite	61	6	?	?	yes

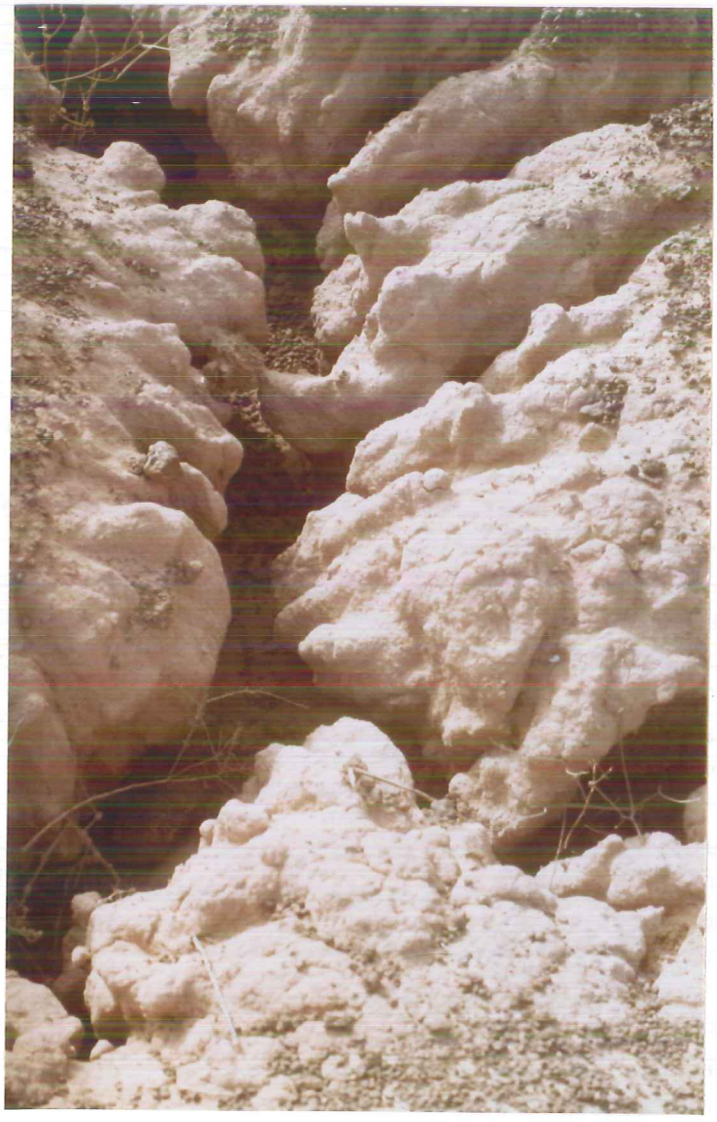

Figure 4.6

Severe erosion at places with high sodium content, just below layers with lime concretions (the gray grains at the surface).

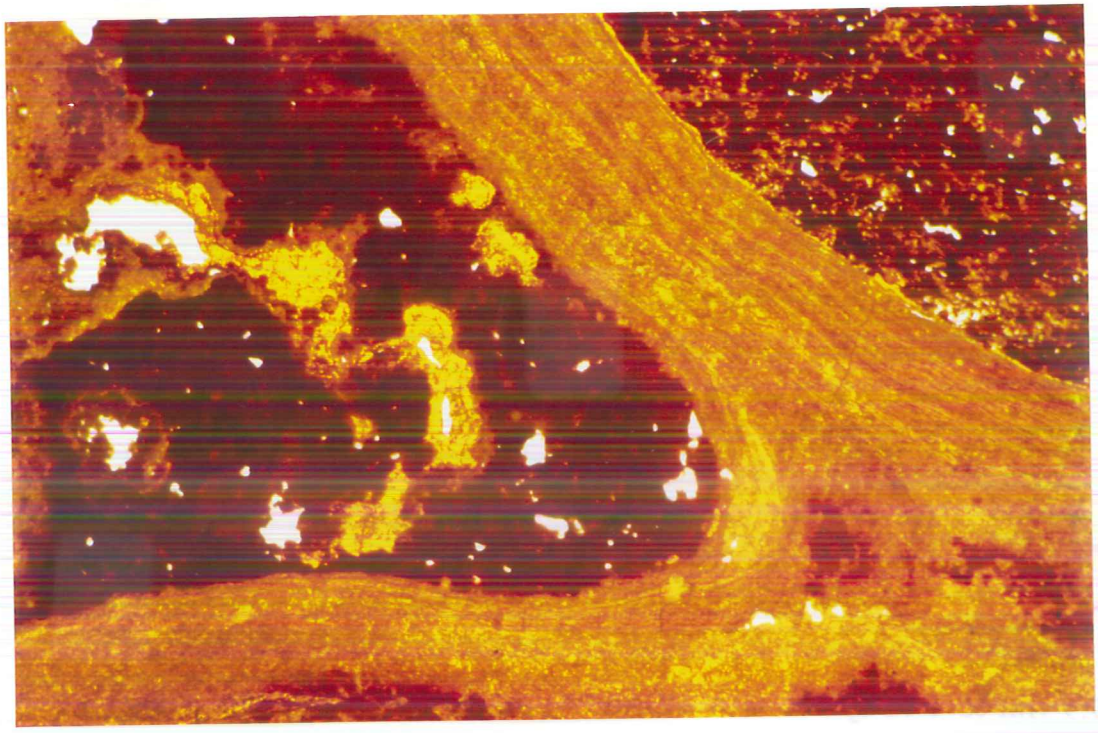

Figure 4.7 Newly formed iron (hydro)oxides minerals

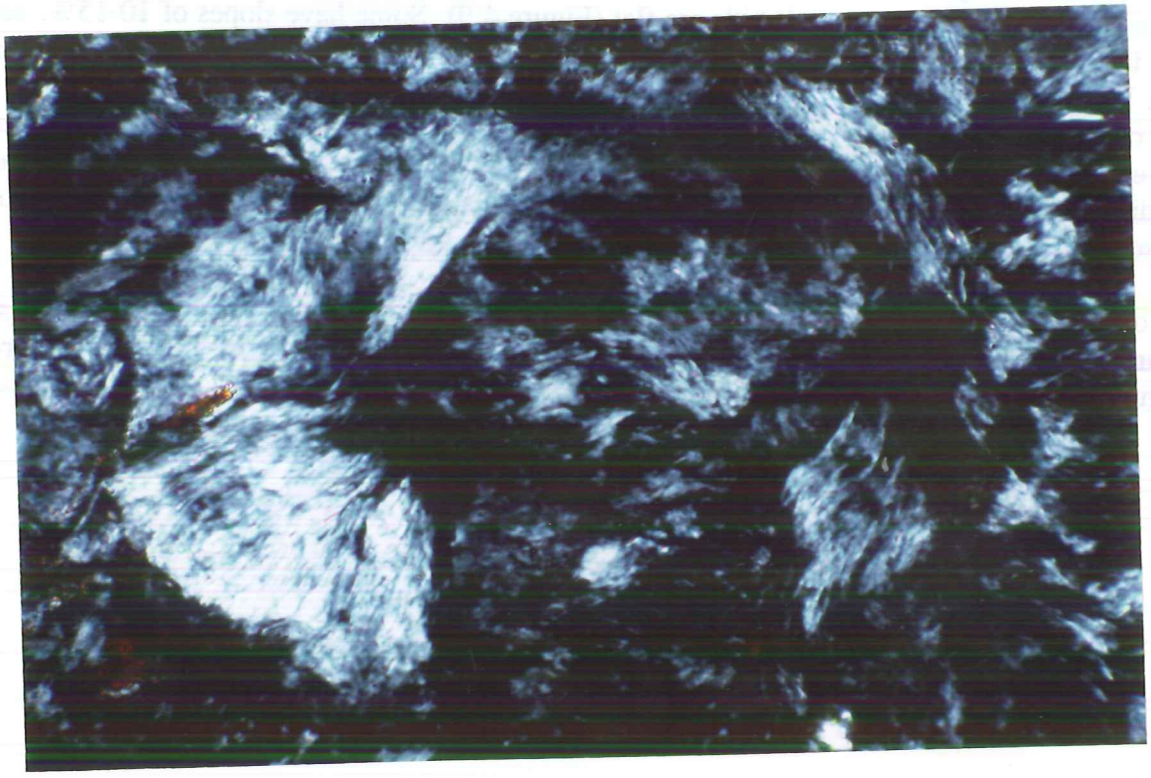

Figure 4.8 Newly formed 'booklets' of kaolinite.

Figure 4.9 Hill covered by a flat iron crust

The iron stone crusts in the project area differ in height, shape, size and state of erosion. The large crusts near Kaya, all on red schists, are slightly tilted in one direction and have a height of up to 10 meters. Those on small hills are flat (Figure 4.9). Some have slopes of 10-15%, and are up to 30 meters high. The last group consists of low 'terrace' iron stones, usually found at or just below the surface. This type of iron crust is found on red schist and on granite. In a trench of the railway under construction even a "burried" iron crust with a wavy appearance was observed (Figure 4.11). Also the rate of erosion strongly differs for one crust to the other. That, depending on the landscape, the process of plinthite formation, as explained before, may result in these various forms of iron crusts will be explained below (McFarlane, 1976).

-Part of the iron in highly located crusts is transported downwards, either in solution or mechanical, where it forms a new 'bottom' laterite (Figure 4.10). The laterite, mentioned before, of Figure 4.11 could be an example of such laterite.

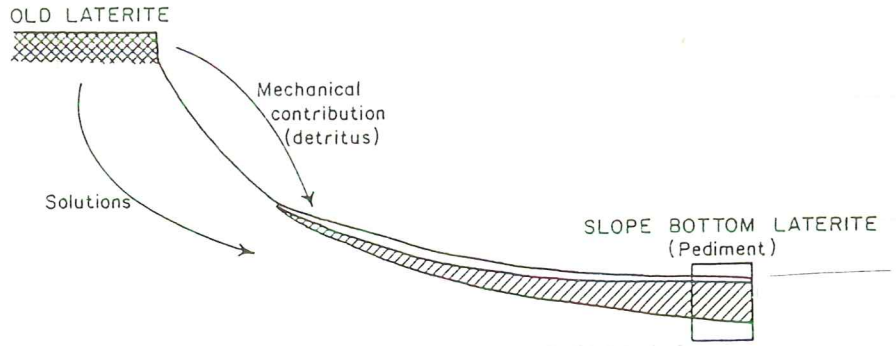

Figure 4.10 Formation of 'bottom' laterite

Figure 4.11 'Bottom' laterite along the railway line under construction near Kaya

-By erosion of the soil, covering plinthite formed on a slope, the concentrated iron is exposed and hardens on dessication. On the upper slope, where no iron precipitated, the soil erodes away, leaving a tilted iron crust with a valley behind its highest part (inversion of the landscape; Figure 4.12);

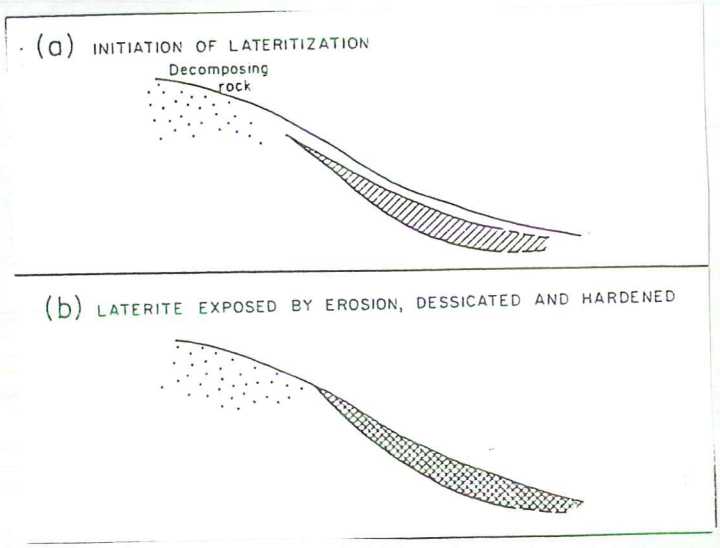

Figure 4.12 Iron crust affected by inversion of the landscape (After Clare, 1960)

-During their development on large peneplains there have always been places with poorly developed iron layers. At places with permanent water not any development occured. These places of weakness could easily erode, forming a strongly incised landschape of separate irregular, both in form and height, iron crust plateaus (iron crust development by incision; Figure 4.13).

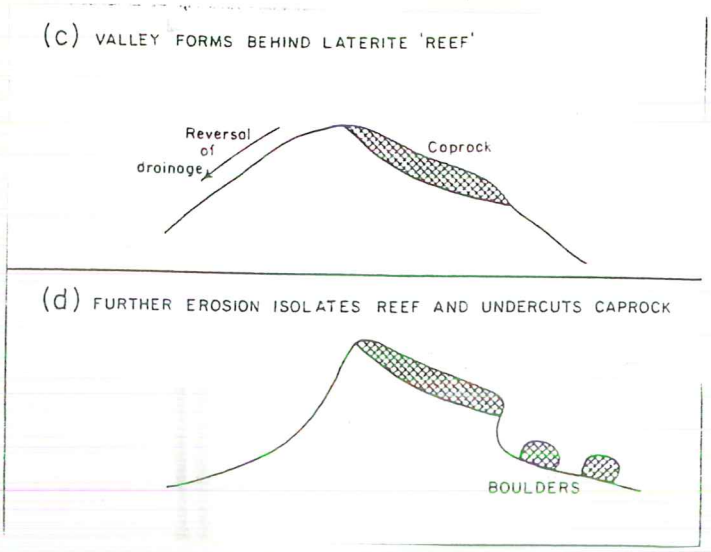

Figure 4.13 Iron crust formation by incision (After Clare, 1960)

The presence of smectites and chlorites, with swelling and shrinking properties, in soils formed on green schist indicate richer soils than those formed on granites or red schists. This is in accordance with the preference of farmers for soils formed on soils of the Dacola group over those of the large peneplains, which have been formed on granites and contain low amounts of lime (Ducellier, 1963). Soils formed on granite but located in the vicinity of hills on different parent material can produce decent crop yields by nutrients being transported from higher areas by drainwater. The granitoid soils are coarser textured than the rest and their subsoils, with high sodium contents, are very sensitive for erosion. Soils formed on red schist-, have an intermediate fertility.

4.3 Soil mapping units

The FAO-Unesco soil map of the world (FAO, 1977), using the Legend of the Soil map of the world (FAO-Unesco, 1974), gives only three soil units for the study area. These, their associated soils and inclusions are:

Soil unit	Associated soils	Inclusions
Lfl8	Re	
Lg9	Bv, Ql	Re
Re33-1 a		

In which:
Bv= vertic Cambisols
Lf= ferric Luvisols:
severely weathered soils well saturated with cations and poor in organic matter. Their fertility depends on texture, iron content and the possible presence of a shallow petroferric horizon (=iron stone)
Lg= gleyic Luvisols: poorly drained Luvisols Qi= luvic Arenosols
Re= Regosols: dunes

The given parent materials, being Basement complex with granitic gneiss, schist, quartzite (to the North and East), Precambrium (Birrimian) with schist, quartzite and greenstone (to the West) and a combination of Basement complex and Cambrian, the latter with sandstone, tillite and minor limestone (around Kaya itself) more or less correspond with the information given in the previous paragraph.

This study resulted in a Reconnaissance soil map (Figure 4.14) of which an extended legend is given below. For the soil description the 'Guidelines for soil description (FAO-ISRIC, 1990) and for the classification the FAO-Unesco Soil map of the world legend (FAO-Unesco, 1988) have been used.

LEGEND

Soils developed on Granite and granodiorite (G)

Plateaus

GPhc Flat to slightly sloping, high level plateau with very shallow soils, directly on continuous, very hard iron stone of up to 300 cm thick, bare with scattered trees and patches of grass, severe run-off, very low water holding capacity, excessively drained; very low agricultural value; where subject to severe erosion they transfer to units GP. f and GP.g; Leptosols.

GPmc Similar to GPhc but at an intermediate level; profile 93-4.

GPbc Similar to GPhc but at a low level.

GPhf Flat to slightly sloping, high level plateau with mostly very shallow, slightly hard and firm, sticky and slightly plastic, very fine sandy loam, with common, medium iron nodules on non continuous, very hard iron crust; 10% of the surface consists of iron stone, 50% is covered with gravel or is bare and 40% is covered with grasses and thick shrubs; slightly hard thin surface crusts; most water is captured in cracks, locally severe run-off, low water holding capacity, severe sheet erosion, excessively drained; only valuable for very extensive rangeland and (limited) production of firewood; Leptosols and some Cambisols.

GPmf Similar to GPhf but at an intermediate level

GPbf Similar to GPhf but at a low level

GPhg Flat to slightly, sloping, high level plateau of gravelly sandy loam, mostly covered with gravel originating from desintegrating iron stone crust; less than 10% is covered with iron crust bolders; scattered patches of grass and shrubs; severe run-off and water erosion, excessively drained, low water holding capacity, extensive grazing; Cambisols, some Leptosols.

GPmg Similar to GPhg but at an intermediate level.

GPbg Similar to GPhg but at a low level.

GPbx Low complex of gravelly, stoney, rocky or deep loamy soils. On the latter, if not very gravelly, millet and sorghum are grown; Cambisols, some Leptosols.

Slopes

GH Rather steep slopes often covered with bolders and stones of desintegrated iron crust, mostly covered with grasses and shrubs; slow internal and a moderately to rapid external drainage resulting in a rapid run-off and erosion, the latter shown by the presence of some gully and common rill erosion; Cambisols.

Valleys

GVg Flat to nearly flat, deep, slightly gravelly loamy sand to sandy loam soils that in most years stay moist below 100 cm for a period of six months; more than 50% of the surface is covered with gravel and less than 10% with bolders, both originating from desintegrating iron crust; slightly hard thin sealing; moderately rapid internal drainage, moderately rapid run-off, somewhat excessively to well drained; moderate agricultural value; millet fields mixed with extensive grazing; Fluvisols, Cambisols.

GVb Flat to nearly flat, deep, brownish yellow to strong brown, soft, friable, slightly sticky and slightly plastic sandy loam to sand, with less than 10% of surface covered with coarse fragments, at places including lime concretions, below 100 cm the sandy soils are moist for nearly six months in most years unless strongly eroded and sealed, pH-H_2O 1:2.5 between 6.5 and 7.0, increasing with depth to very high levels indicating the presence of sodium salts; higher agricultural potential than GVg; millet and scattered trees; Fluvisols, Cambisols; Profile 92-2.

GVx Flat to rolling, deep, well drained, complex of gravelly, stony, boldery, rocky and deep loamy sand to sandy loam soils often with severe gully erosion; Fluvisols, Cambisols; Profile 92-4.

Soils developed on Red schist (= less metamorphized than green schist) (R)

Plateaus

RPhc Flat to slightly sloping, high level plateau with very shallow soils directly on continuous, very hard iron stone of up to 300 cm thick, bare with scattered trees and patches of grass; severe run-off, very low water holding capacity, excessively drained; very low agricultural value, where subject to severe erosion they transfer to units RP.f and RP.g; Leptosols; Profile 93-2.

RPmc Similar to RPhc but at an intermediate level.

RPbc Similar to RPhc but at a low level.

RPhf Flat to slightly sloping, high level plateau with mostly very shallow, slightly hard and firm, sticky and slightly plastic, very fine sandy loam on non continuous very hard iron crust; 30% of the surface consists of very hard iron stones, 60% is covered with gravel or is bare -often with slightly hard thin surface sealing- and 10% is covered with grasses and thick shrubs; locally severe run-off, severe sheet erosion, excessively drained although most water is captured in the cracks between the iron crusts, low water holding capacity, only valuable for very extensive rangeland and (limited) production of firewood; Leptosols and some Cambisols.

RPmf Flat to slightly sloping, medium level plateau with mostly very shallow soils of slightly hard and firm, sticky and slightly plastic, very fine sandy loam, with common, medium iron nodules; shallow on continuous, very hard iron crust; 25 % is occupied with very hard iron crust, 55% with medium gravel and the rest with scattered shrubs and sparce grasses; severe sheet erosion, slightly hard thin surface crusts, excessively drained, rapid run-off, extensive grazing; Leptosols and Cambisols; Profile 93-3.

RPbf Similar to RPhf but at a low level.

RPhg Flat to slightly sloping, high level plateau, with no rock outcrops, and gravel and bolders,

both originating from desintegrating iron crusts, covering respectively more than 50 % and less than 10 % of the surface and 15 % bare patches; in most cases the soil is gravelly; severe erosion, moderately slow internal drainage, external drainage slightly ponded, sometimes some surface sealing; vegetation of shrubs, grasses, millet and some sorghum; Cambisols and some Leptosols.

RPmg Similar to RPhg but at an intermediate level

RPbg Similar to RPhg but at a low level

RPbx Flat to slightly sloping, low level plateau complex of gravelly, stony, boldery, rocky, hardened ironstone or deep multi-coloured, gravelly sandy loam soils with subsoils of silty weathered schist. On the latter, with pH-H_20 1:2.5 values of 6.2-6.6, millet and sorghum are grown; soils (5YR 4/6) are (somewhat) excessively drained; severe sheet erosion but no sealing has been observed, slow to rapid rapid run-off; Leptosols and Cambisols.

RPbp Flat and slightly sloping, low level plateau, of which more than 10% of the surface is covered with stones, e.g. quartz and schists, not originating from iron crust; Cambisols, Leptosols.

RPmb Flat to slightly sloping medium level plateau, for less than 50% covered with coarse fragments and < 10% covered with rocks, the surface can be strongly sealed, at places severe gully erosion, scattered to medium dense vegetation and sorghum fields; Cambisols, Lixisols.

RPbb Similar to RPmb but at a low level

Slopes

RH Rather steep slopes often covered with bolders and stones of surfacing quartz veins and schist bedrock, sometimes bare but mostly covered with grasses, shrubs and millet; slow internal and moderately rapid external drainage resulting in a rapid run-off and moderate erosion, the latter shown by the presence rills and some gullies; Leptosols, Cambisols.

Hills

RLh High longitudinal hills, oriented in two global directions -mostly NW-SE-, very shallow soils directly on hard rock, steep slopes with little vegetation of grasses and small shrubs, rapid run-off, in many places strongly folded, many in vicinity and parallel of 'manganese' outcrops (units MLh/m/b); Leptosols.

RLm Similar to RLh but of a medium level

RLb Similar to RLh but of a low level

RJh High, often covered with up to 3m thick very hard iron crust, with very steep, bare slopes with dominant rock (iron stone and red schist) outcrops, with dominant surface coarse fragments of all sizes, moderate rill erosion, no surface sealing, no surface cracks, excessively drained, slow hydraulic conductivity, rapid run-off, no flooding; Leptosols; Profile 93-2.

Valleys

RVx Complex of gravelly, stony, boldery, rocky or deep loamy soils with various vegetation covers; Fluvisols, Cambisols.

RVg Flat to nearly flat, deep, slightly gravelly, strong brown, soft, firm, sticky and plastic very fine sandy loam to loamy sand soils with respectively > 80 % and less than 10 % of surface covered with coarse gravel and bolders, both originating from desintegrating iron stone crust, few patches are not covered with coarse fragments; a moderate rill erosion has removed most of the A-horizon, somewhat excessively drained with a rapid run-off, some flooding; pH-H_2O 1:2.5 is between 6.0 and 6.5; extensive grazing and some millet; Fluvisols, Cambisols.

RVp Flat to nearly flat, deep, stony, strong brown, soft, firm, sticky and plastic very fine sandy loam to loamy sand soils of which more than 10% of the surface is covered with stones e.g. quartz or schist, excluding remnants of iron crust; Cambisols, Fluvisols, Lixisols.

RVb Flat to nearly flat, deep, stony, dark brown to strong brown, soft, very friable, slightly sticky and slightly plastic, very fine sandy loam to loamy, sometimes slightly gravelly sand soils of which > 50% of the surface is not covered with coarse fragments and less than 10% of the surface is covered with stones, no rock outcrops; grass, peanuts, millet; slightly sealed surface, usely there is a transition zone between soils without coarse fragments at the surface and those covered with gravel. These areas consist of soils with an over-wash of gravel over non gravelly soils; no erosion; slightly hard, thin surface sealing; well to somewhat poorly drained -shown by the presence of pseudogley concretions-, moderately rapid internal drainage, no flooding; pH-H_2O 1:2.5 is 5 at surface to 6 at 120 cm; Cambisols, some Fluvisols; Profile 92-3 and Profile 93-5.

Soils developed on green schist (S)

Plateaus

SPmp Nearly flat to slightly sloping, intermediate level plateau; moderately deep soils covered with grasses, schrubs, arable fields and rangeland; few rock outcrops of quartz veins, abundant coarse fragments of greenschist and locally quartz stones of various sizes, slight sheet erosion, no surface sealing, few fine surface cracks; well drained; no flooding; very fine sandy loam; slightly hard to soft; friable to very friable; slightly sticky and slightly plastic; Regosols and few Leptosols.

Hills

SJh High hills, covered with grasses, schrubs and arable fields with a stony surface (40%-80%), shallow soils; confex slopes, rangeland and extensive farming, few rock outcrops of quartz veins, abundant coarse fragments of various sizes, slight sheet erosion, no surface sealing, few fine surface cracks; somewhat excessively drained; no flooding; pH-H_20 1:2.5 is 6.8; 5Y 4/6 to 4/3 (moist) very fine sandy loam with depth changing to silt; slightly hard to soft; friable to very friable; slightly sticky and slightly plastic; Leptosols and few Regosols.

SJm Similar to SJh but at an intermediate level

SJb Similar to SJh but at a low level

SLh High longitudinal hills parallel and in vicinity of units ML and RL, covered with grasses, shrubs and some arable fields, with a stony surface (40%-80%), shallow soils; confex slopes, rangeland and extensive farming, few rock outcrops of quartz veins, abundant coarse fragments of various sizes, slight sheet erosion, no surface sealing, few fine surface cracks; somewhat excessively drained; no flooding; 7.5YR 4/4 to 5G 7/1 (dry) and 5Y 4/6 to 4/3 (moist) very fine sandy loam with depth changing to silt; slightly hard to soft; friable to very friable; slightly sticky and slightly plastic; Leptosols and eutric Regosols.

SLm Similar to SLh but at a medium level

SLb Similar to SLh but at a low level

Valleys

SVg Similar to SVp (see below) but with a gravelly surface; Regosols.

SVp Gently undulating, gently sloping, yellowish brown to light olive brown (1OYR 5/4 and - 2.5Y 5/6) when moist; apedal; hard, sticky and plastic clay loams with very few rock outcrops, common stones, no erosion, no surface sealing, few fine cracks, slow infiltration rate, moderately slow hydraulic conductivity, slow run-off, extensive farming, moderately rich soil; eutric and vertic Regosols; Profiles 93-1 and 92-1.

SVb Similar to SVg but with a surface not covered with coarse fragments; more than 50% of the surface is not covered with coarse fragments and less than 10% is covered with stones; slightly sealed surface; the texture is sandy loam at the surface and loamy at around 120 cm. At the surface the pH is 4.9 and increases to 6 in the subsoil. There often is a transition zone between SVg and SVb consisting of overwash of gravel over SVb; (nearly) flat, straight slope; no rock outcrops; no erosion; slightly hard, thin surface

sealing; somewhat excessively drained, moderately rapid internal drainage, no flooding; pH-H_20 1:2.5 is 5 at surface to 6 at 120 cm, 7.5YR 5/8 (dry) 4/4 (moist) very fine sandy loam sometimes with few fine iron crust fragments, soft, very friable, slightly plastic and slightly sticky; Regosols, Cambisols.

Outcrops of manganese rocks (M)

Hills

MLh High, longitudinal, very stony hills, parallel or in vicinity of unit RLh, with up to 17% MnO and very shallow soils directly on hard rock, at places inclusions of graphite rocks (e.g close to Lake Dem) are found; high run-off, no infiltration, bare soils, no vegetation; Leptosols.

MLm Similar to unit MLh but at an intermediate level

MLb Similar to unit MLh but at a low level

Valleys

MVp Moderately deep, stony and gravelly, brownish yellow to yellowish red (1OYR 6/6, - 7/5YR 4/6) when moist, non sticky and slightly plastic sandy loams mainly covered with grasses between the many (> 50 %) surface stones, moderate infiltration capacity, moderate gully and rill erosion; Regosols.

Alluvial soils (B)

B Flat to nearly flat, very deep loamy to very fine sandy soils of which more than 50% of the surface is not covered with coarse fragments and less than 10% of the surface is covered with stones; slightly sealed surface, deeper soil layers stay moist during at least four months in most years; pH-H_2O 1:2.5 around 6; dense vegetation of large trees and shrubs; moderate high agricultural potential with sorghum, sometimes maize, ocra and peanuts; Fluvisols.

5. REMOTE SENSING

5.1 FIELD AND LABORATORY REFLECTANCE

In this chapter the main results of study to field and laboratory reflectance in relation with surface characteristics of soil and vegetation are given. Soil surface and vegetation characteristics have been described in the field for the different locations as a whole (see Table 3.1) and for the specific plots. On the specific plots, coverage and type of vegetation, and coverage and type of surface material have been described. Three types of samples have been taken: loose sandy material from the top layer, crusts and gravel/stones (Appendix 5.1 gives an overview). The samples were taken from the different geologic zones and the plateaus. They were analyzed using X-ray fluorescence and X-ray diffraction, while also Carbon and free iron were determined. For crusts both undisturbed samples for determination of laboratory reflectance and bulk samples for the different soil analyses have been taken.

First results of field reflectance measurements with the mini-IRIS are described (Chapter 5.1.1 - 5.1.3). It turned out that only the part up to 1000nm gave reliable results. In chapter 5.1.3 problems with the mini-IRIS will be analyzed in more detail. Results of laboratory reflectance measurements, covering the spectrum from 700-2500nm, are presented in chapter 5.1.4. In this chapter (and more extensive in Appendix 5.2-5.4) also the various soil analyses are given.

5.1.1 Spectral differences between major soil and vegetation types

Reflectance is a function of the characteristics of objects. Scatterplots, in which reflectance at two different wavelengths are compared, can be a good way to separate the different objects.

A useful scatterplot to separate bare soils from vegetation is a comparison of reflectance of red and near infrared. In figure 5.1 a scatterplot between red (651.81nm) and near infrared (NIR, 829.93nm) reflectance is shown. The shrubs can be discriminated from bare soils by their relatively high NIR reflectance and low red reflectance.

The reflectance of most grasses is in between reflectance of bare soils and shrubs. For green grasses a NIR/red ratio comparable to shrubs would be expected. However, almost all measurements were taken at the beginning of the dry season, when the grasses turned yellow. Another reason for the intermediate position of grasses is the not-complete coverage. Therefore, also bare soils influence the total reflectance. This influence depends on soil type and coverage percentage by grasses.

A large variation in reflectance of bare soils exists. The reflectance of bare soils is influenced by factors such as mineralogy, organic matter, particle size and roughness, moisture and Fe content. The effect of these factors will be evaluated extensively in chapters 5.1.3 and 5.1.4. It can be observed already that the following groups can be discriminated with increasing reflectance: ironstone surfaces (called laterite in figure 5.1), sandy surfaces, crusts and kaolin areas. The low reflectance of iron stone is caused by Fe absorption. Crusts have, in average, a higher reflectance than sandy surfaces, probably because of their relative smoothness.

Kaolin, not shown in figure 5.1) has the highest reflectance because of low Fe and organic matter content. Quartz stones show a high reflectance, especially a relatively high red reflectance.

It has to be noted that a spectral distinction between grasses and crusts may be sometimes difficult in comparing red and NIR reflectance.

Besides differences in red and NIR reflectance it has been examined if also other parts of the spectrum show distinct differences between major soil and vegetation types.

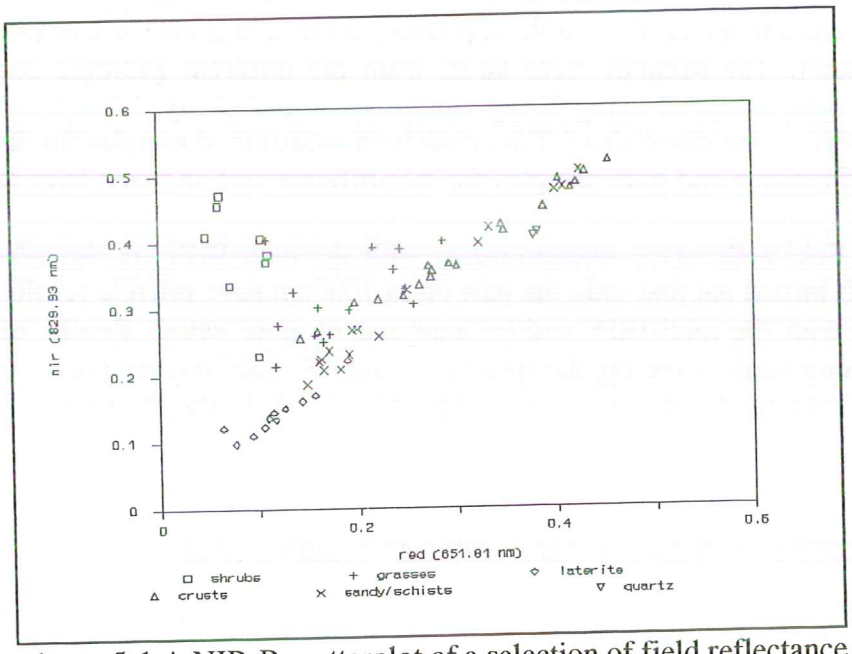

Figure 5.1 A NIR-R scatterplot of a selection of field reflectance measurements.

In figure 5.2 and 5.3 spectral curves of five typical objects are shown: (1) a green shrub (Combretum micranthum, coverage 85%), (2) dry, yellow grass (a combination of Aristida spp., Schoenefeldia gracilis and Pennisetum reticulatum, coverage 90%) and (3) a bare soil dominated by iron stone, (4) a crust and (5) a kaolin surface.

By examining differences in the visible and NIR reflectance (figure 5.2) the following can be observed. The green shrub, which represents a healthy vegetation, has a low reflectance in the visible part of the spectrum and a high reflectance in the NIR part. Low reflectance in the visible is caused by chlorophyll absorption in the blue and red part. The reflectance in the green part is relatively high. In the NIR no such absorption exists and therefore the reflectance is relatively high. The NIR reflectance is a function of the number of leaf layers and orientation of the leaves, moisture content and structure. As a rule one may state that about 50% is reflected by every leaf and 50% is transmitted by cell walls and intracellular structures. Dry, yellow grasses show much higher reflectance in the visible part and no peak in the green part of the spectrum. The rise in the visible part is gradual due to non-complete chlorophyll absorption. Grasses can be distinguished from ironstone by their higher reflectance in the NIR part. The distinction between yellow grass and crusts, which is difficult comparing only red and NIR, can be made in observing blue and green reflectance.

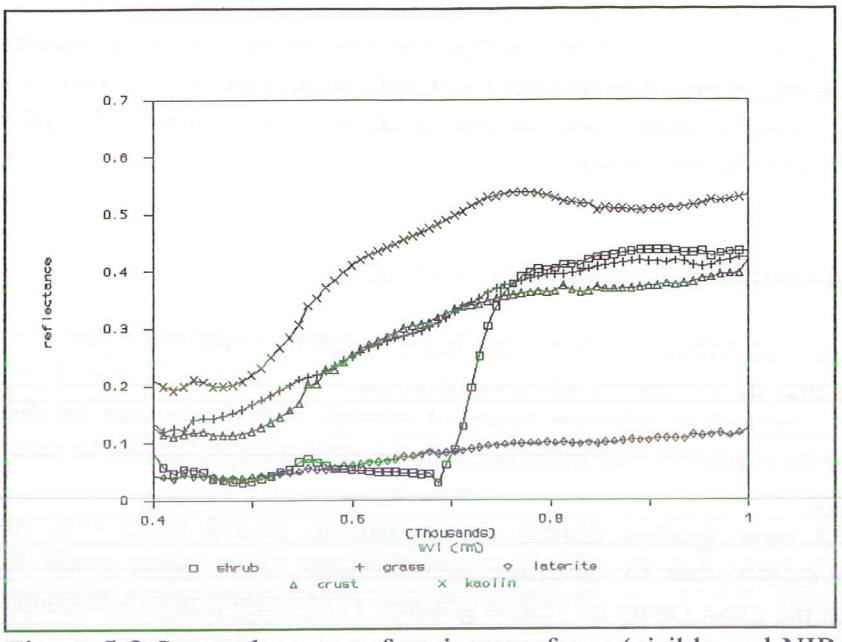

Figure 5.2 Spectral curves of various surfaces (visible and NIR part).

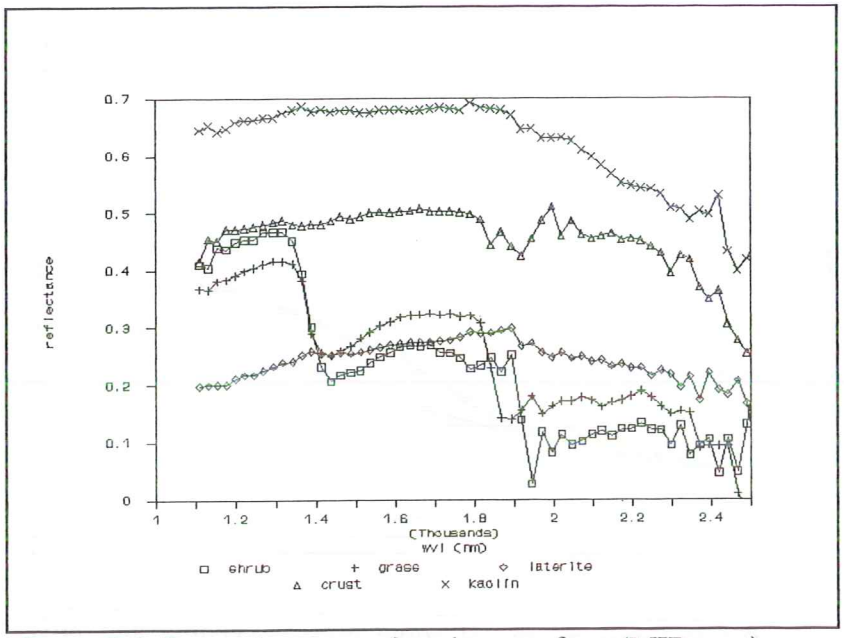

Figure 5.3 Spectral curves of various surfaces(MIR part)

The reflectance of grass is relatively higher than the crust. The low blue and green reflectance of the crust is possibly caused by Fe absorption. Kaolin is easily discriminated from other surfaces by its relatively high reflectance.

In the middle infrared part of the spectrum (MIR, 1000 - 2500nm, figure 5.3) interpretations are somewhat hampered by the problems of the mini-IRIS. The signal to noise ratio turned

out to be worse than expected (see also chapter 3.2 and 5.1.3). In this example spectra are selected which are not saturated. The reflectance of vegetation show a relatively low MIR reflectance in comparison with the NIR. In this way vegetation can be discriminated easily from bare soils. The reflectance dips around 1400 and 1900nm are well known by absorption of features of water. They influence also the rest of the MIR. The noise in the spectra is such that no other water dips can be located.

5.1.2 Spectral characteristics of various shrubs and grasses

In chapter 5.1.1 spectral differences between major vegetation and soil types are examined. It was also shown that in November shrubs and grasses can be discriminated spectrally. In this chapter it is examined if different types of grasses and shrubs can be discriminated spectrally. In order to minimize soil influence, the investigation is limited to plots with high vegetation coverage.
Spectral curves of most grasses during the measuring period were very much alike. Differences were mainly due to coverage and biomass. Two types could however be discriminated from the great group of yellow grasses: (1) Cymbopogon schoenanthus, which shows a peak in the green part of the spectrum because of its relatively greenness at the time of measurement, and (2) Schizachirium exile, which has a red appearance in the dry season. In figure 5.4 these two grasses are compared with Brachiaria lata, which was, like other grasses, yellow at the time of measurement.

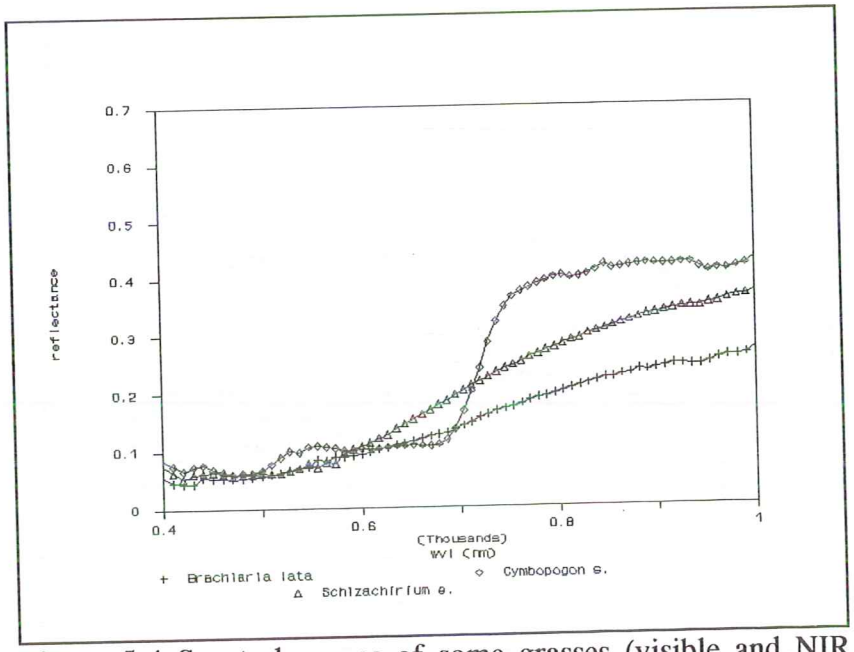

Figure 5.4 Spectral curves of some grasses (visible and NIR part).

The spectral curves of a relatively green and a red/brown shrub (Guiera senegalensis, 70%, and Combretum micranthum, 70%) differ, too. Figure 5.5 shows that the green shrub has a clear peak in the green part of the spectrum.

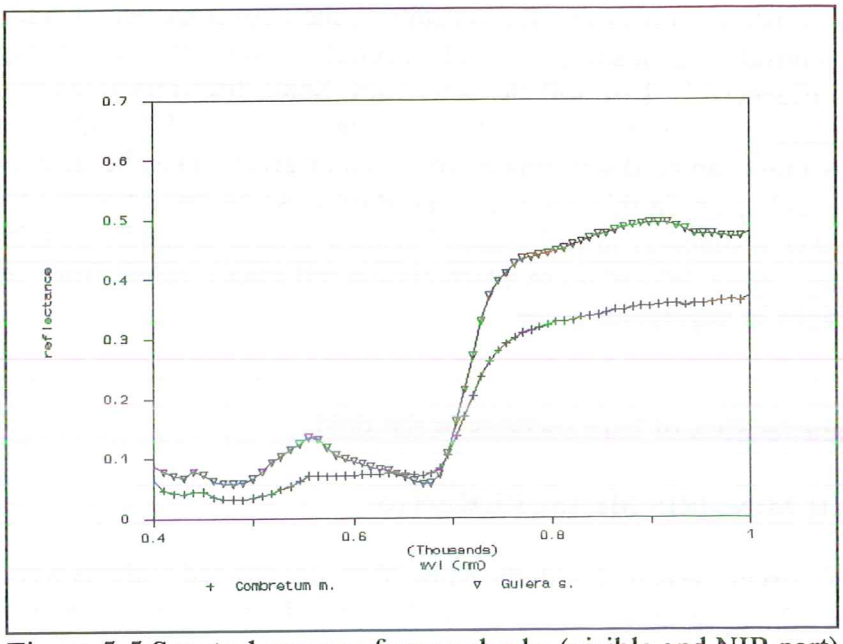

Figure 5.5 Spectral curves of some shrubs (visible and NIR part)

In a scatterplot of different shrubs between red and green reflectance dry, brown shrubs are distinguished from fresh, green shrubs (figure 5.6), due to this peak in the green part.

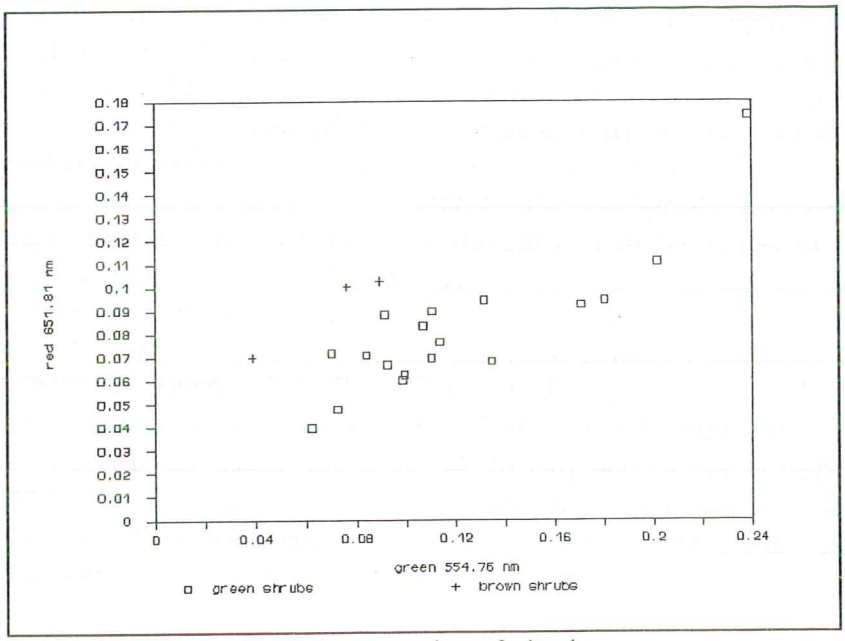

Figure 5.6 A red-green scatterplot of shrubs

A green grass is discriminated from a green shrub by lower green and higher red reflectance of the grass (compare figure 5.4 and 5.5). The shape of the reflectance curve of the grass resembles that of a brown shrub, but is somewhat higher.

Concluding, some major soil and vegetation types can be discriminated relatively easily on their spectral characteristics. Concerning the vegetation, their coverage percentage is of great importance when considering scatterplots and spectral curves. When coverage is low reflectance is also influenced by bare soil characteristics. Some discriminations can be made, however: green grasses and shrubs can be discriminated due to a different green and red reflectance. Yellow grass can be discriminated from red or green grass, because of different reflectance in the visible part. In this manner green shrubs can be discriminated from brown shrubs, too. A further distinction in reflectance between species is hardly possible. Due to these results one may expect difficulties in interpretation reflectance values from satellite data due to large variations in vegetation cover.

5.1.3 Spectral characteristics of bare surfaces in the field.

PROBLEMS WITH MINI-IRIS MEASUREMENTS

Examining spectral curves measured with the Mini-IRIS, unexpected features were observed:
1) high spikiness of the reflectance curves above 1000nm, both using grating 1 and 2. This spikiness was too much to observe specific absorption features, which can be expected for bare soils in the range from 1900 - 2500nm.
2) in most curves, using grating 1, so measuring the whole spectrum, a jump exist between measurements of the first part of the spectrum and the second part.
3) strongly increasing reflectance values above 1000nm with increasing sun elevation.

In Figure 5.7 two examples of reflectance curves (1st grating) are given. Curve A represents a rather smooth curve, while curve B is a more average curve. In curve B the spikiness is clearly visible. The very high spikiness above 1900nm is due to the low amount of incoming radiation in this part of the spectrum. Spikiness using the second grating is still higher. The jump in the curves is visible in both curves and will be due to calibration differences and to saturation in the signal with high sun elevations.
Figure 5.8 shows reflected radiance of the reference panel in two bands throughout the day, one representative for the first part of the spectrum (400 -1000nm) and one for the second part of the spectrum. For the first part reflected radiance increases in time. In the second part of the spectrum reflected radiance does not increase any more after 10 o'clock in the morning. One would normally expect however that reflected radiance increases more or less equally for the total spectrum (Epema, 1992). One may therefore conclude that saturation of the sensors occurred in the second part of the spectrum. Since the signal of the reference panel is higher than of that the target, this saturation will occur already with lower solar elevations for the panel. This will give a too high reflectance in the second part of the spectrum after 10 o'clock and explains also largely the observed jump between the two parts of the spectrum.

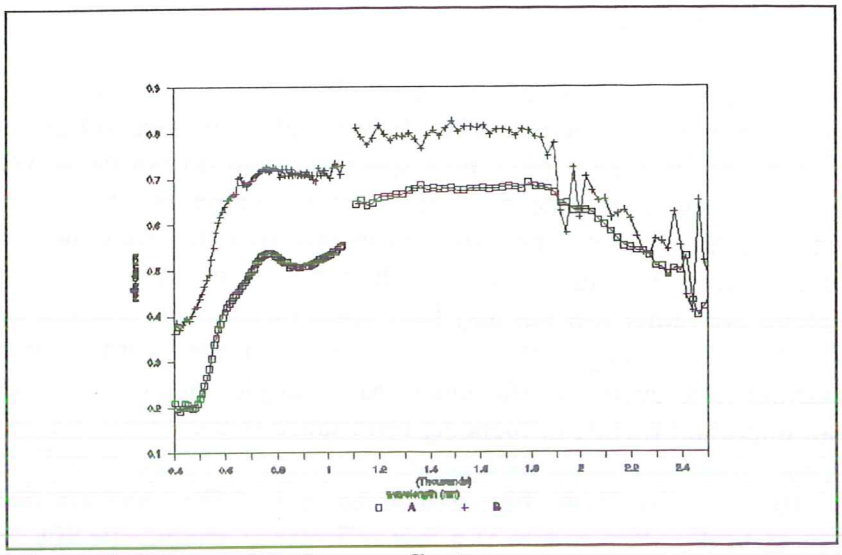

Figure 5.7 Example of two reflectance curves.

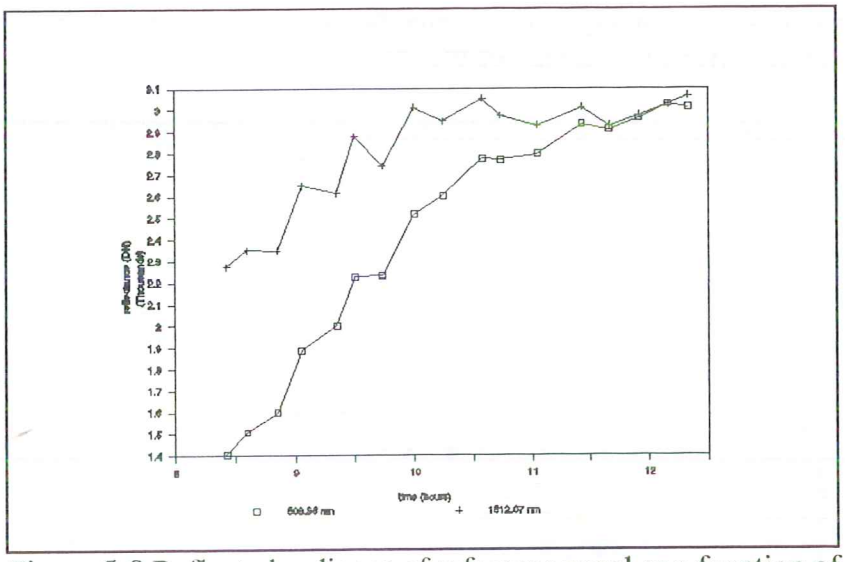

Figure 5.8 Reflected radiance of reference panel as a function of time of the day (day K).

Due to the unreliable results of the second part of the spectrum, the interpretation of the spectral curves measured in the field will be limited to the first part of the spectrum. Absorption features in the second part of the spectrum will be examined using laboratory measurements (chapter 5.1.4).

REFLECTANCE OF BARE SURFACES

Reflectance of bare surfaces is determined by: 1) roughness, 2) organic matter content, 3) moisture content and 4) mineralogy (Asrar 1989). In the visible and near-infrared part of the spectrum factors 1-3 mainly influence the whole spectrum, and do not cause very specific absorption features. Increases in roughness, organic matter content and moisture content all cause a decrease in reflectance. It can be expected in this area that roughness is the most important of the three factors. Moisture content of the top layer is almost always negligible. Organic matter contents are rather low but may have some influence. Variation in roughness between smooth crusts, loose sandy material and surfaces covered with stones can be an important factor causing differences in reflectance. Mineralogic composition, especially the amount of iron is an important factor, influencing reflectance in the visible and near-infrared part of the spectrum. Iron has three effects on reflectance: 1) an overall decrease in reflectance, 2) an extra decrease in the blue and green part of the spectrum due to a very strong absorption band in the ultra-violet, 3) a low reflectance around specific wavelengths due to specific absorption due to different electronic processes. Location and depth of these dips is related to presence of ferri- or ferro ions, type of iron-mineral, goethite or hematite, but also to the exact position of iron in the minerals. In literature a range of absorptions dips are given. Asrar (1989) mentions two large absorption features for ferric iron at 700 and 870nm and two weaker dips at 400 and 550nm. According to Grove et al (1992) the absorption features of goethite are centred at 503, 932, 665, 972nm, while for hematite absorption features are present at 535, 868 and 884nm. Asrar (1989) and Mulders (1987) give additional and slightly different locations of the dips.

Based on the various effects of the factors influencing bare soil reflectance, both variation in overall reflectance and specific absorption features have to be examined.

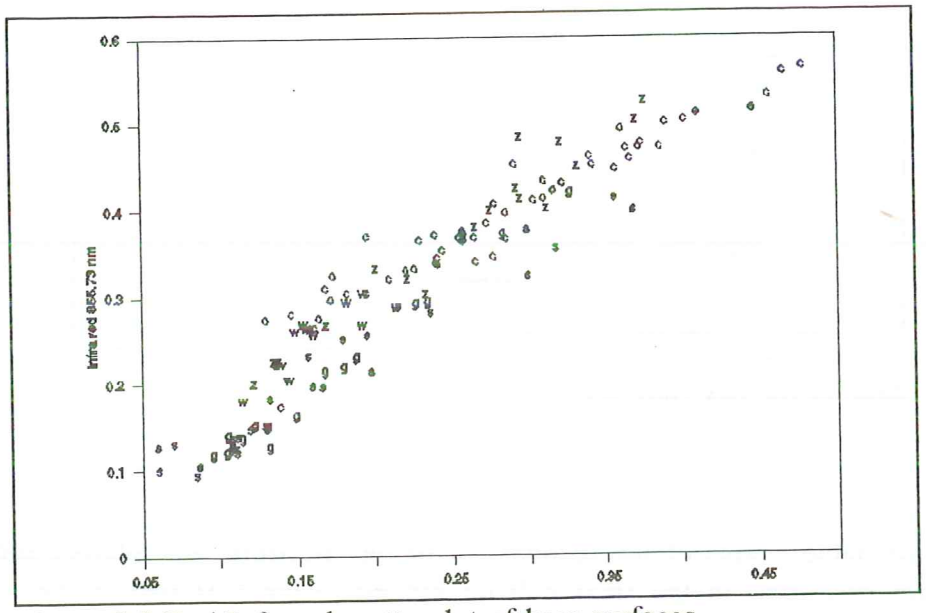

Figure 5.9 Red-Infrared scatterplot of bare surfaces.
(s = stones g = gravel c = crust z = sand e = kaoline)

In order to obtain an overview of the reflectance characteristics of all measured soil surface groups, a red-infrared scatterplot is made. The bands 599.56nm and 855.73nm proved to be most suitable to discriminate the different bare soil surface measurements (figure 5.9). The figure shows that despite large variation within some classes, main groups can be discriminated. Gravel and stones have a low reflectance due to the fact that these are often consist of iron-rich material. Stones with lower iron contents show a higher reflectance. It is striking however that all gravel and stones have a relatively low near-infrared reflectance, due to a strong dip around 850nm. The large overlap between the classes "sand" and "crust" is due to the variations in iron content and roughness and will be examined in more detail in looking to specific curves. Also some of the variation may be due to small differences in organic matter content. Kaolinitic material and some sandy samples contain almost no iron and organic matter and therefore show the highest reflectance.

In the following the variation in spectral curves of the different surface types (parent material, gravel, crusts, sandy material and kaolinitic material) will be examined. They have all in common an increase in reflectance from blue to red. This is a general feature of all bare surfaces and is due to the fact that all samples contain some iron. This causes a large absorption in the ultra-violet which also influence the blue and green part of the spectrum (Asrar 1989).

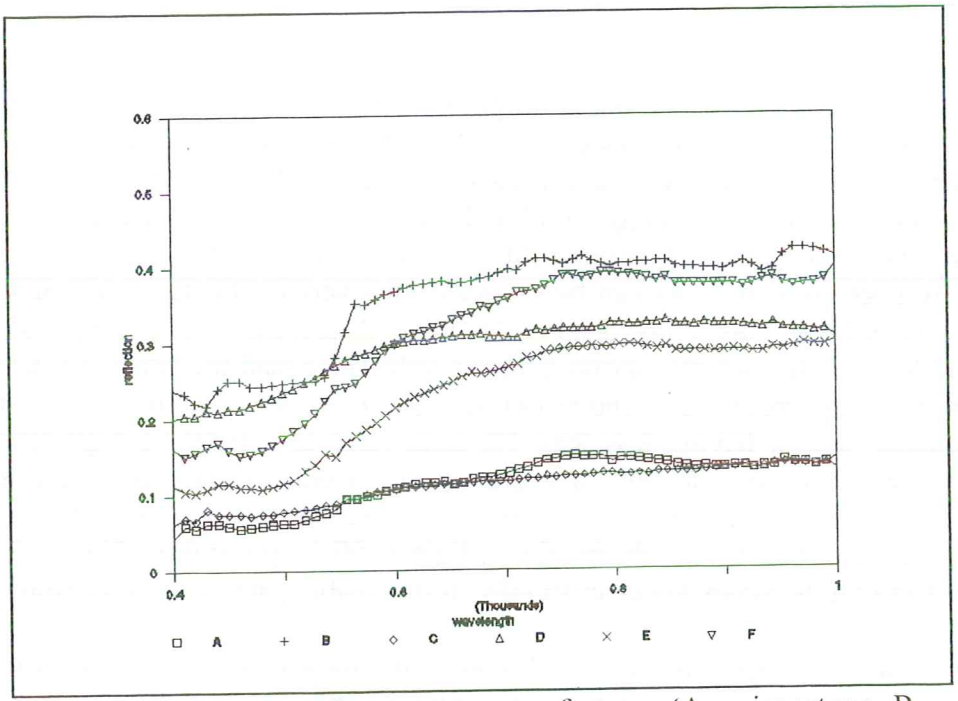

Figure 5.10 Spectral reflectance curves of stones (A = ironstone, B = quartz stone, C = black manganese stone, D = granite stone, E = red weathered granite, F = quartz stone).

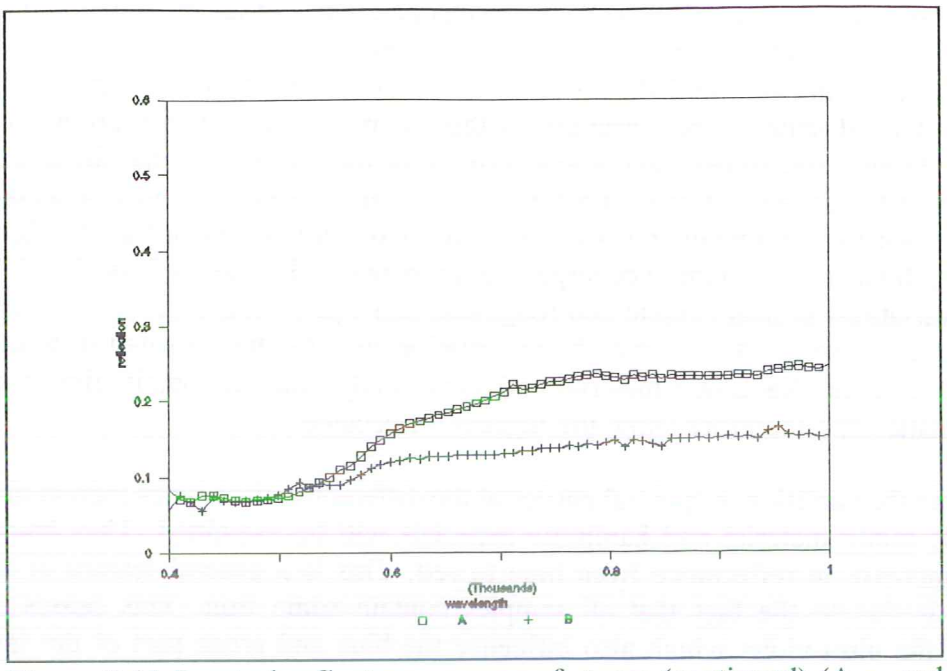

Figure 5.11 Spectral reflectance curves of stones (continued) (A = red schist,B = green schist).

In figures 5.10 and 5.11 spectral curves of parent material, stones with some weathering and ironstone material derived from the plateau caps are shown. In order to perform these measurements in the field, sometimes artificial stone surfaces had to be made. The lowest overall reflectance has been found for ironstones and black manganese stones. The low reflectance of ironstones is due to strong absorption by iron (iron percentage ranges from 35-70%). Three different absorption dips can be seen. The curve of manganese can be easily separated from ironstone since no specific dips are present. Green schist and red schists having respectively an iron percentage of 15 and 30% have a somewhat higher reflectance. Green schists show no specific absorption dips, while red schists have a strong increase in reflectance from green to red. As can be expected the overall reflectance of red schists is higher than greenschists. This can be due to other minerals present. Granitic material, having high iron and low quartz contents, shows a higher reflectance than the other two dominating geological formations: greenschists and redschists. Quartz stones occurring in the same area as the manganese stones, having less than 1% iron, have as expected a high reflectance. Despite this low percentage of iron, a characteristic strong increase from green to red reflectance can be observed for quartz. This is due to iron which is present in a specific way and which gives also with visual observation a light reddish appearance. Upon weathering reflectance of granite becomes lower especially in the visible part of the spectrum.

In figure 5.12 different spectral curves of gravel are shown. The four curves of gravel derived from ironstones still show distinct iron features. It has to be noted that curve A and B are most representative for gravel derived from ironstones. The weathered redschists show relatively lower reflectance values in the near infrared. The chalk concrete (see chapter 4 for a description of their origin) show no distinct features in this part of the spectrum and has a high reflectance.

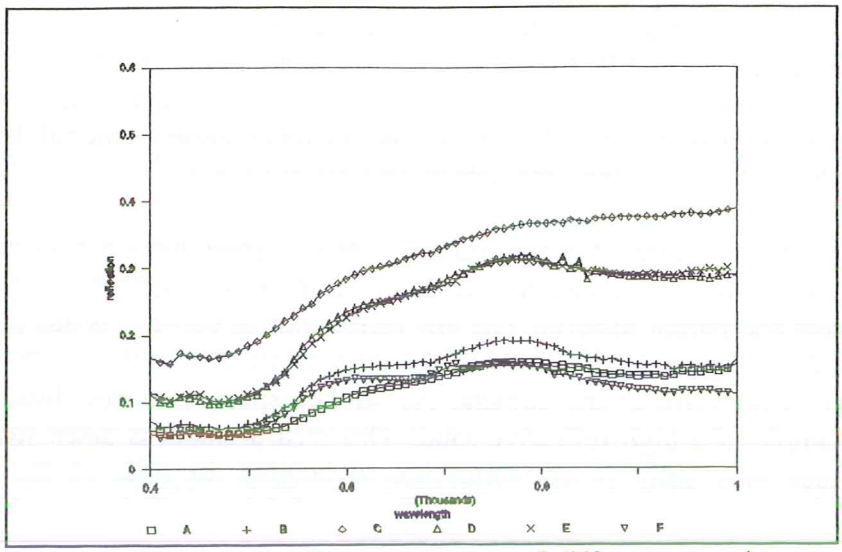

Figure 5.12 Spectral reflectance curves of different gravel types. (A = ironstone gravel, B = yellow ironstone gravel, C = chalk concrete, D = yellow laterite gravel, E = red laterite gravel, F = gravel derived from redschist).

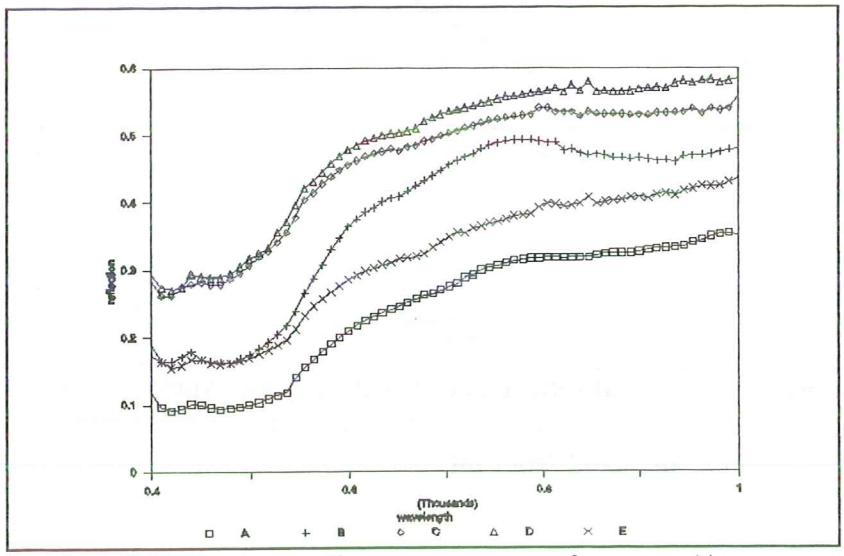

Figure 5.13 Spectral reflectance curves of crusts. (A = crust from agricultural field, B = erosion crust (B), C = curly crust,'decantation', D = light crust, E = algae crust 60%).

In figure 5.13 reflection curves of 5 types of crusts are shown. Curve B, measured on a location, where the top layer has been eroded, show a distinct different curve. This may be due to absorption by iron. It has to be noted however that this measurement has been taken on a very hazy day, which produced strange curves for a lot of surfaces. The other four crusts show no distinct features. The reflectance increases from a crust developed in a field (actually a sealed surface), via a crust covered partially by a thin layer of algae to a curly crust (clayey material) and a very bright greyish crust. The material in the agricultural field has probably a higher iron and organic matter content than the other crusts. Algae are known

for their low reflectance (Epema 1992). Most crusts in the area outside the agricultural fields show curves comparable to A and B, having comparable high or somewhat lower reflectance values. Differences in amount of reflectance are due to variation in roughness, organic matter content, iron content and parent material. Having other factors constant material derived from granite have a higher reflectance than red schists and green schists.

Figure 5.14 shows three spectra of sandy surfaces. Most curves have a reflectance curve comparable to B. Variation is due like for crusts to variation in roughness, organic matter content, iron content and parent material.The low reflectance of curve C is due to the parent material. This sand was taken from a hole in the greenschist area and consists of directly weathered material, with a low quartz content. As can be expected no iron dips are visible. Curve A is an example of a high reflective sand. This measurement is taken from a rather rough sandy surface in a gully (5 cm difference in height). In spite of the roughness, reflectance is high.

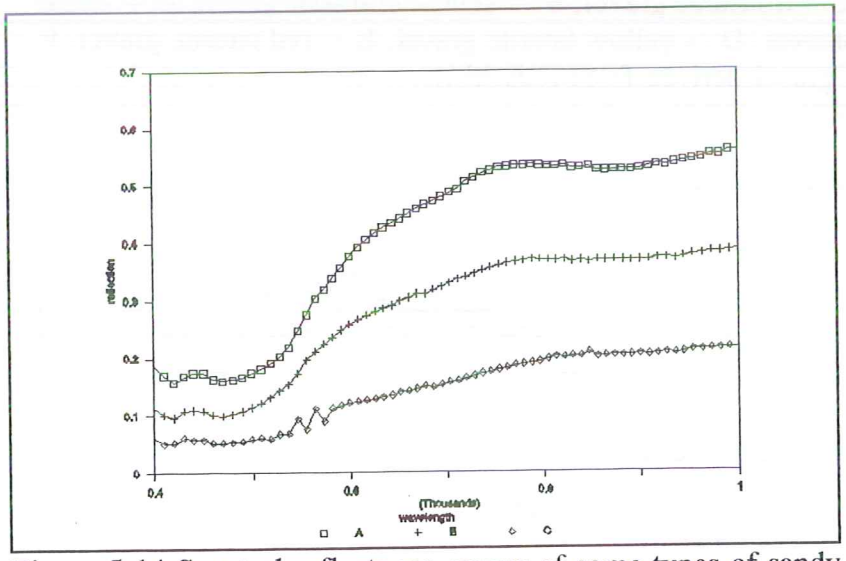

Figure 5.14 Spectral reflectance curves of some types of sandy material (A = sandy material from a gully, B = sandy surface, C = green schist sand from pit).

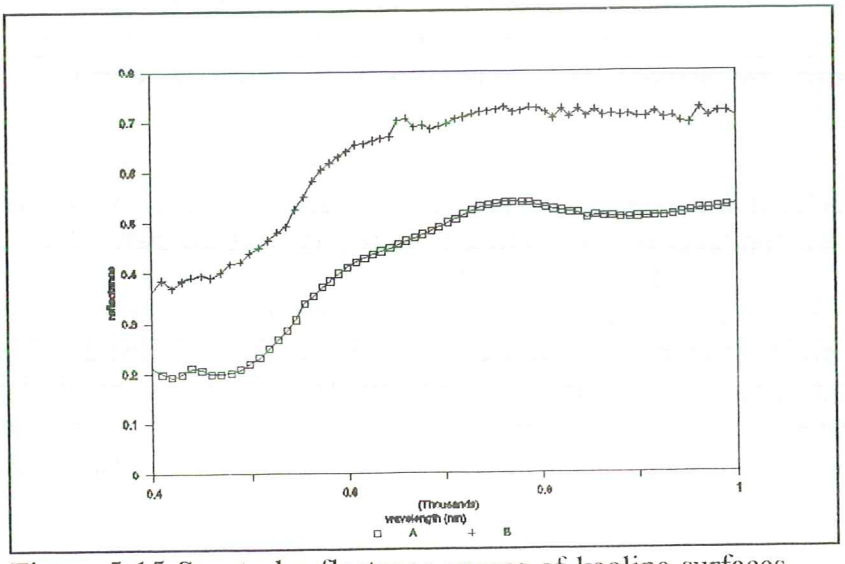

Figure 5.15 Spectral reflectance curves of kaoline surfaces.

In figure 5.15 two spectral curves of kaolinitic material are shown. They both have a high reflectance due to almost absence of iron and organic matter. According to Grove et al (1992) kaolinic material has small absorption dips around 500 and 900nm. It is unclear if the dips visible in curve B can be ascribed to kaolinite or to the presence of some iron.

5.1.4 Analysis of laboratory reflectance spectra for soil surface characteristics.

During the field campaign three types of samples have been taken for subsequent analysis: loose sandy material from the top layer, crusts and gravel/stones. The samples were taken from the different geologic zones and the plateaus. They were analyzed using X-ray fluorescence and X-ray diffraction, while also Carbon and free iron were determined. For crusts both undisturbed samples for determination of laboratory reflectance and bulk samples for the different soil analyses have been taken. First results of different analyses are presented followed by a visual and digital analysis of the spectra (using a specially developed program). Since the used laboratory reflectance measurements cover the spectrum from 700-2500nm, they are complementary to the field measurements.

RESULTS OF X-RAY FLUORESCENCE

All field samples are examined on 11 components: SiO_2, TiO_2, Al_2O_3, MnO, MgO, CaO, Na_2O, K_2O, P_2O_5 and BaO. In addition the loss on ignition (L.o.I.) is measured, which is the amount of weight loss after glowing the sample at 600 °C. L.o.I. can be a measure for the percentage of organic material, but it is strongly influenced by Fe_2O_3. Since the samples show a large variation in Fe_2O_3 content, L.o.I. is not considered in the further analysis. Appendix 5.2 gives an overview of the results of X-ray fluorescence. The main results are resumed below.

Contents of SiO_2 and Al_2O_3 are very variable for the six different types of stones: green schist, red schists, ironstones, granite, quartz and black manganese. Al_2O_3 range from almost zero (quartz stones), to 12% for schists and 15% for granites. Ironstones have an even higher percentage. Fe_2O_3 contents show also a high variability: stones derived from ironstones range from 35% (yellow coloured material) to 70%; redschists 25%, greenschists 13%, granites 5% and quartz almost 0%. Granite samples, having a low iron percentage, contain rather high amounts of MgO, CaO, Na_2O and K_2O.

All sand samples have high contents of siliciumoxide (average 88%) and low contents of aluminumoxide (average 3%). The percentage of SiO_2 in crusts is smaller than that in sands ($\pm$75%). Al_2O_3, Fe_2O_3, MgO, CaO and K_2O are more abundant in crust samples than in sand samples. Both samples of sandy material and crusts of the granite area have higher SiO_2% and a lower Al_2O_3 and Fe_2O_3 content than samples taken in the schist area. Fe_2O_3, MgO and CaO content are especially high for material in the greenschist area, while the contents in the red schist area are somewhat lower. Granite has the lowest amount of Fe_2O_3, MgO and CaO. The relative high K_2O values for sand samples can be explained by the surroundings. Both samples (EP12 and EP19) are derived from small sand dunes within an erosion area dominated by sealed more clayey material. K_2O is probably an element of secondary clay. The sand sample, taken from Niger for reference, is comparable to the granite sands. Although EP9 and EP13 are classified as sandy crusts, their mineralogy is comparable to the loose sands. The crusting of these samples is limited to just a sealing of the surface.

RESULTS OF X-RAY DIFFRACTION

In appendix 5.3 results of X-ray diffraction are presented. Stones have a much larger variation in mineralogy than sands and crusts. Goethite and hematite are found in both redschists and ironstones, but not in granite and the other stones. More reddish colours point to hematite, yellow colours to goethite. Especially the ironstones have large contents of goethite and hematite. Presence of goethite and hematite in greenschists could not shown by this method. Aluminium containing minerals were found for some ironstone samples (boehmite and gibbsite). Greenschist stones have a high content of plagioclase and amphibole, a small amount of epidote and in some samples a little chlorite. Yellow schist holds, besides a large amount of goethite, also anatase. This is a mineral which is found in highly weathered material.
Yellow schists are therefore not considered as a separate geological formation, but only as a weathering product. Granite holds a moderate percentage of quartz and of feldspars (orthoclase and plagioclase), and it also contains amphibole and a little mica. Black manganese stones of the resistant band contain quartz and spessartite. As can be expected no other minerals than quartz are found for quartz stones.

The mineralogical composition of sand is mainly quartz. Quartz is left over after weathering. Granitic sands hold a small amount of kaolinite, produced by the chemical breakdown of feldspars. Epidote and smectite are found in the greenschist samples (the origin is explained in chapter 4.3). Crusts have more or less the same minerals as sands. Crusts only contain more kaolinitic clay, due to secondary mineral enrichment. This higher clay content is sometimes clearly visible in the field. Curly crusts ("croute decantation"; EP20) and greenschist crusts show cracks due to the swelling and shrinking smectite.

RESULTS OF OTHER ANALYSES

In appendix 5.4 free iron and organic carbon of the samples are given. Loose sands and some eroded surfaces have the lowest organic carbon contents. Carbon percentages for crusts and sand range between 0.1 and 0.8%. Highest percentages have been found in some agricultural fields in the south-western part (greenschists) of the study area (1-3%). Relation between free iron content and Fe2O3 determined by X-ray fluorescence is not very straightforward.

VISUAL INTERPRETATION OF REFLECTANCE CURVES FOR SOIL SURFACE CHARACTERISTICS.

In this chapter a selection of laboratory spectra will be discussed. With the laboratory instrument spectra could be achieved between 700nm and 2500nm with a bandwidth of 3nm. Since height of samples varied, especially for stones, it was impossible to put every sample at the same height in the instrument. Therefore it is impossible to compare the overall intensity of the stone samples, while also for crusts and sands heights were not always comparable. Therefore, especially in the discussion on spectra of stones, emphasis is laid on location of absorption dips, which are reliable.

Most spectacular absorption dips have been found for ironstone samples (Figure 5.16). a strong absorption dip is present close to 900nm, dips at 1400 and 1900nm and around 2200nm. The first dip is due to goethite and hematite. A differentiation can be made between yellowish ironstone, having mainly goethite, with a dip centred at about 870nm and reddish

ironstones, mainly hematite, with a dip just above 900nm. This difference between the 2 minerals has also been given in Goetz (1989). The combined absorption dip at 2150 and 2200nm is due to kaolinite (Goetz 1989). The absorption dips around 1400 and 1900nm are found in almost all bare soil curves and stones. These are due to OH^- or H_2O (Goetz 1989). For these curves they can be due to goethite, hematite or kaolinite, having all OH^-.
Spectra of schists and granites show in general much smaller dips than the ironstone samples. Stones which are not weathered show the smallest dips. It is difficult to separate small dips from variation due to instrumental errors. However there seem to be absorption dips near 2300nm, which can be ascribed to epidote or chlorite. These minerals have both absorption dips at 2250 and 2330nm. Chalk concretes show a clear absorption dip near 2330nm.

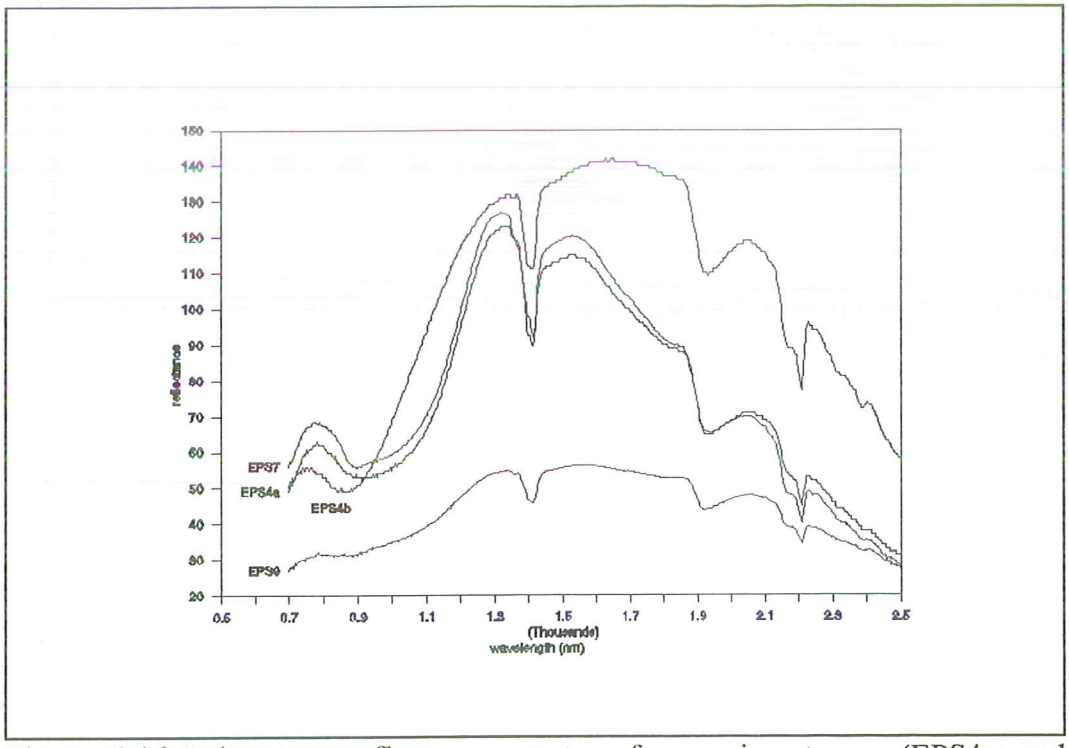

Figure 5.16 Laboratory reflectance spectra of some ironstones. (EPS4a: red coloured ironstone, EPS4b yellow coloured ironstone, EPS7: yellow-red ironstone, EPS9:black ironstone)

In figure 5.17 and 5.18 examples of some spectra of sands and crusts are given. Location of dips are comparable to those found in ironstones, schists and granites. Depth of the dips is between those found for ironstones and those of granites and schists. They are also a function of the mineralogical variation. Remarkably average depths of dips of crusts and sand are hardly different. This can be explained by the chemical analyses, which also show not too large differences.

26)24 pdf

FIG. 4.14

SOIL MAP / CARTE DU SOL, KAYA, BURKINA FASO

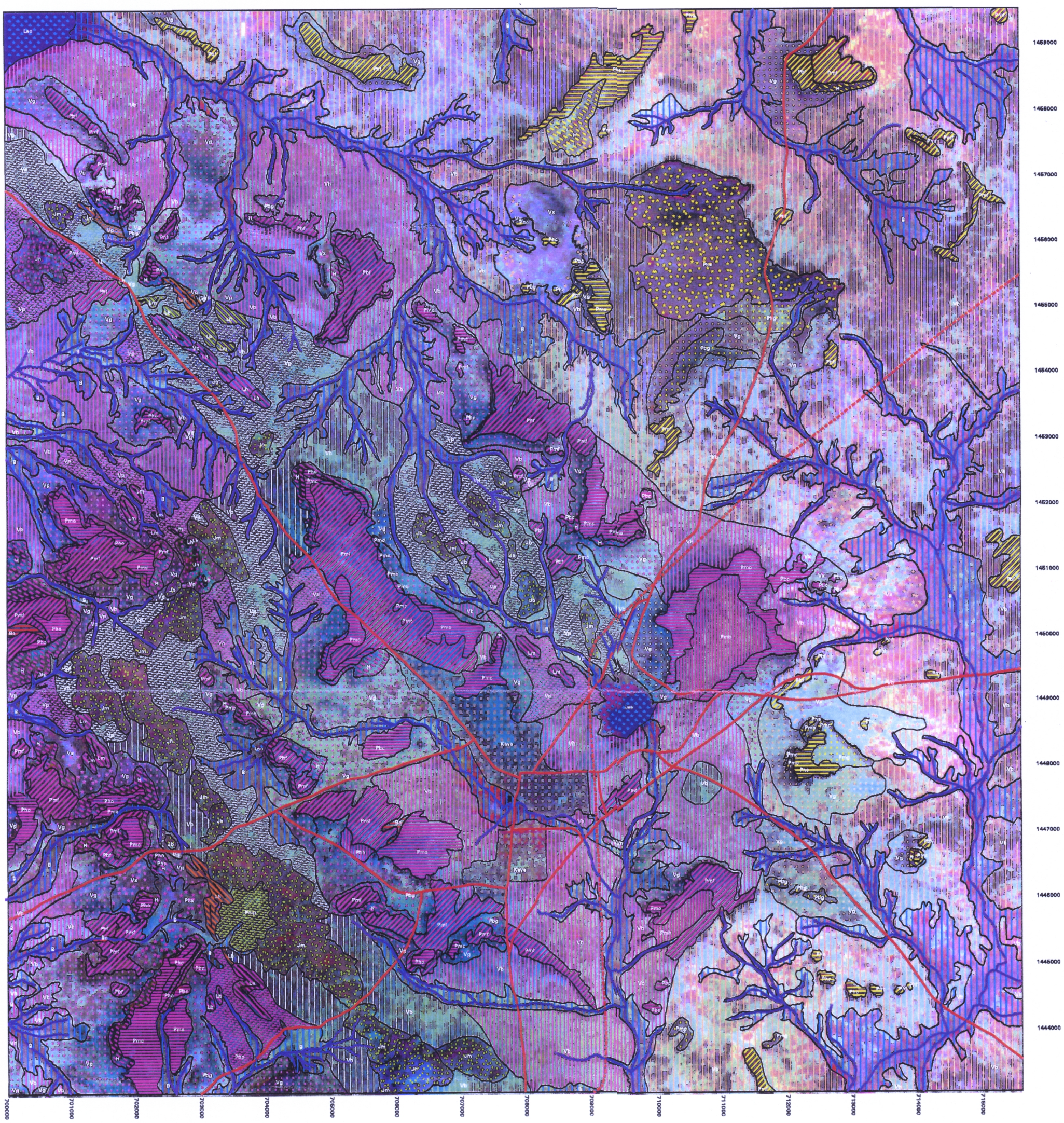

LEGEND / LEGENDE

.h. = high / haute
.m. = middle / moyenne
.b. = low / bas

ANTENNE SAHELIENNE

Image: Landsat-TM, band 4 of May 7, 1988 and band 7 and 2 of January 8, 1991 (RGB)
Fieldata: November and December, 1993
Cover: Digitized with ARC-INFO 6.2

E.M. Elkenbracht, A. ten Holte, D. Legger
Department of Soil science and Geology
Agricultural University of Wageningen
May 1994

GRANITE and/et GRANODIORITE

- P.c Plateau,ironcrust/ Plateau cuirasse
- P.f Plateau,fragmented/Plateau fragment
- P.g Plateau,gravelly / Plateau gravier
- P.x Plateau,complex / Plateau complex
- H Slope / Pente
- Vx Valley,complex / Vallee complex
- Vg Valley,gravelly / Vallee gravier
- Vb Valley,bare / Vallee nue

RED SCHIST / SCHIST ROUGE

- P.c Plateau,ironcrust/ Plateau cuirasse
- P.f Plateau,fragmented/Plateau fragment
- P.g Plateau,gravelly / Plateau gravier
- P.x Plateau,complex / Plateau complex
- P.p Plateau,stony / Plateau pierre
- P.b Plateau,bare / Plateau nue
- H Slope / Pente
- L. Longitudinal hills / Alignement des buttes
- J. Hill / Colline

- Vx Valley,complex / Vallee complex
- Vg Valley,gravelly / Vallee gravier
- Vp Valley,stony / Vallee pierre
- Vb Valley,bare / Vallee nue
- Bc Valley bottom,ironcrust / Bas fond cuirassee

MANGANESE

- L. Longitudinal hills / Alignement des buttes
- Vp Valley,stony / Vallee pierre

GREEN SCHIST / SCHIST VERTE

- P.p Plateau,stony / Plateau pierre
- J. Hill / Colline
- L. Longitudinal hills / Alignement des buttes
- Vg Valley,gravelly / Vallee gravier
- Vp Valley,stony / Vallee pierre
- Vb Valley,bare / Vallee nue

ALLUVIUM

- B Valley bottom / Bas Fond

ADDITIONAL SIGNES / SIGNES ADDITIVES

- Lake / Lac
- Kaya, town / Kaya, ville
- Escarpment / Escarpement
- River / Riviere
- Road / Route
- Railway / Ligne de chemin de fer

0 1000 2000 3000 m

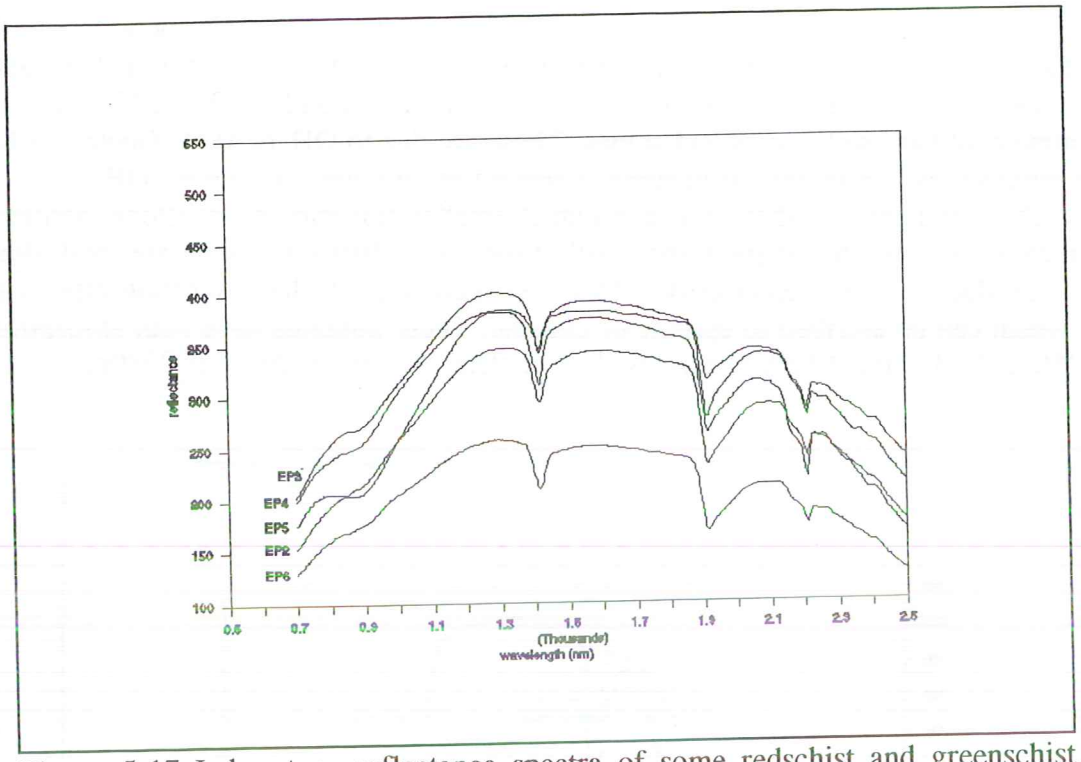

Figure 5.17 Laboratory reflectance spectra of some redschist and greenschist sands.

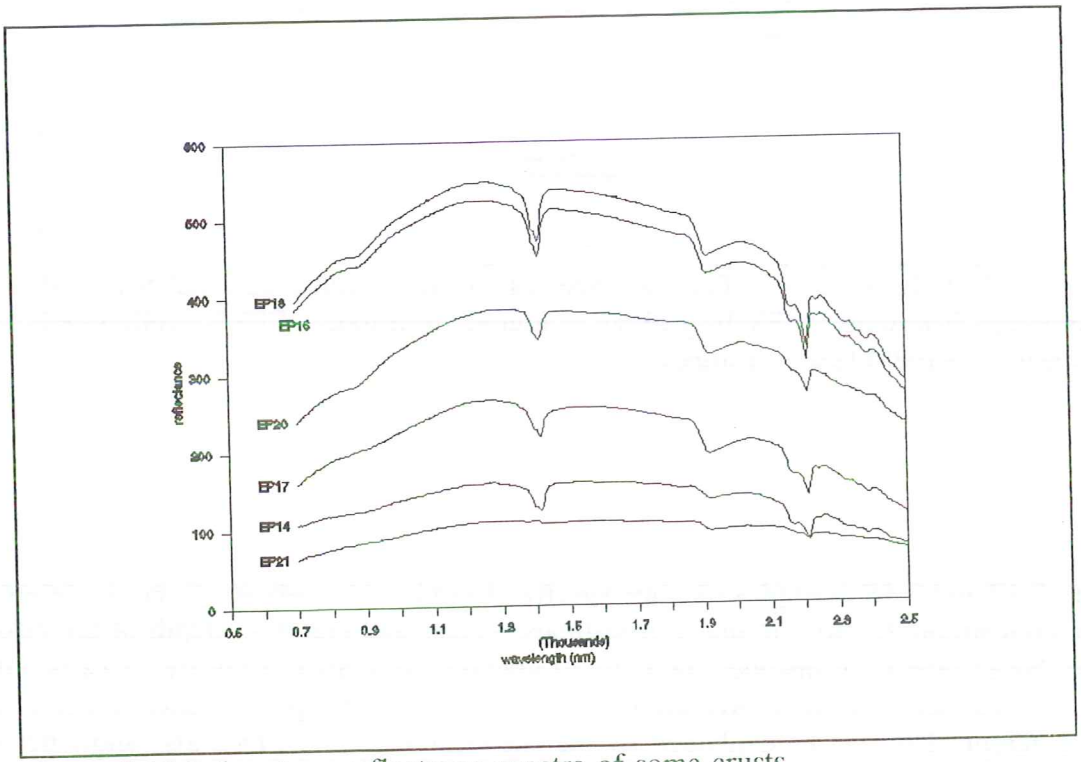

Figure 5.18 Laboratory reflectance spectra of some crusts.

QUANTITATIVE RELATIONS BETWEEN ABSORPTION DIP CHARACTERISTICS AND MINERALOGY

Using the program DISPEC location of the absorption dips can be determined using the hull difference. Hull difference is the difference between the background continuum of a spectrum and the real spectrum. Background continuum or hull is calculated by 'fitting a rubber band over' the spectrum. DISPEC first smooths the calculated hull difference before locating the absorption dips (Anonymous, 1991). The feature search is carried out on the total spectrum (0.7 - 2.5 μm). Search criteria used were: factor for smoothing is 1, minimum depth is set to 0.0001 and maximum number of dips to locate is 15. Results of the search are represented in appendix 5.5.

The relation between percentage iron in the samples and depth or area of the absorption feature around 900nm was examined. No significant relation between percentage of iron and absorption features in the crust, stone or sand curves.
Also the relation between the amount of kaolinite in the samples and the absorption features at 2200nm is examined. The kaolinite absorption feature is a combined dip; a small dip at 2150nm and a large dip at 2200nm (Asrar, 1989 and Grove et al, 1992). DISPEC only recognises the largest dip. Because the amount of kaolinite was not available in percentages, the average of absorption depth and areas of the absorption feature are compared to the qualitative amount of kaolinite (Table 5.1)

Table 5.1. Amount of kaolinite compared to area and depth of absorbtion features.

Type of samples	amount of kaolinite	number of samples	average depth of abs. feat.	average area of abs. feat.
crusts	+	2	0.0035	0.0408
	++	6	0.0053	0.0475
stones	±	1	0.0136	0.0025
	++	3	0.0161	0.0021
sand	±	6	0.0356	0.0025
	+	6	0.0489	0.0039

This table shows that absorbtion features of samples with a small amount of kaolinite are smaller than absorbtion features of samples with a high amount of kaolinite, although the differences between those absorption features are not large. The area of the stone samples absorption feature of the small amount of kaolinite is even larger than the average absorption feature area of samples with a large amount. According to the above results it seems that the shapes of the dips are different. The number of samples are however too limited to draw firm conclusions.

5.2 COMPARISON BETWEEN FIELD AND SATELLITE REFLECTANCE

Field spectra measured with the Mini-IRIS will be compared with spectra of Landsat 4 Thematic Mapper. The Mini-IRIS measures a continous spectra in the wavelengths from 389.25 to 2512.64 nm. The Landsat 4 Thematic Mapper measures only the signal in 6 broad bands (1-5,7) and a thermal band (6) (see table 2.1). In order to compare the spectra derived from the satellite and from the field the raw values have to be calculated to reflectance. In chapter 3.2 it has been described how mini-IRIS reflectance spectra were determined. For comparison reflectance spectra were simply integrated over the TM bandwidths. In this chapter the emphasis is therefore on a discussion on (1) the way to derive reflectance from satellite data and (2) a comparison between field and satellite reflectance.

CALCULATION OF AT-SATELLITE PLANETARY REFLECTANCE FOR LANDSAT 4 THEMATIC MAPPER

Available for this research were two Landsat 4 Thematic Mapper images of respectively 8 January 1991 and 7 May 1988.

The combined surface and atmospheric reflectance can be calculated by:

$$\rho_p = (\pi L_\lambda * d^2) / E_{sun,\lambda} \cos\theta_s \qquad (1)$$

where

ρ_p unitless effective at-satellite planetary reflectance
L_λ spectral radiance at sensor aperture in $mW.cm^{-1}.ster^{-1}.\mu m^{-1}$
d earth sun distance in astronomical units
$E_{sun,\lambda}$ mean solar exoatmospheric irradiances at mean earth-sun distance in $mW.cm^{-1}.\mu m^{-1}$
θ_s solar zenith angle in degrees

Spectral radiance can be determined if the bias ($A_{0\lambda}$) and gain ($A_{1\lambda}$) of the TM sensors are known:

$$L = A_{0,} + A_{1,} * DN \qquad (2)$$

The values of $A_{0,}$ and $A_{1,}$ can be derived in principle from the header information of the TIPS-processed tapes (Markham and Barker, 1985). However, biases and gains on the tape turned out to be wrong. These were actually minimum (B_{tape}) and maximum (G_{tape}) detectable radiance values to the DN range of o to 255 (pers. communication Altman and Collins, October 1993). To obtain biases and gains (in $mW.cm^{-1}.ster^{-1}$) the following equations should be used:

$$A_1 = G_{tape}/254 - B_{tape}/255 \qquad (3)$$

$$A_0 = B_{tape} \qquad (4)$$

To calculate $A_{0,\lambda}$ and $A_{1,\lambda}$ the values calculated in formula (3) and (4) should be divided by by the bandwidth:

$$A_{0,\lambda} = A_0/bw_\lambda \qquad (5)$$

$$A_{1,\lambda} = A1/bw_{\lambda} \quad (6)$$

where
bw_{λ} bandwidth in μm

For this type of processing (TIPS) the bandwidth has to be determined based on the fullwidth at Half maximum method. The bandwidth values were derived from Markham and Barker (1985).

The actual value of the distance earth-sun (d) was derived using the formula of Gurney and Hall (1983):

$$d = 1 + 0.0167 \sin(2\pi(D - 93.5))/365 \quad (7)$$

where
D day number of the year

The mean solar exoatmospheric irradiances were derived from Markham and Barker (1985). The sattelite overpass time was calculated by using formulas described by Verhoef (1989). For this time solar zenith angles on the 2 satellite overpasses were calculated using own developed formulas. The actual values were less than 2 degrees different from that given in the header information.

An overview of the parameters used in the calculations is given in Table 5.2 and 5.3.

Table 5.2 Parameters used in deriving at-satellite planetary reflectance from digital numbers for January 8, 1991 (see text for a description of parameters).

January 8, 1991	TM1	TM2	TM3	TM 4	TM 5	TM 7
B_{tape} ($mW.cm^{-1}.ster^{-1}$)	-.00439	-.01987	-.01094	-.02316	-.0059	-.00235
G_{tape} ($mW.cm^{-1}.ster^{-1}$)	1.009644	2.44842	1.39090	3.11424	0.64522	0.45634
bandwidth (μm)	0.066	0.081	0.069	0.129	0.216	0.250
d (AU)	0.983381	id. TM1	id. TM1	id. TM1	id. TM1	id. TM1
Esun ($mW.cm^{-2}.\mu m^{-1}$)	195.8	182.8	155.9	104.5	21.91	7.457

Table 5.3 Parameters used in deriving at-satellite planetary reflectance from digital numbers for May 7, 1988 (see text for a description of parameters).

May 7, 1988	TM1	TM2	TM3	TM 4	TM 5	TM 7
B_{tape} ($mW.cm^{-1}.ster^{-1}$)	-.00275	-.02048	-.01094	-.02370	-.00501	-.00241
G_{tape} ($mW.cm^{-1}.ster^{-1}$)	1.09644	2.44807	1.39050	3.11247	0.64583	0.45636
bandwidth (μm)	0.066	0.081	0.069	0.129	0.216	0.250
d (AE)	1.009105	id. TM1	id. TM1	id TM1	id. TM1	id. TM1
Esun ($mW.cm^{-2}.\mu m^{-1}$)	195.8	182.8	155.9	104.5	21091	7.457

REMARKS ON ATMOSPHERIC INFLUENCE

The incoming radiation of a satellite is not only influenced by the properties of objects at the earth surface but also by the atmosphere. A schematic overview of atmospheric influence is given in figure 5.19. In the atmosphere four processes occur before radiation from the sun reaches the earth surface: radiation is absorbed, scattered back into space, scattered forward in direction of the earth or is transmitted by the atmosphere directly to the earth surface. At the surface, radiation will be reflected. The kind of reflection depends on surface characteristics such as roughness and chemical contents. Reflected radiation from the surface is again influenced by the atmosphere (absorption, scattering and transmittance) before it reaches the satellite sensors. Planetary reflectance is the radiation reflected by atmosphere and earth surface. In figure 5.19 the atmosphere is simplified to two layers: the ozone layer and the troposphere. In the first layer transmission of radiation is determined by absorption, it affects radiation in downward and upward direction. In the troposphere, besides absorption, scattering also occurs. Due to scattering, a part of the radiation is reflected back to the ozone layer. The rest of the radiation is scattered diffusely to the earth. This diffuse radiation is also reflected back diffusely by objects on earth. Radiation coming direct from the sun (transmitted by the atmosphere) is also reflected direct by the earth.
Different approaches exist to correct for the atmospheric influence. However no data of atmospheric condition were available. Moreover no clear deep water bodies exist in the area, which can be assumed to have zero ground reflectance. In both cases the model of Verhoef could have been used as is done in Epema (1992a). Since however corrections turn out to be almost linear, no further attempts will be done in this study to correct for atmosphere.
It will only be tested if a linear relation exist between measured ground reflectance with the mini-IRIS of selected points and the planetary reflectance derived from the satellite data.

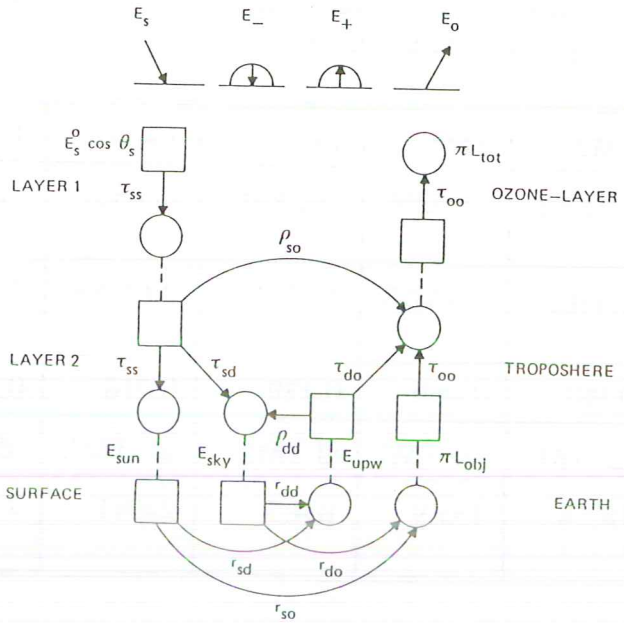

Figure 5.19 Atmospheric influence on incoming radiation from the sun.

COMPARISON PLANETARY AND FIELD REFLECTANCE

The average planetary reflectance is calculated for every band for six areas in the January and May image. Mini-Iris measurements of the same six areas are recalculated to TM-bands. The selected areas are as pure as possible and are chosen in the extremes of reflectance. One area situated in the red schist zone, has an intermediate reflectance percentage. The following areas have been selected:

1 cuirasse (location O)
2 cuirasse (location D)
3 erosion area (location J)
4 erosion area (location L)
5 cuirasse (location P)
6 red schist area (location N)

In the erosion areas it was not possible to select pure areas. Therefore it was necessary to compare these areas not with one field reflectance measurement, but with a combined curve. These combined curves are calculated by multiplying the percentage covering of a surface type and the field reflectance curves measured in these surfaces. Since only these few locations could be used and since only extreme values are used, it is not very useful to analyze the correlation coefficients. At first sight relations were not as good as expected. This can be ascribed partly to a difference in time between field reflectance measurements and the time the satellite images were taken. Field measurements were taken in November. In this month the field is much wetter and has more vegetation than in January. Also difference in pixel size 30 x 30m^2 for Landsat TM and 24 x 24 cm^2 may be of importance. Surfaces represented by large pixels are not as pure as surfaces measured by the Mini-IRIS. Another problem may lay in the calibration of the field reflectance measurements.

CONCLUSION

Field reflectance cannot be converted straightforward to satellite reflectance. In the following chapters in most analyses data from the satellite itself will be used. For instance, endmembers in the unmixing procedure (chapter 5.3.2) are derived from the image data. Calculation to planetary reflectance are however a good way to produce spectral curves of satellite data. In the analysis of satellite data field measurements were vital for understanding the spectral signatures given by the satellite. For further research, for instance to monitor changes, it is better to use planetary reflectance than the original digital counts. Correction for atmospheric influence can be done using information on atmosphere from meteorological stations or assuming some objects to have a constant reflectance.

5.3 ANALYSIS OF LANDSAT TM IMAGERY

Colour composites of satellite images can be a very good means to determine a sampling strategy for soil and vegetation survey. Mostly this type of information, like in this soil survey of the Kaya area, is used in combination with aerial photographs. Besides colour composites, it is possible to use other image processing techniques to make further use of the satellite information. One of the most well-known is supervised classification. Belemviré (1993) tested a range of different classification techniques in the Kaya area. In these techniques the user selects a number of training pixels from an image. These pixels belong to a known class of land cover. Subsequently all pixels with a similar spectral signature are classified to that class of land cover. Results of these techniques are a.o. determined by the spectral differences of landcover classes. Since no image of the wet season was present, we do not expect much better classification results than Belemviré (1993), who used only the January data. Therefore we concentrated our research with satellite data to some other topics:

1) unsupervised classification (Chapter 5.3.1). We compared results of this statistical technique, with our observations of landscape units.

2) mixture modelling (Chapter 5.3.2). With this technique, for every pixel a percentage of a cover class is determined.

3) spectral variation within soil mapping units (Chapter 5.3.3). For one of the soil mapping units, the soils on the plateaus, we analysed statistically the variation based on Landsat TM and field observations.

4) comparison of possibilities of airphotos and Landsat TM for soil mapping (Chapter 5.3.4).

5.3.1 UNSUPERVISED CLASSIFICATION FOR LANDSCAPE MAPPING

INTRODUCTION

Possibilities of unsupervised classification (or clustering) of Landsat TM data of the Kaya area for landscape mapping have been investigated. First the clustering has been refined in several steps to achieve classes, which can be understood in terms of landscape classes. A new clustering of a small part of the area is added to the original clustering of the entire area, whereafter clusters are combined and recoded to 12 final clusters. In order to get a more homogeneous image a filter is applied to the clustered image. The meaning of these clusters has been determined by interpreting spectral values of cluster means, field measurements and field observations.
As a second product a vector overlay on this unsupervised classification has been made. The main entrance of this map layer is physiography. Physiognomy and vegetation coverage classes are added and described in the present text.

SUPERVISED AND UNSUPERVISED CLASSIFICATION

In satellite images like figure 3.1, various colours indicate variation in spectral characteristics. Spectral differences can be used to classify the image.
Based on their original values (called data file values in ERDAS) pixels can be sorted into a number of individual classes or categories of data. When the pixel satisfies a certain set of criteria, the pixel is assigned to the class that corresponds to that criteria. This process is called a multispectral classification (ERDAS, 1990).

Depending on the type of information available, classes may be associated with known features on the ground (supervised) or may simply be represent areas that look different to the computer (unsupervised). Supervised classification is controlled by the analyst: he selects pixels that he recognizes as spatial patterns in the image and, based on these criteria, pixels are associated to classes. It is important to have knowledge of the area before classification (ERDAS, 1990).

Belemviré (1993) performed types of several supervised classifications of the area around Kaya (Maximum Likelihood Classification, Minimum Distance Classification and Parallelepiped Classification). The problem of these classification was the heterogeneity of classes: one class contains several types of landscapes which are different by their geology or land cover. Reasons which cause these problems may be:
- classification is based on the image of January 1991 only, while in this study the image of May 1988 is also available;
- the bands of the January image were not placed rightly one upon the other (bands 3 and 6 were shifted six pixels in comparison with the other bands);
- some landscape types only show small spectral differences;
- a large spatial variation over a short distance sometimes occurs;
- some pixels are mixed pixels, with various land cover types in one pixel.

Unsupervised classification is more computed-automated. The computer uses some parameters which the analyst specifies to uncover statistical patterns that are inherent to the data (ERDAS, 1990). These statistical patterns, or clusters, are not always easily recognizable land cover units, because they are exclusively based on spectral characteristics. The interpretation of the clusters discerned by the computer must be done after classification.

A better co-registration of the bands, use of the May-image in addition and a careful selection of training pixels may give somewhat better supervised classification results than found by Belemviré. However, in this study a unsupervised classification, or clustering, is carried out with subsequent identification of clusters. It is expected that in this way better differences between classes can be made due to small spectral differences and large spatial variation over short distances.

CLUSTERING OF THE SATELLITE IMAGE

Clusters are defined with the sequential clustering algorithm program which uses all or many pixels in the input data file for its analysis, and has no regard for the contiguity of the pixels that define each cluster. The sequential method analyzes the pixels of the image line by line, and groups them on spectral distance. Clusters are determined based on relative spectral distance and the number of pixels per cluster (ERDAS, 1990).

Clustering of different images were done: the January image with and without thermal band (band 6), and a combination of the January-May image with and without band 6. When interpretating the results of the different clusterings it became clear that clustering including the thermal band does not result in more easily definable clusters. Moreover, two lakes on the images ('lac de Dem' and the barrage of Kaya) contain many clusters, because the digital numbers of the thermal band especially vary within water surfaces. The objective of this clustering is to classify landscapes, and not differences in water.

All clustered images show a clear distinction between the north-east granite part and the south-west schist part of the area. Within these two parts valley bottoms, plateaus and surfaces which are more or less densely vegetated are distinguishable. In all clusterings it is difficult to separate green schist hills from red schist plateaus in the south-west part of the area. This is partially due to the shadow effect: both hills and plateaus have dark, shadowed sides with comparable reflectance characteristics. Partially it is due to a comparable vegetation cover. The computer combines parts of plateaus with rather much vegetation and green schist hills in one same cluster.

The difference between the clustering of the January image and the clustering of the January-May image is not very big. The January-May clustering shows most easily interpretable clusters in the granite. Therefore, the multitemporal clustering without band 6 formed the bases for further interpretation.

In order to obtain a better clustering of the south-west part (in which green schist hills can hardly be distinguished from plateaus), this part was cut out of the January-May image and reclustered. The two clusterings were put together. The clusters of the in this way obtained image were combined and recoded, using field knowledge. The 52 original clusters were condensed into 12 new clusters. The most important combinations made were:
- all clusters representing water were combined.
- all clusters representing densely vegetated surfaces (valley bottoms, borders of the lakes and a part of Kaya) were combined.
- all clusters representing granite or schist valleys were combined into four clusters for granite valley and two clusters for schist valley with different vegetation coverages. Several other clusters represent parts of schist valleys, too (in combination with other landscape units).
- all clusters representing exclusively the greenschist hills, a clearly distinguishable landscape unit were combined.
- all clusters representing exclusively shadow of either the edge of the plateau or the greenschist hills were combined.
- all clusters representing plateaus were combined thus forming a separate landscape unit. It was tried to distinguish higher and lower plateaus. These clusters contain some parts of greenschist hills and schist valley also, due to a comparable vegetation coverage.

After recoding, a filter, which gives the dominant value of nine neighbour pixels to the central pixel, was led over the clustered image. This resulted in more homogenous surfaces without loosing information of narrow clusters like bas fonds, which often had a width of only one pixel (Figure 5.20)

The meaning of the final 12 recoded clusters is given in table 5.4.

Table 5.4 Description of clusters

Cluster	Colour on figure	Vegetation coverage	Vegetation type	Geology	Remarks
1	blue	-	-	-	water
2	crimson	very high	trees	alluvial deposits	cultivated; including a part of Kaya, lake borders and one plateau with a high vegetation coverage
3	olive	high	trees	granite valley (bottom)	cultivated
4	ecru	very low	shrubs	granite valley	eroded
5	tan	moderate	trees, shrubs, herbs, grasses	granite valley	less intensive cultivated
6	avocado	high	trees	granite valley	cultivated
7	orange	moderate	trees, shrubs, grasses, herbs	schist valley	cultivated
8	green	high	grasses, herbs, trees, shrubs	greenschist hills	non cultivated
9	black	various	various	various	effect of shadow on edges of plateaus and hills
10	blue-violet	low	trees, shrubs, grasses, herbs	higher parts of plateaus and some parts of hills	including iron crusts and grass vegetation in the centre of the plateau
11	light violet	moderate	trees, shrubs, grasses, herbs	lower parts of plateaus and and some parts of hills	less intensive cultivated; often a high coverage of gravel
12	light grey	moderate	trees, shrubs, grasses, herbs	at the bottom of plateaus	less intensive cultivated; often a moderate coverage of gravel

The clusters composed by the computer are based on spectral characteristics of the pixels. They indicate the coverage by different objects, most essential the vegetation; in case of no vegetation they may indicate the soil type and roughness.

The clustered and interpreted image differs considerably from the supervised classifications of Belemviré (1993):
- the clusters are more homogeneous. For instance, water is represented in one, separate cluster, as are green schist hills and valley bottoms.
- the granite part of the area (north-east) is represented by several clusters with different vegetation density and land use.
- the small green schist longitudinal hills situated north-east of Kaya can not be distinguished very easily in a separate cluster. These hills are discriminated somewhat more clearly in supervised classifications.
- the plateaus are represented by several clusters.

Both supervised and unsupervised classification do not indicate a difference between green and red schist valleys. Probably this is due to the alikeness of land cover; the distinction between green and red schist valley is mainly a geological distinction.

SCATTERPLOTS AND INTERPRETATION OF THE CLUSTERED IMAGE

In order to get more insight in differences in reflectance between January and May, and be able to better interpret the meaning of clusters, some scatterplots and spectral curves are made. An understanding of the spectra may also give enhanced possibilities for extrapolation. Scatterplots and spectral curves are made for the means of the original 27 clusters of the January-May image without band 6, the means of the interpreted and recoded 12 clusters

(Figure 5.20) and the means of 26 polygons which are drawn manually at the image and are supposed to be 'pure' units (for instance, a polygon containing an iron crust only). In the plots original digital numbers or planetary reflectance values are used. The reflectance values are calculated using formulas of chapter 5.2. In Table 5.5 an explanation is given of symbols used in Figure 5.21-5.24.

Table 5.5 Symbols used in figures 5.21-5.24.

b	bare soil
fg	fields in granite area
fs	fields in schist area
h	greenschist hills
p	plateau
s	shadow
v	dense vegetation
w	water
+	difficult to interpret cluster

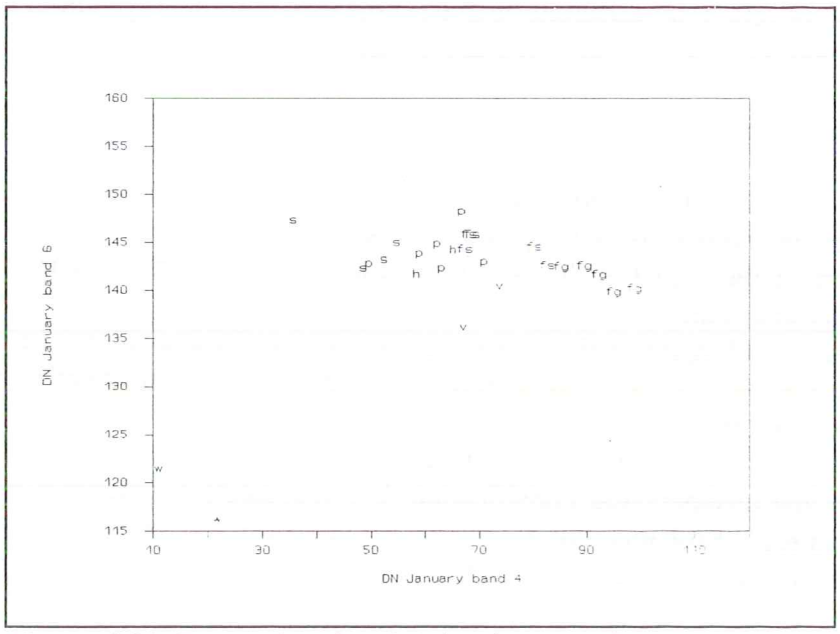

Figure 5.21 Scatterplot (band 4-6) of pure polygon means

In figure 5.21 a scatterplot is given comparing band 4 (NIR) and band 6 (a thermal band). Radiation in the thermal band is low for water and high for bare surfaces, while vegetation has an intermediate reflectance. This is accordance with literature (Asrar, 1989). Within the bare soil group, the temperature of dark surfaces, showing more absorption, is higher than for lighter surfaces. A similar scatterplot of May (not shown) differs only slightly from

KAYA, BURKINA FASO

Figure 5.28 Physiographic vegetation cover map (1-18, see description in text of legend to figure 5.28).

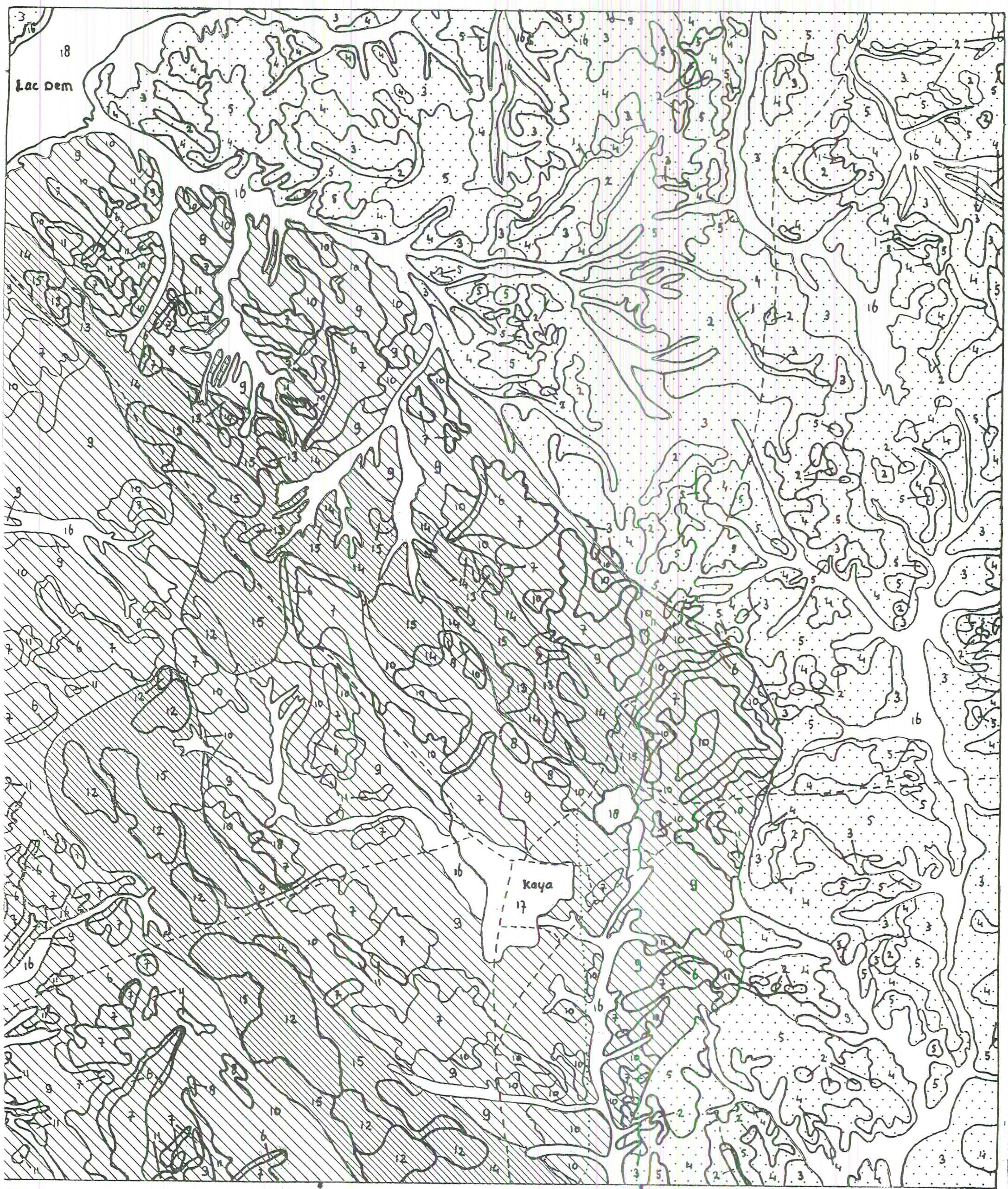

T.H. Slaa
Department of Soil science and Geology
Agricultural University of Wageningen
Antenne Sahélienne, March 1994

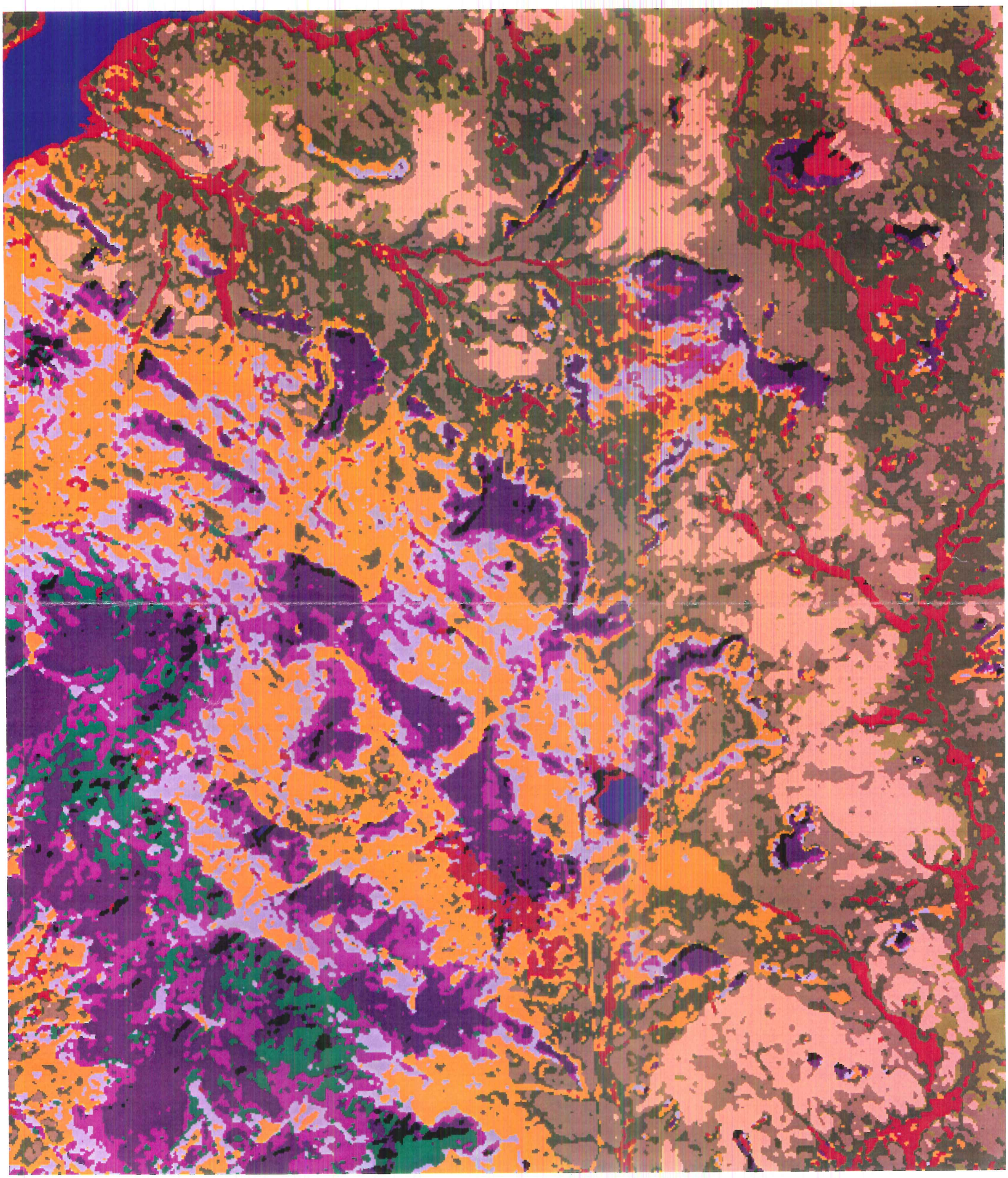

Figure 5.20 Clustered en recoded Landsat TM image (For meaning of colors, see table 5.4)

January. Only the difference between water and vegetation temperature was much less and reflectance of water was higher. This can be explained by the evaporation of water in the lakes, which causes the remaining water to contain more sediment.

A multitemporal comparison was made for the 26 pure polygons, the original 27 clusters and the final 12 clusters. In figure 5.22-5.24 planetary reflectance results are shown for band 7, as an example. Most objects and cluster means are close to a straight line, probably indicating no change. Differences in absolute amount of reflectance are due to atmospheric influence (chapter 5.2).

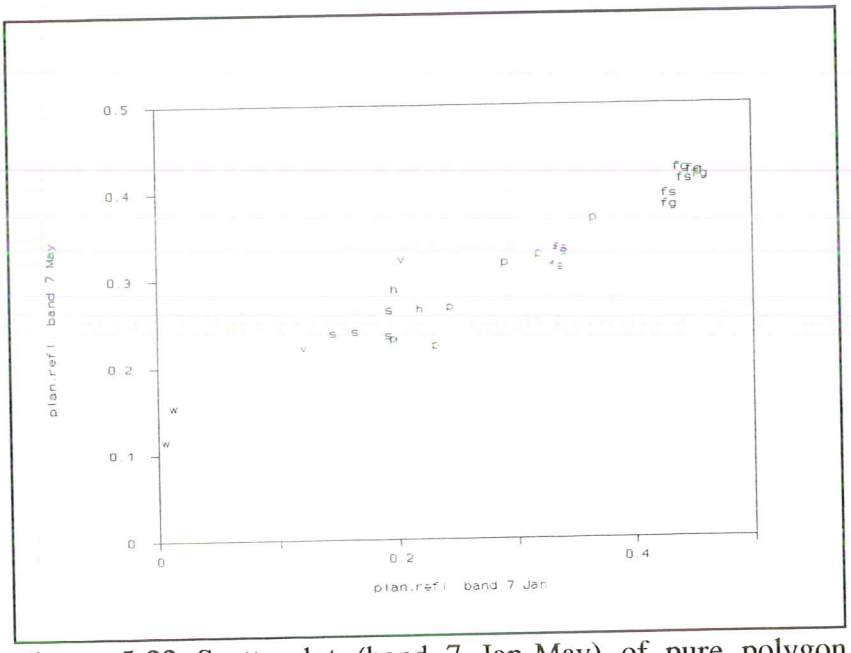

Figure 5.22 Scatterplot (band 7 Jan-May) of pure polygon means.

When examining the pure polygons (Figure 5.22) it can be concluded that eroded, barren land, plateaus and agricultural fields do not show large differences in reflectance between January and May. This is because in both periods they are not covered (or hardly covered) by vegetation. Water and densely vegetated sites (like the greenschist hills), however, have a higher reflectance in May than in January: water in the lakes dries up or contains more sediment and vegetation becomes drier.
Examining the original clusters a comparable relation was found, with the exception of a few clusters (Figure 5.23). These few clusters represent only a small percentage of the area. Some clusters of the original clustering were easy to interpret when looking at the image (Figure 3.1) and with field knowledge; others seemed to be a mixture of different land covers or geological types.
The scatterplot of the final clusters (Figure 5.24) show much similarity to the pure polygons scatterplot. Remarkable are the fields on granite which have a higher reflectance in May, while the schist fields do not show this. Vegetation on both types of fields becomes drier, but the average lower reflectance of schists fields in comparison with granite fields causes a relatively lower reflectance. The cluster representing vegetation does not show a clear higher reflectance in May, because this cluster contains also less densely vegetated parts, apart from the densely vegetated parts of the valley bottom.

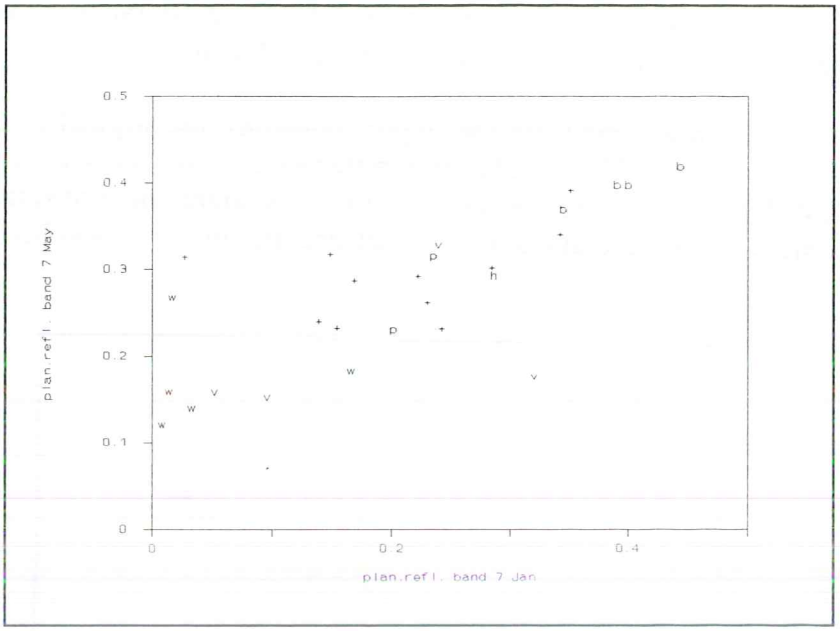

Figure 5.23 Scatterplot (band 7 Jan-May) of cluster means.

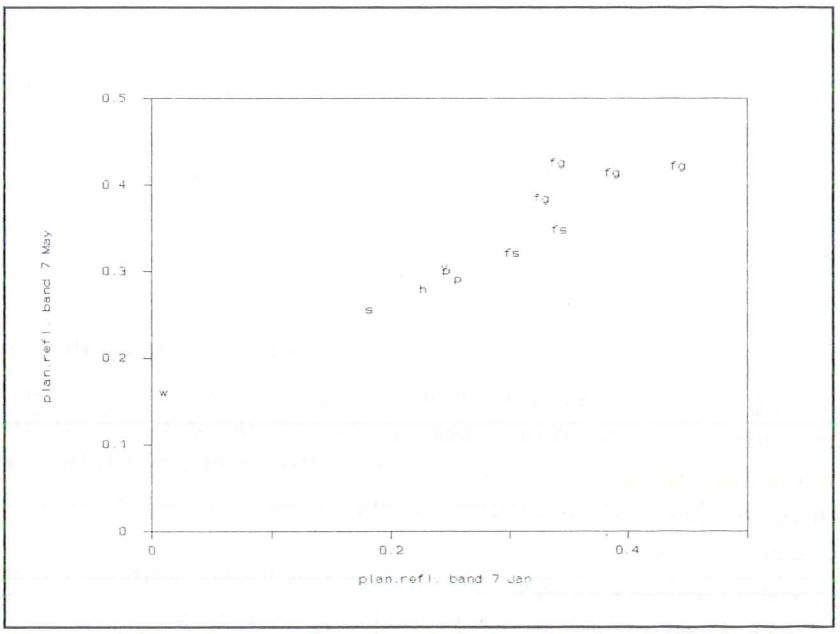

Figure 5.24 Scatterplot (band 7 Jan-May) of final cluster means.

A comparison was made between spectral curves of field measurements with the mini-IRIS (calculated to averages within a bandwidth of the TM, chapter 5.2.1) and curves of some pure polygons and some final clusters (Figure 5.25-5.27). Attention has to be paid to the fact that field measurements were taken of a surface of about 25*25 cm, while the pure polygons and final clusters are of a much bigger size (at least several m^2) which implies that 'pure units' never are really pure (containing only crusts or only iron crust).

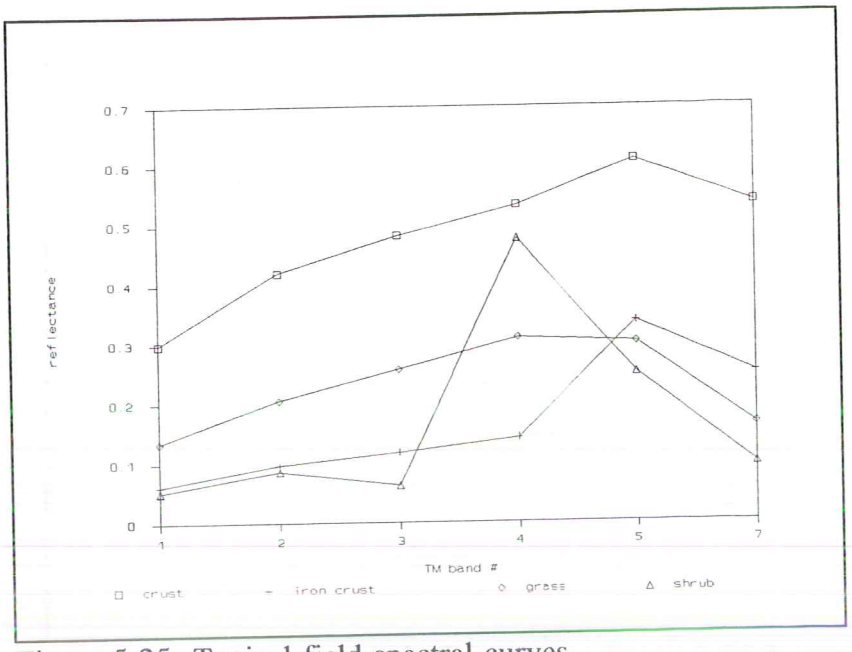

Figure 5.25 Typical field spectral curves.

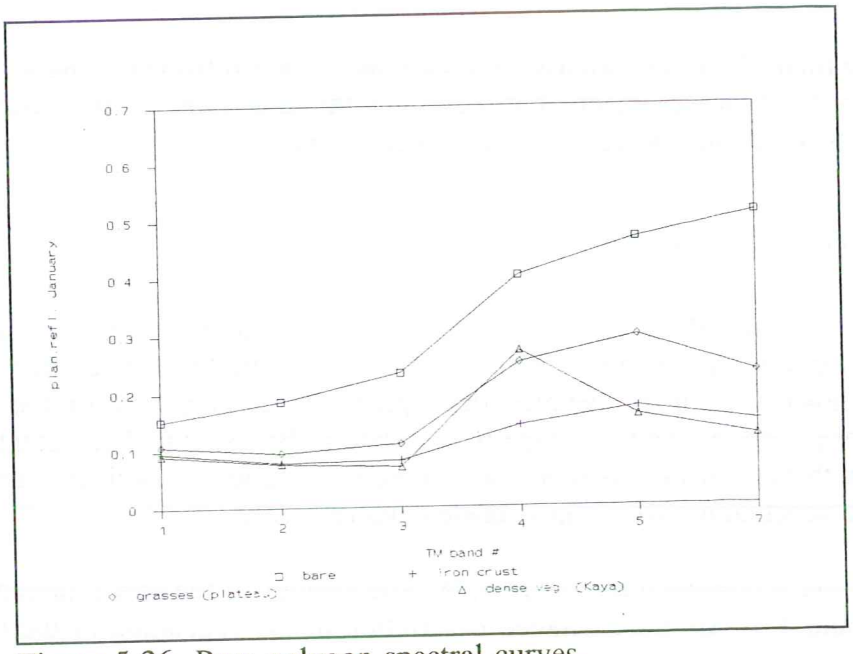

Figure 5.26 Pure polygon spectral curves.

The spectral curves of pure polygons and clusters show less extreme reflectance values than the field curves. This is due to the above mentioned fact of averaging reflectance of a variety of surfaces within one polygon or cluster. However, the curves show similarities in their form. Crusts and bare, eroded surfaces have a high reflectance. Vegetation has a high reflectance in band 4, although the field curve is much more extreme. The reflectance by iron crusts (on plateaus) is low, but the slight increase in band 5 is for the field curve is due to instrumental problems. The grass vegetation of the field curve again does not show a lower reflectance in band 2 and 3, because the grass has turned already yellowish.

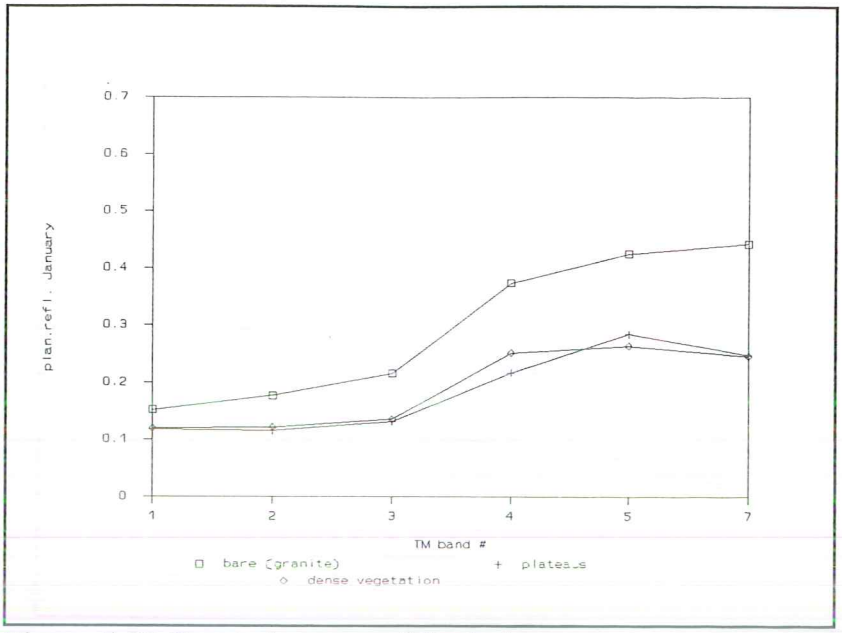

Figure 5.27 Spectral curves of final clusters.

Concluding, the final 12 clusters often are less extreme in their reflectance characteristics than pure polygons or field measurements, but they show the same trends. The clusters are more heterogeneous than the pure polygons or field measurements.

MANUAL CLASSIFICATION

The unsupervised classification, the clustering, gives an indication of how to classify the area based upon land cover. In a manual classification it is possible to include other information obtained by fieldwork: a more detailed description of physiography of the area and a description of physiognomy and coverage by vegetation. By using a physiographic entrance a comparison with the soil map is more easy. Based on clustering, soil map and fieldwork a physiographic vegetation cover map is made (Figure 5.28).

First a short legend is presented for figure 5.28. The geology of the area is already described in chapter 4.2 and 4.3. An more detailed description of the vegetation of the map follows hereafter. Species are then presented in alphabetical order.

Legend to figure 5.28

	UNIT NO FIG. 28
GRANITE AREA	
plateau	
woody vegetation (edge)	1
scrubland (centre of plateau)	2
valley	
open woodland savanna	
high woody vegetation density	3
low woody vegetation density	4
waste land	5
RED SCHIST AREA	
plateau	
woody vegetation (edge)	6
grassland (herb vegetation) with scattered shrubs (centre of plateau)	7
longitudinal hills	
grassland (herb vegetation) with scattered shrubs and trees	8
valley	
open woodland savanna	
high vegetation density	9
low vegetation density	10
waste land	11
GREEN SCHIST AREA	
hill	
grassland (herb vegetation) with scattered shrubs and trees	12
longitudinal hills	
grassland (herb vegetation) with scattered shrubs and trees	13
valley	
open woodland savanna	
high woody vegetation density	14
low vegetation density	15
RECENT ALLUVIAL DEPOSITS	16
KAYA	17
OPEN WATER	18

Extensive description of vegetation for figure 5.28

I. granite
A. plateau
1. woody vegetation (edge)
coverage: woody vegetation 40%, grasses and herbs 10%, iron crusts 50%
species: Combretum micranthum, Guirea sengalensis
Pennisetum pedicellatum
remarks: This is the steep edge of the plateau.

2. scrubland (centre of plateau)
coverage: shrubs 20%, grasses and herbs 10%, gravel 40%, crust 30%
species: Balanites aegyptiaca, Cassia spp., Combretum glutinosum, C. micranthum, Diospyros mespiliformis, Guiera senegalensis, Sclerocarya birrea
Loudetia togoensis, Tripogon minimus
remarks: This vegetation type is also called 'tigerbush', although the shrubs do not always appear in lines. The cover by grass and gravel is not total; bare soil sometimes contributes for 70%.

I. granite
B. valley
1. open woodland savanna
a. high woody vegetation density
coverage: woody vegetation 15%, grasses 15%, sand 70%
species: Acacia seyal, Adansonia digitata, Balanites aegyptiaca, Dicrostachys cinerea, Faidherbia albida, Ficus spp., Guiera senegalensis, Sclerocarya birrea, Piliostigma reticulatum, Vitellaria paradoxa
Cenchrus biflorus, Pennisetum pedicellatum, Schoenefeldia gracilis, Zornia glochiadata
remarks: The bare soil are mainly agricultural fields.

b. low woody vegetation density
coverage: woody vegetation 5%, grasses and herbs 20%, sand 45%, gravel 45%
species: Combretum micranthum, Guiera senegalensis, Piliostigma reticulatum
Andropogon gayanus, Cenchrus biflorus, Loudetia togoensis, Pennisetum pedicellatum, Schoenefeldia gracilis, Zornia glochiadata
remarks: There is some non-permanent agriculture. Sometimes deep gullies cut the area.

I. granite
B. valley
2. barren land
coverage: woody vegetation 1%, small sand dunes (with some grasses) 20%, gullies 5%, sand and crusts 74%
species: Balanites aegyptiaca, Diospyros mespiliformis, Piliostigma reticulatum
Brachiaria lata, Cenchrus biflorus, Schoenefeldia gracilis, Zornia glochiadata
remarks: This is eroded land; often deep gullies are present.

II. red schist
A. plateau
1. woody vegetation (edge)
coverage: woody vegetation 40%, grasses and herbs 10%, iron crusts 50%
species: Combretum micranthum, Guirea senegalensis
Pennisetum pedicellatum
remarks: This is the steep edge of the plateau.

2. grassland (herb vegetation) with scattered shrubs (centre of plateau)
coverage: woody vegetation 5%, grasses 50%, iron crusts (gravel) 45%
species: Combretum glutinosum, C. micranthum, Lannea microcarpa
Cymbopogon schoenanthus, Loudetia togoensis, Schizachirium exile, Schoenefeldia gracilis, Tripogon minimus
remarks: The grass cover can vary considerably between the different plateaus (30-70%) due to local growing conditions.

II. red schist
B. longitudinal hills
1. grassland (herb vegetation) with scattered shrubs and trees
coverage: woody vegetation 10%, grasses 30%, bare soil 60%
species: Acacia seyal, Combretum glutinosum, C. micranthum, Faidherbia albida, Lannea microcarpa
Loudetia togoensis, Pennisetum pedicellatum
remarks:

II. red schist
C. valley
1. open woodland savanna
a.high vegetation density
coverage: woody vegetation 15%, grasses 10%, bare soil 75%
species: Acacia seyal, Balanites aegyptiaca, Faidherbia albida, Sclerocarya birrea, Vitellaria paradoxa
Andropogon gayanus, Pennisetum pedicellatum, Schoenefeldia gracilis
remarks: This class consists mainly of agricultural fields.

b.low vegetation density
coverage: woody vegetation 5%, grasses 20%, bare soil 70%, gravel 5%
species: Acacia seyal, Combretum glutinosum, C. micranthum, Faidherbia albida, Lannea microcarpa
Loudetia togoensis, Pennisetum pedicellatum
remarks: This class consists of both non-permanent and permanent agricultural fields with often a considerable cover by gravel.

II. red schist
C. valley
2. barren land
coverage: shrubs 1%, small sand dunes (with some grasses) 15%, crusts/sand/gravel 84%
species: Combretum micranthum, Guiera senegalensis

Loudetia senegalensis, Pennisetum pedicellatum
remarks: This is eroded land.

III. green schist
A. hill
1. grassland (herb vegetation) with scattered shrubs and trees
coverage: woody vegetation 5%, grasses 80%, bare soil 15%
species: Acacia seyal, Guiera senegalensis
Cymbopogon schoenanthus, Loudetia togoensis, Schizachirium exile
remarks: The presence of Schizachirium exile, which has a red colour when dry, gives a red glow to the hills.

III. green schist
B. longitudinal hills
1. grassland (herb vegetation) with scattered shrubs and trees
coverage: woody vegetation 5%, grasses 30%, bare soil 75%
species: Acacia seyal, Balanites aegyptiaca, Faidherbia albida, Guiera senegalensis
Cymbopogon schoenanthus, Loudetia togoensis, Schoenefeldia gracilis
remarks:

III. green schist
C. valley
1. open woodland savanna
a.high woody vegetation density
coverage: woody vegetation 10%, grasses 5%, bare soil 85%
species: Acacia senegal, A. seyal, Adansonia digitata, Vitellaria paradoxa, Ziziphus mauritiana
Andropogon gayanus, Schizachirium exile, Schoenefeldia gracilis
remarks: This area is an agricultural area.

b.low vegetation density
coverage: woody vegetation 5%, grasses 20%, bare soil 75%
species: Acacia seyal, Balanites aegyptiaca, Faidherbia albida
Cymbopogon schoenanthus, Loudetia togoensis, Schoenefeldia gracilis
remarks: This class consists of both non-permanent and permanent agricultural fields.

IV. recent alluvial deposits
coverage: woody vegetation 20%, grasses 20%, bare soil 60%
species: Acacia seyal, Azadirachta indica, Balanites aegyptiaca, Combretum micranthum, Diospyros mespiliformis, Eucalyptus camaldulensis, Faidherbia albida, Guiera senegalensis, Lannea microcarpa, Piliostigma reticulatum, Sclerocarya birrea, Tamarindus indica, Vitellaria paradoxa
Andropogon gayanus, Pennisetum pedicellatum, Schizachirium exile, Schoenefeldia gracilis
remarks: This class is an agricultural area.

V. Kaya
VI. open water

COMPARISON BETWEEN CLUSTERING AND MANUAL INTERPRETATION

The differences between the clustering and the manual interpretation are:

- Valley bottoms

The valley bottoms are drawn as one class in the manual classification. At the clustered image the valley bottoms often are interrupted or not continued. This is due to the variable vegetation density within the valley bottom class. The vegetation of Kaya is classified as city area and the plateau in the north-east is classified as plateau.

- Plateaus

The plateaus are distinguished upon their location in either granite or (red or green) schist. The clustered image puts all plateaus in one cluster, which is due to similarity in vegetation density and material (iron crusts).

- Longitudinal hills

The longitudinal hills are distinguished, which form one single cluster with plateaus in the clustered image. It was not possible to separate them spectrally because of the similarity in vegetation density and their relatively smallness.

- Schists

The manual classification makes a difference between the red and the green schist. The clustered image does not show this difference.

- Schist/granite

Based upon field observations the boundary between the schists and the granite is located more to the north east than the clustered image indicates. The granite sand is blown into the schist area by the wind, coming every year from the north east (harmattan), and forming a thin layer of sand over the schist area. This explains why the granite seems to penetrate the schist area.

- Manganese

In neither the clustering nor the manual classification manganese has been distinguished, because of the relative small size of these hills.

The physiographic vegetation cover map can be used in combination with other sources, like the soil map. Eventually, more detail can be included.

CONCLUSIONS

Unsupervised classification (clustering) of the satellite image gives a good impression of landscape types, especially when clustering is applied in different steps and also clusters are combined. The manual classification, based on a combination of clustering, soil map and field work, gives more information on vegetation characteristics.

Extrapolation of the computer-based classification to other areas is possible if these areas do not differ too much in physiography and vegetation. However extrapolation can not be done without some fieldwork in order to be able to adequately interpret and process the imagery.

5.3.2 MIXTURE MODELLING OF LANDSAT TM DATA

Mixture modelling is carried out on the Landsat TM image of January. With this procedure, maps can be derived from remotely sensed data, which represent the cover percentages of a specific cover type. These coverage maps have continuous values, in contrast to, for example, unsupervised classification and interpretation maps (described in chapter 5.3.1), which produces a choropleth landcover map. The mixture modelling maps are more detailed because the resulting data is on sub pixel level. The mixture modelling procedure is explained and the resulting coverage maps are described in this chapter.

The unmixing method seeks to determine the fractional abundance of all endmembers within each pixel. An endmember is a reflectance curve of a component of the landscape. An endmember can be, for example, an reflectance curve of a plateau or vegetation. With a number of endmembers it is possible to calculate percentage of surface which is covered by each component within a pixel. The unmixing module of SIPS uses a simple linear mixing model. This model assumes that pixel spectra can be modeled as linear combinations of endmembers. The program uses the singular value decomposition for inverting the spectral library (Kruse et al, 1993). A schematic overview is given in figure 5.29.

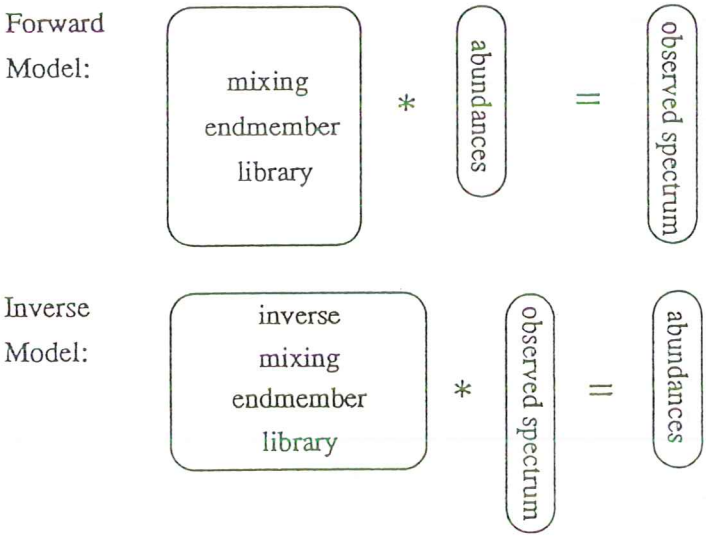

Linear spectral mixing forward and inverse models. If the number of endmembers in the library is less than the number of bands in the data, then the problem is an over-determined linear least squares inversion.

Figure 5.29 Linear spectral mixing (Kruse et al, 1993)

The program SIPS has three different unmixing algorithms: unconstrained, partly constrained and fully constrained. The first option is a classic least-squares method for solving the problem. Surface covering of endmembers can be any value, negative and positive. The second method derives coverings, which are required to be positive. The fully constrained method requires that the sum of the coverings must be unity or less (Kruse et al, 1993).

The endmember library can be selected from a library of curves, containing laboratory, field reflectance data or image data. When using field and laboratory curves for unmixing, the image has to contain reflectance percentages and has to be corrected for atmospheric influences. The endmember library used for the unmixing procedure should contain reflection curves of all materials believed to be mixing in the scene. This means also that this library should not contain members that are not present. Before starting the unmixing procedure it is possible to exclude bad or noisy bands (Kruse et al, 1993).

Endmembers used in the unmixing procedure of the January and May images are spectral curves derived from the images. As shown in chapter 5.2 it was not possible to correct adequately the image for atmospheric influences. The selected endmembers are as pure as possible. In order to obtain a representative endmember, the mean curve is calculated from a number of pixels. The endmember curves are represented in figure 5.30-5.31. A short description of the place were the endmembers were taken is given in table 5.6.

Table 5.6 Description of endmembers.

nr.	description
EM1	Greenschist hills shade side
EM2	Greenschist hills illuminated side
EM3	Plateau with ironstone
EM4	Vegetation in Kaya
EM5	Lac Dem
EM6	Erosion area in the East
EM7	Redschist area in the South
EM8	Manganese hills

If all endmembers and all 6 bands of the January image are used for unmixing, the result is not very satisfying. The best result is unmixing with the combination of EM2, EM3, EM4, EM6, EM7 and EM8 and the unmixing method: fully constrained. The result is an image with 8 bands. The first 6 bands are representing the percentage of the endmembers which the pixels contain. The DN in the 7th band are representing the percentages of all endmembers added for one pixel. The last band is representing the least mean square of the endmember computation.

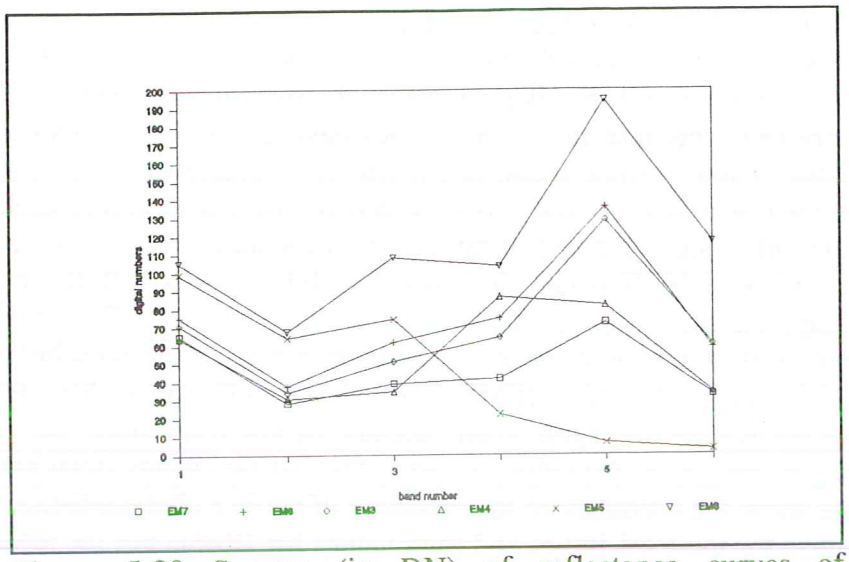

Figure 5.30 Spectra (in DN) of reflectance curves of endmembers (EM1 - 6)

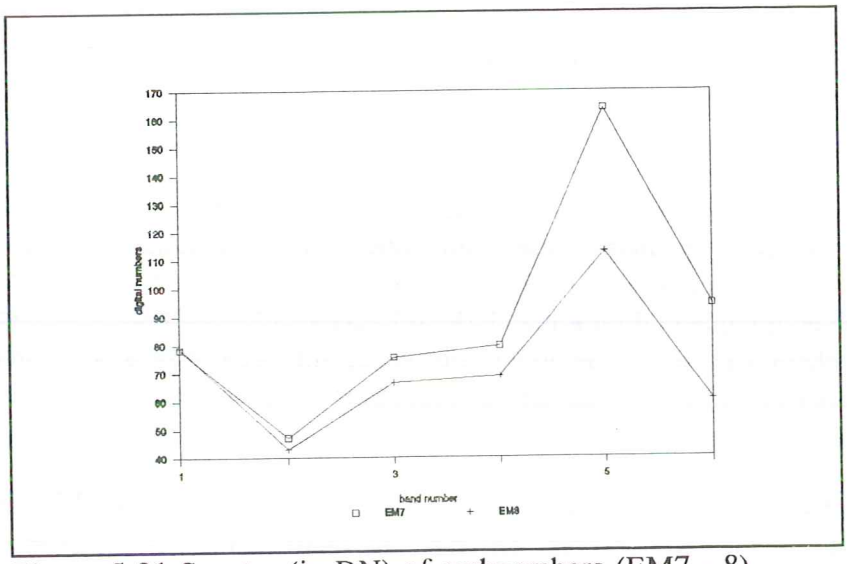

Figure 5.31 Spectra (in DN) of endmembers (EM7 - 8)

In the appendix 5.6 a selection of unmixed images of EM2, EM3, EM4, EM6, EM7 and EM8 is given. If unmixing is carried out with EM1, the result is an image of which all dark places (such as cuirasse, shade and water) are mapped as greenschist shaded sides. So, endmember EM1 is not used in the unmixing procedure. EM2 results in an image, which maps accurately the illuminated greenschist hill sides. It also maps vegetated areas with a few percent as greenschist hills. EM3 maps accurately the non-vegetated cuirasse areas. EM4 is

an endmember of which the reflectance characteristics are very different from the other endmembers, so this endmember maps the vegetation very well. In this image the vegetation in the neighbourhood of Kaya and the lake can clearly be seen and also the river basins are distinct. EM5 is not used, because its characteristics have a too close resemblance to the characteristics of shades and cuirasse areas. So, when this endmember is being used, water is mapped all over the research area. Water is very easy to distinguish in this satellite image. Moreover, there are only a small amount of mixed pixels containing water, mostly the water pixels represent a surface of 100% water. So it is not useful to unmix with this endmember. EM6 accurately maps the erosion areas and areas with light crusts. EM7 is an endmember with an intermediate reflectance percentage. It results in a map of the redschist agriculture area around Kaya. The last endmember (EM8) has very low reflectance characteristics, but it distinguishes the manganese hills quite good. Because of low reflectance, the endmember also locates a few percentages in the cuirasse areas. The last two bands (total and RMS) of the unmixed image show the adequacy of the matching of surface characteristics. The worst matching, low values for the total image and high values for RMS() are for areas with low reflectance. In this way the RMS image can be used as a shade map.

To evaluate the unmixing procedure, two types of areas in the unmixed image are compared. For both area types the following is computed: the average score in the area of each endmember, standard deviation of the endmember score, and minimum and maximum score of all endmembers. The first type of areas are the places of which the reflection characteristics of the endmembers are taken from. The second type of areas, control areas, are places where the endmembers are known to be present for almost 100%. In appendix 5.7, some statistics has been given. The endmembers map the control areas quite good. The greenschist endmember locates 62% greenschist in the pixels of the control area. The cuirasse endmember locates 74% cuirasse in the pixels of the control area. The vegetation endmember, erosion area endmember, redschist endmember and manganese band endmember recognise respectively 61%, 84% 83% and 91% of their own surface type in the pixels of the control area.

Appendix 5.7 also shows the average of the endmember scores of a water surface. The figures indicate that only the manganese endmember slightly matches the water reflectance characteristics, but the other endmembers do not match. The RMS is very high. This indicates that the endmembers do not match the reflectance characteristics of a water surface. The reflectance characteristics of the greenschist shade side area show a better match with the used endmembers especially the manganese endmember. This is because the manganese hills and the greenschist shade side have both rather low reflectance.

It can be concluded that the unmixed image is not perfect, but gives a good impression of the spatial distribution of the endmembers. The type and quality of the endmembers are strongly related to the quality of the resulting unmixed image.

5.3.3 SPECTRAL VARIATION WITHIN SOIL MAPPING UNITS DETERMINED WITH THEMATIC MAPPER AND CROPSCAN

The soil map is presented in Chapter 4.3. Reflectance measured with TM within a soil mapping unit is not uniform. In this chapter variation of this reflectance is determined and compared with variation in ground reflectance of the same units, measured with Cropscan. The variation is explained by a difference in surface cover. The different types of surface cover are statistically correlated with the reflectance measurements. This gives the possibility to predict surface coverage from TM and Cropscan data.
Spatial dependence is analyzed to determine possibilities of another kind of prediction: the interpolation of surface coverage and reflectance within a soil mapping unit on basis of measurements already performed in that unit.

As an example seven plateaus were selected (figure 5.32), representing relatively homogeneous soil mapping units. An advantage of selecting plateaus is the distinct borders of the soil mapping unit, recognizable both in the field and on the aerial photograph. This was necessary in order locate the transects exactly. In the TM image these borders are less clear.

The ground reflectance is measured with the Cropscan (Chapter 3.2). The planetary reflectance, measured by the TM is calculated from digital numbers (DN-s) of the pixels, representing a transect.

REFLECTANCE OF DIFFERENT SURFACE COVERS

The variation within a transect is caused by different types of surface cover. Representative reflectance curves of these types, measured by the Cropscan, are given in figures 5.33 and 5.34. Surfaces can roughly be divided in two main types: With and without vegetation.
The last group can be subdivided in the next types in order of increasing reflectance:

- **Ironcrust and gravel**: These two surfaces have nearly the same reflectance curve. The curves have the lowest level with regard to other curves. A marked feature of the curves is the dip between 800 and 1000nm, caused by hematite and goethite.
- **Algae**: Surfaces covered with algae reflect relatively high, nearly as high as grass and increasing with wavelength.
- **Bare soil (loose sand)**: Bare, but not crusted surfaces reflect intermediate between algae and crusts. The lower reflectance is caused by higher roughness with regard to crusts.
- **Crust**: A crusted surface acts like a mirror and reflects the strongest of all surface covers.

The group of surfaces with vegetation consists of grass and shrubs:

- **Grass**: Grass appears yellow (very dry) during our field trip (November) and reflectance increases with increasing wavelength. The amount of reflectance depends on the density of grass and the type of surface between grass. When the density of grass is nearly 100%, the reflectance is as high as that of bare crust.
- **Shrubs**: Shrubs reflect very high in NIR compared to the reflectance in R. This peak is caused by strong increasing reflectance of chlorophyll in NIR. Also a little peak was to be expected in the green interval. The absence of this little peak can be explained by the low coverage of the shrubs (only 20 - 30%).

Figure 5.32 Location of the 7 transects on the plateaus

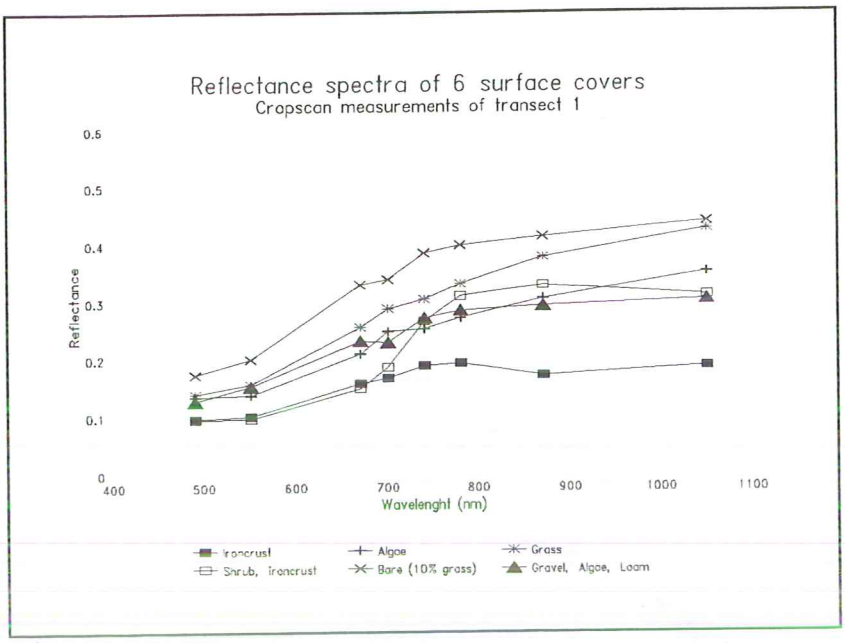

Figure 5.33

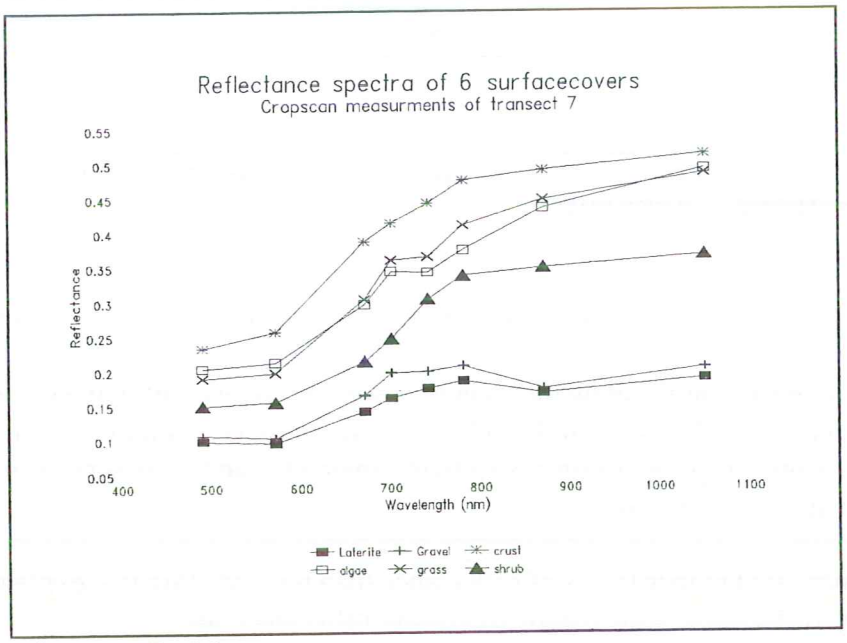

Figure 5.34

To provide an extra illustration of the specific reflectance of the different surface covers, a scatter plot of R against NIR is shown (figure 5.35). The "soil line" is well recognizable: It starts with the lowest values, the ironcrust (i) which is clustered with gravel (g). Bare soil (b) succeeds gravel upwards the soil line and is clustered with crusts (c) which have the highest values. At the left side of this line shrubs (s) attract attention, reflecting relative higher in NIR than in R. Grasses (h) and algae (a) are hardly to distinguish from each other and appear in a cluster intermediate between the soil line and the shrubs. The well clustered scatter plot confirms that the distinction made in types of surface cover is right.

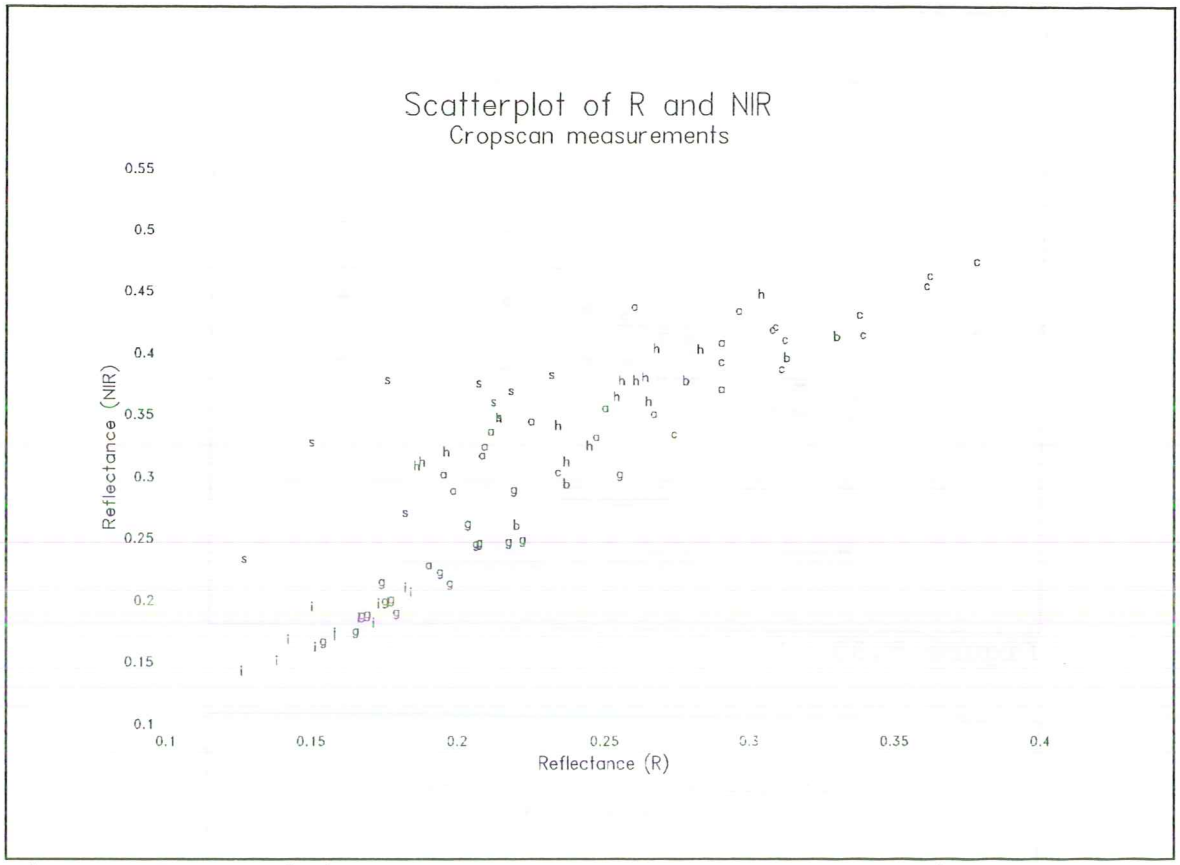

Figure 5.35 (i=ironcrust, g=gravel, b=bare soil, c=crust, a=algae, h=grass, s=shrub)

SPECTRAL VARIATION ALONG A TRANSECT THROUGH A SOIL MAPPING UNIT

Measurements along a transect show the change of surface covers within the soil mapping unit. In figure 5.36 and 5.37 reflectance in R and NIR along transect 1 is indicated. In these figures measurements of the Cropscan (with respectively method 1 and 2, described in chapter 3.2) are compared with those of TM.

The cropscan measured higher levels of reflectance than the TM. Possible explanations for this lower planetary reflectance with regard to ground reflectance are:

- Differences in calibration of Cropscan and TM.
- Influence of the atmosphere on TM measurements. It is possible that reflected radiance is more lowered by the atmosphere than incoming radiation.
- Influence of shadow on TM measurements. Shadow lowers reflectance measured by TM, while the Cropscan does not measure shadow with measuring directly above the object.

Although the reflectance differs in level, it is possible to compare trends between Cropscan and TM measurements.

In order to compare Cropscan measurements of method 1 with TM data, the distinguished parts (with various sizes) of the transect are summed to create parts of 25m, the same size of a pixel of the TM. The weighted summation is performed in order to obtain final reflectance percentages according to the contribution of the surface to the distance of 25m. In this way a comparison with the "mixed pixels" of the TM is possible.

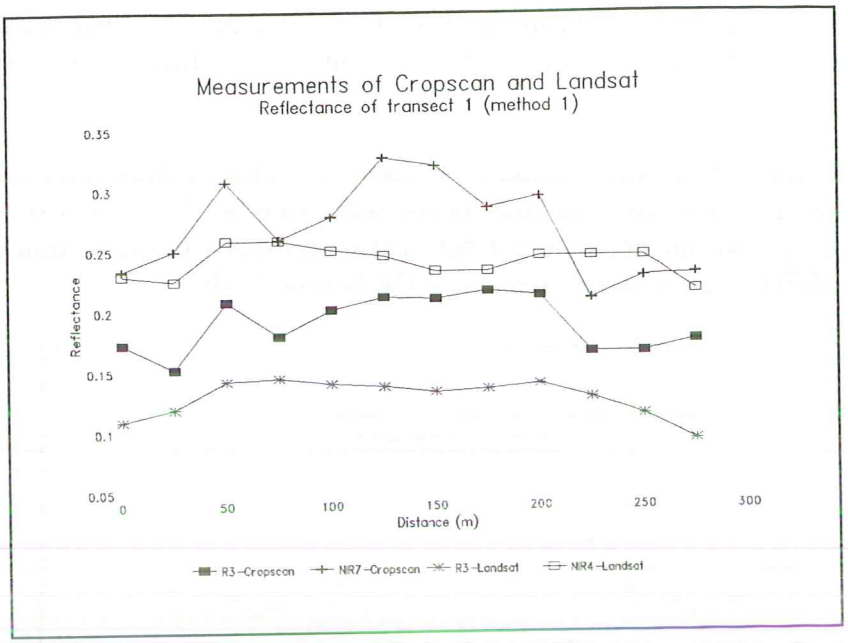

Figure 5.36

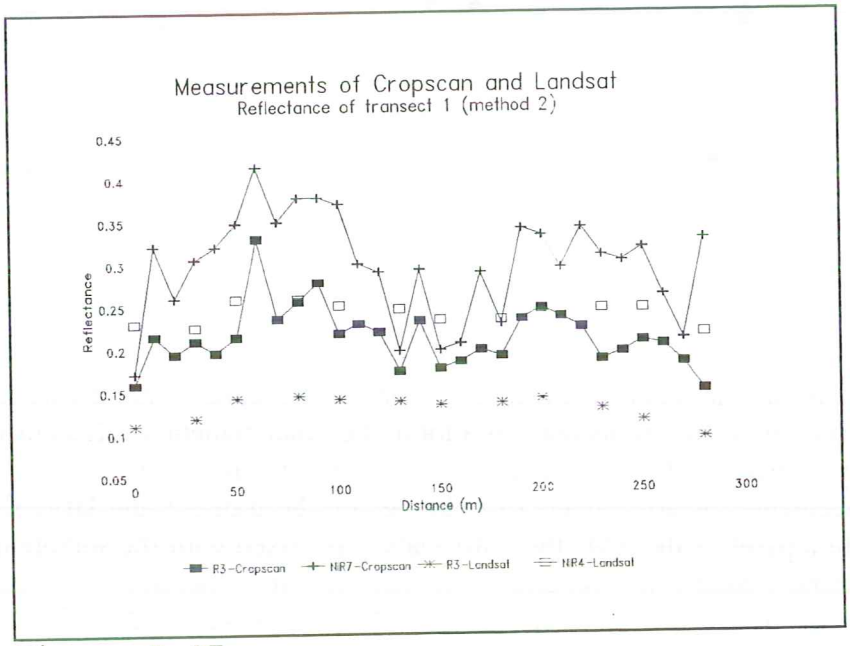

Figure 5.37

The results are given in figure 5.36. The curves do not show exactly the same trend. The upward trend in the beginning of the transect is alike, but the succeeding part is not. There are two possible explanations for the differences in the curves:

- The Cropscan measurements are perhaps not representative for a specific part of the transect. In each part three measurements are randomly performed, so it is possible that an extreme (the Cropscan is very sensible to extremes) has a strong influence on the result.

- It is a problem to point out on a TM-image exactly the same pixels, which represent a field transect. So it is possible that transects in the field and on the image do not correspond to each other.

Measurements of transect 1 with method 2 show a better correspondence with TM measurements (figure 5.37) than measurements with method 1. It is likely that field measurements with the two methods are not performed on exactly the same transects. Figure 5.38 shows clear differences between results of the two methods.

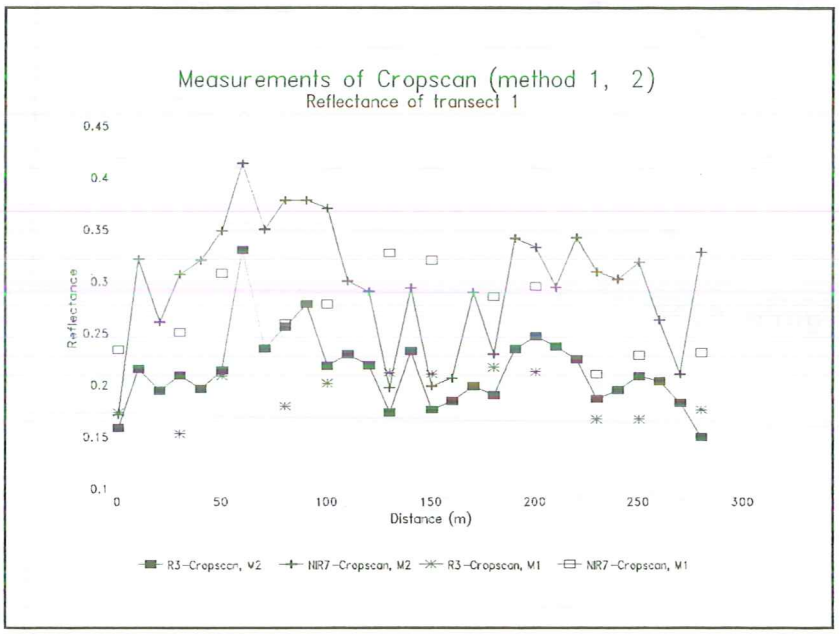

Figure 5.38

TM and Cropscan measurements with method 2 show the same trend. However, as can be expected variability of ground reflectance is a lot higher than planetary reflectance. This difference is mainly explained by difference of scale: Cropscan measurements are strongly influenced by accidental measurements of extremes on the transect and large differences on little distance. In a pixel of the TM, this information is mixed with the surrounding environment and sometimes hardly to recognize. In this way it is possible to explain the high Cropscan values of the last measurement (of a shrub) of transect 1 and the low TM values of the same location.

A well known approach (Burrough, 1986) to smooth a curve is the method of "moving average". This method is applied to match the data of the Cropscan with those of the TM. A calculation of the vegetation index NDVI ((NIR-R)/(NIR+R)) is used for this example because of the enormous variation in this variable caused by the vegetation. The moving average is calculated with a window of 5 data. The result is a smoother curve than the curve in figure 5.39 and is well to compare with the NDVI of the TM and has about the same amount of variation (figure 5.40).

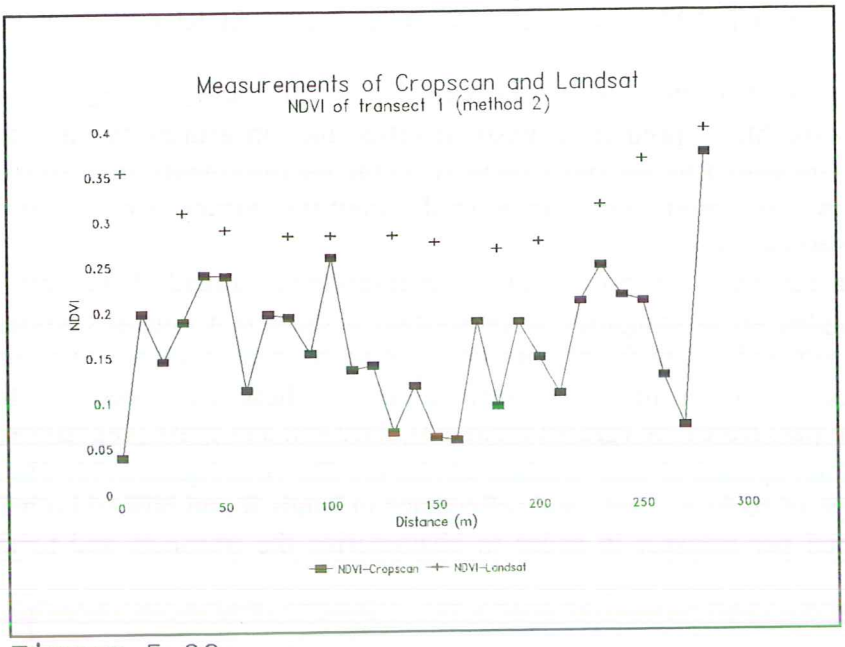

Figure 5.39

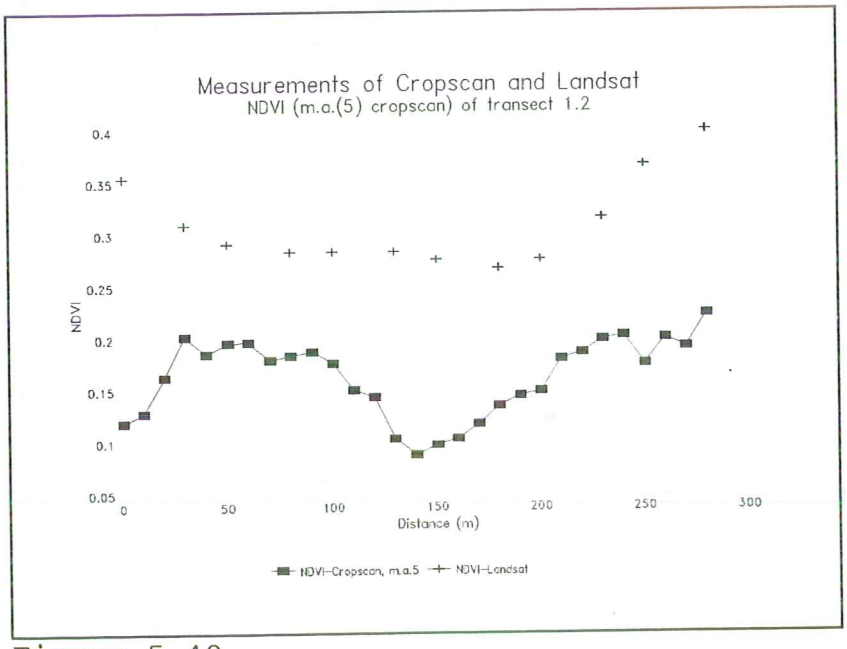

Figure 5.40

The curves show the same trend except for the beginning of the transect. There the TM values are high, while the Cropscan values are low. Two explanations are possible for this difference:

- The transects of the TM and Cropscan do not start at the same point.
- High TM values are caused by a large amount of shrubs on the slope of the plateau. This influences the high value of the pixel on the edge of the plateau. Cropscan measurements are performed until the edge of the plateau and not on the slope, so the last measurements of Cropscan are performed on ironcrust or gravel which cause low reflectance.

CORRELATION OF CROPSCAN- AND TM-DATA AND SURFACE COVERS

It is important to analyze the correlation between the two ways of measurement. With a correlation it is possible to predict on basis of reflectance measured by one of the methods reflectance to be measured by the other method. If the measurements are also correlated with the surface covers, valid predictions can be made about the surface coverage with help of the reflectance measurements.
Although various results of Cropscan and TM measurements already have been illustrated in previous paragraphs, an investigation is performed if there is a mutual correlation between these measurements and a significant correlation of these measurements with surface covers. In order to reduce the large amount of surface classes, these are joined into three well to recognize main types: Ironstone (gravel included), bare soil and grass (vegetation). The representative reflectance spectra of these surface covers are shown in figure 5.41. The means (table 5.7) of percentage of surface covers and reflectance in bands R and NIR of both Cropscan and TM are calculated per transect in order to characterize the transects and to determine the correlations.

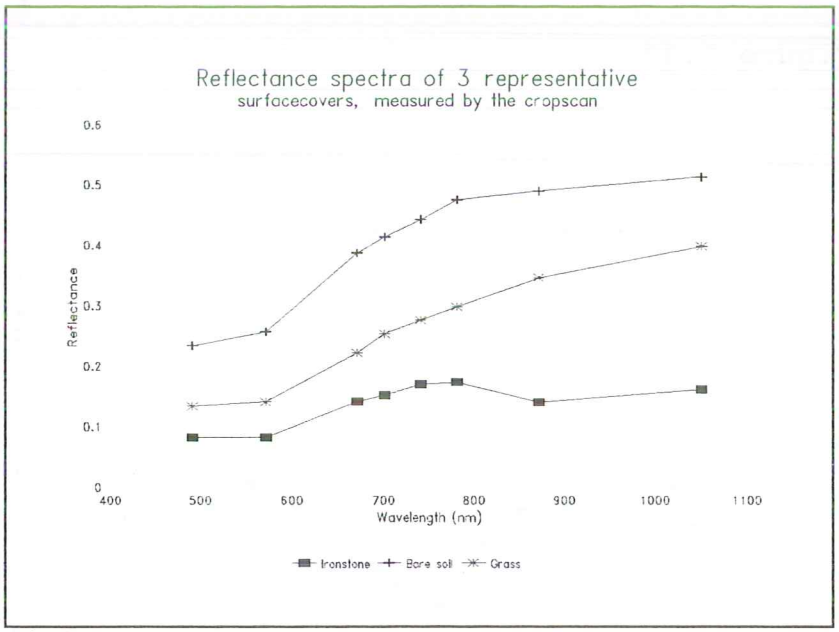

Figure 5.41

To compare the levels of reflectance in R and NIR measured by Cropscan and TM, the means (given in table 5.7) are presented in a scatter plot (figure 5.42). The scatterplot shows some interesting facts:

- Transect 1, 3, 5, 6 and 7 have nearly the same level of reflectance in NIR measured by TM.
- Reflectance measured by Cropscan shows a clear distinction between the transects 5 and 6 and the transects 1, 3 en 7.

The large amount of ironstone in transects 5 and 6 causes low reflectance in NIR, represented in relatively low Cropscan values. A possible explanation for the relative high TM-values could be a change in surface coverage in the period between the TM measurements (january 1988) and the Cropscan measurements (december 1993). The higher TM-values could result from a denser cover of grasses in 1988 compared with 1993. If this assumption is true and the process of a reducing vegetation coverage is structural there is an indication of land

degradation.

- Transect 2 and 4 show both for the TM and Cropscan high reflectance in R and NIR, caused by respectively a high percentage of grass and bare soil.

Table 5.7 Means of surface cover and reflectance measured by Cropscan and Landsat of all 7 transects.

Transect	Grass	Ironsto-ne	Bare Soil	C3	L3	C7	L4
1	25%	29%	46%	0.203	0.124	0.292	0.238
2	53%	30%	17%	0.210	0.117	0.322	0.227
3	26%	30%	44%	0.211	0.138	0.309	0.233
4	22%	8%	70%	0.260	0.172	0.351	0.305
5	2 %	49%	49%	0.200	0.147	0.234	0.242
6	15%	59%	26%	0.179	0.144	0.243	0.244
7	16%	44%	40%	0.233	0.143	0.304	0.235

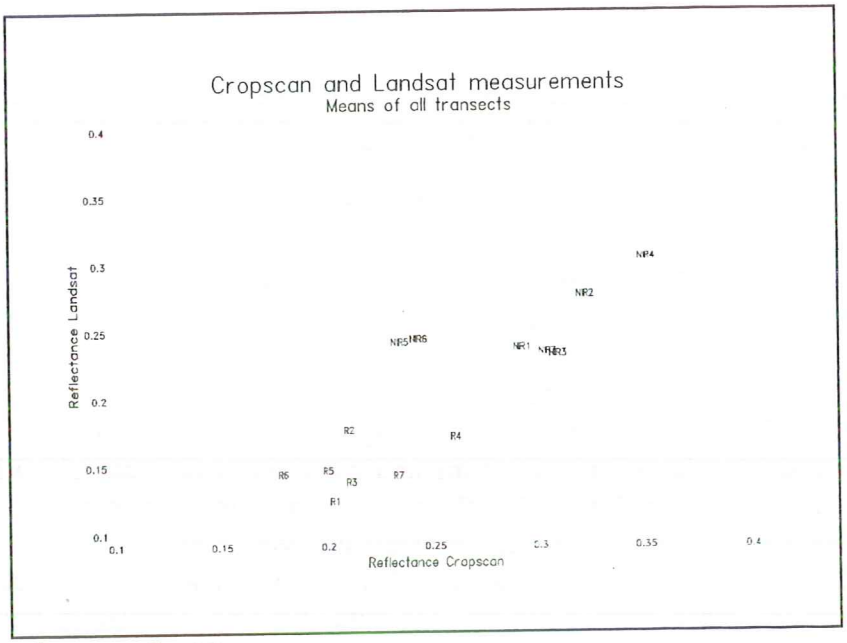

Figure 5.42

The scatter plot (figure 5.42) shows already some correlations. Table 5.8 shows the correlations of all the variables of table 5.7 calculated with simple regression.

Table 5.8 Correlation of surface covers, reflectance measured by Cropscan and by TM of R and NIR (band 3 and 4, respectively 7).
Significant correlation coefficients are underlined.

VARIABLE	GRASS	IRON-STON	BARE SOIL	C3	L3	C7	L4
GRASS	1						
IRONSTONE	-.44	1					
BARE SOIL	-.50	-.56	1				
C3	.10	-.82	.69	1			
L3	.49	-.40	-.06	.46	1		
C7	.61	-.91	.31	.81	.48	1	
L4	.40	-.67	.28	.63	.86	.63	1

With this regression analysis is assumed that two variables are correlated with each other if one variable explains 60 % or more of the variance of an other variable; $r^2 \geq 0.6$, so the regression coefficient $r \geq 0.7746$.

Table 5.8 shows the next results:
- C3 and C7 are strongly negative correlated with ironstone. The reflectance curves showed already the very low reflectance of ironstone (figures 5.33, 5.34 and 5.41).
- There are no other significant correlations of surface covers and reflectance measurements.
- The highest correlation of Cropscan and TM is of NIR ($r = 0.63$), but is not significant (nearly 40 % of the variance is explained).
- There is a mutual correlation between the two Cropscan bands and the two TM-bands, which is not surprising for measurements at the same time and place in different bands.

The conclusion about these correlations is:
- Cropscan and TM measurements are not significantly correlated with each other. Differences caused by the other scale, time and place (not exact enough to locate) are of strong influence on the correlation. On the basis of these measurements it is not sensible to predict Cropscan data with TM-measurements and vice versa.
- Cropscan data are significantly correlated with ironstone. These reflectance data are not correlated with the other surface covers. TM-data show no correlation with the surface covers. This means that either reflectance is dependent on more variables (surface covers) at the same time or of variables, which are not determined.

If the reflectance is dependent on more variables, is it possible to determine this dependence with multiple regression analysis, which calculates the dependence of one dependent variable on more independent variables (Webster and Oliver, 1990). The degree of change of the dependent variable per independent variable is expressed in the standardized partial regression coefficient (B) of the independent variable. Besides this regression coefficient the multiple determination R^2 is calculated. The multiple determination represents the amount of variance of the dependent variable, which is explained by the independent variables. With a Student's t-test is tested if a standardized independent variable significantly differs of the main mean

zero. The hypothesis H_0 of this test is that the standardized independent variable doesn't differ significantly of zero. The assumption is made that the H_0 is rejected if the probability of the $H_0 \leq 5\%$ ($p \leq 0.05$). When the standardized variable differs significantly of zero, it can be stated that this independent variable influences the dependent variable significantly (table 5.9).

A large part (75% of C3 and 89% of C7) of the variance of reflectance, measured by Cropscan is explained by surface covers.

- Ironstone is of strong influence on the reflectance in R and NIR.
- Bare soil is only of significant influence on C7. C7 is not dependent on grass. In the first instance this seems strange, but there are some explanations:
  - Yellow grass reflects in general high, but with a large variation because of the different kind of grasses, a different height of grasses (high grass causes a larger roughness of surfaces than low grass, so the reflectance of low grass will be higher) and the influence of the soil between the blades of grass.
  - In the range of band 7 there is an absorption dip of iron (figure 5.41). A measurement of a surface covered with grass and iron, will strongly be determined by iron.

Table 5.9 Multiple regression: The contribution of the surface covers to the explained variance of the Cropscan and Landsat-TM measurements.
Independent variables: IRONSTONE, GRASS and BARE SOIL.
Dependent variables: bands 3 and 7 of the Cropscan (C3 and C7) and bands 3 and 4 of the Landsat-TM (L3 and L4).

	IRONSTONE	GRASS	BARE SOIL
C3 R^2 = 0,7459	B = -0,0015 p = 0,0002	*B = -0,0005* *p = 0,0882*	
L3 R^2 = 0,2366		*B = 0,0006* *p = 0,0778*	
C7 R^2 = 0,8872	B = -0,0028 p = 0,000003		B = -0,0007 p = 0,0358
L4 R^2 = 0,4507	B = -0,0011 p = 0,0086		

N.B. These values are significant if a probability-level of 5 % is handled. The values, printed in *italic*, are only significant if a probability-level of 10 % is handled.

- Grass does influence the reflectance in R, both in Cropscan as in Landsat-TM measurements, at least if a probability level of 10% is handled. Apparently the variation of the reflectance in R is less than in NIR and is there no influencing absorption dip of iron.

A smaller part of the variance of the reflectance, measured by Landsat-TM is explained. The reflectance in R and in NIR, is explained for respectively 24% and 45% by two surface covers.

- Ironstone influences the reflectance in NIR.

- Grass has an influence on the reflectance in R (see above).

There are two possible reasons for this low explained variance:

- The reflectance measured by the TM is dependent on more and other variables, which are not measured.
- The determinations of the surface covers don't correspond exactly with the TM-measurements, because of a small difference of location of the transects.

On the basis of these results it is possible to predict the coverage by ironstone both with Cropscan and TM with a probability of 95%. The coverage of grass can be predicted with a probability of 90% with these two methods. The coverage of bare soil can only be predicted with the help of the Cropscan, for only C7 is significantly influenced by bare soil with a probability of 95%.

SPATIAL DEPENDENCE

In the paragraph above dependence has been investigated of the selected reflectance variables (C3, C7, L3 and L4) and surface covers (Grass, Ironstone and Bare soil) on each other. In this paragraph spatial dependence of these variables will be investigated. If a variable is spatial dependent it is possible to determine spatial behavior of this variable. This means a certain distance which still explains the variance of a variable and on which a variable can be interpolated.

A variogram is computed of each of the selected variables (Table 5.10 and 5.11) for transects 4 and 7. In a variogram semi-variance of a variable is plotted against the distance between the data points (lag). In theory semi-variance at lag zero is zero, but in reality the measured semi-variance tends towards a positive value near a lag distance of zero. This value is called the *nugget variance* c_0 (Webster and Oliver, 1990)

Usually semi-variance is small at short lags and increases steadily with increasing distance. A steep initial slope shows that there is more change with increasing separation. The semi-variance increases until eventually its maximum is reached and the graph curves horizontally. This level is called the *sill variance (c)*. The sill variance estimates the variance (in advance) of the random variable. The lag at which the variogram reaches its sill is the *range (r)*. This is the limit of spatial dependence, beyond this the variance has no relation to the separating distance.

Lines are fitted through the variograms with a Gaussian model. This model showed the best fit for most of the variables and is used for all variables for a good comparison. The ratio SS_D/SS_T is a measure for the quality of fit. The total variance (SS_T) is computed together with the variance caused by the difference of the points compared to the fitted curve (SS_D). The ratio SS_D/SS_T is the percentage of variance, compared to the total variance (SS_T), not explained by the fit. So this parameter has to be as small as possible: The more variance of the total variance is explained by the fit, the smaller the parameter SS_D/SS_T, the better the fit.
The parameter $(c_0/(c+c_0))*100\%$ expresses the percentage of nugget compared to the sill. A variable with low spatial correlation shows a value of this parameter in the neighborhood of 100%.

The parameters mentioned above are computed for transect 4 and 7 and are shown in respectively Table 5.10 and 5.11.

The lag increments used for the Cropscan measurements and the surface covers are 10m. and for the Landsat-TM measurements 25m. The maximal lag distance is one third of a transect, so the this distance is different for the both transects.

Table 5.10 Parameters of the variograms of TRANSECT 4

	c_0	c	r	SS_D/SS_T	$(c_0/(c+c_0)) * 100\%$
C3	$1.39*10^{-3}$	$6.45*10^{-4}$	8.34*10	0.350	68.30
L3	$3.70*10^{-5}$	$3.33*10^{-4}$	$1.44*10^{2}$	0.038	10.00
C7	$3.09*10^{-3}$	$1.53*10^{-3}$	7.60*10	0.178	66.88
L4	$1.83*10^{-4}$	$1.62*10^{-3}$	$1.43*10^{2}$	0.010	10.15
GRASS	5.08*10	-2.73*10	$5.00*10^{2}$	0.964	100
IRON-STONE	$5.74*10^{2}$	$1.48*10^{2}$	4.88*10	0.526	79.50
BARE SOIL	$5.33*10^{2}$	$1.18*10^{2}$	5.25*10	0.716	81.87

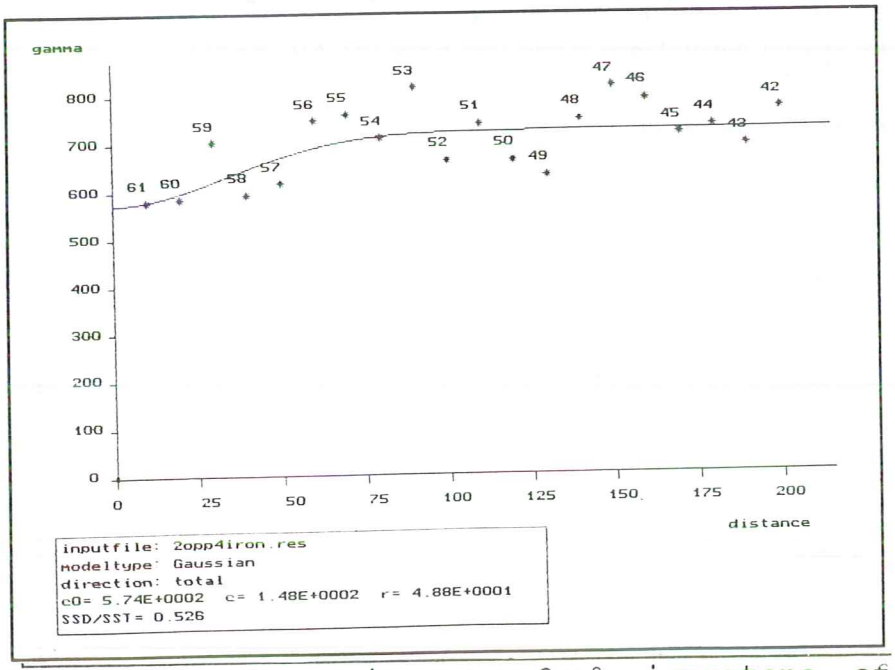

Figure 5.43: Variogram of % ironstone of transect 4 (gamma = semi-variance)

Table 5.10 shows the next facts of transect 4:

- All variables except L3 and L4 have no or little spatial correlation because the parameter $(c_0/(c+c_0))*100\%$ is larger than about 35%. This means that the sill is smaller than the nugget variance, so the variable exists for more than 50% of nugget-variance (figure 5.43). These variables with a very low spatial component can be supposed as uniform over the

whole transect.

- The Landsat-TM measurements show spatial dependence up to a lag distance of somewhat more than 140 meters. These are also the only measurements with a good fit.

Table 5.11 Parameters of the variograms of TRANSECT 7

	c_0	c	r	SS_D / SS_T	$(c_0/(c+c_0)) * 100\%$
C3	$1.51*10^{-3}$	$2.49*10^{-3}$	$1.25*10^{2}$	0.104	37.75
L3	0	$2.47*10^{-4}$	5.79*10	0.021	0
C7	$3.53*10^{-3}$	$6.13*10^{-3}$	$1.08*10^{2}$	0.100	36.54
L4	$3.18*10^{-5}$	$9.48*10^{-4}$	6.29*10	0.003	3.25
GRASS	$3.85*10^{2}$	$1.98*10^{2}$	$1.45*10^{2}$	0.658	66.04
IRON-STONE	$6.65*10^{2}$	$5.34*10^{2}$	$1.03*10^{2}$	0.341	55.46
BARE SOIL	$4.01*10^{2}$	$9.24*10^{2}$	$1.92*10^{2}$	0.053	30.26

Table 5.11 shows the next results for transect 7:

- There is more spatial dependence along this transect: All variables are well or reasonably correlated except Gras and Ironstone.
- The Landsat-TM measurements even have a nugget variance of nearly zero (figure 5.44), but the range is smaller than in transect 4.

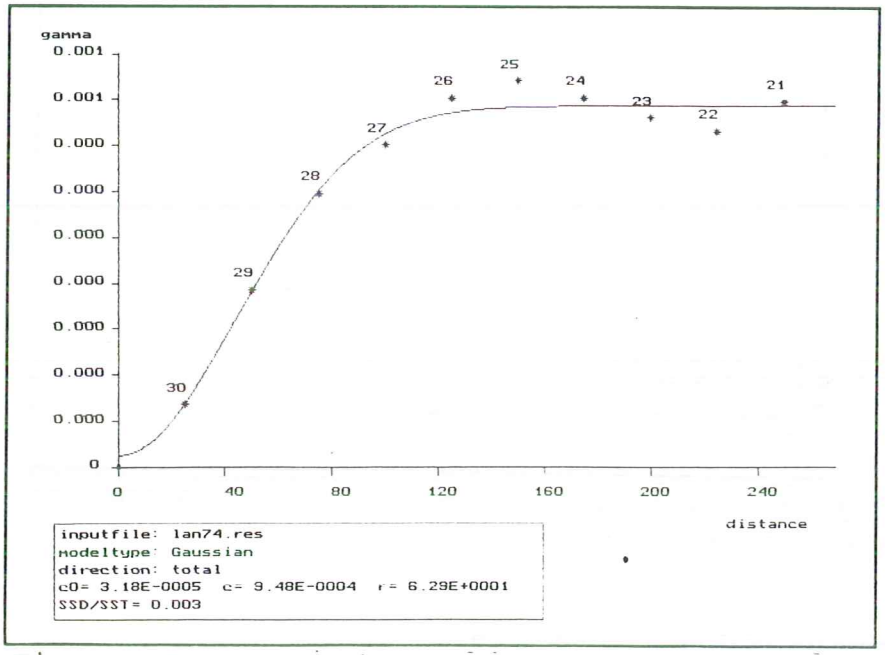

Figure 5.44: Variogram of TM band 4 for transect 7 (gamma = semivariance)

It is striking that Landsat-TM measurements show a lot more spatial correlation than Cropscan

measurements together with surface covers. Also the best variogram of Cropscan measurements shows 50% nugget variance (figure 5.45). The main explanation is the method of sampling. Every 10m. one sample of 1 m^2 is taken, so this is also the shortest possible lag distance.

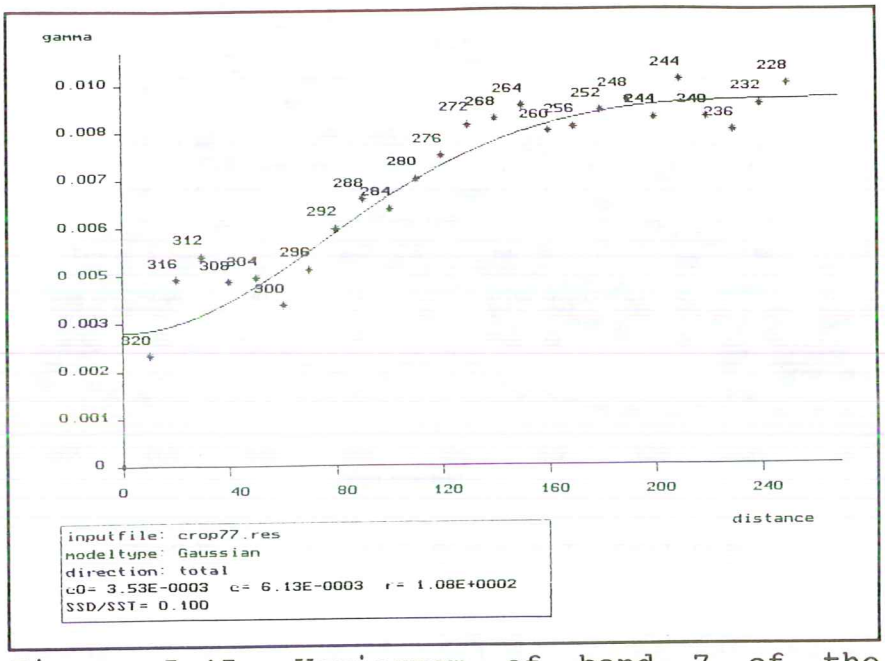

Figure 5.45: Variogram of band 7 of the cropscan of transect 7 (gamma = semivariance)

This lag appears to be too large on the basis of this support (support = size of sampling in relation to the area). If a smaller lag was used with the same support there would be more spatial dependence. The measurements in this research were too little in heterogenic units like transect 4. The succeeding measurements show strong peaks and dips, where for instance respectively some grass blades or ironstone are measured. The short distance relations can only be determined if some of the Cropscan measurements are taken closer together, for example in a nested way.

Transect 7 is more homogeneous and exists of large surfaces with the same cover (figure 5.46). Although there are still some peaks and dips, there is a reasonable spatial correlation of bare soil.
Figure 5.47 shows the constant increasing variogram of bare soil in this transect. This continual increasing semi-variance with increasing lag distance indicates that there is a possible trend in this transect. In that case the variogram does not comply with the condition of stationarity.
Figure 5.46 showed that the second part of transect 7 reflects a lot higher than the first parts because of the large amount of crusts in the second part of the transect. Therefore it would be better to divide this transect in two parts to comply with the condition of stationarity.
Although there is spatial correlation of bare soil in this transect, the nugget variance is still nearly 50% of the sill variance and the other surface covers show little spatial correlation. So also here the lag distance is too long for short distance relations.

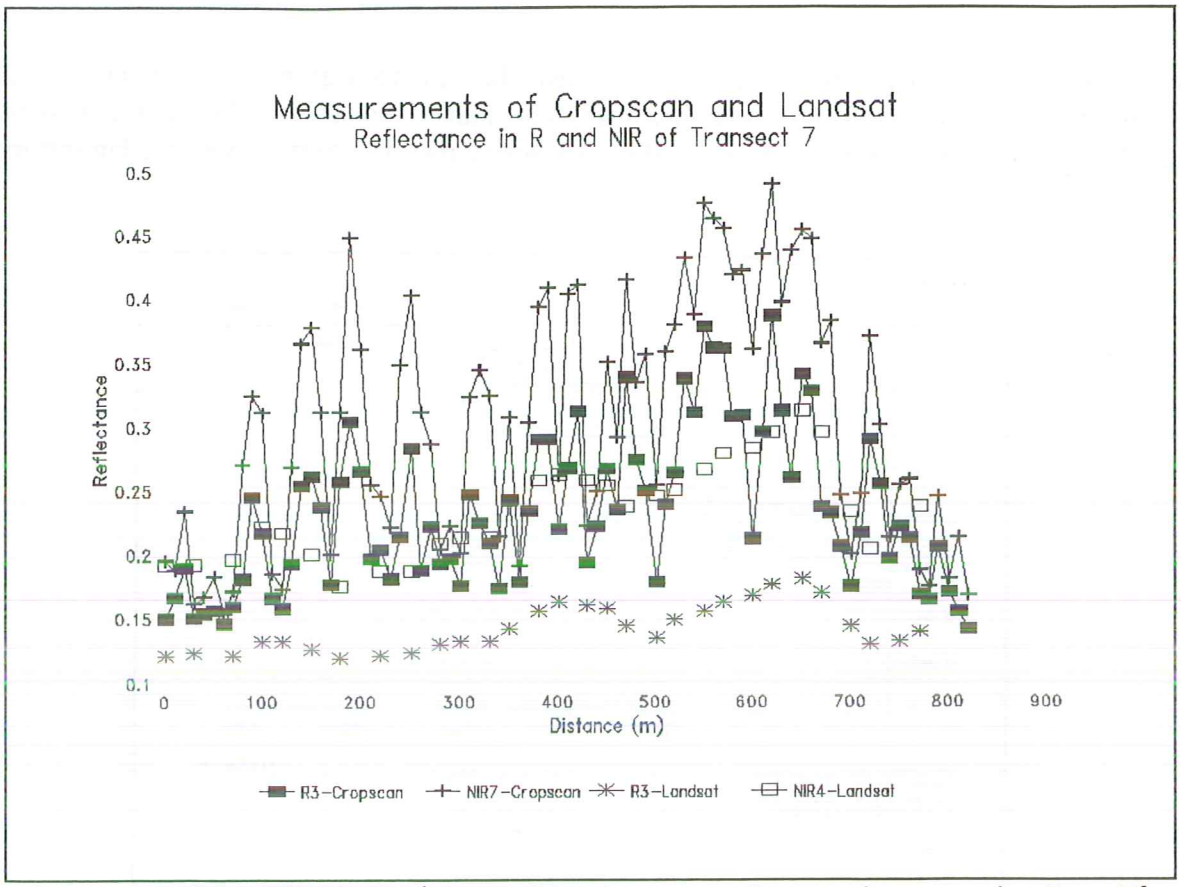

Figure 5.46 Change in reflectance along transect 7; The transect exists of two parts, before 350 m with relative low reflectance and after 350 m with higher reflectance.

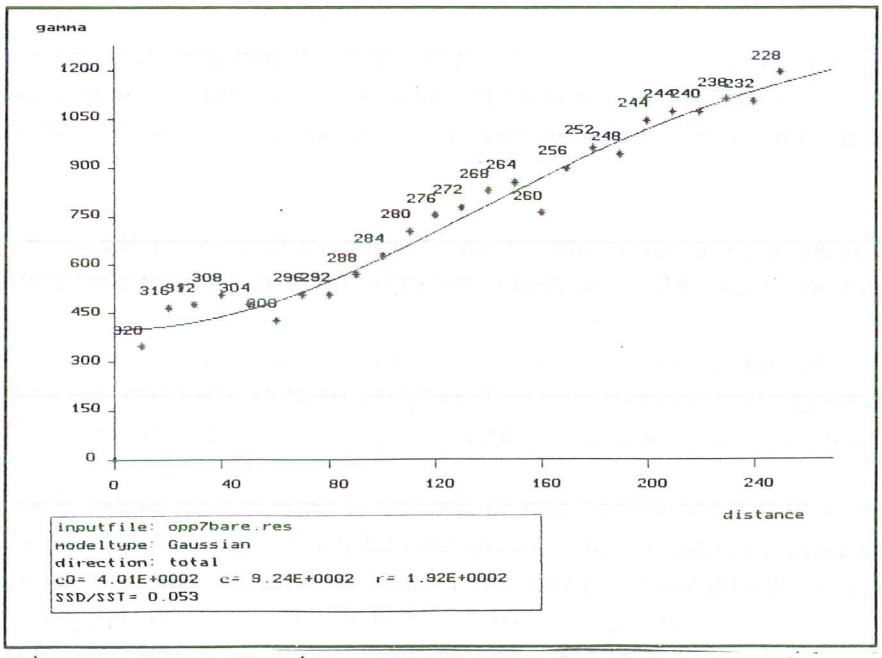

Figure 5.47 Variogram of the % of bare soil of transect 7 (gamma = semivariance)

It is possible to determine long distance relations if the support is larger. These are well determined by the Landsat-TM because of the measuring of larger surfaces (of $25m^2$) which are also joined together. This is the reason why a well spatial correlation of long distances is determined with the Landsat-TM. The same result would be reached if there are a lot of measurements with Cropscan and surface descriptions performed next to each other. If this results in a better spatial correlation of Cropscan measurements and surface covers, they can be related to TM more directly.

Summarized the conclusions of this paragraph are:
- TM measurements are strongly spatially correlated.
- Cropscan measurements and surface covers show spatial correlation in large uniform surfaces, but in most cases there is too much nugget variance. This means that the variable has a low spatial component and can be supposed as uniform over the transect. This high nugget variance is caused by the method and scale of the cropscan measurements and surface descriptions:
  - The measurements are too randomly performed.
  - The support is too small, so larger surfaces are to be measured when the same distance is used.
  - The lag is too large, it would be useful to perform some measurements on shorter distances and in a nested way.
- TM measurements are useful to determine long distance relations.
- Cropscan measurements could be useful to determine both large and short distance relations if respectively the support is large enough and the distances between the measurement points short enough.

CONCLUSIONS

- Spectral variation within soil mapping units depends on the difference in surface covers and the method and scale with which the reflectance of these covers is measured.

- TM measurements show differences in reflectance between extremes in surface covers like vegetation and ironstone. But the represented variation is little and the calculated correlation with the surface covers is weak because of mixing of reflectance of surface covers within a pixel. Besides, it is difficult to link the measurements with the corresponding surface covers in the field. The same problem of not exactly corresponding transect appears with comparing the two methods of Cropscan measurements and the TM measurements.

- Cropscan measurements are performed in two ways:
  - Method 1 measured three times random in each estimated homogeneous unit along a transect with a surface coverage estimation of the whole unit.
  - Method 2 measured one time in each ten meter with a surface coverage estimation of the measured square meter.
- Method 1 of the Cropscan is best to compare with TM, if the measurements of this method are representative for the cover unit and registered including the distance between these measurements and an estimation of the surface cover exactly on the measure point.

- In this research the results of method 2 are best, because of the more accurate registration of the surface covers corresponding with the measurements. These point measurements on a distance of 10 m lead to problems of difference of scale with comparison of the TM measurements. Because of the point measurements this method shows also a larger variation in reflectance.
- The application of a moving average on the Cropscan data provides a solution for these scale-problems.

- No correlations have been found between the Cropscan and TM measurements with simple linear regression, because of the differences between the data sets, mentioned above. This analysis was based on the means of the transects and also used to analyze the correlation with the surface covers.
- TM measurements show no correlation with surface covers, because of the same reason of the non-correlation with Cropscan measurements, mentioned above.
- There is a correlation between surface cover Ironstone (ironcrust and gravel) and reflectance in R and NIR measured by Cropscan. Ironstone is a distinct variable for its extreme low reflectance, clearly to distinguish from grass and bare soil. These two surface covers reflect a lot higher, but are difficult distinguish from each other because there is more variation in the variables themselves. That is the reason why they are not correlated with Cropscan measurements.

- A multiple regression analysis shows that reflectance measured by the Cropscan is significantly dependant on a large part of the surface covers at the same time.
- A little part of the variance of the reflectance measured by the TM is explained by the surface covers (mainly by ironstone).
- The conclusion is that the coverage of ironstone can be predicted by both Landsat-TM and Cropscan and the coverage of grass and bare soil only by Cropscan measurements.

- Spatial dependence determines uniformity within the soil mapping unit. TM measurements are strongly spatially correlated, so on basis of these the 7 plateaus appear to be clearly distinctive units.
- Cropscan measurements and surface coverage show some spatial correlation in large uniform surfaces, but not in heterogeneous units. In these units there are too less measurements on too large distances to determine spatial dependance.

- On large scale there is spatial dependance for TM. There is also already a multiple correlation of TM with Ironstone. So with this correlation and the spatial dependence of TM it is possible to predict the percentage of Ironstone coverage on plateaus.
- On small scale there is a multiple correlation of Cropscan with all surface cover types. So it is possible to predict surface coverage on places where measurements are performed with Cropscan. Interpolation is not yet possible, for there is no spatial correlation measured. But also this will be possible with an nested sampling design on shorter distances.

5.3.4 AERIAL PHOTOGRAPHS AND LANDSAT TM FOR SOIL MAPPING

Aerial photographs and Landsat TM image contain a different kind of information. But they are both useful for soil mapping.
Advantage of aerial photographs over TM images are (Lillesand and Kiefer, 1987):
-Since a TM image consist of pixels, the information is discontinuous. An aerial photograph is continuous, so discrete elements such as roads can be distinguished;
- Pixels of 25m of a TM image provide a lower resolution than aerial photographs. This results in e.g. less distinct borders of landscape elements on the TM image;
-Stereoscopic observation of aerial photographs makes a three-dimensional analysis of a landscape possible.

The advantage of TM images over aerial photographs are:
- TM images provide information of reflectance in 7 narrow bands, also in the non-visible light, while black and white aerial photographs only have one broad band in the visible light. Each of the 7 bands of the TM image gives information about different properties of the surface like moisture content, vegetation, soil and geology.
- As opposed to aerial photographs, TM data are digital. This makes it possible to perform digital image processing techniques. Although photos can be scanned to get these in a digital format, a range of corrections have to be made before the digital information (for black and white photographs only 1 band) can be used for image processing.

A combination of aerial photographs and TM images gives a good base for soil mapping. In the study area a range of geomorphological landscapes can be distinguished well using stereoscopic aerial photographs. For example borders of ironstone plateaus can be delineated easily, while on TM images due to shadow it is difficult to delineate. Geological differences can be discerned very well using TM data, green and red schists can be separated.
Active vegetation can be discerned very well using information of Landsat TM band 4 in combination with visible bands. Also different types of crusts can be discerned much better with TM. For example transect 7 on the ironstone plateau (chapter 5.3.3), appeared to be homogeneous on the aerial photograph. On the satellite image a gradual change from light to dark was observed which coincide in reality with a change from non crusted to crusted soil.

As a conclusion one may state that the information of aerial photographs and TM images are complementary. Therefore on scales as used in this research they have to be used both.

6. CONCLUSIONS AND DISCUSSION

The main objectives of this study were: (1) to study the genesis and produce a soil map of the Kaya area, Burkina Faso; (2) to understand the Landsat Thematic mapper satellite images of the area for mapping.

The first objective has been fulfilled by studying the genesis of the area, in combination with the mapping of soils using satellite images, aerial photographs and fieldwork.
A genetical study revealed that the parent material consists of both plutonic rocks and those subjected to different degrees of metamorphosis. The presence of high amounts of amorphous iron and goethite indicates that the soils have been subjected to ferralitisation, an extreme case of weathering and leaching. This process is typical for wet tropical climates. The presence of haematite, clay illuviation and the effects of ferrolyses indicate alternating wet and dry seasons, so a monsoon climate. The presence of secondary lime and -probably- of gypsum are symptoms of very dry climates. As the effects, of each of the above mentioned processes, alternate in the studied soil samples indicates several changes from wet tropical to savannah (or desert), or visa versa, climates.
Fieldwork showed that, with soil mapping at this scale, mono temporal satellite images are very useful to indicate the general geomorphology but that most information, to produce a soil map of the required detail, has to be obtained from aerial photographs. With the availability of multi-temporal images, the usefulness of satellite images are expected to increase substantial. The objective of the production of a soil map has been met by its production (Figure 4.14).
In the mapping of soils at this scale, it was observed that the information of aerial photographs and TM images are complementary.

To achieve the second objective a range of studies has been performed:

a. the relation between soil and vegetation reflectance and their properties;
b. the relation between field reflectance and at-satellite planetary reflectance and between field reflectance and laboratory reflectance;
c. possibilities of landscape classification based on satellite images and fieldwork;
d. the abundance of typical surfaces within a pixel using mixture modelling;
e. the variation in spectral values within one soil mapping unit using geostatistics.

(a) The relation between reflectance and soil and vegetation properties was studied using a combination of field and laboratory reflectance. It was shown that the mini-IRIS field radiometer presented good results for the first part of the spectrum (up to about 1000nm). However the second part of the spectrum (1000-2500nm) could not be measured adequately in the field. For the field measurements it could be concluded that some major soil and vegetation types can be discriminated relatively easily on their spectral characteristics.

Concerning the vegetation, their coverage percentage is of great importance when considering scatterplots and spectral curves. When coverage is low reflectance is also influenced by bare soil characteristics. Some discriminations can be made, however: green grasses and shrubs can be discriminated due to a different green and red reflectance. Yellow grass can be discriminated from red or green grass, because of different reflectance in the visible part. In this manner green shrubs can be discriminated from brown shrubs, too. A further distinction in reflectance between species is hardly possible.

Most bare soil reflectance curves show an increase in reflectance with increasing wavelength in the visible part of the spectrum. This is due to absorption in the ultraviolet

part of the spectrum by iron, having their influence up to the visible part of the spectrum. The reflectance between 700 and 1000nm is in general the highest. Most prominent absorption features are due to iron. Soils with a very high iron content show the lowest overall reflectances. Erosion surfaces, crusts and sandy surfaces do not show such strong absorption features as stones. Still differences between greenschists, redschists and granite could be observed.

For a small selection of samples reflectance was determined in the laboratory. With the Infraspectrometer reflectance could be determined between 700 and 2500nm. Most reflectance curves show a convex shape, with distinct absorption features caused by OH^- or H_2O (around 1400 and 1900 nm), iron (900 nm), and kaolinite (about 2200 nm). The spectral curves were analyzed using the program DISPEC, which enables to calculate a range of dip characteristics, like location, depth and width. Good results have been found for location of the dip and irontype, and depth of the dip and percentage kaolinite. However the limited number of samples makes firm conclusions difficult.

(b) Field reflectance could not be converted straightforward to satellite reflectance. Therefore for the different image processing techniques, like mixture modelling and classification, data from the satellite itself have been used. Satellite calibration has been evaluated. This evaluation can be used in subsequent studies if information on weather conditions is present and if reliable field reflectance measurements over the whole spectrum are available. In the analysis of satellite data for this study, field measurements were vital for understanding the spectral signatures given by the satellite.

(c) Since supervised classification has been investigated already extensively by Belemvire, emphasis in this study was to unsupervised classification and mixture modelling. It was shown that unsupervised classification (clustering) of the satellite image gives a good impression of landscape types, especially when clustering is applied in different steps and also clusters are combined. The manual classification, based on a combination of clustering, soil map and field work, gives more information on vegetation characteristics. Extrapolation of the computer-based classification to other areas is possible if these areas do not differ too much in physiography and vegetation. However extrapolation can not be done without some fieldwork in order to be able to adequately interpret and process the imagery.

(d) The unmixing of pixels from the Landsat TM image of January resulted in different surface type maps of percentages covered by green schists, cuirasse plateaus, vegetation, erosion areas, red schists and manganese hills. Such types of maps are especially useful in areas with a large variability over short distances. The results are promissing, but a better selection of endmembers will enhance the accuracy of these types of maps.

(e) The variation in spectral values within one soil mapping unit, the plateaus, has been investigated using geostatistics. Spectral variation within this soil mapping unit is caused by different surface covers like grass, bare soil and ironstone. With multiple regression these surface covers are well correlated with Cropscan measurements. So with help of cropscan measurements surface coverage can be predicted. The correlation with Landsat TM measurements is less, for exact location of these measurements is difficult and so the comparision with ground measurements. Semi-variance analysis shows some spatial correlation of both reflectance measurements and surface covers. However results would be better if nestled sampling design was selected.

It is believed that the results of this study are a good base for further work in the field of remote sensing and soil science for the Province of Sanmatenga at both detailed and less detailed scale.

At a detailed scale field reflectance measurements can be used to map surface characteristics. To make optimal use of it, calibration of the radiometer has to be improved.

Large scale aerial photographs can be a good aid for mapping on village level.

At the scale used in this study, results of mixture modelling and supervised classification can be ameliorated having: (1) imagery from the wet season, (2) adequate selection of endmembers, (3) calibration of radiometer.

At smaller scales, mapping can be done mainly using satellite imagery, including imagery from the wet season, and a fieldcheck.

REFERENCES

Ambrosi, J.P. and Nahon, D., 1986.
Petrological and geochemical differentiation of lateritic iron crust profiles. Chemical Geology, 57 (1986) 371-393.

Ambrosi, J.P., Nahon, D. and Herbillon, A.J., 1986.
The epigenetic replacement of kaolinite by hematite in laterite - petrographic evidence and the mechanisms involved. Geoderma, 37 (1986) 283-294.

Anonymous, 1990.
ERDAS Field Guide, version 7.4, Atlanta.

Anonymous, 1990.
Cropscan, users manual, Internal Publication Cropscan Inc., Fargo ND, USA, 25p.

Anonymous, 1991.
Manual DISPEC version 1.0 California Institute of Technology. Jet propulsion laboratory, Pasadena, California.

Anonymous, 1992a.
ARC/INFO Data Model, Concepts, & Key Terms, Environmental Systems Research Institute, Inc., Redlands CA, USA, 176 p.

Anonymous, 1992b.
Understanding GIS, The ARC/INFO Method, Environmental Systems Research Institute, Inc., Redlands CA, USA, 426 p.

Anonymous, 1993.
Operation manual GER's mini-IRIS RT spectroradiometer. Geophysical and environmental research corporation (GER), New York.

Asrar, G., 1989.
Theory and applications of optical remote sensing. John Wiley & sons, New York.

Belemviré, 1993.
Contribution à l'étude de la cartographie des états de surface et à l'estimation de la biomasse ligneuse aerienne à partir de l'image Landsat Thematic Mapper. Université de Ouagadougou/Université Agronomique de Wageningen, Ouagadougou.

Blot, A., Leprun,J.C. and Pion, Jc. 1978
Notes des membres et coffespondants et notes presentées ou transmises par leurs soins. C.R. Acad. Sc. Paris t. 286, serie D. 1331-1334

Bougère, J. 1976
Recherches sur les paysages Soudano-Birrimiens de la région de Kaya (Haute Volta). Université Paris.

Boulange, B., Bocquier, G., 1983.
Le role du fer dans la formation des pisolites alumineux au sein des cuirasses bauxitiques lateriTiques. Sci. Géologiques Mém., 72:29-36. Institut de géologie, université Louis Pasteur, Strasbourg.

Boulet, R. 1968.
Etude Pédologique de la Haute-Volta Région: centre Nord. Centre 0RST0M de Dakar-Hann, L'Institut Gégraphique National, Paris.

Boulet, R. 1972.
Modalités d'action du lessivage dans les sols tropicaux développés sur granites (Haute Volta). Étude micromorphologique. Cah. ORSTOM vol X, no 4: 321-343.

Buiten H.J. and Clevers, J.G.P.W., 1990
Remote Sensing, theorie en toepassingen van landobservatie, Pudoc Wageningen

Burrough, P.A., 1986
Principles of Geographical Information System for Land Resources Analysis, Oxford University Press
Casenave, A. and C. Valentin, 1989.
Les états de surface de la zone sahélienne. Influence sur l'infiltration. Editions de l'ORSTOM, Bondy, 230p.
Dam, O. van, 1993
Recherche du sol et de la télédetection a Kaya (Burkina Faso). Antenne Sahélienne, Universite de wageningen, Universite de Ouagadougou.
Ducellier, J. 1963
Contribution a 1'étude des formations cristallines et métamorphiques du centre et du nord de la Haute-Volta. Carte 1:500 000. Mémoires du Bureau de Recherches Geoloques et Minières, no. 10, 1963.
Eastman, J.R., 1992.
IDRISI User's Guide version 4.0 Clark University, Graduate School of Geography, Worcaster, Massachusetts
ERDAS, 1990.
Field guide ERDAS version 7.4. ERDAS, Atlanta.
Epema, G.F., 1992.
Spectral reflectance in the Tunisian desert. 1992 Agricultural University Wageningen.
FAO, 1977
Soil map of the world (1:5 000 000). Volume VI Africa. Unesco-Paris.
FAO, ISRIC. 1990
Guidelines for soil description, 3rd edition, FAO, Rome.
FAO-Unesco, 1974
Soil map of the world (1:5 000 000). Volume I, legend.
FAO-Unesco, 1988
Soil map of the world. Revised legend. World soil resources report 60.
Goetz, A.F.H., 1989.
Spectral remote sensing in geology. Chapter 12 in G.Asrar, Theory and applications of optical remote sensing, John Wiley and sons, 1989, p.491-526.
Grove, C.I., S.J. Hook, E.D.Paylor II, 1992.
Laboratory reflectance spectra of 160 minerals, 0,4 to 2.5 micrometers, NASA, Jet propulsion laboratory, California institute of technology Pasadena, California.
Grove, C.I., S.J. Hook and E.D. Paylor II. 1992.
Users manual for DISPEC. 1992
Gurney, R.J. and D.K. Hall, 1983.
Satellite-derived surface energy balance estimates in the Alaskan Sub-Arctic. Journal Climate and Applied Meteorology, 22, p.115-125.
Guyot, G., 1989.
Proriétés spectrales des sols et de la végétation: application à la télédetection. INRA, Montfavet.
Harland, W.B, 1989 et al.
A geologic time scale 1989, Cambridge university press.
Hottin, G. and Ouedraogo, O.-F., 1975.
Carte Géologique a 1:1 000 000 de la République de Haute Volta, notice explicative Direction de la Géologie et des mines, Ministère du commerce, du développement industriel et des mines, République de Haute-Volta, 1975.

Iqbal M., 1983
An introduction to solar radiation.Department of mechanical engineering The universityy of Britoch Colombia, Vancover, Britich Columbia, Canada.
Kaloga, B. 1966.
Etude pédologique des bassins versants des volta blanche et rouge en Haute-Volta. Centre ORSTOM de Harm-Dakar, L'Institut Géographique National, Serie Pedol; Vol IV, no 1-1966, p.23-60, Paris.
Kruse, F.A., A.B.Lefkoff, J.W.Boardman, K.B,Heidebrecht, A.T.Shapiro, A.F.H.Goetz, 1993.
The spectral image processing system (SIPS) Interactive visualization and analysis of imaging spectrometer data. Remote sensing of environment 44,145-163, 1993.
Leneuf, N. and Aubert, G. 1960.
Essai d'évaluation de la vitesse de ferrallitisation. Proc. 7th Int. Congr. Soil Sci., Madison, Wisc., U.S.A.:225-228.
Léprun, J.P. 1979.
Les cuirasse ferrugineuses des pays cristallins de L'Afrique occidentale sèche: genese, transformations, degradation. Sciences pédologiques memorie no 58. Institut de géologie, université Louis Pasteur, Strasbourg.
Markham, B.L., and J.L. Barker, 1985.
Spectral characterization of the Landsat Thematic Mapper sensors. Int. J. Remote Sensing, 6(5):697-716.
Maydell, H.-J., von, 1990.
Arbres et arbustes du sahel; leurs caractéristiques et leurs utilisations. GTZ, Eschborn.
McFarlane, M.J. 1976.
Laterite and landscape, academic press inc., London
Morgan, W.B. and Pugh, J.C. 1969
West Africa. Methuen, London.
Mulders, M.A., 1987.
Remote Sensing in Soil Science, Developments in soil science 15, Elsevier, Amsterdam.
Mulders, M.A. and G.F. Epema, 1992.
Application of multispectral and multitemporal remote sensing in landcover and soil mapping of tropical and temperate zones. Wageningen Agricultural University, 1992.
Péron, Y. and Zalacain, V. 1975
Atlas de la Haute-Volta. Editions jeune Afrique. Institut Géographique National, Paris.
Reeuwijk, L.P. van. 1987
Procedures for soil analyses, Technical paper no. 9 (2nd edition); ISRIC, Wageningen.
Soil Survey Staff, 1975
Soil Taxonomy: A basic system for making and interpreting soil surveys. Agric. handbook no.436, SCS, USDA. US Government printing office, Washington D.C.
Verhoef, W., 1989.
The calculation of satellite overpass time, Chapter 3, in: National Points of Contact, Products and Services "Annex to Remote Sensing Newsletter no 38", NLR, Emmeloord.
Wambeke, A. van, 1982.
Calculated soil moisture and temperature regimes of Africa. Technical Monograph 3. Soil management services, Ithake, NY.

Webster, R. and Oliver, M.A., 1990
Statistical Methods in Soil and Land Resource Survey, Oxford University Press
Whittow, J. 1984.
Dictionary of physical geography, The Penguin, London.

APPENDIX 2.1 CHARACTERISTICS OF LANDSAT THEMATIC MAPPER IMAGES

HEADER INFORMATION OF LANDSAT TM IMAGE OF JANUARY 8, 1991.

```
PRODUCT =92090002-01
WRS =195/05100
ACQUISITION DATE =19910108
SATELLITE =L4
INSTRUMENT =TM10
PRODUCT TYPE =MAP ORIENTED
PRODUCT SIZE =FULL SCENE
TYPE OF GEODETIC PROCESSING =SYSTEMATIC
RESAMPLING =CC
RAD GAINS/BIASES =  1.09644/-.00439  2.44842/-.01987
TAPE SPANNING FLAG=1/1
START LINE #=    1
LINES PER VOL= 8180
ORIENTATION =  0.00
PROJECTION =UTM
USGS PROJECTION # =     9
USGS MAP ZONE =    30
USGS PROJECTION PARAMETERS =
0.6378206400000000D+07   0.6356583800000000D+07   0.9996000000000000D+00
0.0000000000000000D+00  -0.3000000000000000D+05   0.0000000000000000D+00
0.5000000000000000D+06   0.0000000000000000D+00   0.0000000000000000D+00
0.0000000000000000D+00   0.0000000000000000D+00   0.0000000000000000D+00
0.0000000000000000D+00   0.0000000000000000D+00   0.0000000000000000D+00
EARTH ELLIPSOID =CLARKE_1866
SEMI-MAJOR AXIS =6378206.400
SEMI-MINOR AXIS =6356583.800
PIXEL SIZE =25.00
PIXELS PER LINE= 8790
LINES PER IMAGE= 8180
UL 0023615.1388W 135744.3698N    542750.000   1543500.000
UR 0003414.4016W 135701.8404N    762475.000   1543500.000
LR 0003519.0300W 120611.0114N    762475.000   1339025.000
LL 0023625.6804W 120647.7311N    542750.000   1339025.000
BANDS PRESENT =1,2
BLOCKING FACTOR =   3
RECORD LENGTH =26370
SUN ELEVATION =40
SUN AZIMUTH =135
CENTER 0013552.3743W 130124.9899N    652048.897   1440076.532  4373  4138
OFFSET=-210 REVB
```

HEADER INFORMATION OF LANDSAT TM IMAGE OF MAY 7, 1988.

```
PRODUCT =92090003-01
WRS =195/05100
ACQUISITION DATE =19880507
SATELLITE =L4
INSTRUMENT =TM10
PRODUCT TYPE =MAP ORIENTED
PRODUCT SIZE =FULL SCENE
TYPE OF GEODETIC PROCESSING =SYSTEMATIC
RESAMPLING =CC
RAD GAINS/BIASES =  1.09644/-.00275  2.44807/-.02048
TAPE SPANNING FLAG=1/1
START LINE #=     1
LINES PER VOL= 8190
ORIENTATION =  0.00
PROJECTION =UTM
USGS PROJECTION # =      9
USGS MAP ZONE =     30
USGS PROJECTION PARAMETERS =
0.6378206400000000D+07    0.6356583800000000D+07    0.9996000000000000D+00
0.0000000000000000D+00   -0.3000000000000000D+05    0.0000000000000000D+00
0.5000000000000000D+06    0.0000000000000000D+00    0.0000000000000000D+00
0.0000000000000000D+00    0.0000000000000000D+00    0.0000000000000000D+00
0.0000000000000000D+00    0.0000000000000000D+00    0.0000000000000000D+00
EARTH ELLIPSOID =CLARKE_1866
SEMI-MAJOR AXIS =6378206.400
SEMI-MINOR AXIS =6356583.800
PIXEL SIZE =25.00
PIXELS PER LINE= 8840
LINES PER IMAGE= 8190
UL 0023246.9256W 135655.1776N     549000.000    1542000.000
UR 0003005.1949W 135610.5268N     769975.000    1542000.000
LR 0003111.6640W 120511.9039N     769975.000    1337275.000
LL 0023259.0082W 120550.4424N     549000.000    1337275.000
BANDS PRESENT =12
BLOCKING FACTOR =    3
RECORD LENGTH =26520
SUN ELEVATION =59
SUN AZIMUTH =079
CENTER 0013159.2617W 130051.1867N     659078.264    1439077.537   4404   4118
OFFSET=  74 REVB
```

APPENDIX 2.2 CHARACTERISTICS OF THE REFERENCE PANEL

The hemispherical reflectance factor of the reference panel has been determined in the laboratory (TFDL) before the field campaign of November/December 1993.

Target No. SRT-99-050-10122-A

Wavelength (um)	8°/Hemispherical Reflectance Factor
0.250	0.933
0.300	0.978
0.350	0.988
0.400	0.990
0.450	0.989
0.500	0.990
0.550	0.989
0.600	0.989
0.650	0.988
0.700	0.988
0.750	0.988
0.800	0.987
0.850	0.986
0.900	0.988
0.950	0.987
1.000	0.986
1.050	0.988
1.100	0.987
1.150	0.988
1.200	0.987
1.250	0.986
1.300	0.986
1.350	0.984
1.400	0.983
1.450	0.984
1.500	0.982
1.550	0.983
1.600	0.983
1.650	0.983
1.700	0.981
1.750	0.981
1.800	0.980
1.850	0.974
1.900	0.972
1.950	0.970
2.000	0.961
2.050	0.946
2.100	0.934
2.150	0.929
2.200	0.953
2.250	0.954
2.300	0.943
2.350	0.928
2.400	0.922
2.450	0.927
2.500	0.920

8° /Hemi. Spectral Retlectance Factor

SRT-99-050-10122-A

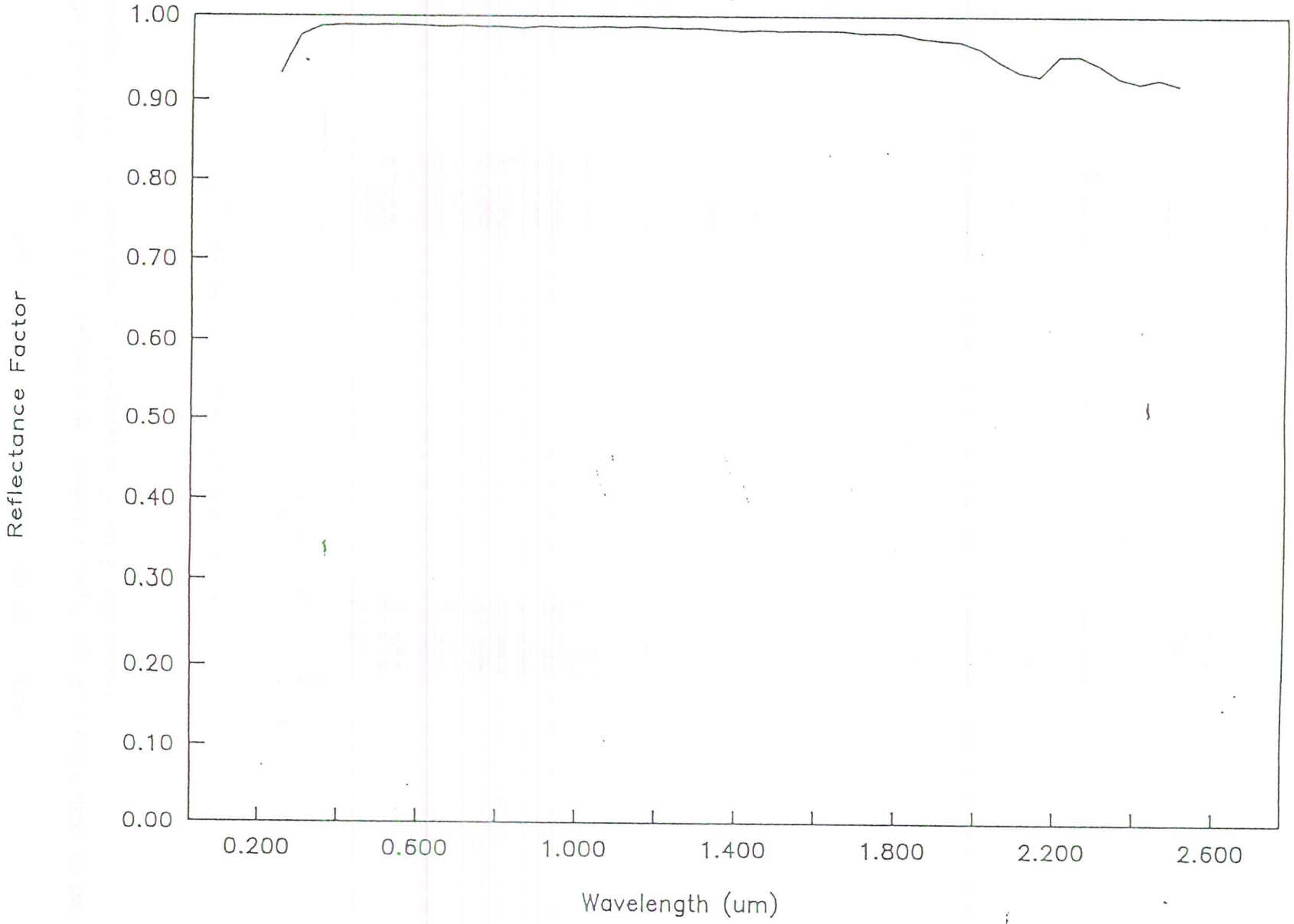

APPENDIX 3.1 FILE AND MAP COORDINATES OF TM IMAGES OF JANUARY AND MAY.

The following values are for files present in the department of soil science and geology. This information is therefore for internal use only.

File: subset of January Landsat TM image:
upper left pixel number (from the original scene) :
6292,3295
lower right pixel number (from the original scene) :
6945,4020
number of columns and rows:
654,726
coordinate of the centre of the upper left pixel in UTM (meters):
700025,1461150
coordinate of the centre of the lower right pixel in UTM (meters):
716350,1443025

File: subset of May Landsat TM image:
upper left pixel number (from the original scene) (X,Y):
5981,3237
lower right pixel number (from the original scene) (X,Y):
6675,3957
number of columns and rows:
695,721
coordinate of the centre of the upper left pixel in UTM (meters):
698500,1461100
coordinate of the centre of the lower right pixel in UTM (meters):
715850,1443100

File: multitemporal image of January and May subsets (12 bands):
upper left pixel number (from the original scene) (X,Y):
5981,3238
lower right pixel number (from the original scene) (X,Y):
5604,3957
number of columns and rows:
623,721
coordinate of the centre of the upper left pixel in UTM (meters):
700025,1461000
coordinate of the centre of the lower right pixel in UTM (meters):
715575,1443050

APPENDIX 3.2 MINI-IRIS REFLECTANCE MEASUREMENTS

An overview of surface reflectance measurements and plot descriptions.

grass 1: Loudetia togoensis
grass 2: Tripogon minimus
grass 3: Schoenefeldia gracilis
grass 4: Aristida paniculata?
grass 5: Schizachirium exile
grass 6: Poacea spp
grass 7: Pennisetum pedicellatum
grass 8: Brachiaria lata
Cymbopogon schoenanthus

cru=crust
shr=shrub
gras=grass
grav=gravel
san=sand
kao=kaolin
sto=stone
str=straw
ter=termites hill

ref=reference
dif=diffuse
wet=wet surface

MINI IRIS

LOC.	DATE	CODE	TIME	NR	DESCRIPTION
A1	5 NOV	sto	7.45	10101	ironstone, 80 %
		cru		10102	algue crust
		cru		10103	crust
		gras		10105	grass 2, 80%
		cru	9.00	10106	curled crust
A2		cru	10.48	10201	crust clay
		cru		10202	idem
		cru		10203	crust eroded
		shr		10204	Guiera s.
		shr		10205	Combretum m.
		san		10206	sand of dune
		grav		10207	gravel red
B1	6 nov	sto	9.02	10101	ironstone
		sto	9.16	10102	ironstone
		shr	9.31	10103	Combretum m.
		cru	10.40	10104	algue crust, 70 %
		grav	10.55	10105	gravel 1cm, 80%
		gras	11.02	10106	grass 1, 40 cm, 70%
		shr	11.15	10107	Combretum g., 40%
		shr	11.30	10108	Combretum m., 30%, iron crust, 70%
		gras	11.40	10109	Brachiaria lata, 80%
		ter	11.47	10110	termites hill
		cru	11.55	10111	crust, 70%, fine gravel, 30%
B2		kao	10.30	10201	kaolin
C1	8 nov	sto	8.19	10101	schist stone red and green
		gras	8.30	10102	grass 1, 30 cm, 80%
		gras	8.43	10103	grass 1, 30cm, 70%
		gras	8.54	10104	grass 1, 30cm, 90%
		sto	9.08	10105	schist stone red and green
		sto	9.18	10106	schist stone red 80 %
		gras	9.30	10107	grass 1, 50%, grass 5, 50%
		shr	9.40	10108	Guiera s., 90%
C2		cru	10.05	10201	bare field, straw 3%
		str	10.15	10202	straw, 50%
		sto	10.25	10203	quartz stone
		gras	10.35	10204	grass 5, 70%
D1	10 nov	grav	9.50	10101	gravel red schist
		cru		10102	sealed surface, gravel, 5%

	grav		10103	gravel, .5cm
	cru		10104	crust in field
	cru		10105	Pennisetum p., 50cm
	gras		10106	grass, 1m
	shr	10.55	10201	Combretum micranthum, 70%
	sto		10202	black stone
	gras	8.48	10301	grass 1, 90%
	sto		10302	iron stone cuirasse
11 nov	cru	8.12	10101	sealed surface in field, 5% fine gravel
	san		10102	rough surface field
	san	8.30	10103	sandy rough surface
	cru	8.45	10104	crust
	cru	9.00	10105	idem, in shadow
	san	9.15	10201	sandy
	cru		10202	crust, 95%
	gras	10.33?	10301	Cymbopogon s., 100%
	gras		10302	grass 2, 50%
	cru		10303	crust, 58%, algue, 40%, gravel, 2%
	ref	9.20	101	reference
	ref		102	small reference panel
	dif		103	reference diffuse
12 nov	sto	8.55	10101	degr. green schist stone
	sto	9.20	10102	quartz stone
	sto	10.35	10103	schist green, 70%, red, 30%
	gras	9.50	10104	grass 4,3,7, 90%
	gras	10.10	10105	Cymbopogon s., 80%
16 nov	grgav	8.45	10101	cuirasse gravel, 85%
	cru	9.10	10102	crust, 1.5cm
	gras	9.15	10103	grass 1, 40%
	sto	9.30	10104	cuirasse
	cru	9.50	10105	crust with algues, 80%
	cru	9.55	10106	crust with algues, 30%
	cru	10.05	10107	crust
	grav	10.10	10108	yellow cuirasse gravel, 1.5cm
	san	10.25	10109	sandy field
	cru	10.35	10110	sandy/silty crust
	cru	10.45	10111	ahor. crust
	san	10.53	10112	sandy surface
	cru	11.02	10113	rough surface (B?)
	shr	11.15	10114	Combretum m., 85%
	shr	11.20	10115	Combretum m. red/green, 70%
	cru	11.30	10116	sandy crust, fine gravel 5%
	grav		10117	kalk gravel, 1cm, 60%
	dif	9.40	101	diffuse
17 nov	kao	8.05	10101	kaolin dark
	kao	8.15	10102	kaolin light
	cru	8.25	10103	algue crust, grass 2%, sand 10%
	gras	8.30	10104	Zornia g. 50%, grass 8 10cm 10%, crust 40%
	gras		10105	grass 8 10cm 50%, crust 50%
	san	8.50	10106	sand in gully 5 cam
	grav	8.57	10107	gravel
	cru	9.20	10108	sandy crust

2		sto	9.45	10201	black stone
3		sto	10.15	10301	quartz
		gras		10302	Cymbopogon s., 90%
		gras	10.25	10303	grass 4 3 7 90%
		sto		10304	green schist stone
		sto	10.40	10305	red schist gravel
4		sto	11.13	10401	quartz gravel, red sand
		cru		10402	red sand, crust 80%, quartz 1%
		sto	11.35	10403	black stone
		sto		10404	gray stone 70%, red 30%
I1	18 nov	sto	9.18	10101	granite stone not degr.
		sto	9.28	10102	red degr. granite
		sto	9.35	10103	yellow degr. granite
		cru	9.47	10104	light crust
		san	9.53	10105	sand in gully 3 cm
		cru		10106	clay crust
		sto		10107	cuirasse 4cm 90%, sand 10%
		gras	10.28	10108	Leptadenia hastata 90%
		cru		10109	dark sandcrust with algues
		san		10110	sanddune grass 15%
		cru	10.54	10111	red, rough crust 1cm
		grav		10112	kalk grind .5cm 60%
		grav		10113	yellow gravel 1cm 65%
		grav	11.30	10114	red gravel .5cm 40%
		dif	10.13	101	diffuse
K1	23 nov	cru	8.26	10101	red sealed surface, gravel 5%
		sto	8.36	10102	greenschist stone
		sto	8.51	10103	redschist stone
		cru	9.03	10104	bare greenschist field
		wet	9.21	kw1010	wet surface
		sto		10105	roodverweerde groenschist steen
		gras	9.44	10106	grass 9 30cm 80%
		sto		10107	quartz stone
		cru	10.15	10108	somewhat red field, gravel 1%
		wet	10.35	kw1010	wet surface
		san	10.44	10109	sandy surface gravel.2cm 1%
		grav	11.03	10110	gravel on red schist .5cm
		str	11.26	10111	straw 100%
		shr	11.40	10112	Balanites aegyptiaca 60%
		gras	11.55	10114	grass 20cm 70%
		gras	12.20	10113	grass 5 90%
		san	12.10	10115	sand greenschist (profile)
		dif	8.56	101	diffuse
		dif	12.04	102	idem
L1	25 nov	shr	9.05	10101	Guiera s. 1m 70%
		cru	9.12	10102	grey crust with sand .15cm 5%: Bhor erosion
		cru	9.25	10103	light curled crust (decantation)
		cru	9.35	10104	light crust in between: Ahor erosion
		wet	9.45	lw1010	wet surface (1mm water)
		wet		lw1010	wet surface later
		wet		lw1010	wet 30%, dried up 70%
		gras	10.12	10105	Brachiaria lata on sanddune 50%
		san	10.20	10106	sand

	shr		10107	Combretum micranthum 60%
	san	10.40	10108	varios coloured sand rough .15cm 60%, fine 40
	cru	10.50	10109	rough sand 20%, algues 30%, light surface 50%
	shr	11.55	10101aidem	10101
	dif	9.20	101	diffuse
	dif		102	diffuse
	cru	11.00	10201	field with crust
	san		10202	field sandy
	wet		lw1020	wet surface
	wet	11.25	lw1020	less wet
	shr		10203	Piliostigma r., very green 90%
	wet	11.45	lw1020	less wet
	dif	11.40	103	diffuse
	dif		104	diffuse
29 nov	cru	8.01	10101	crust in field greenschist
	wet	8.25	nw1010	wet surface
	wet	8.30	nw1010	less wet
	cru	8.40	10102	broken crust in field, straw 5%
	wet	9.00	nw1010	less wet
	shr		10103	Ziziphus m. 80%
	shr	9.20	10104	Diospyros m. 90%
2	cru	10.00	10201	crust 20cm
	san	10.13	10202	sand
3	sasn	10.55	10301	sand
	wet		nw1030	wet surface
	wet	11.45	nw1030	less wet
	ref	8.10	nr101	reference
	ref	8.20	nr201	idem
	ref	10.20	nr102	idem
	ref		nr202	idem
	ref	12.30	nr103	idem
	ref	12.40	nr204	idem
	dif	9.15	nn101	diffuse
	dif		nn102	diffuse
	dif	11.20	nn103	diffuse
	dif		nn104	diffuse
1 2 dec	grav	8.55	10101	gravel .2-1.5cm 100%
	cru	9.10	10102	sandy crust 3mm gravel 5%
	gras	9.16	10103	grass 20 cm 70%
	shr	8.30	10104	Guiera s. 100%
	shr	8.40	10105	Combretum glutinosum 90%
	shr	9.32	10106	Diospyros mespiliformis 70%
	shr	10.00	10107	Combretum micranthum brown leaves (50%), gree
	shr	10.13	10108	Cassia 70%
	shr	8.15	10109	Combretum micaranthum 80% green 5% woody
	cru	10.25	10110	curled crust, gravel 10%
	cru		10111	algue crust 60%
	grav	10.55	10112	gravel .5cm 70%
	ter	11.05	10113	termites hill
	shr	11.20	10101aidem	10109
	shr	11.30	10104aidem	10104

```
          shr   11.40 10105aidem 10105

          ref   8.47  or101 reference
          ref        or201 idem
          ref   10.45 or102 idem
          ref        or202 idem
          ref   11.50 or103 idem
          ref        or203 idem

          dif   9.40  oo101 diffuse
          dif        oo102 diffuse
          dif   11.45 oo103 diffuse
          dif        oo104 diffuse

P1  3 dec cru   8.35  10101 field sandy crust 5cm, gravel 5%
          san   8.45  10102 field no crust, gravel 5%
          cru         10103 crust, gravel 10%
          cru         10104 curled crust
          gras        10105 grass 25cm 70%
          cru         10106 algue crust 80%
          grav 9.45   10107 gravel 80%

          dif   9.50  pp101 diffuse
          dif        pp102 diffuse
          ref   9.58  pr101 reference
          ref        pr201 idem

Q1  4 dec cru   8.05  10101 sandy crust with gravel
          sto         10102 dark cuirasse stones

          dif   8.40  qq101 diffuse
```

APPENDIX 4

SOIL PROFILE DESCRIPTIONS

KAYA 92-1 (Van Dam, 1993, adapted)

GENERAL INFORMATION

Date	1992-08-18
Authors	M. Mulders, A. Belemvire and 0. van Dam.
Location	Zablou, 11 km. NW of Kaya (road to lake Dem)
Coordinates	1°7'43"LO, 13°8'55"LN, photo 1:30.000 7940
Classification FAO	Eutric Regosol
French	Sol brun eutrophe tropical
Landform	Valley bottom
Slope gradient	Rolling
Micro topography	Irregular
Slope	Class 2
Vegetation/ land use	Herbs and some shrubs
Parent material	Colluvium on chlorate and epidote schist
Drainage	Class 3, moderate
Groundwater depth	Very deep
Erosion	Rills
Alkalinity/ salinity	None
Biological activity	At 44 cm some krotovina's (0-2/m^2) some roots (0-2/dm^2) mainly between 0-64 cm

HORIZON DESCRIPTION

Ah 0- 5cm Strong brown (7.5YR 4/6) moist and (7.5YR 5/6) dry; loam with 30% gravel; medium plates, medium subangular blocks and medium granules; very friable, non sticky and slightly plastic; pH 5 (Hellige); nine roots < 0.5 mm, ten 0.5-2 mm and one > 2 mm; gradual and wavy to:

AB 5- 21cm Yellowish red (5YR 4/6) moist and dry, clay loam with 30% gravel; medium angular blocky; friable, slightly sticky, (slightly) plastic; pH 5 (Hellige); twelve roots < 0.5 mm, two 0.5-2 mm and one > 2 mm; four biopores; gradual and wavy to:

Bw 21- 33cm Dark red (2.5 YR 3/6) moist, yellowish red (5 YR 4/6) dry; clay with 3% gravel; fine angular blocky; very friable, (slightly) sticky and (slightly) plastic; pH 4.5 (Hellige); seven roots < 0.5 mm, one 0.5-2 mm and one > 2 mm; ten biopores; gradual and wavy to:

BC 33- 44cm Dark red (2.5YR 3/6) moist, yellowish red (5YR 4/6) dry; clay with 1 % gravel;

fine angular blocky; very friable, (slightly) sticky and (slightly) plastic; pH 4.5 (Hellige); nine roots < 0.5 mm, one 0.5-2mm and one > 2 mm; five biopores; gradual and wavy to:

Cl 44- 66cm Yellowish red (5YR 5/8) moist, reddish brown (5YR 4/4) dry; clay with 5% gravel; very fine angular blocky; very friable, (slightly) sticky and (slightly) plastic; pH 5 (Hellige); five roots < 0.5 mm, one 0.5-2 mm and one > 2 mm; four biopores; gradual and wavy to:

C2 66- 84cm Yellowish red (5YR 4/6) moist and dry with 2% red (2.5YR 5/8) mottles; clay loam; 50% rotten rock (plinthite d= 10 cm, with schist stratification); massive stratified; friable, slightly sticky and (slightly) plastic; pH 4.5 (Hellige); five roots < 0.5 mm, one 0.5-2 mm and one > 2 mm; three biopores; gradual and wavy to:

C3 84-100cm Strong brown (7.5YR 5/6) moist, yellowish red (5YR 4/6) dry, with 30% light red (2.5 YR 6/8) mottles, 70% yellow rotten rock; clay loam; massive, stratified; friable, slightly sticky and slightly plastic; pH 4.5 (Hellige); four roots < 0.5 mm, one 0.5-2 mm and one > 2 mm 1; one biopore.

Remark: pores and roots/dm_2.

Analytical data

Horizon		Ah	AB	Bw	BC	C1	C2
Depth, cm		0-5	5-21	21-33	33-44	44-66	66-84
Moisture %		nd	2.5	nd	nd	nd	nd
CaCO3 equiv. %		nd	0	nd	nd	nd	nd
pH H_2O 1:5		nd	6.4	nd	nd	nd	nd
pH KCl ,,		nd	4.8	nd	nd	nd	nd
EC mS cm_1 ,,		nd	21	nd	nd	nd	nd
C %		nd	nd	nd	nd	nd	nd
Sand %		nd	31	nd	nd	nd	nd
Silt %		nd	37	nd	nd	nd	nd
Clay %		nd	32	nd	nd	nd	nd
Texture		nd	CL	nd	nd	nd	nd
CEC	$cmol^{(+)}kg^{-1}$	nd	13.7	nd	nd	nd	nd
Exch.Ca,	,,	nd	8.5	nd	nd	nd	nd
,, Mg,	,,	nd	6.0	nd	nd	nd	nd
,, Na,	,,	nd	0.5	nd	nd	nd	nd
,, K,	,,	nd	0.3	nd	nd	nd	nd
,, H,	,,	<0.1	<0.1	<0.1	<0.1	<0.1	<0.1
,, Al,	,,	<0.1	<0.1	<0.1	<0.1	<0.1	<0.1
Free Fe%		4.0	5.6	6.2	6.1	5.4	5.0
Free Al%		0.2	0.3	0.4	0.3	0.3	0.3
BS %			100+				

nd = not done or unreliable

KAYA 92-2 (Van Dam, 1993, adapted)

GENERAL INFORMATION

Date	1992-08-18.
Authors	M. Mulders, P. Zombré, A. Belemvire and 0. van Dam.
Classification FAO	Dystric Fluvisol
French	Sol minéraux brut d'apport alluvial
Location	Silmiougou, 7 km. North of Kaya (road to Barsalogo)
Coordinates	1°3'17"LO, 13°7'39"LN, photo 1:30.000 7959.
Elevation	± 700m
Physiography	Plain
Slope	Class 1, flat to nearly flat
Vegetation/ land use	Millet field close to village with some large trees
Parent material	Alluvial deposits on granodiorite
Drainage	Class 4, well drained
Groundwater table	Very deep
Erosion	Rill
Salt and alkali	None
Biological activity	Some roots (0-2/dm²) mainly between 0-10 cm. Termite activity throughout the profile.

HORIZON DESCRIPTION

Ah 0- 6cm Brownish yellow (10YR 6/6) moist, yellow (10YR 7/6) dry; sandy loam; weak medium subangular blocky; soft, very friable, slightly sticky and non plastic; pH 6,5 (Hellige); ten roots < 0.5 mm, two 0.5-2 mm and one > 2 mm; one biopore; gradual and smooth to:

AB 6- 43cm Strong brown (7.5YR 4/6) moist, reddish yellow (7.5YR 6/6) dry; sandy loam; weak medium subangular blocky; soft, friable, slightly sticky, non plastic; pH 5.5 (Hellige); five roots < 0.5 mm, one 0.5-2 mm and one > 2 mm; one biopore; gradual and smooth to:

Bw 43- 89cm Reddish yellow (7.5YR6/6) moist, strong brown (7.5YR 5/6) dry with yellowish red (5YR 5/8) mottles, sandy loam; massive, slightly hard, (very) friable, slightly sticky and non plastic; pH 5.5 (Hellige); four roots < 0.5 mm, one 0.5-2 mm and one > 2 mm; three biopores; abrupt and wavy to:

Bt 89- 90cm Very irregular hardened strong brown (7.5YR 5/8) moist and (7.5YR 5/6) dry with 20% reddish brown (5YR 4/4) mottles; loam; slightly hard, friable, slightly sticky and non to slightly plastic; pH 5 (Hellige); abrupt and wavy to:

BC90-120cm Brownish yellow (10YR 6/6) moist, very pale brown (10YR 7/4) dry, with 30 % reddish brown (5YR 4/4) and 15 % vefy pale brown (10YR 7/3) mottles; sandy

clay loam; soft, very friable, slighty sticky and non to slightly plastic; pH 5 (Hellige); one root < 0.5 mm, one 0.5-2 mm and one > 2 mm; two biopores.

Remark: roots and pores dm^2

Laboratory data

Horizon	AB	Bw
Depth, cm	6-20	43-89
Moisture %	0.3	5.7
CaCO3 equiv. %	1.3	0.3
pH H_2O 1:5	6.4	6.9
pH KCl ,,	5.3	5.3
EC mS cm^{-1} ,,	22	13
Sand %	72	62
Silt %	21	16
Clay %	7	22
Texture	SL	SCL
CEC $cmol^{(+)}kg^{-1}$	4.0	7.3
Exch. Ca, ,,	1.6	3.6
,, Mg, ,,	0.7	2.0
,, Na, ,,	0.1	0.6
,, K, ,,	0.1	0.1
,, Al, ,,	<0.1	<0.1
,, H, ,,	<0.1	<0.1
Free Fe %	0.3	0.3
Free Al %	0.1	0.0
BS %	63	85

KAYA 92-3 (Van Dam, 1993, adapted)

GENERAL INFORMATION

Date	1992-09-29
Authors	A. Belemvire and 0. van Dam.
Classification FAO	Eutric Fluvisol
French	Sol peu évolué d'apport alluvial
Location	Tiouéga, 4 km. South east of Kaya
Coordinates	1°7'43"LO, 13°8'55'LN, photo 1:30.000 7942.
Elevation	± 700m
Physiography	Plain
Topography	Flat to nearly flat
Micro topography	Regular
Slope	Class I
Vegetation/land use	millet field
Parent material	Alluvial deposits on chlorite and epidote schist
Drainage	Class 4, well drained
Depth groundwater	Very deep
Erosion	Sheet
Salt/ alkali	None
Biological activity	Some krotovina's (0-2/dm^2) Some roots (2-5/dm^2) mainly beween 5-10 cm

HORIZON DESCRIPTION

Ah 0- 9cm — Strong brown (7.5 YR 4/6) moist, reddish yellow (7.5 YR 6/6) dry; loamy sand; medium platy; slightly hard, slightly sticky and slightly plastic; pH 5.5 (Hellige); 18 roots of < 0.5 mm; 20 very fine and 15 fine biopores; distinct and smooth to:

AB 9- 40cm — Strong brown (7.5 YR 4/6) moist and (7.5 YR 5/6) dry, sandy clay loam; weak and strong angular blocky; slightly hard to hard, slightly sticky and slightly plastic; pH 5.5 (Hellige); 36 roots of < 0.5 mm 36 and two of 0.5-2 mm; 220 very fine and 20 fine biopores; gradual and wavy to:

BA 40- 54cm — Strong brown (7.5 YR 4/6) moist and (7.5 YR 5/8) dry; sandy clay loam; weak to strong angular blocky; very friable, slightly sticky and slightly plastic; pH 5 (Hellige), two roots of < 0.5 mm and five of 0.5-2 mm; 104 very fine and three fine biopores; gradual and wavy to:

Bw1 54- 77cm — Yellowish red (5 YR 4/6) moist and (5 YR 5/8) dry; sandy clay loam; medium angular blocky; slightly hard, sticky and (slightly) plastic; pH 5 (Hellige); two roots of < 0.5 mm; 92 very fine and six fine biopores;

gradual and wavy to:

Bw2 77-110cm — Strong brown (7.5 YR 4/6) moist and (7.5YR 5/8) dry; sandy clay loam; moderately developed angular blocky; (very) friable, sticky and (slightly) plastic; pH 5.5 (Hellige); two roots of < 0.5 mm; 92 very fine, four fine and four medium biopores.

Remark: roots and pores /dm²

Laboratory data

Horizon	Ah/AB	Bw2
Depth, cm	0-20	90-110cm
Moisture %	0.4	6.9
CaCO3 equiv. %	0.0	0.0
pH H_2O 1:5	7.1	5.9
pH KCl ,,	5.9	4.4
EC mS cm^{-1} ,,	24	14
Sand %	57	46
Silt %	33	28
Clay %	10	26
Texture	SL	(SC)L
CEC, $cmol^{(+)}kg^{-1}$	5.2	8.0
Exch. Ca, ,,	2.6	3.8
,, Mg, ,,	1.0	2.0
,, Na, ,,	0.5	0.0
,, K, ,,	0.1	0.1
,, H, ,,	-	0.2
,, Al, ,,		<0.1
,, H, ,,		<0.1
Free Fe %		4.2
Free Al %		0.2
BS %	80	73

KAYA 92-4 (Van Dam, 1993, adapted)

GENERAL INFORMATION

Date	1992-09-30
Authors	A. Belemvire and 0. van Dam.
Classification FAO:	Eutric Fluvisol
French	Sol peu évolué d'apport alluvial
Location:	Dimassa, 4 km. East of Kaya
Coordinates	1°7'43"LO, 13°8'55"LN, photo 1:30.000 7940.
Physiography	Concave slope
Topography	Rolling
Micro topography	Irregular
Slope	Class 2
Vegetation/ land use	?
Parent material	Alluvial deposits on chlorite and epidote schist
Drainage	Class 4, well drained
Groundwater depth	Very deep
Erosion	Severe gully erosion
Salt/ alkali	None
Biological activity	Some krotovina's (2-5/dm^2), some roots (0-2/dm^2)

HORIZON DESCRIPTION

Ah 0- 4cm	Reddish yellow (7.5 YR 6/8) moist, pink to reddish yellow (7.5 YR 7/5) dry; sand; fine, moderately developed platy; loose, non sticky and non plastic; pH 5.5 (Hellige), twenty very fine and one fine biopores; abrupt and smooth to:
AB 4- 11cm	Strong brown (7.5YR 5/6) moist, pink (7.5 YR 7/4) dry; sandy loam; moderately developed medium angular blocky; slightly hard, slightly sticky and non plastic; pH 5.5 (Hellige); one root of 0.5-2 mm; 44 very fine and one fine biopores; abrupt and smooth to:
Bwl 11- 23cm	Strong brown (7.5YR 5/8) moist, reddish yellow (7.5YR 6.5/8) dry; sandy loam with 4% iron nodules gravel; moderately developed medium angular blocky; slightly hard, non sticky and non plastic; pH 6 (Hellige); four roots of 0.5-2 mm; 24 fine biopores; abrupt and smooth to:
Bw2 23- 45cm	Strong brown (7.5YR 5/6) moist, reddish yellow (7.5YR 6/6) dry with 10% yellowish red and reddish yellow (5YR 5/6 and 6/6) mottles; sandy loam; moderately developed medium angular blocky; slightly hard, slightly sticky and slightly plastic; pH 5.5 (Hellige); five roots of 0.5-2 mm and one of > 2 mm; 72 fine biopores; gradual and smooth to:
2Ah 45- 61cm	(Dark) brown (7.5YR 4/4) moist, brown (7.5YR 5/4) dry, with 15%

reddish yellow (5YR 6/6) mottles; loamy sand; strongly developed fine angular blocky; hard, slightly sticky and slightly plastic; pH 5.5 (Hellige); three roots of 0.5-2 mm; 48 fine and five large biopores; abrupt and smooth to:

2AB 66- 81cm — Strong brown (7.5YR 5/6) moist and dry with 15% reddish yellow (5 YR 6/6) mottles; loamy sand; strongly developed fine angular blocky; (very) hard, slightly sticky and slightly plastic; pH 5.5 (Hellige); six roots of 0.5-2 mm; 12 fine and 28 large biopores; abrupt and smooth to:

2Bw 81-120+cm — Strong brown (7.5YR 5/8) moist and dry with 3% reddish yellow (5 YR 6/6) mottles; loamy sand with many iron concretions; moderately developed fine and medium angular blocky; very hard, sticky and slightly plastic; pH 5.5 (Hellige); one root of 5-2 mm; 48 fine and six large biopores

Remark: roots and pores /dm^2

Laboratory data

Horizon	Ah+Bw1	2Bw
Depth, cm	0-20	90-110cm
Moisture %	0.8	2.3
CaCO3 equiv. %	1.3	0.5
pH H_2O 1:5	9.0	9.7
pH KCL ,,	8.7	8.1
EC mS cm^{-1} ,,	469	280
Sand %	25	35
Silt %	45	46
Clay %	30	19
Texture	SL	(SC)L
CEC cmol$^{(+)}$kg^{-1}	3.9	10.1
Exch. Ca, ,,	9.3	10.6
,, Mg, ,,	3.0	3.3
,, Na, ,,	1.8	3.7
,, K, ,,	1.5	1.8
,, H, ,,	<0.1	<0.1
,, Al, ,,	<0.1	<0.1
Free Al %	0.1	
Free Fe %	0.5	
BS%	100+	100+

KAYA 93-1

GENERAL SOIL INFORMATION

Date	1993-11-23
Authors	A. Ten Holte, E. Elkenbracht
Coordinates	Latitude:13° 06' 23.3" Longitude: 1° 04' 16.7"
Elevation	± 340m
Topography	Gently undulating
Landform	Valley
Position	Lower slope
Slope gradient	Gently sloping
Slope form	Straight
Parent material	Green schist
Micro topography	Flat
Vegetation/ Land use	Extensive farming
Rock outcrops	Very few
Surface coarse fragments	Common stones
Erosion/deposition	None
Surface sealing	None
Surface cracks	Fine
Infiltration rate	Slow
Internal drainage	Moderately slow
External drainage	Slow run-off
Flooding	No

PROFILE DESCRIPTION

AB 0 - 8cm Yellowish brown (10YR 5/4) moist, and (10YR 5/6) dry; (fine sandy) clay loam; apedal; slighly hard, friable, sticky and plastic; no pores; no cutans; no cementation; no nodules; very few very fine and fine roots;
Micromorfology, at Ocm: More sandy than its subsoil with a few concretions, some saprolite, an average quantity of quartz, some muscovite and fine crystalline lime;
Clear and smooth boundary of fine gravel to:

2Bw 8 - 47 cm Light olive brown (2.5Y 5/6) moist, yellowish brown (10YR 5/4) dry; few, medium, prominent black mottles; clay loam; weak to moderate fine, angular blocky; hard, friable, sticky and plastic; no pores; no cutans; no cementation, few very fine black nodules; few, medium roots;
Micromorfology, at 14cm: Dense microstructure with litte biological activity in the form of infillings, little concretions with goethite, very few amphiboles, some saprolite with unweathered goethite, quartz and staurolites;
Gradual and smooth to:

2BR 47 - 55 cm Light olive brown (2.5Y 5/4) moist, brown (10YR 5/3) dry; common, medium, prominent, 7.5 YR mottles; clay loam; weak to moderate fine angular block; hard, friable, very sticky and slightly plastic; no pores; no cutans; no cementation; few, very fine, hard, iron-manganese black nodules; very few, fine roots;
Micromorphology, at 43 cm: Schisteus material with soil. In the former are found: staurolite, amphibole, chlorite and quartz. The staurolite concentration is higher than in the parent material. The amphiboles and chlorites are covered with iron. The quartz is not weathered yet. The soil material consists of clay in which the rock structure is completely changed to a dense microstructure. Further there are found: quartz, staurolites, pieces of rock material, iron concretions with sharp borders and some biological activity in the form of infillings.
Clear smooth boundary to:

2R 55+ cm Hard rock.
Micromorphology: The parent rock contains large quantities of quartz, green amphiboles, chlorite and staurolite. The structure is a typical schist with, along cracks, accumulation of amorphous iron. The rotten rock, abrupt on top of it, doesn't contain all the minerals found in the parent material. Quartz, staurolite and amphibole are still present, however, the latter in lower quantities. No chlorite could be traced. The soil mass consists of clay and spots of amorphous iron. Rock structure is absent. Further very little plagioclase and saprolite, strongly covered by goethite, are found. The borders of the goethite are angular and subangular.

SEMI-QUANTATIVE ESTIMATION OF THE MINERALOGY (GUINIER-METHOD)

Depth cm	Quartz	Kaol.	Goeth.	Hemat.	Various
0	++++	+	±	-	Ep: + ; PI:+ ; Sm: +
14	++++	+	+	-	Ep: + ; PI:+ ; Sm: +
43	++++	+	++	-	Ep: + ;
55	+++	-	-	-	Am: + + +; Ep: + ; PI: + ; Sm: + ; Ch: +

1. Relative amount: - not present ± very little or doubtfull + little
++ moderate +++ much ++++ very much

2. All samples with kaolinite also contain anatase.

3. The diffraction pattern of the amphibole indicates a Ca- and Mg-rich (Al-poor) type: tremolite/actinolite.

4. Am=amfibole; Ch=chlorite; Ep=epidote; Pl=plagioklaas; Sm=smectite

XRFS-analysis

Depth cm	SiO_2 %	TiO_2 %	$A1_2O_3$ %	Fe_2O_3 %	MnO %	MgO %	CaO %	Na_2O %	K_20 %	P_2O_5 %	BaO %
0	79.8	1.0	7.6	5.3	0.1	0.6	1.0	<tr	0.6	tr	tr
14	66.8	1.3	11.8	9.1	0.3	0.8	1.4	<tr	0.4	tr	tr
43	54.5	1.7	12.3	18.5	0.4	0.8	4.1	<tr	0.2	tr	tr
55	57.4	1.7	12.7	13.0	0.2	3.1	8.3	0.5	tr	0.1	tr

Depth cm	Ni	Pb	Rb	Sr	V	Zn	Zr
0	29	26	28	75	190	<10	550
14	50	20	22	66	244	<10	455
43	66	22	15	94	446	13	249
55	40	14	<10	53	347	46	112

	0-20cm
CaCO3 equiv. %	1.0
pH-H20]:5	7.7
pH-KCI 1:5	6.2
EC mS cm^{-1} 1:5	34
Sand %	33
Silt %	28
Clay %	39
Text.	clay loam
CEC $cmol^{(+)}$ kg^{-1}	20.6
Exch. Ca ,,	19.8
Mg ,,	5.7
Na ,,	0.2
K ,,	0.3
BS %	100+

CONCLUSIONS

The accumulation of amorphous iron in cracks and on amphiboles and chlorites suggests weathering of the parent material. This weathering process has been disturbed because not only some minerals of the parent material are absent in the surface layers but also minerals are found that suggest mixing with material from elsewhere. The "alien" elements are plagioclase, muscovite, fine crystalline lime and concretions with goethite. The lime is probably deposited after having been formed elsewhere (secondary lime). Although some biological activity and some plasma reorientation, which suggests swell and shrink, have been observed, there is no evidence of heterogenisation processes.

KAYA 93-2

GENERAL INFORMATION

Date:	1993-11-24
Authors:	Elkenbracht, ten Holte
Coordinates	Latitude 702325 longitude 1446550
Topography	Steeply dissected
l,andform	Hill
Land element	Upper slope and top
Slope gradient	Steep
Slope form	Straight to convex
Parent material	Schist
Vegetation/land use	Bare
Rock outcrops	Dominant
Surface crse fragm.	Dominant, all sizes
Erosion/deposition:	
Area affected	5-10%
Source	Water
Types	Rill
Degree	Moderate
Surface sealing:	None
Surface cracks	None
Drainage class	Excessively
Internal drainage	Slow
External drainage	Rapid run-off
Floodin	No

HORIZON DESCRIPTION, eastern site of hill

R1 0-1]Ocm — Extremely hard, continuous, iron stone
Micromorphology: see 'Western site of hill' at 40 cm;
clear and smooth to:

R2 110-170 cm — Porous hardened plinthite
Micromorphology: see 'Western site of hill' at 160 cm;
clear and smooth to:

BC 170-700 cm — Red (2.5YR 5/6) moist, reddish yellow (5YR 6/6) dry; slightly hard, friable, sticky and plastic; fine sandy loam with continuous, abundant, coarse, strongly weathered ironstone gravel; weak, medium, subangular blocky structure; no pores; no cutans; no roots;
Micromorphology, at 500cm: Rotten rock and saprolite with quartz, muscovites and moderate clay precipitation, which has been followed by ferrolyses, in the soil mass;

diffuse and wavy to:

C 700 cm + Yellow (10YR 8/6) and pale red (10R 6/2) moist and red (10R 4/6) and yellow (10YR 8/8) dry; hard, firm, sticky and plastic; apedal, (loamy) sand with no pores; no cutans; no cementation; no nodules; no roots
Micromorphology, at 7.00 cm: Saprolite in which the rock structure is still visible. The micas have desintegrated and turned yellow. Along cracks iron has accumulated, is crystalline (haematite/goethite) and has a droplet form, indicating gleying.

HORIZON DESCRIPTION, Western site of hill

1R 0-110cm Extremely hard, continuous, iron stone.
Micromorphology, at 40 cm: The rotten rock and soil mass have not been coloured by iron. The clay accumulation is much better visible. Micas and clays, formed out of micas, are absent. Only large quartz crystals and fragments remain. These fragments were not found in the parent material. No ferrolyses, possibly some clay accumulation;
clear and smooth to:

R2 110-170 cm Porous hardened plinthite;
Micromorphology, at 160 cm: Some saprolite, rotten rock, rock and soil mass. Goethite is squarly orientated on the walls of cracks. Clay accumulation, covered with iron coatings, is present. Also haematite and amorphous iron are found;
clear and smooth to:

RC 170-365 cm Layered hardened plinthite;
Micromorphology, at 270 cm: Soil mass with small pieces of weathered rock and saprolite. The latter has lost its orientation. Only part of the micas is still visible. Haematite, goethite and amorphous iron are found in regular veins in layers. The ground mass, like the clay coatings present on grey, red and brown spots, has been affected by ferrolyses. The accumulated clay is sometimes covered with iron compounds;
clear and smooth to:

C 365-395 cm White (kaolinite) and yellowish brown (10YR 5/8) when dry, poreus massive saprolite sandy loam with few, fine, angular blocky ironstone nodules;
Micromorphology, at 380 cm: Saprolite with a good schist structure. The micas are impregnated with amorphous iron. High amounts of accumulated iron in cracks. Haematite and goethite are found in the sample;
diffuse and smooth to:

2R 395-900+cm Hard red schist

Micromorphology, at 425 cm: Schist with quartz, muscovite, primary iron and haematite. The schist has a typical structure with lengthwise orientation. In cracks, accumulation of secondary clay minerals, possibly kaolinite, has taken place.

SEMI-QUANTITATIVE ESTIMATION OF THE MINERALOGY (GUINIER METHOD)

Depth cm	Qtz	Kaol.	Goeth.	Hemat.	Various
40	±	+++	+++	+++	
160	±	+++	++	++	Mi: ± ; Mi(9.6A): ±
270	++	+++	++	++	Mi: ± ; Mi(9.6A): ±
380	++	+++	+	++	Mi: + ; Mi(9.6A): +
420	+++	+++	+	+	Mi: + ; Mi(9.6A): +
500	++	+++	+	++	Mi: ± ; Mi(9.6A): ±
700	+++	+++	++	+	Mi: + ; Mi(9.6A): +

1. Relative amount: - not present ± very little or doubtfull + little
++ moderate +++ much ++++ very much

2. All samples contain anatase.

3. Mi=mica (1O A).

XRFS-analysis

Depth cm	SiO_2 %	TiO_2 %	$A1_2O_3$ %	Fe_2O_3 %	MnO %	MgO %	CaO %	Na_2O %	K_2O %	P_2O_5 %	BaO %
40	17.6	>3.2	17.2	51.8	>0.1	0.1	0.2	tr	tr	0.7	tr
160	27.0	1.8	21.6	37.8	>0.1	0.1	tr	0.3	0.5	0.4	tr
270	31.6	1.7	21.2	34.7	>0.1	0.1	tr	0.2	0.4	0.2	tr
380	38.9	1.2	26.7	21.7	tr	0.1	0.2	1.3	1.4	0.1	tr
420	52.2	1.0	22.7	14.0	tr	0.1	0.1	1.5	1.3	0.1	tr
500	45.9	1.4	24.8	17.7	tr	0.1	tr	0.4	0.8	0.1	tr
700	54.2	0.9	23.4	12.1	tr	0.1	0.1	1.0	1.5	0.1	tr

Depth cm	Ni	Pb	Rb	Sr	V	Zn	Zr
	--------- in		mg/kg	--------			
40	26	34	<10	25	1000+	37	135
160	32	34	28	44	699	<10	184
270	19	35	23	43	615	<10	178
380	60	26	62	114	346	<10	177
420	42	16	51	125	209	<10	165
500	42	34	41	78	366	<10	283
700	131	22	57	130	176	38	184

Depth, cm		365-395
CaCO3 equiv.	%	0.3
pH-H_2O	1:5	6.7
pH-KCl	1:5	5.6
EC mS cm^{-1}	1:5	16
Sand	%	75
Silt	%	12
Clay	%	13
Texture		Sandy loam
CEC $cmol^{(+)}/kg^{-1}$		3.1
Exch. Ca	,,	1.4
Mg	,,	1.0
Na	,,	0.1
K	,,	0.0
H	,,	-
BS%		78

CONCLUSIONS

The soil has been weathered from schist to saprolite, on which an iron cap has been formed. In some samples the effects of ferrolyses, which affected the iron and/or clay coatings, are visible. The profile is deeply weathered, what can by concluded from the accumulation of high amounts of iron in cracks and the impregnation of micas with amorphous iron.

KAYA 93-3

GENERAL INFORMATION

Date	1993-11-25
Authors	Elkenbracht, Ten Holte
Coordinates	Latitude 13° 04' 37N Longitude 1° 06' 37.5"W
Topography	Plateau escarpment
Slope gradient	Not relevant
Slope form	Not relevant
Parent material	Schist
Micro topography	Not relevant
Vegetation/ land use	Bare
Rock outcrops	None, surfacing quartz veins of 5 cm thick
Surface coarse fragments	Not relevant
Erosion/deposition:	
Area affected	25-50%
Source	Water
Type	Rill
Degree	Moderate
Surface sealing:	None
Surface cracks	None
Drainage class	Somewhat excessively
Internal drainage	Slow
External drainage	Rapid run-off
Flooding	None

SOIL HORIZON DESCRIPTION

R1 0- 32 cm — Hard, massive, continuous, ironstone;
Micromorphology, at 0 cm: The iron (haematite, goethite and probably other iron minerals) content is higher than deeper located samples. In this crust infillings of yellow clay are present; clear and smooth to:

R2 32- 70 cm — Hard, porous, continuous, ironstone;
Micromorphology, at 47 cm: A yellow soil mass with kaolinite, quartz and many iron concretions. Locally a few red spots with red clay coatings are found. The much lower number of red coatings cannot be explained; abrupt and smooth to:

CR 70-152 cm — Yellowish red (5YR 5/8) moist and reddish yellow (5YR 6/6) dry; slightly hard, very friable, sticky and slightly plastic; apedal to weak, coarse, angular blocky; fine sandy loam with few, medium and coarse strongly weathered quartz gravel; abundant, fine, hard, dark yellowish brown (10YR 3/4), yellow (10YR 7/8) and red (10R 5/8) iron-manganese

nodules; very few, fine roots; pH-H_2O 1:2.5 is 4.7;
Micromorphology, at 110 cm: A kaolinitic soil mass with iron, quartz of various sizes and red spots with red fragmented yellow clay coatings that are sometimes once again covered with yellow clay coatings. Sometimes these coatings penetrate into the red spots along pores and cracks; clear and smooth to:

C 152-620+cm

White with abundant, fine, prominent yellowish red (5YR 5/8) moist and reddish yellow (5YR 6/8) dry mottles; apedal, soft, very friable, slightly sticky and slightly plastic; clay or pseudo silt loam; very few, fine, weathered quartz gravel; few fine roots; pH-H_2O 1:2.5 at 620 cm is 7.6
Micromorphology, at 155 cm: The saprolite is more desintergrated than below. Clay precipitation may have occured in the saprolite and the soil mass. A red clay coating is covered with a yellow clay coating. It is possible that the coating coloured red as a result of dehydration of amorphous iron into crystalline iron (haematite/ goethite).
At 200 cm: Large quartz crystals, muscovite, saprolite, booklets of kaolinite, haematite. The original rock structure is visible. Also plutonic rock structure. It also contains soil clumb with small pieces of quartz and pieces of saprolite which have fallen apart. Clay precipitation may have occured.
At ±300cm: More schist structure than at 200cm, with large quartz crystals, muscovite, haematite/goethite, pieces of rock with plutonic appearance, of red schist, and of kaolinite in clusters with muscovite. The kaolinite is associated with large quartz crystals and sometimes appears in veins. The sample was damaged during collection.

Remark: Augered from 200cm onwards

SEMI-QUANTITATIVE ESTIMATION OF THE MINERALOGY (GUINIERMETHOD)

Depth cm	Qrtz	Kaol	Goeth	Hemat.
0	++	+++	+++	++
47	++	+++	++	++
110	++	+++	++	+
155	+++	+++	+	±
200	+++	+++	±	±

1. Relative amount: ± = very little or doubtfull; + = little; ++ = moderate; +++ = much

2. All samples contain anatase.

XRFS-analysis

Depth	SiO_2	TiO_2	Al_2O_3	Fe_2O_3	MnO	MgO	CaO	Na_2O	K_2O	P_2O_5	BaO
cm	%	%	%	%	%	%	%	%	%	%	%
0	65.0	0.6	23.2	3.9	tr	tr	tr	tr	0.2	tr	tr
47	28.8	1.6	19.4	>39.7	0.1	0.1	0.1	tr	tr	0.2	tr
110	37.0	1.3	23.5	28.9	tr	tr	tr	tr	0.1	0.1	tr
155	44.8	1.3	24.2	20.2	tr	0.1	tr	tr	0.1	tr	tr
200	64.9	0.7	22.5	5.4	tr	tr	tr	tr	tr	tr	tr

Depth	Ni	Pb	Rb	Sr	V	Zn	Zr
cm	---------- in mg/kg----------						
0	18	11	<10	<10	107	<10	195
47	23	52	11	18	663	<10	284
110	28	36	11	<10	441	<10	243
155	30	32	14	<10	350	<10	243
200	21	15	11	<10	135	<10	228

CONCLUSIONS

In the deepest sample both schist and a structure of plutonic rock is found. It is possibile that before the metamorphosis the parent material was a granite. Throughout the profile, weathering and laterization can be observed. The parent material changes into saprolite with an increasing iron content and at the surface the sample consists nearly entirely of iron. The two different clay coatings indicate that there have been two different periods of clay precipitation. After the clay precipitation iron has covered the clay in some cases. The red coating is older then the yellow one. Some of the red clay coatings are fragmentaled which could have been caused by biological activity. These fragments can be covered with the yellow clay coating.

KAYA 93-4

GENERAL INFORMATION

Date	1993-11-26
Author	Ten Holte
Coordinates	Latitude 13° 05' 35.6" Longitude 01° 02' 28.0"
	712382 1448266
Topography	Flat
Landform	Escarpment and upper valley slope
Slope gradient	Sloping
Slope form	Straight
Parent material	Granodiorite
Vegetation/Land use	Bare
Rock outcrops	None
Surface coarse fragments	
Abundance	Dominant
Size	Medium and coarse gravel and boulders
Erosion/deposition:	
Area affected	> 50%
Source	Water erosion and wind deposition
Type	Gully
Degree	Extreme
Surface sealing:	None
Surface cracks	None
Drainage class	Somewhat excessively
Internal drainage	Moderately rapid
External drainage	Moderately rapid run-off
Flooding	No

HORIZON DESCRIPTION

R 0-300 cm Hard, porous, white, red (2.5YR 6/6) and yellow (10YR 8/8), when dry, iron crust;
Micromorphology: Mainly crystalline with high amounts of amorphous iron, the former in the form of goethite and haematite, and large biotites. Clay coatings are conserved by an iron coating that completely covers them. Grey spots, the result of ferrolyses, are also covered by iron; at 0 cm, the situation looks more extreme than at 150cm, here also manganese is found;
diffuse and smooth to:

Btc 300-380 cm White, red (2.5YR 4/6) and yellow (10YR 7/8), when moist, and white, light red (2.5YR 6/6) and yellow (2.5Y 8/8), when dry, sandy loam with abundant, medium and coarse, prominent multi-coloured mottles; no rocks; apedal; consistence not relevant because of presence of abundant,

fine, hard, iron nodules; few, fine roots; pH-H_2O 1:2.5 is 8.1;
Micromorphology, at 300cm: Grey spots with clay coatings, fragmented by severe ferrolyses, have been covered with brown clay coatings followed by lime accumulation. Furthermore large biotites, quartz and kaoline are present.
At 330 cm: Many pieces of red schist and large biotites, covered with iron, a lot of kaolinite, pieces of saprolite and colluvium. In situ clay precipitation has been followed by lime accumulation in cracks; diffuse and smooth to:

BCk 380-455 cm White, red (2.5YR 4/6) and yellow (10YR 7/8) when moist and white, light red (2.5YR 6/6) and yellow (2.5Y 8/8) when dry; sandy loam with abundant, medium and coarse, prominent multi-coloured mottles; no rocks; apedal; pseudo-silt yellow and white mottles with soft consistency; common lime concretions; few, fine roots; pH-H_2O 1:2.5 is 8.2;
Micromorphology, at ±380cm: Sand and some clay with quartz, kaolinite, secondary lime and schists. In the soil mass red iron nodules and pieces of fragmented clay coatings are visible. The same grey spots with the fragmented clay coatings, as those at 470cm, are present. Through the red and grey spots in situ formation of clay coatings has been followed by lime accumulation; diffuse and smooth to:

CB 455-550 cm Multi-coloured white, strong brown (7.5YR 5/8) when moist and white and brownish yellow (10YR 6/6) when dry; hard, firm, sticky and plastic; apedal; fine sandy loam; pH-H_2O 1:2.5 is 7.6; no pores; no cutans; no cementation; common lime concretions; common, fine (dead) roots;
Micromorphology, at ±470cm: Sand with less clay than higher in the profile and with pieces of hardened plinthite and kaolinite that are surrounded by a dough like soil mass of kaolinite. Further, quartz, plagioclase, staurolite, biotite (strongly covered by iron), muscovite and homblende are present. There have been different stages of clay precipitation. In grey, iron free spots pale yellow greyish granular clay has precipitated. Within these grey spots are areas that are coloured red by iron and have a yellow to red coloured clay precipitate. The yellow-red coatings are the same as the grey ones. Locally the yellow-grey coating is covered by a younger clay coating with a brownisch colour which is not affected by ferrolyses. Secondary lime covers the youngest clay coatings. The grey spots are preferent waterflows or root cracks. The pieces of hardened plinthite found contain large quartz and crystalline iron and have been formed elsewhere; diffuse and smooth to:

C 550-800+cm Similar but more white than overlying horizon, softer, less concretions, no HCl efflorescence, pH-H_2O 1:2.5 is 8.2.

SEMI-QUANTITATIVE ESTIMATION OF THE MINERALOGY (GUINIER-MFTHOD)

Depth cm	Qrtz	Kaol.	Goeth	Hemat.
0	++	+++	+++	+++
150	++	+++	++	±
300	+++	+++	++	-
330	+++	+++	++	-
390	+++	+++	++	-
470	+++	+++	-	-

- = not present
± = very little or doubtfull
\+ = little
++ = moderate
+++ = much
All samples contain anatase.

XRFS-ANALYSIS FOR MAJOR AND MINOR COMPONENTS

Depth cm	SiO_2 %	TiO_2 %	$A1_2O_3$ %	Fe_2O_3 %	MnO %	MgO %	CaO %	Na_2O %	K_2O %	P_2O_5 %	BaO %
0	30.16	1.71	20.16	>37.75	0.21	0.05	tr	tr	tr	0.25	0.03
150	49.20	1.19	23.54	16.97	0.05	0.06	tr	0.04	tr	0.06	tr
300	58.45	0.94	22.59	9.58	0.07	0.08	tr	tr	0.13	0.06	tr
330	58.02	0.93	24.58	8.26	0.03	0.08	0.07	tr	0.18	0.05	tr
380	58.4	11.11	24.60	7.36	0.03	0.11	0.06	tr	0.27	0.05	tr
470	62.61	0.88	19.19	6.12	0.02	0.32	0.26	tr	0.42	0.02	tr

	Ni	Pb	Rb	Sr	V	Zn	Zr
	---------- in mg/kg ----------						
0	11	57	<10	25	658	<10	305
150	14	34	10	45	330	<10	277
300	10	28	<10	45	178	<10	289
330	18	16	<10	46	192	17	244
380	16	26	13	55	205	<10	408
470	15	21	22	86	162	20	362

< = lower than detection limit
> = higher than standard series
tr = trace

Laboratory data

Depth, cm	380-400	470-490
$CaCO_3$ equiv. %	1.3	0.5
pH H_2O 1:5	9.0	9.7
pH KCl ,,	8.7	8.1
EC mS cm^{-1} ,,	469	280
Sand %	25	35
Silt %	45	46
Clay %	30	19
Texture	CL	L
CEC $cmol^{(+)}kg^{-1}$,	3.9	10.1
Exch. Ca ,,	9.3	10.6
Mg ,,	3.0	3.3
Na ,,	1.8	3.7
K ,,	1.5	1.8
BS%	100+	100+

CONCLUSIONS

Iron mottles were formed during poor drainage conditions. During the following well drained period, clay precipitated on aggregates, forming the present grey spots, and in the iron mottles. During a next wetter period, with alternating periods of oxidation and reduction, again heterogenisation of iron resulted in the creation of more grey and red spots. During this period also the clay coatings present were affected by ferrolyses. The clay, accumulated in the iron nodules, was completely covered with iron, protecting it from ferrolyses. After this period the drainage improved again, leading to a second precipitation of brown clay in, between, and around red and grey spots. The iron concentrations hardened irreversible during dry periods. Both the fragmentation of some of the clay coatings and the presence of various parent materials indicates disturbance by transport so of the presence of colluvial or eolian material.

KAYA 93-5

GENERAL INFORMATION

Date	1993-11-29
Author	Legger
Coordinates	Latitude: 705489 Longitude: 1447445 13° 05' 11.5" 1° 06' 17.7" 2.3 km southwest of centre of Kaya, 1.55 km from turn off to Yako, 75 m left of the road.
Elevation	± 340 m
Topography	Flat
Landform	Valley
Land element	Bottom
Slope gradient	Flat
Slope form	Straight
Parent material	Red schist
Micro topography	Smooth
Vegetation/Land use	Sorghum
Rock outcrops	None
Surface coarse fragments	None
Erosion/deposition:	None
Surface sealing- Abundance	10% of surface affected
Thickness	< 2mm
Consistency	slightly hard
Surface cracks	None
Drainage class	Well
Internal drainage	Moderately slow
External drainage	Slightly ponded
Flooding	None

PROFILE DESCRIPTION

Ap 0 - 17 cm — Yellowish red (5YR 5/6) moist and dry; fine loamy sand; no rocks; weak very coarse subangluar blocky structure; slightly hard, very friable, slightly sticky and slightly plastic; very few, very fine pores; no cutans and no cementation; few, fine, hard, dusky red (2.5YR 3/2) iron nodules; common fine roots, gradual and smooth to:

Bwl 17 - 50 cm — Yellowish red (5YR 4/6) moist, reddish yellow (5YR 6/6) dry; fine loamy sand; no rocks; apedal, slightly hard, very friable, slightly sticky and slightly plastic; very few, very fine pores; no cutans and no cementation, no nodules; very few, very fine roots; gradual and smooth to:

Bw2 50 - 105 cm — Yellowish red (2.5YR 4/6) moist and (5YR 5/6) dry; fine sandy loam; no rocks; apedal; slightly hard, very friable, sticky and plastic; very few, very fine pores, no cutans and no cementation; no nodules; in transition zone to the next horizon common yellowish red (2.5YR 4/6) dry, fine iron-manganese nodules, very few, very fine roots; diffuse and smooth to:

Bg 105 - 220 cm — Strong brown (7.5YR) moist, reddish yellow (7.5YR 6/8) dry; few, with depth increasing in abundance, fine distinct, yellowish red (2.5YR 4/6) when dry mottles; fine loamy sand; no rocks; apedal; slightly hard, very friable, slightly sticky and slightly plastic; very few, very fine pores; no cutas, no cementation and no nodules; no roots; diffuse and smooth to:

BCg 220- 360+ cm — Red (2.5YR 4/8) and yellow (10YR 7/6) when dry; fine loamy sand; no rocks; apedal; very friable, slightly sticky and slightly plastic; no cutans, no cementation; common, fine, hard iron-manganese nodules, the location of the manganse -inner part- indicates pseudo-gley conditions; no roots.

Remark: augered from 160cm onwards.

Laboratory data

		Ap	Bw1
Depth, cm		0-17	40-50
$CaCO_3$ equivalent		0	0
pH H_2O	1:5	6.3	6.4
pH KCl	,,	4.9	5.0
EC mS cm^{-1}	,,	11	15
Sand %		85	84
Silt %		8	9
Clay %		7	7
Texture		LS	LS
CEC $cmol^{(+)}kg^{-1}$,		2.4	3.0
Exch. Ca,	,,	0.8	0.6
Mg	,,	0.6	0.7
Na	,,	0.0	0.1
K	,,	0.1	0.1
H	,,	0	0
BS%		64	51

KAYA I (adapted from Leprun, Jean-Claude, 1979)

GENERAL INFORMATION

Date	
Authors	Jean Claude Leprun
Coordinates	Lattitude 714300; Langitude 1445500
Elevation	± 400m
Topography	Inselberg
Position	Slope
Slope form	Straight
Parent material	Granodiorite
Micro topography	Not relevant
Vegetation/ land use	Bare
Rock outcrops	None
Surface crse fragm.	Not relevant (iron crust)
Erosion/deposition	Severe gully erosion
Surface sealing	None
Surface cracks	None
Infiltration rate	Low
Internal drainage	Well drained
External drainage	Rapid
Flooding	None
Precipitation	700 mm

PROFILE DESCRIPTION

0 - 70cm Very hard iron crust, with mainly vertical cracks. Outside, each block consists of 0.5- 5cm large, dusky to weak red (10R 3.5/3) round, partly connected nodules and, less frequent, dusky red to dark reddish brown (2.5YR 3/3) compact nodules. The surface of these nodules is covered with very thin shiny skins. Inside the blocks, of hard multi-coloured light brown, yellow and bright red clayey sand, some pores with thin dark red clay around bright centres are visible. If crushed with a hammer, these nodules show, with a magnification glass, pores and black holes where sometimes small, weathered and bleached quartz grains persist;

70 - 120cm In general the same as above. The nodules are more fixed to each other, smaller, less distinct with less black coloured pores, and more quartz. Some large sub-verticale pores with fine, very red iron circles;

120 - 185cm Less hard and less massive, continuous porous, multi-coloured matrix with very clear purple and fine rusty brown mottles. The purple nodules become diffuse. At 185cm the vertical cracks, mentioned above, widen and are filled with a mixture of fine earth and loose nodules. White sandy 'tracks'

suggest leaching with rainwater;

185 - 330cm Sandy clay, that turns into a powder when crushed between the fingers, with small white, yellow, ocre, red and light red mottles. In the very fine structured, clayey and uniform red (2.5YR 5/7) areas termite channels and holes can be recognized. Iron concentrations and iron nodules have sharp colour boundaries. The matrix consists of two types: the majority has a purple, dark red, fine mottled structure, the minor one is sandy clayey and iron brown;

330-1200cm With depth, each mottle looks more like a very friable granule of which the colour: bloodred, greyish white chalkish, and the form indicate various strongly weathered minerals of which the form and composition have been preserved. The reddish clay areas decrease wih depth and cease at a depth of 1000 cm. The iron, shown with brown and ocre mottles, decreases with depth;

1200-2000cm The orientation and micaciation of the mottles increases. The granulated mottles get even more resistant with fainter colours;

2000-2200cm The matrix is a mix of pale purple and clear greyish green. The granules are easier to separate but cannot be pulverized between the fingers anymore. The greyish green colouring increases. The reddish purple colouring can be attributed to weathering biotites, the white chalky granules to feldspars and the pale grey green to undifferentiated ferro magnesian minerals.

2200-2500cm The cohesion and the granulair structure increase. The small greyish green mottles become pistache green. The pastel colour and the consistence of the material resemble that of 'tweed'. The original mineralogy of each granule is well recognisable.

ANALYTICAL DATA

Depth (m)	Clay %	Silt %	Sand %	pH H_2O	pH KCl	Ca	Mg	K	Na	CEC	ESP %
						----------$cmol^{(+)}kg\text{-}1$----------					
4.5	16	40	44	9.0	7.0	1.3	tr	0.1	2.0	4.6	43
6	18	39	43	8.6	7.0	1.4	tr	0.2	2.1	5.1	41
7	14	49	37	10.0	9.3	1.0	0.2	tr	2.0	4.5	44

Remark: The presence of sodium in soils with very low CEC values can result in extreme high ESP values. So very low amounts of sodium may already have a detrimental effect on the stability of strongly weathered soils.

APPENDIX 5.1 SHORT DESCRIPTION OF LABORATORY SAMPLES

sands and crusts

EP1	D1	Red schist crust
EP2	D1	sand 0.5 - 5 cm in red schist
EP3	E1	sand in gully
EP4	E2	sand
EP5	I4	red sand
EP6	K	0.5 - 5 cm soil in greenschist
EP7	K	0 - 0.5 cm crusts in greenschist
EP8	H	sand in little gully trampled on
EP9	H	crust in millet field
EP10	H	gray crusts
EP11	H	sand of small dunes with gras
EP12	J	sand of dunes
EP13	J	crusts gray
EP14	I1	crusts and sands of dunes in the near kaolinite
EP15	Niger,red sand from degraded bush	
EP16	L	clay 'decantation'crust
EP17	L	clay B erosion
EP18	L	clay A erosion
EP19	L	sand dunes
EP20	M/A	clay, curl crust
EP21	M/A	crust B erosion
EP22		red sand taken north of tigerbush
EP23		red sand taken north of tigerbush

crusts

GFE1	D1	red schist crust (EP1)
GFE2	H	curst (EP24)
GFE3	H	algae curst
GFE4	H	gray crust (EP10)
GFE5	H	crust in field (EP9)
GFE6	H	B2t crust (broken) (EP25)
GFE7	J	gray crust (EP13)
GFE8	I1	crust in erosion area (EP14)
GFE9	L1	clay 'decantation' curl crust (EP16)
GFE10	L2	erosion B crust (EP17)
GFE11	L2	erosion A crust (EP18)
GFE12	M/A	curl crust (EP20)
GFE13	M/A	crust B erosion (EP21)
GFE14	K	green schist crust (EP7)

stones

EPS1	D1	a:redschist b:yellowschist c: greenschist
EPS2	D2	black stone
EPS3	E2	a: black b: red c: yellow laterite gravel
EPS4	E2	red and yelow laterite stone
EPS5	I	a: gray stone b: quarts on hill b: shining red laterite stone

EPS6	K	a: quarts b:weathered greenschist
EPS7	H	yelow laterite gravel from tree hole
EPS8	H	chalk gravel
EPS9	H	black laterite stone
EPS10	J	granite a:non weathered b: yelow weathered c: red weathered
EPS11	K	non weathered greenschist stone
EPS12	I2	black stone

APPENDIX 5.2 CHEMICAL COMPOSITION (X-RAY FLUORESCENCE) OF LABORATORY SAMPLES

				SiO2 %	TiO2 %	Al2O3 %	Fe2O3 %	Mno %	MgO %	CaO %
D1	R	EP2	89	85.11	0.53	3.33	4.25	0.05	0.19	0.15
E1	R/G	EP3	90	78.19	1.1	8.64	7.62	0.74	0.53	0.89
E2	R	EP4	91	83.8	0.71	5.44	4.48	0.12	0.39	1.32
I4	R	EP5	92	80.63	0.83	6.67	7.45	0.13	0.26	0.08
K	G	EP6	93	76.91	0.98	7.97	5.7	0.07	0.58	1.06
H	A	EP8	94	87.12	0.61	4.73	3.31	0.01	0.13	0.01
H	A	EP11	95	93.38	0.49	1.68	1.54	0.01	0.1	0.01
J	A	EP12	96	92.98	0.29	2.59	1.22	0.01	0.13	0.11
I	R	EP14	97	94.91	0.44	2.15	1.07	0.01	0.13	0.02
NIGER		EP15	98	88.69	0.5	5.27	1.88	0.01	0.12	0.01
L	A	EP19	99	92.21	0.38	2.78	1.58	0.01	0.11	0.03
O	A	EP22	100	90.85	0.68	1.87	3.18	0.03	0.11	0.01
			100r	91.43	0.69	1.85	3.19	0.03	0.14	0.01
O	A	EP23	101	91.93	0.49	2.65	1.72	0.02	0.13	0.01
P1	G	EP1	102	74.32	1.1	7.72	7.7	0.54	0.48	0.84
K	G	EP7	103	73.18	1.2	9.11	6.6	0.18	0.64	1.36
H	A	EP9	104	89.53	0.55	4.14	2.01	0.02	0.15	0.03
H	A	EP10	105	76.88	1.34	8.92	4.14	0.04	0.19	0.04
			105r	77.6	1.34	8.95	4.14	0.03	0.2	0.05
J	A	EP13	106	86.42	0.47	5.86	1.94	0.02	0.18	0.09
L	A	EP16	107	72.3	1.09	13.4	3.33	0.05	0.28	0.13
L	A	EP17	108	79.98	0.73	9.6	3.02	0.02	0.19	0.08
L	A	EP18	109	73.17	1.06	12.03	3	0.04	0.26	0.13
			109r	74.52	1.05	12.2	3.01	0.04	0.25	0.13
M/A	R	EP20	110	68.8	1.1	10.99	5.04	0.05	0.45	0.33
M/A	R	EP21	111	72.95	1.1	9.94	5.2	0.03	0.38	0.29
			111r	73.1	1.14	9.92	5.19	0.03	0.4	0.29
H	A	EP24	112	75.97	0.71	11.95	3.76	0.02	0.13	0.01
H	A	EP25	113	40.28	1.14	16.84	30.78	0.33	0.1	0.01
D1	G/R	EPS1a	114	55.45	0.53	11.98	24.88	0.02	0.11	0.04
D1	G/R	EPS1b	115	62.29	1.83	13.39	13.24	0.03	0.08	0.01
			115r	62.88	1.82	13.58	13.21	0.03	0.08	0.01
D1	G/R	EPS1c	116	53.52	1.61	12.59	13.8	0.2	5.84	8.44
D2	G/R	EPS2	117	46.14	0.73	12.71	13.41	16.76	0.15	0.79
			117r	46.02	0.7	12.71	13.46	16.83	0.15	0.79
E2	R	EPS3a	118	3.23	2.14	11.63	70.41	0.41	0.13	0.01
			118r	3.33	2.17	11.67	70.34	0.4	0.13	0.01
E2	R	EPS3b	119	18.23	2.7	16.72	55.06	0.06	0.03	0.01
E2	R	EPS3c	120	2.09	5.15	68.54	5.03	0.02	0.03	0.01
E2	R	EPS4a	121	16.86	2.71	17.52	56.43	0.09	0.09	0.01
E2	R	EPS4b	122	31.42	1.5	19.6	36.77	0.13	0.07	0.01
I	R	EPS5a	123	97.39	0.04	0.03	0.17	0.01	0.09	0.01
			123r	98.55	0.04	0.03	0.17	0.01	0.07	0.01
I	R	EPS5b	124	98.28	0.04	0.06	0.04	0.01	0.09	0.01
I	R	EPS5c	125	93.59	0.08	0.09	4.76	0.01	0.1	0.01
K	G	EPS6a	126	99.05	0.04	0.03	0.23	0.01	0.1	0.01
K	G	EPS6b	127	58.41	1.76	12.62	14.4	0.18	3.43	7.25
			127r	57.3	1.78	12.2	14.28	0.18	3.43	7.3
H	A	EPS7	128	33.17	1.34	19.62	35.67	0.05	0.08	0.01
H	A	EPS8	129	28.34	0.31	5.24	1.43	0.1	1.49	33.16
H	A	EPS9	130	34.36	1.23	17.85	34.35	0.49	0.11	0.13
J	A	EPS10a	131	62.05	0.67	14.94	5.87	0.09	3.4	4.76
J	A	EPS10b	132	61.28	0.66	15.12	7.38	0.1	2.69	3.75
J	A	EPS10c	133	63.74	0.61	15.01	5.65	0.1	2.78	4.22
K	G	EPS11	134	53.09	1.91	11.56	17.68	0.19	4.08	8.15
I2	R	EPS12	135	62.15	0.73	10.33	5.58	13.05	0.2	0.83

	Na2O	K2O	P2O5	BaO	L.o.I	sum
	%	%	%	%	%	%
EP2	0.04	0.31	0.03	0.03	4.74	98.47
EP3	0.04	0.55	0.04	0.03	2.44	100.67
EP4	0.04	0.57	0.02	0.03	2.02	98.92
EP5	0.04	0.27	0.03	0.03	3.67	99.78
EP6	0.04	0.56	0.03	0.03	5.12	98.93
EP8	0.04	0.38	0.03	0.03	2.4	98.54
EP11	0.04	0.32	0.01	0.03	0.79	98.07
EP12	0.04	0.95	0.01	0.03	0.69	98.95
EP14	0.04	0.45	0.01	0.03	1.42	100.4
EP15	0.04	0.11	0.02	0.03	2.4	98.68
EP19	0.04	0.72	0.01	0.03	1.03	98.76
EP22	0.04	0.15	0.01	0.03	0.95	98
	0.04	0.15	0.01	0.03	0.95	98.14
EP23	0.04	0.44	0.02	0.03	1.27	98.48
EP1	0.04	0.57	0.04	0.03	4.95	98.21
EP7	0.04	0.55	0.04	0.03	5.58	98.42
EP9	0.04	0.46	0.03	0.03	2.65	99.4
EP10	0.04	0.59	0.04	0.03	4.62	98
	0.04	0.6	0.05	0.03	4.62	98
EP13	0.04	1.04	0.02	0.03	2.3	98.33
EP16	0.04	1.19	0.04	0.03	6.5	98.34
EP17	0.04	0.96	0.03	0.03	4.25	98.83
EP18	0.05	1.03	0.04	0.03	5.95	98
	0.04	1.04	0.04	0.03	5.95	98.28
EP20	0.04	1.06	0.13	0.03	10.16	98.16
EP21	0.04	0.82	0.08	0.03	7.16	98
	0.04	0.81	0.08	0.03	7.16	98.1
EP24	0.04	0.36	0.03	0.03	5.54	98.23
EP25	0.04	0.13	0.08	0.06	9.27	98.72
EPS1a	0.68	0.9	0.1	0.03	3.62	98.31
EPS1b	0.04	0	0.2	0.03	6.88	98
	0.04	0	0.2	0.03	6.88	98.33
EPS1c	3.82	0.31	0.14	0.03	1.23	101.47
EPS2	0.04	0.02	0.15	0.05	6.99	98
	0.04	0.02	0.15	0.05	6.99	98
EPS3a	0.04	0	0.17	0.03	9.8	98
	0.04	0	0.17	0.03	9.8	98
EPS3b	0.04	0	0.12	0.03	7.65	99.98
EPS3c	0.04	0	0.32	0.03	18.33	98.7
EPS4a	0.04	0	0.22	0.03	6.59	99.98
EPS4b	0.04	0	0.08	0.03	10.15	99.37
EPS5a	0.04	0	0.01	0.03	0.15	98
	0.04	0	0.01	0.03	0.15	98.54
EPS5b	0.04	0	0.01	0.03	0.14	98.23
EPS5c	0.04	0	0.02	0.03	0.64	98.9
EPS6a	0.04	0	0.01	0.03	0.17	99.12
EPS6b	2.78	0.18	0.12	0.03	1.11	102
	2.72	0.18	0.13	0.03	1.11	100.58
EPS7	0.04	0	0.08	0.03	10.57	100.24
EPS8	0.04	0.2	0.01	0.09	28.14	98.42
EPS9	0.04	0	0.1	0.15	9.83	98.32
EPS10a	4.33	2.84	0.22	0.11	0.59	99.88
EPS10b	3.68	2.81	0.15	0.11	1.88	99.62
EPS10c	4.19	2.83	0.19	0.1	0.74	100.15
EPS11	2.95	0.02	0.11	0.03	0.92	100.64
EPS12	0.04	0.11	0.12	0.06	4.57	98
	0.04	0.1	0.11	0.05	4.57	98

APPENDIX 5.3 MINERALOGICAL COMPOSITION (X-RAY DIFFRACTION) OF LABORATORY SAMPLES

sn.	name	pl	Qu	Ka	Or.	Pl.	Ep.	Go.	He.	An.	Am.	dif.
	sand											
89	EP2	D1	+++ +	±	±	±	+	-	-	-	-	
90	EP3	E1	+++ +	±	±	+	+	-	-	-	-	
91	EP4	E1	+++ +	±	±	-	±	-	-	-	-	
92	EP5	I4	+++ +	±	±	-	±	-	-	-	-	
93	EP6	K	+++ +	+	±	±	+	-	-	-	-	sm:+
94	EP8	H	+++ +	+	±	-	±	-	-	-	-	
95	EP11	H	+++ +	±	±	-	-	-	-	-	-	
96	EP12	J	+++ +	±	±	±	±	-	-	-	-	
97	EP14	I	+++ +	±	±	-	±	-	-	-	-	
98	EP15	Ni	+++ +	+	-	-	-	-	-	-	-	
99	EP19	L	+++ +	+	±	±	±	-	-	-	-	
100	EP22	O	+++ +	+	-	-	-	-	-	-	-	
101	EP23	O	+++ +	+	±	_	±	-	-	-	-	
	crusts											
102	EP1	P1	+++ +	+	±	±	+	-	-	-	-	Sm:+
103	EP7	K	+++ +	+	±	±	+	-	-	-	-	Sm:+
104	EP9	H	+++ +	+	±	-	±	-	-	-	-	
105	EP10	H	+++ +	++	±	±	±	-	-	-	-	
106	EP13	J	+++ +	+	±	±	±	-	-	-	-	
107	EP16	L	+++ +	++	±	±	±	-	-	-	-	
108	EP17	L	+++ +	++	±	±	±	-	-	-	-	
109	EP18	L	+++ +	++	±	±	±	-	-	-	-	
110	EP20	M/A	+++ +	++	±	±	±	-	-	-	-	
111	EP21	M/A	+++ +	++	±	±	±	-	-	-	-	
112	EP24	H	+++ +	++	±	-	±	-	-	-	-	
113	EP25	H	++	++	-	-	-	++	+	±	-	
	stones											

sn.	name	pl	Qu	Ka	Or.	Pl.	Ep.	Go.	He.	An.	Am.	dif.
114	EPS1a	D81	+++	+	-	-	-	-	++	-	-	Mi:+
115	EPS1b	D1	+++	++	-	-	-	++	-	+	-	
116	EPS1c	D1	+	-	±	+++	+	-	-	-	+++	Ch:+
117	EPS2	D2	+++	+	-	-	-	-	-	-	-	Sp:+++,?:+
118	EPS3a	E2	-	±	-	-	-	+++	+++	-	-	Bo:++,gi:++
119	EPS3b	E2	-	++	-	-	-	+	+++	±	-	
120	EPS3c	E2	±	±	-	-	-	±	-	++	-	Bo:+++,Gi:++
121	EPS4a	E2	±	++	-	-	-	-	+++	-	-	
122	EPS4b	E2	+	++	-	-	-	++	++	-	-	
123	EPS5a	I	+++ +	-	-	-	-	-	-	-	-	
124	EPS5b	I	+++ +	-	-	-	-	-	-	-	-	
125	EPS5c	I	+++ +	-	-	-	-	±	±	-	-	
126	EPS6a	K	+++ +	-	-	-	-	-	-	-	-	
127	EPS6b	K	++	-	-	++	±	-	-	-	+++	
128	EPS7	H	+	++	-	-	-	++	++	±	-	
129	EPS8	H	++	+	-	-	-	-	-	-	-	Ca:++++
130	EPS9	H	+	++	-	-	-	++	++	±	-	
131	EPS10a	J	++	-	+	++	±	-	-	-	++	Mi:+
132	EPS10b	J	++	-	+	++	±	-	-	-	++	Mi:+
133	EPS10c	J	++	-	+	++	±	-	-	-	++	Mi:+
134	EPS11	K	++	-	±	-	+	-	-	-	++	Ch:±
135	EPS12	I2	+++	+	-	-	-	-	-	-	-	Sp:+++,?++

Relative amount of the minerals:

- not present
± very little amount or not present
\+ little amount
++ moderate
+++ abundance
++++ very abundance

abbreviations:

sn. sample number
name name of sample (corresponding with names in appendix 5.1)
pl place were sample is taken

Qu Quartz
Ka Kaolinite
Or. Orthoclase
Pl. Plagioclase
Ep. Epidote
Go. Goethite
He. Hematite
An. Anatase
Am. Amphibole
dif. Different types of minerals
Sm Smectite
Mi Micas
Ch Chlorite
Sp Spessartite
Bo Boehmite
Gi Gibbsite
Ca Calcite

APPENDIX 5.4 ORGANIC CARBON AND FREE IRON CONTENT (ANALYTICAL CHEMICAL ANALYSIS) OF LABORATORY SAMPLES

Sample Code	Moisture Content	Organic Carbon	Free
	%	%	%
94/89	0.8	0.54	2.7
94/90	0.2	0.16	1.4
94/91	0.2	0.29	1.8
94/92	0.2	0.16	3.2
94/93	1.0	0.65	1.7
94/94	0.2	0.27	1.4
94/95	0.0	0.17	0.7
94/96	0.0	0.09	0.6
94/97	0.0	0.46	0.5
94/98	0.2	0.12	0.8
94/99	0.0	0.12	0.7
94/100	0.0	0.05	1.3
94/101	0.0	0.23	0.8
94/102	0.9	0.62	3.1
94/103	0.7	0.80	2.7
94/104	0.1	0.63	0.8
94/105	0.1	0.58	1.5
94/106	0.2	0.23	0.6
94/107	0.3	0.86	1.4
94/108	0.1	0.38	1.1
94/109	0.2	0.82	1.2
94/110	0.7	3.39	1.6
94/111	0.6	1.70	1.7
94/112	0.4	0.24	1.4
94/113	0.8	0.11	12.2

APPENDIX 5.5 ABSORPTION FEATURES OF LABORATORY SAMPLES USING DISPEC

GFE1

wavel	depth	area	asym
1.915	0.0345	0.0043	0.2356
1.417	0.0149	0.0011	0.6086
0.949	0.0049	0.001	1.6357
1.723	0.0004	0	2.4008
1.804	0.0003	0	2.087
1.198	0.0001	0	2.4117
1.243	0.0001	0	2.2706

GFE10

2.209	0.0429	0.0064	3.873
1.414	0.0426	0.0027	1.2435
0.916	0.0042	0.0006	0.6661
0.709	0.0006	0	0.9438
1.726	0.0004	0	4.2436
1.237	0.0004	0	1.2192

GFE11

2.209	0.0793	0.0091	2.6823
1.414	0.0677	0.0032	2.0174
0.895	0.0128	0.0011	0.8512
2.449	0.0073	0.0003	0.5197

EP5

1.915	0.0776	0.0109	0.2202
1.414	0.0668	0.0039	0.9142
0.91	0.0466	0.0102	0.5912
1.795	0.0017	0.0001	1.233
1.687	0.0003	0	2.005

EP6

1.912	0.0644	0.0063	0.305
1.414	0.0446	0.0025	0.7208
2.209	0.0218	0.0014	1.0304
0.898	0.0079	0.0009	0.6607
0.715	0.0014	0	0.3839
1.684	0.0002	0	1.1208
1.195	0.0002	0	0.1864

EP14A

2.209	0.0395	0.0027	1.042
1.414	0.0334	0.0015	1.2485
1.915	0.0264	0.0024	0.4808
0.901	0.0108	0.001	0.7641
2.452	0.0043	0.0002	0.5959

EP15

2.206	0.0772	0.0054	1.4501
1.414	0.0732	0.0042	1.4897
1.915	0.0472	0.0039	0.4455
0.898	0.0342	0.005	0.9126
2.446	0.0053	0.0002	0.4602
1.798	0.0022	0.0001	0.6474
0.706	0.0006	0	0.094
1.672	0.0004	0	0.5938
1.171	0.0001	0	0.9077

EPS1A

0.892	0.034	0.0052	1.3303
1.414	0.0173	0.0076	0.1011

EPS1B

2.329	0.0039	0.0007	2.9159
0.73	0.0014	0.0003	0.0678

EPS5A

0.934	0.0287	0.0084	0.7606
1.402	0.0151	0.0024	0.1468
2.209	0.0131	0.0012	0.9552

EPS5B

0.748	0.0012	0.0002	0.1397
1.795	0.0012	0.001	0.9162

EPS10C

1.915	0.0111	0.0017	0.1891
1.441	0.0038	0.0007	1.7179
0.865	0.0021	0.0002	3.4809

EPS11

2.317	0.0027	0.0004	1.5974
1.441	0.0025	0.0011	4.2609

GFE2

wavel	depth	area	asym
1.414	0.1043	0.0059	1.9481
2.209	0.0804	0.0068	1.3249
1.915	0.051	0.0046	0.5076
0.91	0.0311	0.007	0.5102
1.669	0.0003	0	0.4069

GFE3

wavel	depth	area	asym
1.933	0.0499	0.0104	0.1841
1.444	0.0212	0.0041	0.2622
0.784	0.0099	0.001	0.9601
1.102	0.0002	0	3.4706
1.192	0.0002	0	0.9827
1.138	0.0002	0	0.7079
1.24	0.0001	0	0.9291

GFE12

1.411	0.0368	0.0014	1.3005
2.209	0.0327	0.0053	2.9811
0.883	0.0106	0.001	0.8285
1.243	0.0002	0	1.8595
1.576	0.0001	0	0.3693

GFE13

2.209	0.0093	0.0007	0.837
1.918	0.0091	0.0008	0.5021
1.447	0.0041	0.0004	1.0066
0.961	0.0016	0.0003	2.6336
1.099	0.0003	0	0.6186
1.18	0.0001	0	0.4975

EP7

1.912	0.0705	0.0062	0.3378
1.414	0.0439	0.0025	0.697
2.209	0.0273	0.0018	1.0157
0.904	0.0098	0.0014	0.5292
1.672	0.0003	0	0.6182

EP8

2.209	0.0662	0.0046	1.1638
1.414	0.0542	0.0024	1.886
1.915	0.0275	0.0024	0.4958
0.895	0.0151	0.0014	0.6846
2.449	0.0059	0.0002	0.4868
1.129	0.0004	0	3.6741
2.089	0.0003	0	1.1132
1.492	0.0002	0	0.2444
1.18	0.0002	0	0.68

EP16

2.209	0.071	0.0051	1.0934
1.414	0.0612	0.0028	1.8684
1.915	0.0361	0.003	0.4985
0.901	0.0132	0.0011	0.9981
2.089	0.0005	0	0.8703
1.111	0.0004	0	0.3668
1.237	0.0004	0	0.84
1.189	0.0002	0	0.6529
1.591	0.0001	0	0.68

EP17

1.414	0.0651	0.004	3.3537
2.209	0.0531	0.0064	3.1212
2.449	0.0051	0.0002	0.5309

EPS1C

1.015	0.0451	0.0133	1.1339
2.209	0.0322	0.0022	1.2977
1.414	0.0313	0.0015	1.7228
1.918	0.018	0.0023	0.8786
2.449	0.0034	0.0001	0.5459
1.33	0.0002	0	2.8029

EPS1BA

2.332	0.0042	0.0013	6.2292

EPS5C

1.927	0.0341	0.0055	0.3915
1.42	0.0215	0.003	0.3014
0.889	0.0024	0.0003	1.5722

EPS6A

1.924	0.0727	0.0192	1.2417
0.937	0.0094	0.0017	0.8707
2.47	0.0012	0.0001	3.7523

EPS12

1.45	0.006	0.0019	0.088
1.372	0.0049	0.0008	8.5159

GFE4

wavel	depth	area	asym
2.209	0.0613	0.004	1.3515
1.414	0.0582	0.0027	1.7959
1.918	0.0313	0.0027	0.6216
0.898	0.0172	0.002	0.8497
2.449	0.0061	0.0003	0.493
2.089	0.0004	0	1.8725
1.237	0.0003	0	0.5506
1.204	0.0002	0	5

GFE5

wavel	depth	area	asym
2.209	0.0381	0.0047	2.394
1.414	0.0302	0.0015	1.5833
0.892	0.0083	0.0011	0.9207
1.801	0.0012	0.0002	2.5266

GFE31A (BROKEN)

2.209	0.0196	0.0014	0.9749
1.915	0.019	0.0016	0.3369
1.417	0.0136	0.0008	0.7189
0.928	0.0033	0.0004	1.1709
1.729	0.0008	0.0001	0.4596

GFE14

1.912	0.0862	0.0086	0.275
1.417	0.0542	0.0034	0.6136
2.209	0.0268	0.0019	0.7882
0.919	0.0157	0.0026	0.5419
1.786	0.0013	0.0001	1.062
1.672	0.0003	0	0.3956
1.246	0.0002	0	0.1924

EP9

2.209	0.0458	0.0031	1.1771
1.414	0.039	0.0018	1.7913
1.918	0.0311	0.0027	0.5535
0.886	0.0094	0.0011	0.8599
2.452	0.0047	0.0002	0.6042
1.123	0.0002	0	0.2209
1.204	0.0002	0	0.8518
1.243	0.0002	0	1.3579
1.57	0.0001	0	0.1768

EP10

2.209	0.0565	0.004	1.0938
1.414	0.0549	0.0025	1.5917
1.915	0.0285	0.0024	0.5445
0.904	0.018	0.0017	0.7768
1.243	0.0003	0	2.7611

EP18

2.209	0.0612	0.0046	1.0724
1.414	0.0552	0.0026	1.5968
1.915	0.0315	0.0027	0.512
0.91	0.0132	0.0012	0.9379
1.24	0.0004	0	1.6794

EP19

2.209	0.047	0.0061	2.7905
1.414	0.0432	0.0019	1.5303
0.898	0.0133	0.0012	0.7934
2.449	0.0042	0.0002	0.4734
1.132	0.0003	0	0.9587
1.234	0.0002	0	1.2515
1.183	0.0002	0	0.551

EPS2

1.405	0.0124	0.0006	0.9395
1.915	0.008	0.0014	0.174
0.898	0.0053	0.0012	0.9548
1.729	0.0002	0	3.4315

EPS3A

0.982	0.028	0.0085	0.8037
1.417	0.0265	0.0103	0.0627
2.269	0.0136	0.0025	0.8403

EPS6B

0.934	0.0068	0.0015	0.534
2.32	0.0039	0.0009	3.5178
1.441	0.0037	0.0003	0.4698
1.372	0.0033	0.0001	1.8901

EPS7

1.057	0.0359	0.0116	1.4034
1.414	0.0338	0.002	1.3811
1.921	0.0184	0.0047	0.4299

GFE6

wavel	depth	area	asym
1.414	0.042	0.0027	1.2165
2.209	0.0269	0.0049	3.9817
0.931	0.0176	0.0052	0.4293
0.709	0.0012	0	0.2699
1.669	0.0002	0	0.8021

GFE7

wavel	depth	area	asym
2.209	0.0574	0.004	1.3202
1.414	0.051	0.0027	1.4665
1.915	0.0442	0.0038	0.4256
0.898	0.0082	0.0008	0.8782
2.446	0.0047	0.0002	0.3642
1.669	0.0005	0	0.5431
1.732	0.0005	0	1.172
1.24	0.0003	0	1.4
1.138	0.0002	0	0.5395

EP1

1.912	0.0705	0.0065	0.3098
1.414	0.0418	0.002	0.7747
2.209	0.0321	0.0018	1.3171
0.901	0.015	0.0017	0.6437
2.452	0.0031	0.0002	0.4863
1.132	0.0002	0	0.4552
1.174	0.0001	0	0.616

EP2

1.912	0.085	0.0086	0.2761
1.414	0.0514	0.0032	0.5736
2.209	0.0292	0.0017	1.3138
0.907	0.0134	0.002	0.5677
2.449	0.0027	0.0001	0.4872
1.78	0.0011	0.0001	0.7382
1.669	0.0003	0	0.3641

EP11

2.209	0.0391	0.0031	0.8472
1.414	0.034	0.0016	1.4038
1.915	0.0233	0.0022	0.4923
0.904	0.0175	0.0026	0.5874
1.234	0.0001	0	0.616

EP12

2.209	0.0393	0.0028	1.0179
1.915	0.0353	0.0032	0.4132
1.414	0.0351	0.0017	1.1586
0.904	0.0146	0.0018	0.6422
2.449	0.0035	0.0001	0.5009
1.237	0.0001	0	1.1176

EP20

1.918	0.0299	0.0046	0.1778
1.417	0.0128	0.0012	0.3798
0.955	0.0053	0.0007	1.7151
2.452	0.0036	0.0002	0.4931
1.729	0.0021	0.0002	0.4965
1.249	0.0002	0	1.891

EP21

1.414	0.0391	0.0016	1.3996
2.209	0.0364	0.0027	0.8891
1.918	0.0347	0.0033	0.5621
0.904	0.0075	0.0007	1.1213
0.718	0.0012	0.0001	0.2375
1.234	0.0002	0	0.8008

EPS3B

0.892	0.0217	0.0061	0.4054
2.209	0.0183	0.0016	1.1234
1.921	0.0116	0.0011	0.3772
1.819	0.0009	0.0001	2.5467

EPS3C

0.988	0.0233	0.0082	0.8476
1.411	0.0141	0.0007	1.0426
1.924	0.0114	0.0027	0.5213

EPS8

1.414	0.0377	0.0021	1.62
1.915	0.0354	0.0059	0.1776
0.907	0.0038	0.0005	1.5739
2.446	0.0025	0.0001	0.2624
1.816	0.0007	0	2.3069
1.681	0.0003	0	1.5575

EPS9

1.411	0.0093	0.0027	11.928
1.915	0.0076	0.0008	0.5303
2.209	0.0075	0.0007	0.8627

GFE8

wavel	depth	area	asym
2.209	0.0359	0.0041	2.0529
1.414	0.035	0.0019	2.4787
0.892	0.004	0.0006	0.7228
0.712	0.0008	0	0.4072
1.24	0.0006	0	1.232
1.72	0.0004	0	1.8986
1.57	0.0001	0	0.2969

GFE9

wavel	depth	area	asym
2.209	0.0724	0.005	1.2864
1.414	0.0626	0.0029	1.9379
1.915	0.0379	0.003	0.3945
0.898	0.0114	0.0009	0.8919
2.449	0.0071	0.0003	0.4981
1.816	0.002	0.0002	4.1708
2.089	0.0005	0	1.0295
1.063	0.0004	0	1.0618
1.24	0.0004	0	0.8844
1.138	0.0002	0	0.2772
1.579	0.0001	0	2.68

EP3

1.912	0.0857	0.0077	0.3218
1.414	0.0535	0.0032	0.6465
2.209	0.0327	0.0023	0.8344
0.901	0.0159	0.0028	0.3211
2.449	0.0023	0.0001	0.3892
1.795	0.0008	0.0001	1.2496
1.681	0.0004	0	1.2335

EP4

1.915	0.0473	0.0041	0.3618
1.414	0.036	0.0019	0.9367
2.209	0.0337	0.0023	1.1003
0.895	0.02	0.0029	0.7291
1.798	0.001	0.0001	2.1703
1.195	0.0002	0	0.9755
1.237	0.0001	0	0.4824

EP13

1.414	0.0634	0.003	1.6088
2.209	0.0602	0.0042	1.304
1.915	0.0471	0.004	0.4454
0.901	0.0092	0.0011	1.3929
2.449	0.0048	0.0002	0.5295
1.24	0.0003	0	3.283
2.089	0.0003	0	1.446

EP14

1.414	0.0442	0.002	1.4245
1.921	0.0367	0.0057	0.3108
0.874	0.0078	0.0008	0.8513
2.455	0.0053	0.0003	0.6621
1.057	0.0005	0.0001	0.4231

EP22

2.209	0.037	0.0026	1.1467
1.414	0.0369	0.0017	1.4081
1.915	0.0292	0.0026	0.352
0.901	0.026	0.0044	0.6609
2.449	0.0033	0.0001	0.524
1.798	0.0013	0.0001	2.1113
2.113	0.0003	0	0.6774

EP23

2.209	0.0444	0.0032	0.9884
1.414	0.0407	0.0018	1.4371
1.915	0.033	0.0028	0.3535
0.895	0.018	0.0021	0.7315
1.801	0.0012	0.0002	3.1235
2.113	0.0003	0	0.6882

EPS4A

1.063	0.0345	0.0111	1.4988
1.414	0.0272	0.0016	0.9749
1.921	0.0187	0.0044	0.4455

EPS4B

0.916	0.0278	0.0074	0.661
1.411	0.0233	0.0011	1.2551
2.209	0.0227	0.004	4.057
1.795	0.0008	0	0.398
1.327	0.0001	0	1.439
1.669	0.0001	0	0.2412

EPS10A

1.918	0.0307	0.003	0.3522
2.209	0.0211	0.0017	0.6849
1.417	0.0183	0.0011	0.8172
0.943	0.0155	0.0039	0.4887
1.798	0.0006	0	1.4824
1.678	0.0004	0	1.248

EPS10B

1.918	0.0153	0.0015	0.3235
2.323	0.009	0.0009	1.1024
1.411	0.0076	0.0004	0.8169
0.895	0.0046	0.0007	1.0641
1.72	0.0003	0	0.6726
2.11	0.0002	0	0.6129

APPENDIX 5.6 A SELECTION OF UNMIXED IMAGES

Unmixed image of EM manganese hills

Stretched between: 0 - 90

Unmixed image of EM redschist area

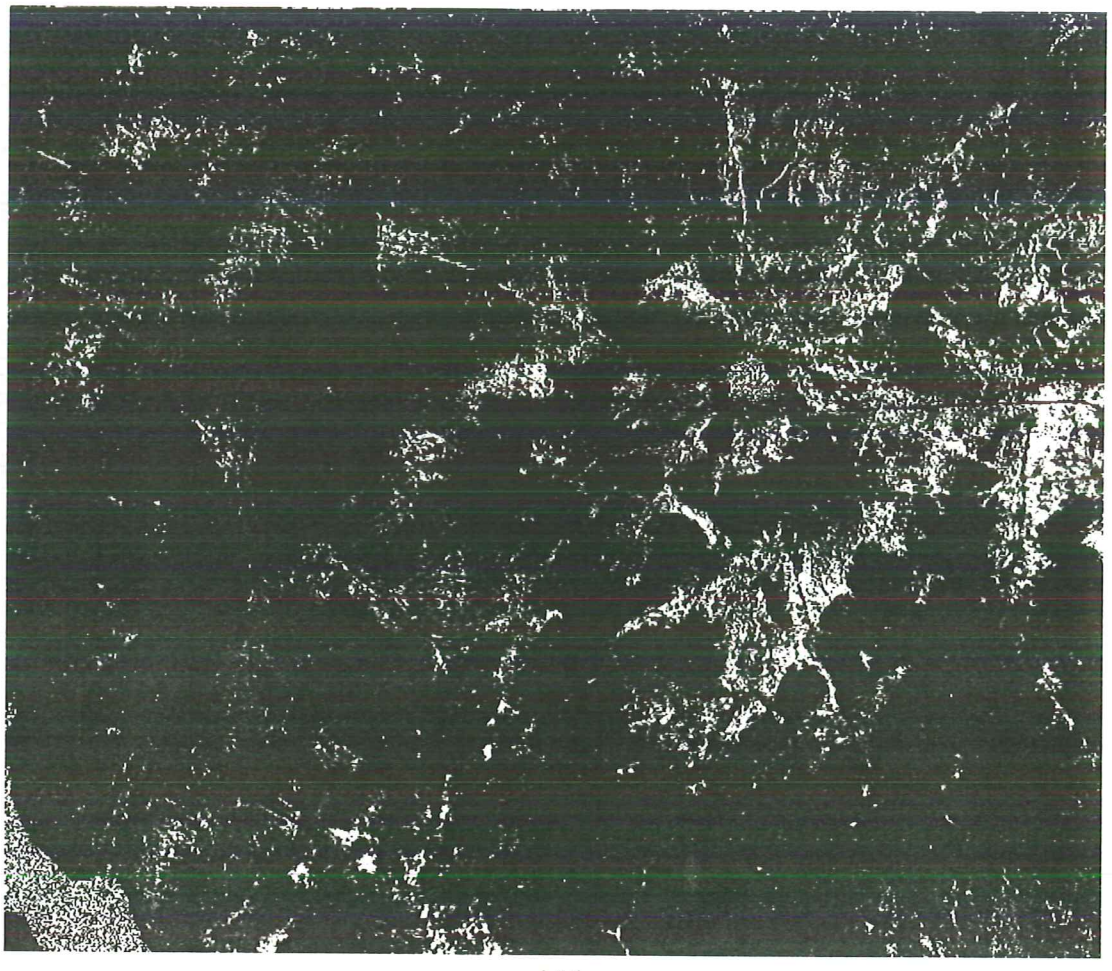

Stretched between: 0 - 85

Unmixed image of EM greenschist

Stretched between: 0 - 50

Unmixed image of EM cuirasse

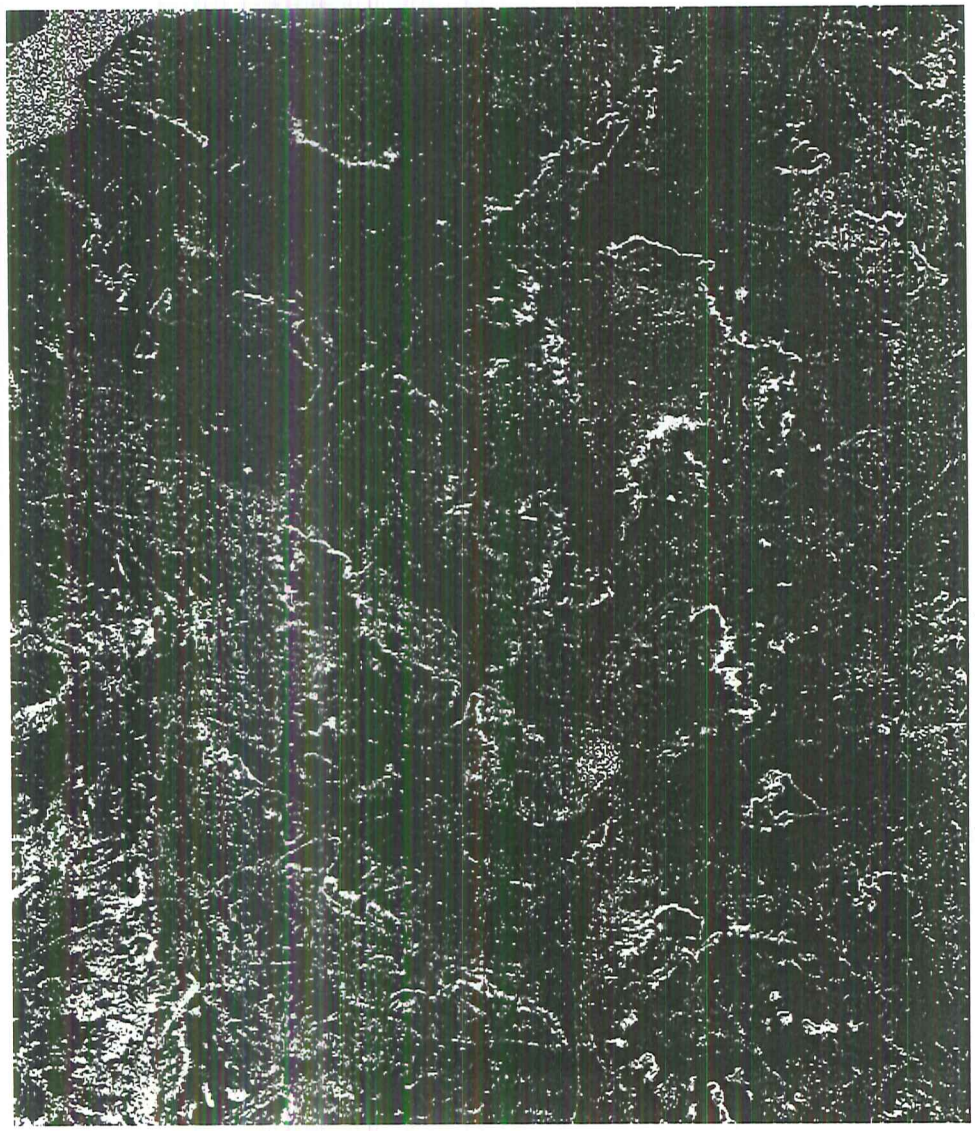

Stretched between: 0 - 70

Unmixed image of EM vegetation

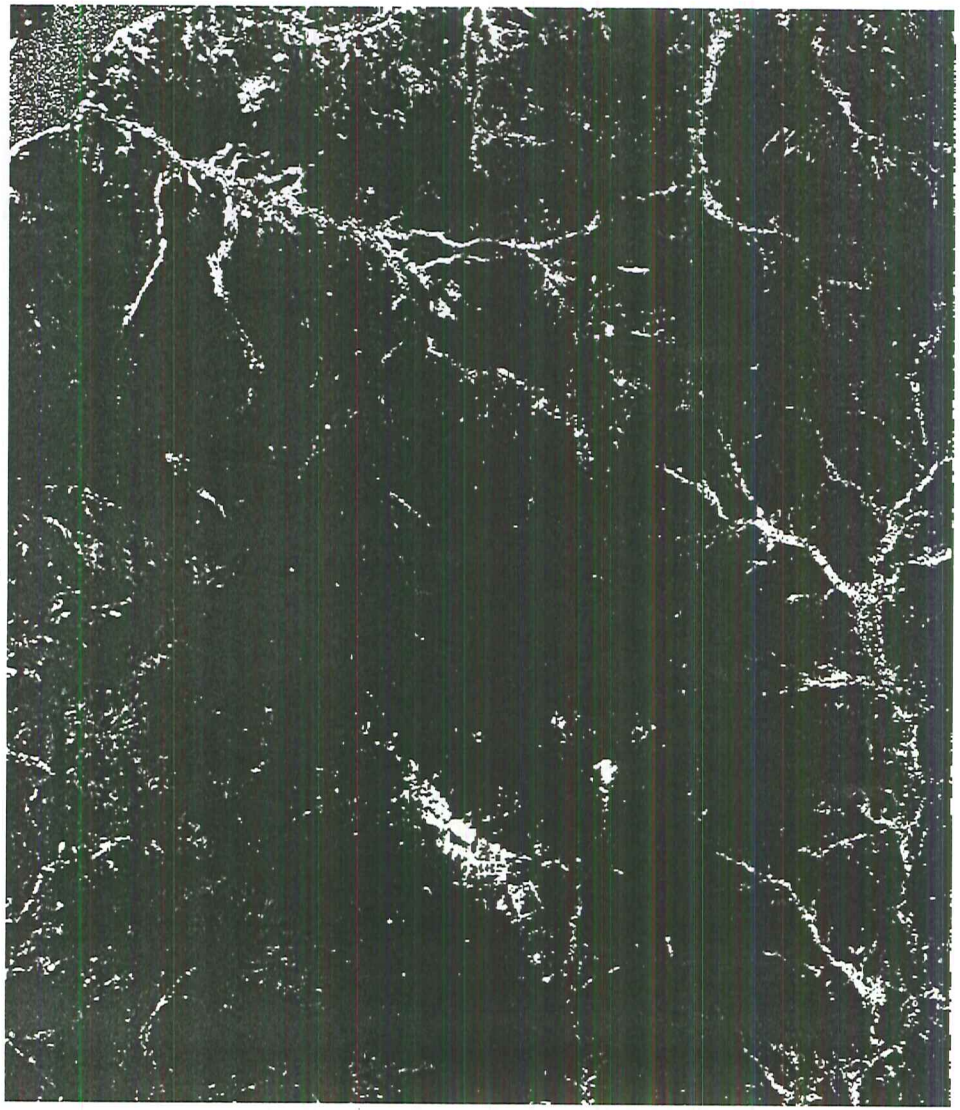

Stretched between: 0 - 25

Unmixed image of EM erosion area

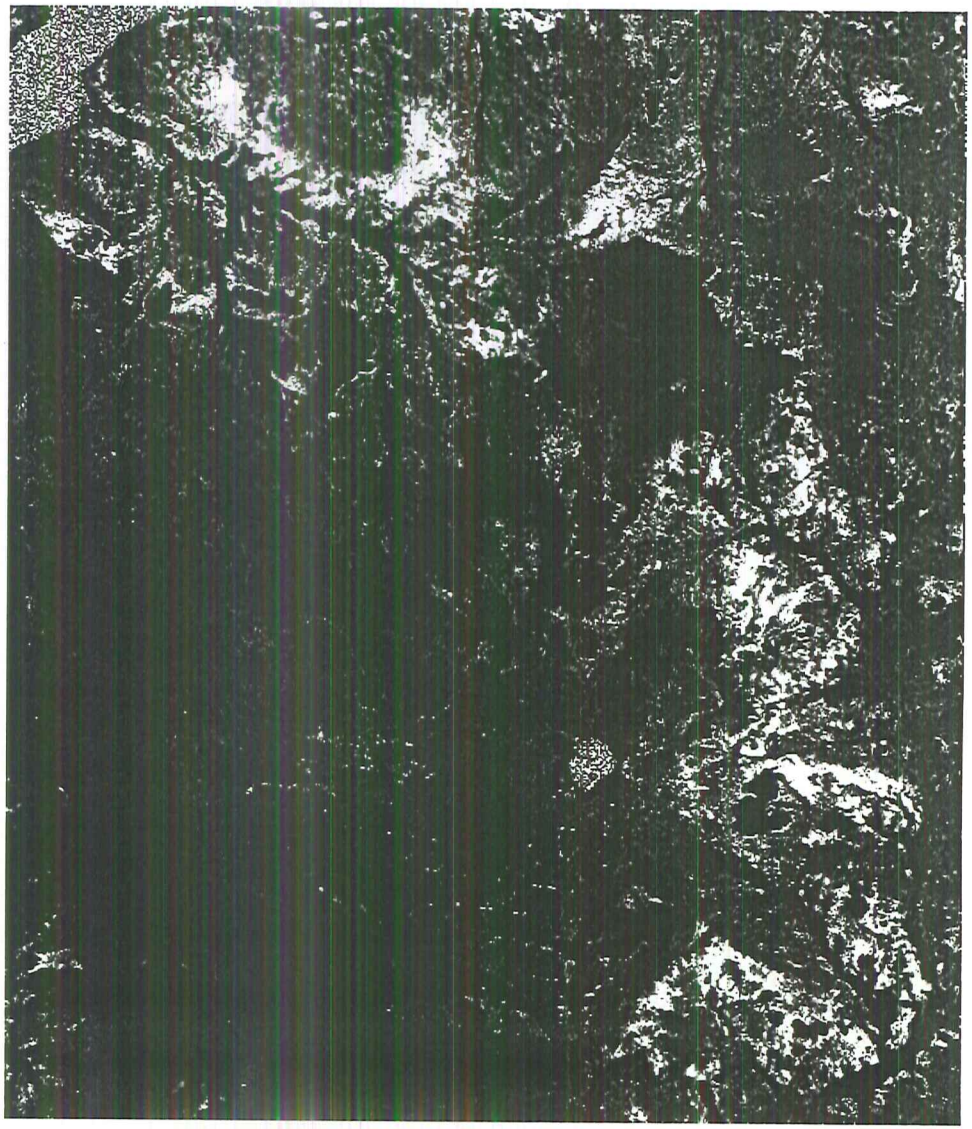

Stretched between: 0 - 80

Unmixed image: total sum of all EM

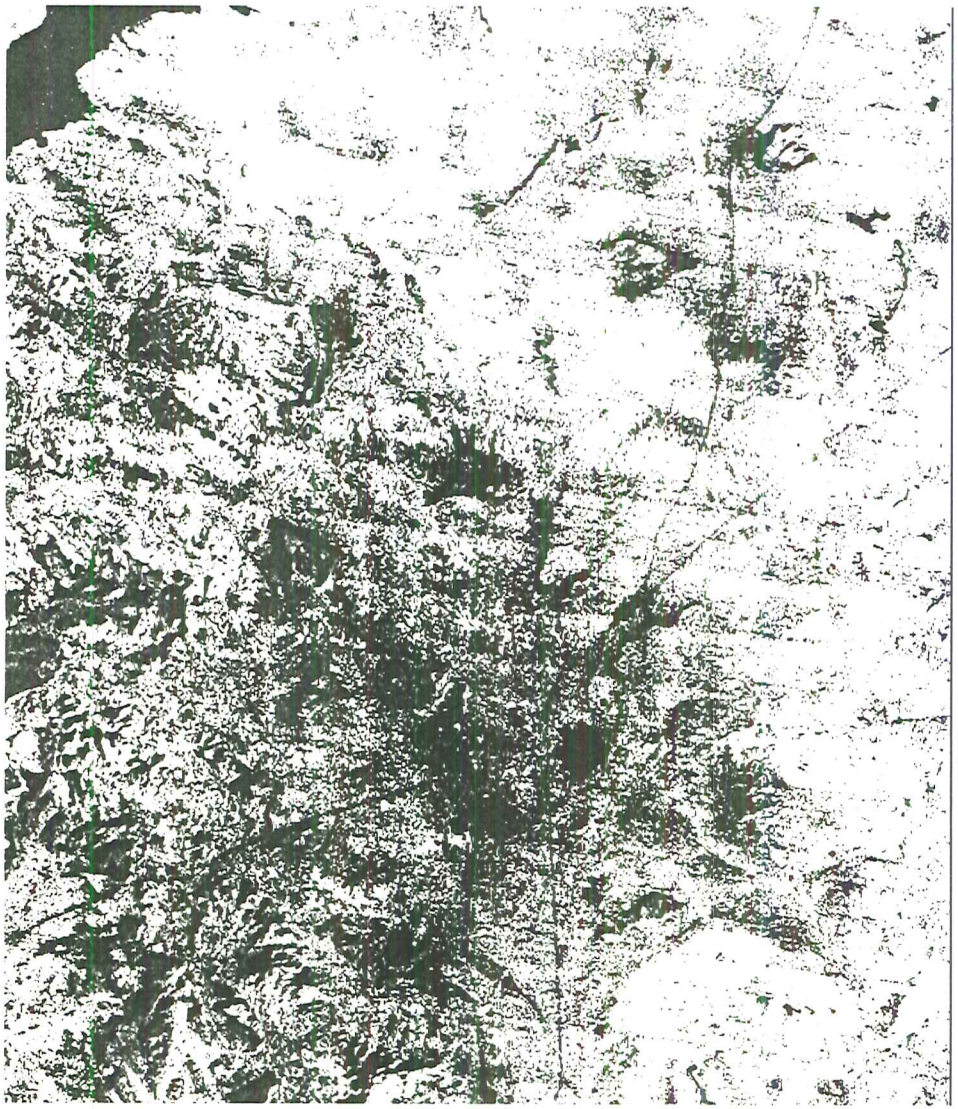

Stretched between: 80 - 100

Unmixed image: RMS

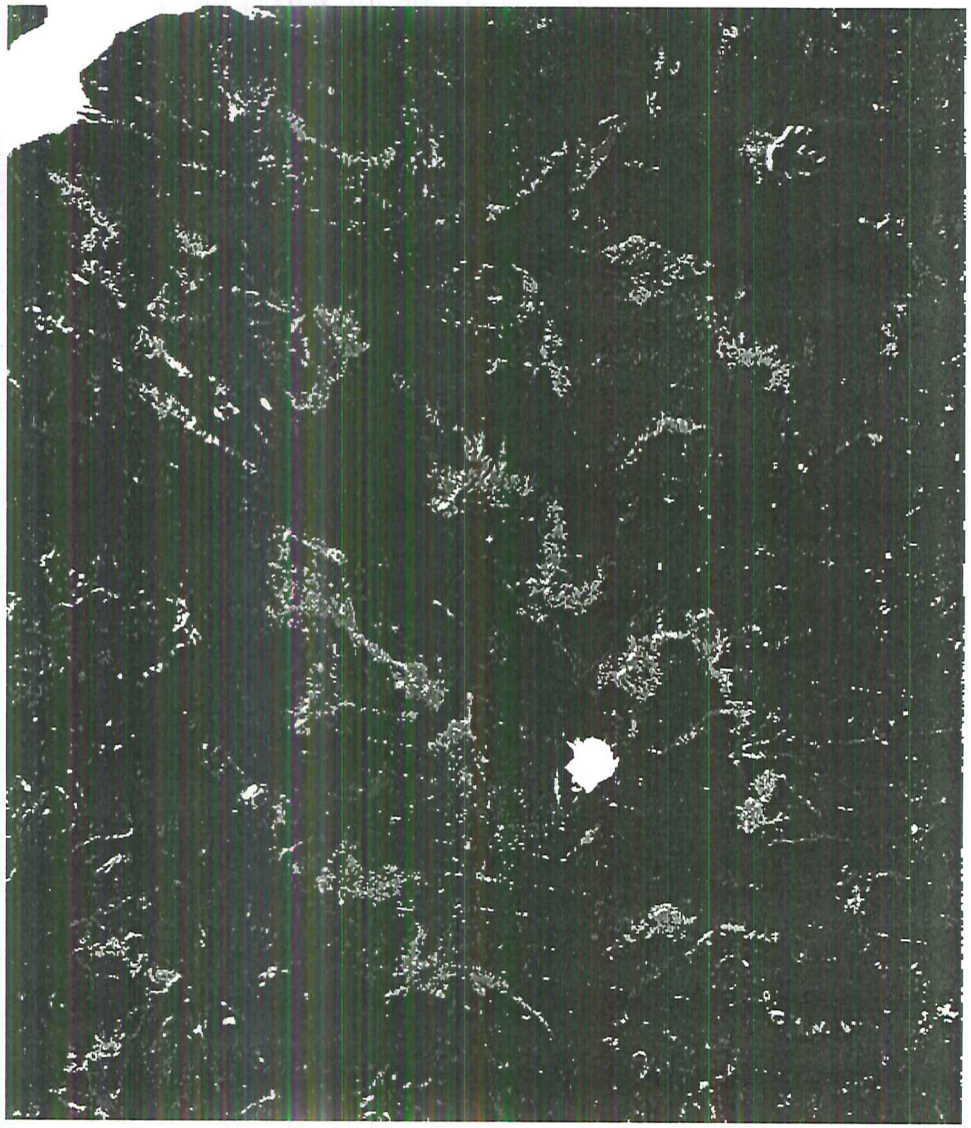

Stretched between: 1 - 5

APPENDIX 5.7 STATISTICAL RESULTS OF UNMIXING

Cuirasse	ave.	st.dv	min	max
EM1	53.33	73.14	0	206
EM2	750.0	100.3	550	911
EM3	18.21	24.12	0	100
EM4	3.952	12.73	0	60
EM5	32.28	53.23	0	178
EM6	121.9	138.2	0	399
TOTAL	980.9	21.99	932	1000
RMS	0.619	0.696	0	2

Control area cuirasse	ave.	st.dv	min	max
EM1	0	0	0	0
EM2	739.4	91.64	582	899
EM3	0	0	0	0
EM4	84.64	62.29	0	232
EM5	18.97	48.33	0	195
EM6	106.3	110.2	0	380
TOTAL	950.3	21.60	898	999
RMS	4	0.707	2	5

Greenschist	ave.	st.dv	min	max
EM1	837.6	87.71	600	982
EM2	39.46	85.19	0	382
EM3	19.70	23.95	0	89
EM4	38.12	42.08	0	160
EM5	24.96	44.43	0	210
EM6	30.55	52.34	0	260
TOTAL	991.6	14.14	952	1000
RMS	0.344	0.578	0	3

Control area greenschist	ave.	st.dv	min	max
EM1	622.2	149.9	190	940
EM2	20.36	49.02	0	198
EM3	9.414	17.51	0	78
EM4	53.34	42.82	0	145
EM5	0	0	0	0
EM6	289.3	156.4	0	615
TOTAL	995.8	9.721	955	1000
RMS	0.682	0.609	0	2

vegetation	ave.	st.dv	min	max
EM1	18.78	44.34	0	232
EM2	4.495	25.89	0	182
EM3	16.13	28.21	0	118
EM4	837.7	57.05	734	990
EM5	0.056	0.580	0	6
EM6	121.4	57.26	0	255
TOTAL	999.4	0	999	1000
RMS	1.887	0.924	0	5

Vegetation controle area	ave.	st.dv	min	max
EM1	0.436	3.236	0	24
EM2	48.36	110.8	0	501
EM3	609.0	195.9	224	935
EM4	9.254	40.42	0	278
EM5	2.2	10.42	0	69
EM6	234.7	180.4	0	641
TOTAL	904.8	49.74	770	1000
RMS	1.6	1.285	0	6

erosion surface	ave.	st.dv	min	max
EM1	3.853	13.30	0	100
EM2	2.439	10.63	0	78
EM3	0.586	2.702	0	16
EM4	939.1	61.23	737	1000
EM5	41.71	61.23	0	262
EM6	9.068	27.38	0	140
TOTAL	997.3	6.019	971	1000
RMS	0.818	0.667	0	2

erosoin surface control area	ave.	st.dv	min	max
EM1	18.78	44.34	0	232
EM2	4.495	25.89	0	182
EM3	16.13	28.21	0	118
EM4	837.7	57.05	734	990
EM5	0.056	0.580	0	6
EM6	121.4	57.26	0	255
TOTAL	999.4	0	999	1000
RMS	1.887	0.924	0	5

redschist	ave.	st.dv	min	max
EM1	2.993	17.29	0	186
EM2	22.52	56.25	0	391
EM3	3.436	11.35	0	80
EM4	61.74	62.86	0	377
EM5	866.1	117.0	284	1000
EM6	29.65	56.77	0	274
TOTAL	987.3	18.19	890	1000
RMS	0.832	0.743	0	4

red schist control area	ave.	st.dv	min	max
EM1	0	0	0	0
EM2	45.48	63.39	0	254
EM3	3.1	12.94	0	85
EM4	18.2	42.82	0	194
EM5	826.0	92.72	616	983
EM6	55.92	65.06	0	230
TOTAL	949.5	29.94	869	1000
RMS	1.16	0.509	0	2

manganese hills	ave.	st.dv	min	max
EM1	0.946	8.198	0	71
EM2	0	0	0	0
EM3	16.01	29.44	0	132
EM4	32.73	45.81	0	175
EM5	0	0	0	0
EM6	938.6	49.46	811	1000

manganese control area	ave.	st.dv	min	max
EM1	2.094	15.28	0	133
EM2	9.803	30.95	0	206
EM3	8.726	21.86	0	134
EM4	23.47	47.90	0	198
EM5	0.034	0.369	0	4
EM6	911.5	64.51	693	1000

TOTAL	988.8	22.95	888	1000	TOTAL	956.0	49.26	811	1000
RMS	2.773	0.847	1	5	RMS	2.205	0.760	1	4

Greenschist shade side					Water area				
EM1	18.62	43.28	0	220	EM1	-0.02	6.200	-15	16
EM2	0.558	3.659	0	24	EM2	-0.11	14.84	-38	33
EM3	125.5	30.12	75	229	EM3	0.006	0.083	0	1
EM4	0	0	0	0	EM4	-0.09	11.72	-30	26
EM5	0	0	0	0	EM5	0.174	17.98	-39	45
EM6	693.3	44.75	617	761	EM6	326.3	6.818	311	348
TOTAL	838.7	50.97	717	922	TOTAL	326.3	6.249	313	347
RMS	3.093	0.647	2	5	RMS	16.46	0.500	16	17

PUBLICATIONS DEJA PARUES:
(SUITE DE LA PAGE INTERIEURE DU FRONTISPICE)

15	H.J.M Gijsbers J.J. Kessler M.K. Knevel	Dynamics and natural regeneration of woordy species in farmed parklands in the Sahel region (Province of Passore, Burkina Faso) In: Forest Ecology and Management 64 (1994) 1-12
16	J.J. Kessler	Usefulness of the human carrying capacity concept in assessing ecological sustainability of land-use in semi-arid regions. In Agriculture, Ecosystems & Environment 48 (1994) 273-284
17	J.J. Kessler P. Laban	Planning strategies and funding modalities for land rehabilitation. In: Land Degradation & Rehabilitation, Vol. 5, 25-32 (1994)
18	A. Blokland L. Stroosnijder	Sustainable agriculture and food security - a challenge to farmers, research and development in the Sahel. Chapter 4 from: Development-related research collaboration. A second look at the role of the Netherlands.C. Schweigman and I.A. van der Werf(eds), Royal Tropical Institute, Amsterdam, 1994
19	J. de Graaff L. Stroosnijder	L'évaluation économique des mesures CES au Sahel (présenté lors des 11ème Journées du Réseau Erosion "L'environnement humain de l'érosion, 20-22 septembre 1994, ORSTOM/E.N.S. St. CLOUD-Université PARIS VII)

Rapports des étudiants (violet)

1	M. Rietkerk	Les differences locales du sol et la capacité de régénération: une étude pour la régénération des écosystèmes sylvo-pastoraux Sahéliens, dans la Forêt Classée de Yabo (Burkina Faso)
2	S.J.T. Poutsma	Geografische Informatie Systemen en bodem- en waterconservering: een praktijkvoorbeeld
3	J. van Etten	Mesures de rendement dans les Bas-fonds de Damana, Kawara et Moadougou, rapport de stage
4	A. de Wit	L'effet du bilan hydrique sur la croissance des arbres tropicaux: une étude sur la distance optimale des diguettes à l'aide de quantité d'eau utilisée par l'Acacia Seyal
5	A. Florijn	Etude sur l'impact hydrologique des digues filtrantes sur l'humidité volumétrique du sol dans le bas-fond de Noh
6A	H.B. Tammes	Carte des états de surface du bassin versant de Solmiougou
6B	H.B. Tammes	L'effet de la matière organique des sols sableux de Burkina Faso sur la formation des croûtes et sur l'érosion
7	F. Kologo	Evaluation des techniques de restauration des sols dans les zones sylvo-pastorales de la province du Sanmatenga
8	A. Belemviré	Contribution à l'étude de la cartographie des états de surface et à l'estimation de la biomasse ligneuse aérienne à partir de l'image Landsat Thematic Mapper. Essais de Mesures radiométriques au sol. Etudes menées au Kaya
9	S. Idi	Evaluation des contraintes socio-économiques et techniques des plantations villageoises dans le Sanmatenga: étude de cas
11	M. de Haas	Assessment of aggregate stability of Sahelian soils from Burkina Faso
12	O. van Dam	Recherche du sol et de la télédétection à Kaya, Burkina Faso
13	J.C. den Boef	Les mesures de conversation des eaux et du sol dans trois villages de la province du Zoundwéogo.
14	P.A.J. Schaper	Les mesures de conservation des eaux et des sols dans trois villages de la province du Sanmatenga
15	A.R. Vriend	Un inventaire agro-socio-économique des ménages du plateau central du Burkina Faso
16	M.C. Minnaard	Une étude sociologique sur la coopération autour des mesures des conservations des eaux et des sols, dans un village Mossi, Burkina Faso.
19	T. Slaa	Contribution à la classification des espaces sylvo-pastoraux au niveau villageois dans le Sahel
21a	A. Bleumink	La goutte qui se fait déborder la surface: une recherche indicative à l'influence du climat local sur la dégradation des états de la surface
21b	A. Bleumink	La goutte qui se fait déborder la surface, supplément: les données obtenues de la station météo
23	K.O. Trouwborst	Soil moisture reserve development at soil-water conservation measures in Burkina Faso
24	I.H. Janssen	De invloed van korsten op afstroming en nutriëntenverliezen in de Sahel
26	L. Coolegem	Recherche des intensités de la pluie dans trois stations au Burkina Faso
27	L.A. Timmer	Une étude sur les buts et les types de taille du néré (Parkia biglobosa (Jacq.) Benth.) et la relation avec sa structure
29	A.T.A. Loozekoot	A plusieurs mains l'ouvrage avance! Une étude socio-économique de Barcé, Yakin et Salmintenga, trois villages dans la province de Zoundwéogo au sud de Burkina Faso
29a	A.T.A. Loozekoot	Land degradation, population pressure and agricultural intensification
30	J.D. Wijnhoud/A.J. Otto	Physical properties of soils in the Kaya area, Burkina Faso
31	C.M.J. Jans	Les occupations et les revenues des plusieurs ménages au Burkina Faso
32	E. Elkenbracht/A. ten Holte/ L. Otter/T.Slaa	Remote sensing and soil science of the Kaya area (Burkina Faso)
44a	M. Kempkes	Analyse financière des cordons pierreux. Cas d'étude de Tagalla, province du Sanmatenga au Burkina Faso.
44b	M. Kempkes	Enquête socio-économique menée dans la provive du Sanmatenga au Burkina Faso durant la période sèche de 1994. Les résultats et leur analyse.
51	J. Suurmond	Rôle de l'élevage dans la zone traditionnelle de la province du Zoundwéogo.
58	A.A.C.	Faire une carte d'utilisation de la terre à l'aide de données-Landsat-TM, de photographies aeriènnes, et d'observations sur le terrain.

PUBLICATIONS DEJA PARUES (SUITE):

AUTRES PUBLICATIONS

- Stroosnijder, L. et al. (1990). Bijdragen Saheldag LUW-KIT 1990: Aménagement du Terroir Villageois. LUW, Wageningen
- Kessler, J.J. et J. Boni (1991). L'Agroforesterie au Burkina Faso: Bilan et analyse de la situation actuelle. Tropical Resource Management Paper No. 1. Ministère de l'Environnement et du Tourisme et UAW, Wageningen, Pays-Bas
- Bognetteau-Verlinden, E., S van der Graaf et J.J. Kessler (1992). Aspects de l'aménagement intégré des ressources naturelles au Sahel. Tropical Resource Management Paper No. 2, SNV et AUW, Wageningen, Pays-Bas
- Vlaar, J.C.J. (Ed.), 1992. Les techniques de conservation des eaux et des sols dans les pays du Sahel. Rapport d'une étude effectuée dans le cadre de la collaboration entre le Comité Interafricain d'Etudes Hydrauliques (CIEH), Ouagadougou Burkina Faso, et l'Université Agronomique Wageningen (UAW), Wageningen, Pays Bas
- Graaff, J. de (1993). Soil Conservation and sustainable land use, an economic approach. Development Oriented Research in Agriculture no. 4, Royal Tropical Institute, Amsterdam, Pays-Bas
- Boer de, F. et J.J. Kessler (1993). Le système d'élevage Peulh dans le sud du Burkina Faso: une étude agro-écologique du département de Tô. Tropical Resource Management Paper No. 3, AUW, Wageningen, Pays-Bas
- Hoek van der, R. et al. (1994). Perspectives pour le développement soutenu des systèmes de production agrosylvopastorale au Sanmatenga, Burkina Faso. Tropical Resource Management Paper No. 4, AUW, Wageningen, Pays-Bas
- Briel van den, J. et al. (1994). L'aménagement des terroirs villageois: une contribution à la gestion durable des ressources naturelles. Etude de cas du projet Reboisement Rive Droite Téra, Niger. Tropical Resource Management Paper No. 5, AUW, Wageningen, Pays-Bas